UNIVERSITY OF
BIRMINGHAM

Forest Structural Controls on Boreal Peatland Ecohydrology

Rhoswen Mair Leonard

A thesis submitted to the University of Birmingham for the degree of DOCTOR OF PHILOSOPHY

School of Geography, Earth & Environmental Sciences (GEES)

College of Life and Environmental Sciences (LES)

University of Birmingham

July 2019

ABSTRACT

Boreal peatlands are globally important carbon stores, holding ~22% of terrestrial Carbon. The composition and structure of their vegetation controls the rates and direction of globally important mass and energy fluxes. However, the effect of system structure on functioning and disturbance response remains largely un-known. This PhD investigates how forested peatland structure and organisation influences key eco-hydrological processes at the peatland-atmosphere interface. The primary research outcomes are: (1) disturbance of forest-canopy layers changes the spatio-temporal dynamics of peatland surface temperatures which, vary substantially in space and time, (2) different system structural layers have varying controls on peat-surface temperatures, and their disturbance changes the thermal regime even when no change in mean temperature is observed, (3) meter-scale spatial variability in surface energy balance induced by the tree-canopy, substantially impacts simulated peatland evapotranspiration (ET), increasing ET by 25% and reducing unexplained variance between modelled and measured ET by 8%, (4) responses of key bryophytes to canopy removal is lagged in peatlands (unlike mineral soils), highlighting the potentially important influence of transition periods (system lags) on eco-hydrological feedbacks mechanisms to disturbance. This research provides important new understating of the eco-hydrological functioning of peatland-atmosphere interfaces. It characterises the dynamics of system variability (both intact and disturbed), evidences of how energy and mass flux estimates may be improved, and details how small scale-research could yield important information for assessing changes to system functioning.

ACKNOWLEDGEMENTS

Firstly, I thank Dr Nick Kettridge and Dr Stefan Krause for their truly valued support, advice and guidance throughout this entire process. I'm grateful for the opportunities they have provided, offering training and guidance on a range of research methods, opportunities to use new and innovative technology and the chance to work as part of exciting research groups. They have fuelled my enthusiasm for peatland eco-hydrology research and pushed the boundaries of what I thought I could achieve. Thank you.

I thank Dr Paul Moore for providing his valuable time and skills to collaborate on the modelling component of the work and Dr Laura Chasmer for the use of Lidar data and CHM. I am also grateful to the wider URSA research group for insightful discussions, feedback, and welcoming me into the Boreal research community.

Thanks also go to Samantha Leader, Cameron McCann, Greg Carron, Patrick Pow, Midori Depante, Lindsay James, Kristyn Housman, Rebekah Ingram, Silvia Folegot, Cierra Hoecherl and Dom Eardly among others for their support in the field over for two intense but incredible summers. I thank Alex Hurley and forum users for providing useful advice on R.

I also thank to Dr Peter Jones for sparking my interest in peatland eco-hydrology in the first place, providing positive encouragement to embark on PhD research, and his unwavering faith in my ability.

In addition, I thank Dr Fiona Schulz, Dr Amaia Marruedo, Dr Silvia Folegot, Dr Sophie Comer-Warner and Dr Sophie Briffa for their true and valued friendships. Together we have shared successes, struggles and a lot of laughter.

Diolch o galon i'm teulu am eu cariad a chefnogaeth trwy'r broses hir o waith ymchwil yma: Sian, John, Dwynwen, Ifanwy a Delun.

Diolchaf Sam Giles yn bennaf, am ei gariad, ei amynnedd a dealltwriaeth, am bob amser cynnig clyst i wrando, a'i ffydd ddiflino.

CANDIDATE'S CONTRIBUTION

The work presented in this thesis is the result of collaborative research, and the specific contributions of the candidate are outlined below.

CHAPTER ONE: INTRODUCTION, was completed by candidate.

CHAPTER TWO: DISTURBANCE IMPACTS ON THERMAL HOT SPOTS AND HOT MOMENTS AT THE PEATLAND-ATMOSPHERE INTERFACE

Authorship: **R. Leonard**, N. Kettridge, K.J. Devito, R. Petrone, C. Mendoza, J.M. Waddington, S. Krause.

Status: Published 27 December 2017 in *Geophysical Research Letters*

Candidate's contribution:

All data were collected and analysed by the candidate.

Manuscript preparation was completed by the candidate; N. Kettridge, S. Krause, K.J. Devito, G. Granath, R. Petrone, C. Mendoza, J.M. Waddington provided feedback to the manuscript. *Geophysical Research Letters* Editor M Bayani Cardenas and two anonymous peer-reviewers provided feedback on the manuscript and statistical analysis approach during publication process.

CHAPTER THREE: THE INFLUENCE OF SYSTEM HETEROGENEITY ON PEAT-SURFACE TEMPERATURE DYNAMICS

Authorship: **R. Leonard,** P. Moore, S. Krause, K.J. Devito, R. Petrone, C. Mendoza, J.M. Waddington, N. Kettridge.

Status: To be submitted to *Environmental Research Letters*

Candidate's contribution:

All field data were collected and analysed by the candidate. Numerical modelling support was provided by Paul Moore. All modelling outputs were analysed by the candidate.

Manuscript preparation was completed by the candidate.

CHAPTER FOUR: FOREST STAND COMPLEXITY CONTROLS ECOSYSTEM-SCALE EVAPOTRANSPIRATION DYNAMICS: IMPLICATIONS FOR LANDSCAPE FLUX SIMULATIONS

Authorship: **R. Leonard**, P. Moore, S. Krause, L. Chasmer, K.J. Devito, R. Petrone, C. Mendoza, J.M. Waddington, N. Kettridge.

Status: To be submitted

Candidate's contribution:

All field data were collected and analysed by the candidate, except Eddy Covariance and lidar data (CHM) which was provided by R. Petrone and L Chasmer. Numerical modelling support was provided by Paul Moore. Sub-model predicting ground layer vegetation cover (MARS) was prepared by the candidate. All modelling outputs were analysed by the candidate

Manuscript preparation was completed by the candidate.

CHAPTER FIVE: PEATLAND BRYOPHYTE RESPONSES TO INCREASED LIGHT FROM BLACK SPRUCE REMOVAL

Authorship: **R. Leonard**, N. Kettridge, S. Krause, K.J. Devito, G. Granath, R. Petrone, C. Mendoza, J.M. Waddington.

Status: Published 04 November 2016 in *Ecohydrology*

Candidate's contribution:

All data (except 2010 data collection) were collected and all data (including data from 2010) were analysed by the candidate.

Manuscript preparation was completed by the candidate; N. Kettridge, S. Krause, K.J. Devito, G. Granath, R. Petrone, C. Mendoza, J.M. Waddington provided feedback to the manuscript. Two anonymous peer-reviewers provided feedback on the manuscript during publication process.

CHAPTER SIX: SYNTHESIS, was completed by the candidate.

TABLE OF CONTENTS

List of Figures

List of Tables

List of Movies

CHAPTER ONE : INTRODUCTION

1.1 BOREAL FORESTED PEATLANDS

Forests in the circumpolar bio-geographic zone, called the boreal (the world's second largest biome), occupy approximately 10% of the earth's vegetated surface (McGuire *et al.*, 1995). Globally they are estimated to store ~703 GtC, which is five times more than in temperate forests (121 GtC) and twice as much carbon as tropical forests (375 GtC) (Kasischke, 2000). Most of this carbon store is found below the surface (Kasischke, 2000), in the region's peatlands, which cover 24% of the land area (Joosten & Clarke, 2002) and represent 80% of global peatland cover (Gorham, 1991; Joosten & Clarke, 2002). Conservative estimates suggest they contain ~500 GtC (Yu, 2012; Bradshaw and Warkentin, 2015), the equivalent to around 22% of total terrestrial carbon (Watson *et al.*, 2000), making them one of the world's largest terrestrial carbon stores (Yu, 2012).

Northern forested peatlands are subject to a multitude of disturbances that include naturally occurring wildfire (but increasing frequency: Chapin *et al.*, 2000), insect outbreaks (capable of destroying entire canopies: Raffa *et al.*, 2008), oil and gas exploration (~1.8 million km of 10m wide seismic lines where trees have been removed, in Alberta alone; Strack *et al.*, 2019), herbivory, ice storms, peat extraction and forestry (Turetsky & St. Louis, 2006). Climate change is likely to exacerbate these disturbances further with changes predicted to disproportionately affect systems in northern latitudes (IPCC, 2013). Understanding the resilience of northern latitude systems, especially carbon rich systems such as peatlands is a clear priority for peatland research and climate change predictions. Northern peatlands have the potential to exacerbate global warming if the net carbon flux across the peat-atmosphere interface becomes an atmospheric source of carbon by mobilising their dense carbon reserves (Freeman *et al.*, 1992; Gorham, 1991; Worrall & Evans, 2009; Worrall *et al.*, 2007). The capacity of these important systems to regulate carbon depends

largely on the dynamic eco-hydrological processes occurring across the peatland-atmosphere interface (Belyea & Malmer, 2004; Christensen *et al.*, 2004; Gorham, 1991; Holden, 2005; Laine *et al.*, 1996; Malmer & Wallén, 2004; Moore, 2002; Roulet *et al.*, 1992; Strack *et al.*, 2004; Turetsky *et al.*, 2002; Vasander & Kettunen, 2006; Waddington *et al.*, 2015). Whilst it is recognised that dissolved organic carbon (DOC) and particulate organic carbon (POC) provide important carbon transport pathways, (Roulet *et al.*, 2007; Worrall *et al.*, 2009; Worrall *et al.*, 2002; Worrall *et al.*, 2003), the peatland atmospheric interface provides the primary boundary across which energy and mass are gained or lost from the system. For example, the carbon content of peatlands, and the importance of their functions as atmospheric Carbon (C) sinks or sources is largely regulated by respiration and productivity (Clymo *et al.*, 1998, ; Peichl *et al.*, 2018; Wang *et al.*, 2018), while hydrological balance (an important regulator of carbon storage and regional water resources; Devito *et al.*, 2005a; Devito *et al.*, 2017; Holden, 2005) is largely dictated by rates of evapotranspiration (Lafleur, 2008; Price & Maloney, 1994; Wu *et al.*, 2010; Zhang *et al.*, 2009). Understanding important and dynamic processes across this boundary is essential to understanding peatland function and resilience.

These important peatland-atmosphere boundaries are highly complex, especially in treed peatlands, such as those found in the boreal region. The total structural complexity of a boreal peatland-atmosphere interface may be conceptualised as vertical (variability in structure across a vertical space) and horizontal heterogeneity (variability across each layer found in the vertical space :Filotas *et al.*, 2014, Kelliher *et al.*, 1993). The vertical layers of boreal forested peatlands comprise of: (i) an open-canopy tree cover of *Picea mariana* (Vitt *et al.*, 1994; Wieder *et al.*, 2006), (ii) a vascular sub canopy of ericaceous shrubs (e.g. *Ledum groenlandicum, Chamaedaphne calyculata,*

Kalmia polifolia, Vaccinium oxycoccos, V. vitis-idaea and *Rubus chamaemorus* (Vitt *et al.*, 1994; Wieder *et al.*, 2006), (iii) a moss groundcover (of *Sphagnum* mosses, true mosses (e.g. *Pleurozium schreberii*) (Wieder *et al.*, 2006), lichen (Dunford *et al.*, 2006) and patches of bare peat (Leonard *et al.*, 2018; Thompson *et al.*, 2014; Thompson & Waddington, 2013)) and (iv) variable micro-topography. Each of these vertical layers varies in space within each layers' horizontal plane. The system functioning (total flux of mass and balance of energy exchange) is the sum of complicated small-scale, spatio-temporal interactions across and between its horizontal and vertical layers. For example, vascular species such as trees and shrubs impact the energy available at lower system layers. These spatio-temporally variable interactions not only control the energy available to drive processes such as evaporation (Villegas *et al.*, 2014), but modify species composition and their associated controls on system processes (Koerselman & Beltman, 1988; Lafleur, 1990; De Sena *et al.*, 2007).

Fluxes across the peatland atmosphere interface may be measured at the ecosystem scale using the Eddy Covariance (EC) method. Eddy covariance is a micro-meteorological method of measuring turbulent momentum, heat and gas exchange between an ecosystem surface and the atmosphere, that has been used globally since the seventies (Baldocchi, 2003). Measurements from the EC method are beneficial due to their ability to provide net exchange estimates of mass and energy between the system and the atmosphere that are spatially averaged for a given area and a specified time-interval. Eddy covariance however, does not provide information about within system factors and processes that drive and control exchanges and provides little indication of the within system spatial and temporal variability in flux magnitude or direction (Launiainen *et al.*, 2005). Point-scale methods of measuring fluxes can provide valuable quantification of individual system component

contributions to net fluxes. Chamber based systems provide small-scale (size depends on field practicality but is usually < $1m^2$) flux measurements over a defined area and time that can be attributed to individual system components e.g. a given groundcover type (Heijmans *et al.*, 2004a). Chamber methods work best on surfaces with short vegetation where a chamber can easily be placed over the top of the desired measurement component and create a seal at the ground-surface. Within forested systems however, vascular system components such as trees may be too large to contain within a standard field chamber and alternative methods are required to estimate their fluxes, such as direct measurements of sap flow or measurements of stomatal conductance (Thompson *et al.*, 2014; Warren *et al.*, 2018). Efforts employed to measure boreal peatland-atmosphere interface fluxes incorporate both the EC and point-scale measurements (Angstmann *et al.*, 2012; Angstmann *et al.*, 2013; Bond-Lamberty *et al.*, 2011; Heijmans *et al.*, 2004a, b, Thompson *et al.*, 2014; Warren *et al.*, 2018) in attempts to understand and simulate system flux dynamics (Kettridge *et al.*, 2013; Sutherland *et al.*, 2014; Sutherland *et al.*, 2017; Wu *et al.*, 2010). However, understanding of the dynamic interaction of the system structural layers, its associated impact on fluxes, and response to disturbances remain largely unknown and unpredictable due to the small-scale variability of this interaction. Understanding how the partitioning of fluxes in vertical and horizontal space and in time across the boundary is likely important not only for better numerical representations of dominant system fluxes but for understanding system dynamics, shifts in response to disturbances, and the corresponding effect on peatland-atmosphere exchanges and peatland functioning.

1.2 RESEARCH GAPS

The structurally tall, heterogeneous and interdependent organisation of the peatland-atmosphere boundary makes researching the dynamics of important system processes such as carbon and water exchange challenging (Drexler *et al.*, 2004). However, understanding these dynamics and small-scale variability in processes that occur across peat-atmosphere interfaces is increasingly identified as a priority for peatland research (Aleina *et al.*, 2015; Frei *et al.*, 2012; Griffiths *et al.*, 2017; Holden, 2005; Kettridge & Baird, 2010; Premke *et al.*, 2016). The following are identified as priority research areas for peatland-atmosphere interface dynamics (detailed literature evaluations presented in chapter 2-5):

1. Soil-surface temperature controls a wide array of key system processes (Buchan, 2011), yet current understanding of peat-surface temperatures are limited to few discrete point measurements. More detailed understanding of the small-scale dynamics of surface temperature and how it is affected by modification to the system architecture is an important first step to understand the intricate nature of temperature-driven process dynamics (Chapter 2).
2. Identifying the contribution of individual system structural layers to the dynamic thermal regime of the peat surface is needed to understand how each system component influences the spatial distribution, frequency, and duration of thermally driven processes (Chapter 3).
3. Understanding of how small-scale stand complexity, composition and layer inter-dependencies affect evapotranspiration (ET) dynamics remains limited. Better understanding of the small-scale controls on ET across the whole system boundary is required to support more informed

and targeted future research efforts on system fluxes and improve assessments of peatland function and resilience (Chapter 4).

4. Better understanding of bryophyte responses to disturbance of higher system vertical layers is needed to provide important information for models simulating eco-hydrological transitions and feedbacks in response to disturbance. These bryophyte species act as a first order control on the small-scale atmospheric carbon and water fluxes from peatlands (chapter 5).

1.3 AIMS AND OBJECTIVES

The aim of the research presented in this thesis is to determine how small-scale heterogeneity and organisation in forest structure, controls peatland ecohydrological system processes (Chapter 2, 3 and 4) and the associated impact of structural disturbance on these system dynamics (Chapter 2 and 5). The aim of each stand-alone chapter is detailed here:

Chapter 2 aims to determine how small-scale peat-surface temperature dynamics vary in space and time, and how they change with disturbance to the system architecture (removal of trees and shrubs).

Chapter 3 aims to determine the influence of both individual layers of system heterogeneity (subsurface ice-layers, ground cover vegetation, microtopography, tree, and sub-canopy vascular cover) on surface temperature distributions, and how different combinations of these layers influence peat-surface temperature patterns.

Chapter 4 aims to determine how ET dynamics are influenced by stand structure and related organisational complexity.

Chapter 5 aims to determine the eco-hydrological, biogeochemical and compositional response of two key northern bryophytes to tree-canopy removal.

1.4 STUDY AREA

Utikuma Region Study Area

The study site is part of the wider Utikuma Region Study Area (URSA) in the Boreal Plains Ecotone, Canada. This region is approximately 150 km south of the discontinuous permafrost zone (Woo & Winter, 1993), covering Alberta, Saskatchewan, and Manitoba in western / central Canada. This landscape comprises around 50% peatland (Vitt *et al.*, 2000) with spruce, and aspen forests growing on the surrounding mineral uplands. Monthly mean air temperatures range from -16.7 °C (January) to 16.3 °C (July) (Devito *et al.*, 2005a) with mean annual air temperatures between 0.2 and -0.1 °C (Devito *et al.*, 2017). Mean annual precipitation experienced during the study years 2010 to 2015 was 426 (±85 SD) mm (mean precipitation in the region is 462 mm : Devito *et al.*, 2005a) with ~70% of this precipitation received during the growing season summer months (Devito *et al.*, 2005, Mwale *et al.*, 2010). Snow inputs usually account for ~25% of the annual mean precipitation (Devito *et al.*, 2005a). The region is characterised as sub-humid because the annual potential evapotranspiration is usually higher than or almost equal to precipitation at ~517 mm (Bothe & Abraham, 1993; Devito *et al.*, 2005a; Devito *et al.*, 2005b). This sub-humid climate is typical of most years but at 10 to 15 year intervals it is punctuated by cool summer temperatures and above average precipitation (Devito *et al.*, 2005b). URSA sits on glacial derived glaciofluvial, moraine, and glaciolacustrine sediment deposits over bedrock, that range in thickness from 20 to 240 m (Pawlowicz & Fenton, 2002).

The study site: BC35

Research presented in this thesis is focused on an exemplar poor fen, (55.81°N, 115.11°W) within the URSA, ~370 km north of Edmonton in central Alberta. The site is commonly referred to as BC35 after it was last burned around 1935. The site is characteristic of treed peatlands in this region with an open-canopy tree cover of *Picea mariana* (Vitt *et al.*, 1994; Wieder *et al.*, 2006), a vascular sub canopy of ericaceous shrubs (e.g. *Ledum groenlandicum, Chamaedaphne calyculata, Kalmia polifolia, Vaccinium oxycoccos, V. vitis-idaea* and *Rubus chamaemorus* (Vitt *et al.*, 1994, Wieder *et al.*, 2006) and a moss groundcover of *Sphagnum* mosses, true mosses (e.g. *Pleurozium schreberii*) (Wieder *et al.*, 2006), lichen (Dunford *et al.*, 2006) and bare peat (Thompson *et al.*, 2014; Thompson & Waddington, 2013). Data was collected over field seasons of 2010, 2014 and 2015 and each chapter (2-5) describes data collection methods and dates in more detail.

1.5 THESIS LAYOUT

This thesis follows a research paper style format, where chapters 2 to 5 address the research questions outlined in *Aims and Objectives.* Each chapter is self-contained and may be considered in isolation of other chapters. Each chapter reviews relevant literature, identifies research gaps, describes methods and data analysis, discusses and interprets results and draws conclusions. Chapters 2 to 4 are followed by supporting information (SI) that support relevant sections of the main text. Chapter 6 then provides a synthesis of the thesis, drawing together and contextualising the new knowledge gained in chapter 2 to 5 and outlines further research needs.

1.6 REFERENCES

Aleina, F. C., Runkle, B. R. K., Kleinen, T., Kutzbach, L., Schneider, J. & Brovkin, V. (2015)

Modeling micro-topographic controls on boreal peatland hydrology and methane fluxes. *Biogeosciences* **12**(19), 5689–5704. doi:10.5194/bg-12-5689-2015

Angstmann, J L, Ewers, B. E. & Kwon, H. (2012) Size-mediated tree transpiration along soil drainage gradients in a boreal black spruce forest wildfire chronosequence. *Tree Physiol.* **32**(5), 599–611. doi:10.1093/treephys/tps021

Angstmann, Julia L., Ewers, B. E., Barber, J. & Kwon, H. (2013) Testing transpiration controls by quantifying spatial variability along a boreal black spruce forest drainage gradient. *Ecohydrology* **6**(5), 783–793. doi:10.1002/eco.1300

Baldocchi, D. (2003) Assessing the eddy covariance technique for evaluating carbon dioxide exchange rates of ecosystems: past, present and future. *Glob. Chang. Biol.* **9**(October 2002), 479–492. doi:10.1046/j.1365-2486.2003.00629.x

Belyea, L. R. & Malmer, N. (2004) Carbon sequestration in peatland: patterns and mechanisms of response to climate change. *Glob. Chang. Biol.* **10**(7), 1043–1052. John Wiley & Sons, Ltd (10.1111). doi:10.1111/j.1529-8817.2003.00783.x

Bond-Lamberty, B., Gower, S. T., Amiro, B. & Ewers, B. E. (2011) Measurement and modelling of bryophyte evaporation in a boreal forest chronosequence. *Ecohydrology* **4**, 26–35. doi:10.1002/eco.118

Bothe, R. A. & Abraham, C. (1993) *Evaporation and Evapotranspiration in Alberta 1986 to 1992 Addendum*. Surface Water Assessment Branch, Technical Services & Monitoring Division, Water Resources Services, Alberta Environmental Protection.

Bradshaw, C. J. A. & Warkentin, I. G. (2015) Global estimates of boreal forest carbon stocks and flux. *Glob. Planet. Change* **128**, 24–30. Elsevier B.V. doi:10.1016/j.gloplacha.2015.02.004

Buchan, G. D. (2011) *Encyclopedia of Agrophysics*. Springer. doi:10.1007/978-90-481-3585-1

Chapin, F. S., Mcguire, A. D., Randerson, J., Pielke, R., Baldocchi, D., Hobbie, S. E., Roulet, N., Eugster, W., Kasischke, E., Rastetter, E. B., Zimov, S. A., Running, S. W. (2000) Arctic and boreal ecosystems of western North America as components of the climate system. *Glob.*

Chang. Biol. **6**(SUPPLEMENT 1), 211–223. doi:10.1046/j.1365-2486.2000.06022.x

Christensen, T. R., Johansson, T., Åkerman, H. J., Mastepanov, M., Malmer, N., Friborg, T., Crill, P., *et al*. (2004) Thawing sub-arctic permafrost: Effects on vegetation and methane emissions. *Geophys. Res. Lett.* **31**(4). John Wiley & Sons, Ltd. doi:10.1029/2003GL018680

Clymo, R. S., Turunen, J. & Tolonen, K. (1998) Carbon Accumulation in Peatland. *Oikos* **81**(2), 368. doi:10.2307/3547057

Devito, K., Creed, I., Gan, T., Mendoza, C., Petrone, R., Silins, U. & Smerdon, B. (2005a) A framework for broad-scale classification of hydrologic response units on the Boreal Plain: Is topography the last thing to consider? *Hydrol. Process.* **19**(8), 1705–1714. doi:10.1002/hyp.5881

Devito, K. J., Creed, I. F. & Fraser, C. J. D. (2005b) Controls on runoff from a partially harvested aspen-forested headwater catchment, Boreal Plain, Canada. *Hydrol. Process.* **19**(1), 3–25. doi:10.1002/hyp.5776

Devito, Kevin J., Hokanson, K. J., Moore, P. A., Kettridge, N., Anderson, A. E., Chasmer, L., Hopkinson, C., *et al*. (2017) Landscape controls on long-term runoff in subhumid heterogeneous Boreal Plains catchments. *Hydrol. Process.* **31**(15), 2737–2751. doi:10.1002/hyp.11213

Drexler, J. Z., Snyder, R. L., Spano, D. & Paw U, K. T. (2004) A review of models and micrometeorological methods used to estimate wetland evapotranspiration. *Hydrol. Process.* **18**(11), 2071–2101. doi:10.1002/hyp.1462

Dunford, J. S., Sciences, B., Biological, C. W. & Centre, S. (2006) Lichen abundance in the peatlands of northern Alberta: Implications for boreal caribou. *Ecoscience* **13**(4), 469–474. doi:10.2980/1195-6860(2006)13[469:LAITPO]2.0.CO;2

Filotas, E., Parrott, L., Burton, P. J., Chazdon, R. L., Coates, K. D., Coll, L., Haeussler, S., *et al*. (2014) Viewing forests through the lens of complex systems science. *Ecosphere* **5**(1), art1. doi:10.1890/ES13-00182.1

Freeman, C., Lock, M. A. & Reynolds, B. (1992) Fluxes of CO2, CH4 and N2O from a Welsh peatland following simulation of water table draw-down: Potential feedback to climatic change. *Biogeochemistry* **19**(1), 51–60. doi:10.1007/BF00000574

Frei, S., Knorr, K. H., Peiffer, S. & Fleckenstein, J. H. (2012) Surface micro-topography causes hot spots of biogeochemical activity in wetland systems: A virtual modeling experiment. *J. Geophys. Res. Biogeosciences* **117**(4), 1–18. doi:10.1029/2012JG002012

Gorham, E. (1991) Northern peatlands : role in the carbon cycle and probable responses to climatic warming. *Ecol. Appl.* **1**(2), 182–195.

Griffiths, N. A., Hanson, P. J., Ricciuto, D. M., Iversen, C. M., Jensen, A. M., Malhotra, A., McFarlane, K. J., Norby, R J., Sargsyan, K, Sebestyen, S. D., Shi, X, Walker, A. P., Ward, E. J., Warren, J. M., Weston, David J.*et al*. (2017) Temporal and Spatial Variation in Peatland Carbon Cycling and Implications for Interpreting Responses of an Ecosystem-Scale Warming Experiment. *Soil Sci. Soc. Am. J.* **0**(0), 0. doi:10.2136/sssaj2016.12.0422

Heijmans, M. M. P. D., Arp, W. J. & Chapin, F. S. (2004) Carbon dioxide and water vapour exchange from understory species in boreal forest. *Agric. For. Meteorol.* **123**, 135–147. doi:10.1016/j.agrformet.2003.12.006

Heijmans, M. M. P. D., Arp, W. J. & Chapin, F. S. (2004) Controls on moss evaporation in a boreal black spruce forest. *Global Biogeochem. Cycles* **18**(2), n/a-n/a. doi:10.1029/2003GB002128

Holden, J. (2005) Peatland hydrology and carbon release: why small-scale process matters. *Philos. Trans. R. Soc. A Math. Phys. Eng. Sci.* **363**(1837), 2891–913. doi:10.1098/rsta.2005.1671

IPCC. (2013) *Climate Change 2013: The Physical Science Basis. Contribution of Working Group I to the Fifth Assessment Report of the Intergovernmental Panel on Climate Change*. (T. F. Stocker, D. Qin, G.-K. Plattner, M. Tignor, S. K. Allen, J. Boschung, A. Nauels, *et al*., Eds.). Cambridge, United Kingdom and New York, NY, USA: Cambridge University Press.

Joosten, H. & Clarke, D. (2002) *Wise Use of Mires and Peatlands - and Including Framework for Decision - Making*. *Transformation*.

Kasischke, E. S. (2000) Boreal Ecosystems in the Global Carbon Cycle. (E. S. Kasischke & B. J. Stocks, eds.), 19–30. New York, NY: Springer New York. doi:10.1007/978-0-387-21629-4_2

Kelliher, F. M., Leuning, R. & Schulze, E. D. (1993) Evaporation and canopy characteristics of coniferous forests and grasslands. *Oecologia* **95**(2), 153–163. doi:10.1007/BF00323485

Kettridge, N., Thompson, D. K., Bombonato, L., Turetsky, M. R., Benscoter, B. W. & Waddington, J. M. (2013) The ecohydrology of forested peatlands: Simulating the effects of tree shading on moss evaporation and species composition. *J. Geophys. Res. Biogeosciences* **118**(2), 422–435. doi:10.1002/jgrg.20043

Kettridge, Nicholas & Baird, A. J. (2010) Simulating the thermal behavior of northern peatlands with a 3-D microtopography. *J. Geophys. Res.* **115**(G3), G03009. doi:10.1029/2009JG001068

Koerselman, W. & Beltman, B. (1988) Evapotranspiration from fens in relation to Penman's potential free water evaporation (E O) and pan evaporation. *Aquat. Bot.* **31**(3–4), 307–320. doi:10.1016/0304-3770(88)90019-8

Lafleur, P. (1990) Evaporation From Wetlands. *Can. Geogr. / Le Géographe Can.* **34**(1), 79–82. doi:10.1111/j.1541-0064.1990.tb01072.x

Lafleur, P. M. (2008) Connecting Atmosphere and Wetland: Energy and Water Vapour Exchange. *Geogr. CompasS3*(4), 1027–1057. doi:10.1111/j.1749-8198.2007.00132.x

Laine, J., Silvola, J., Tolonen, K., Alm, J., Nykänen, H., Vasander, H., Sallantaus, T., Savolainen, I, Sinisalo, J, Martikainen, P.J. (1996) Effect of Water-Level Drawdown on Global Climatic Warming: Northern Peatlands. *Ambio* **25**(3), 179–184. [Springer, Royal Swedish Academy of Sciences].

Launiainen, S., Rinne, J., Pumpanen, J., Kulmala, L., Kolari, P., Keronen, P., Siivola, E., Pohja, T, Hari, P, Vesala, T. (2005) Eddy covariance measurements of CO2 and sensible and latent heat fluxes during a full year in a boreal pine forest trunk-space Eddy covariance measurements of CO 2 and sensible and latent heat fluxes during a full year in a boreal pine forest.

Leonard, R. M., Kettridge, N., Devito, K. J., Petrone, R. M., Mendoza, C. A., Waddington, J. M.

& Krause, S. (2018) Disturbance Impacts on Thermal Hot Spots and Hot Moments at the Peatland-Atmosphere Interface. *Geophys. Res. Lett.* 1–9. doi:10.1002/2017GL075974

Malmer, N. & Wallén, B. (2004) Input rates, decay losses and accumulation rates of carbon in bogs during the last millennium: internal processes and environmental changes. *The Holocene* **14**(1), 111–117. SAGE Publications Ltd. doi:10.1191/0959683604hl693rp

McGuire, D. A., Melillo, J. M., Kicklighter, D. W. & Joyce, L. A. (1995) Equilibrium Responses of Soil Carbon to Climate Change: Empirical and Process-Based Estimates. *J. Biogeogr.* **22**(4/5), 785–796. Wiley.

Moore, P. D. (2002) The future of cool temperate bogs. *Environ. Conserv.* **29**(1), 3–20. Cambridge University Press. doi:DOI: 10.1017/S0376892902000024

Mwale, D., Gan, T. Y., Devito, K. J., Silins, U., Mendoza, C. & Petrone, R. (2010) Regionalization of Runoff Variability of Alberta, Canada, by Wavelet, Independent Component, Empirical Orthogonal Function, and Geographical Information System Analyses. *J. Hydrol. Eng.* **16**(2), 93–107. doi:10.1061/(asce)he.1943-5584.0000284

Pawlowicz, J. G. & Fenton, M. M. (2002) Drift thickness of the Peerless Lake map area (NTS 84B), Map 253. Edmonton, Alberta, Canada: Alberta Geologic Survey,.

Peichl, M., Gažovič, M., Vermeij, I., Goede, E. De, Sonnentag, O., Limpens, J. & Nilsson, M. B. (2018) Peatland vegetation composition and phenology drive the seasonal trajectory of maximum gross primary production. *Sci. Rep.* **8**(1), 1–11. doi:10.1038/s41598-018-26147-4

Premke, K., Attermeyer, K., Augustin, J., Cabezas, A., Casper, P., Deumlich, D., Gelbrecht, J., Gerke, H.H., Gessler, A., Grossart, H-P., Hilt, S., Hupfer, M., Kalettka, T., Kayler, Z., Lischeid, G., Sommer, M., Zak, D., (2016) The importance of landscape diversity for carbon fluxes at the landscape level: small-scale heterogeneity matters. *Wiley Interdiscip. Rev. Water* **3**(4), 601–617. doi:10.1002/wat2.1147

Price, J. & Maloney, D. (1994) Hydrology of a patterned bog-fen complex in southeastern Labrador, Canada. *Nord. Hydrol.* **25**(5), 313–330. doi:10.2166/nh.1994.020

Raffa, K. F., Aukema, B. H., Bentz, B. J., Carroll, A. L. & Hicke, J. A. (2008) Cross-scale Drivers of Natural Disturbances Prone to Anthropogenic Amplification : The Dynamics of Bark Beetle Eruptions. *Bioscience* **58**(6), 501–517.

Roulet, N., Moore, T., Bubier, J. & Lafleur, P. (1992) Northern fens: methane flux and climatic change. *Tellus B* **44**(2), 100–105. John Wiley & Sons, Ltd (10.1111). doi:10.1034/j.1600-0889.1992.t01-1-00002.x

Roulet, N. T., Lafleur, P. M., Richard, P. J. H., Moore, T. R., Humphreys, E. R. & Bubier, J. (2007) Contemporary carbon balance and late Holocene carbon accumulation in a northern peatland. *Glob. Chang. Biol.* **13**(2), 397–411. doi:10.1111/j.1365-2486.2006.01292.x

Sena, J. O. A. De, Zaidan, H. A. & Camargo e Castro, P. R. De. (2007) Transpiration and stomatal resistance variations of perennial tropical crops under soil water availability conditions and water deficit. *Brazilian Arch. Biol. Technol.* **50**(2), 225–230.

Strack, M, Waddington, J. M. & Tuittila, E.-S. (2004) Effect of water table drawdown on northern peatland methane dynamics: Implications for climate change. *Global Biogeochem. Cycles* **18**(4). John Wiley & Sons, Ltd. doi:10.1029/2003GB002209

Strack, Maria, Hayne, S., Lovitt, J., McDermid, G. J., Rahman, M. M., Saraswati, S. & Xu, B. (2019) Petroleum exploration increases methane emissions from northern peatlands. *Nat. Commun.* **10**(1), 2804. doi:10.1038/s41467-019-10762-4

Sutherland, G., Chasmer, L. E., Petrone, R. M., Kljun, N. & Devito, K. J. (2014) Evaluating the use of spatially varying versus bulk average 3D vegetation structural inputs to modelled evapotranspiration within heterogeneous land cover types. *Ecohydrology* **7**(6), 1545–1559. doi:10.1002/eco.1477

Sutherland, George, Chasmer, L. E., Kljun, N., Devito, K. J. & Petrone, R. M. (2017) Using High Resolution LiDAR Data and a Flux Footprint Parameterization to Scale Evapotranspiration Estimates to Lower Pixel Resolutions. *Can. J. Remote Sens.* **43**(2), 215–229. doi:10.1080/07038992.2017.1291338

Thompson, D. K., Benscoter, B. W. & Waddington, J. M. (2014) Water balance of a burned and unburned forested boreal peatland. *Hydrol. Process.* **28**(24), 5954–5964. doi:10.1002/hyp.10074

Thompson, D. K. & Waddington, J. M. (2013) Wildfire effects on vadose zone hydrology in forested boreal peatland microforms. *J. Hydrol.* **486**, 48–56. doi:10.1016/j.jhydrol.2013.01.014

Turetsky, M. R. & Louis, V. L. St. (2006) Disturbance in Boreal Peatlands. *Boreal Peatl. Ecosyst.* **188**(Iucn 2000), 359–379. doi:10.1007/978-3-540-31913-9_16

Turetsky, M., Wieder, K., Halsey, L. & Vitt, D. (2002) Current disturbance and the diminishing peatland carbon sink. *Geophys. Res. Lett.* **29**(11), 7–10. doi:10.1029/2001GL014000

Vasander, H. & Kettunen, A. (2006) Carbon in Boreal Peatlands. *Boreal Peatl. Ecosyst.* **188**(Lappalainen 1996), 165–194. doi:10.1007/978-3-540-31913-9_9

Villegas, J. C., Espeleta, J. E., Morrison, C. T., Breshears, D. D. & Huxman, T. E. (2014) Factoring in canopy cover heterogeneity on evapotranspiration partitioning: Beyond big-leaf surface homogeneity assumptions. *J. Soil Water Conserv.* **69**(3), 78A-83A. doi:10.2489/jswc.69.3.78a

Vitt, D. H., Halsey, L. A., Bauer, I. E. & Campbell, C. (2000) Spatial and temporal trends in carbon storage of peatlands of continental western Canada through the Holocene. *Can. J. Earth Sci.* **37**(5), 638–693.

Vitt, D. H., Halsey, L. A. & Zoltai, S. C. (1994) The Bog Landforms of Continental Western Canada in Relation to Climate and Permafrost Patterns. *Arct. Alp. Res.* **26**(1), 1. doi:10.2307/1551870

Waddington, J. M., Morris, P. J., Kettridge, N., Granath, G., Thompson, D. & Moore, P. (2015) Hydrological feedbacks in northern peatlands. *Ecohydrology* (8), 113–127. doi:10.1002/eco.1493

Wang, S., Zhuang, Q., Lähteenoja, O., Draper, F. C. & Cadillo-Quiroz, H. (2018) Potential shift

from a carbon sink to a source in Amazonian peatlands under a changing climate. *Proc. Natl. Acad. Sci.* **115**(49), 12407–12412. doi:10.1073/pnas.1801317115

Warren, R. K., Pappas, C., Helbig, M., Chasmer, L. E., Berg, A. A., Baltzer, J. L., Quinton, W. L., *et al*. (2018) Minor contribution of overstorey transpiration to landscape evapotranspiration in boreal permafrost peatlands. *Ecohydrology* **11**(5), 1–10. doi:10.1002/eco.1975

Watson, R. T., Noble, I., Bolin, B., Ravindranath, N. H., Verardo, D. J. & Dokken, D. J. (2000) Land Use, Land-Use Change and Forestry. A Special Report of the International Panel on Climate Change. Montreal, Canada. WMO & UNEP, Geneva.

Wieder, R. K., Vitt, D. H. & Benscoter, B. W. (2006) Peatlands and the Boreal Forest. In: *Boreal Peatland Ecosystems* (R. K. Wieder & D. H. Vitt, eds.), 1–8. Berlin, Heidelberg: Springer Berlin Heidelberg. doi:10.1007/978-3-540-31913-9_1

Woo, M. K. & Winter, T. C. (1993) The role of permafrost and seasonal frost in the hydrology of northern wetlands in North America. *J. Hydrol.* **141**(1–4), 5–31. doi:10.1016/0022-1694(93)90043-9

Worrall, F., Burt, T. P., Rowson, J. G., Warburton, J. & Adamson, J. K. (2009) The multi-annual carbon budget of a peat-covered catchment. *Sci. Total Environ.* **407**(13), 4084–4094. Elsevier B.V. doi:10.1016/j.scitotenv.2009.03.008

Worrall, F, Burt, T. P., Jaeban, R. Y., Warburton, J. & Shedden, R. (2002) Release of dissolved organic carbon from upland peat. *Hydrol. Process.* **16**(17), 3487–3504. John Wiley & Sons, Ltd. doi:10.1002/hyp.1111

Worrall, F & Evans, M. (2009) The carbon budget of upland peat soils. In: *Drivers of Environmental Change in Uplands* (S. J. Bonn A, Allott T, Hubacek K, ed.), 93–112. Abingdon, UK.: Routledge.

Worrall, Fred, Burt, T., Adamson, J., Reed, M., Warburton, J., Armstrong, A. & Evans, M. (2007) Predicting the future carbon budget of an upland peat catchment. *Clim. Change* **85**(1–2), 139–158. doi:10.1007/s10584-007-9300-1

Worrall, Fred, Reed, M., Warburton, J. & Burt, T. (2003) Carbon budget for a British upland peat catchment. *Sci. Total Environ.* **312**(1–3), 133–146. doi:10.1016/S0048-9697(03)00226-2

Wu, J., Kutzbach, L., Jager, D., Wille, C. & Wilmking, M. (2010) Evapotranspiration dynamics in a boreal peatland and its impact on the water and energy balance. *J. Geophys. Res. Biogeosciences* **115**(4), 1–18. doi:10.1029/2009JG001075

Yu, Z. C. (2012) Northern peatland carbon stocks and dynamics: A review. *Biogeosciences* **9**(10), 4071–4085. doi:10.5194/bg-9-4071-2012

Zhang, K., Kimball, J. S., Mu, Q., Jones, L. A., Goetz, S. J. & Running, S. W. (2009) Satellite based analysis of northern ET trends and associated changes in the regional water balance from 1983 to 2005. *J. Hydrol.* **379**(1–2), 92–110. Elsevier B.V. doi:10.1016/j.jhydrol.2009.09.047

CHAPTER TWO : DISTURBANCE IMPACTS ON THERMAL HOTSPOTS AND HOT MOMENTS AT THE PEATLAND-ATMOSPHERE INTERFACE

2.1 ABSTRACT

Soil-surface temperature acts as a master variable driving non-linear terrestrial ecohydrological, biogeochemical and micrometeorological processes, inducing short-lived or spatially isolated extremes across heterogeneous landscape surfaces. However, sub-canopy soil-surface temperatures have been, to date, characterised through isolated, spatially discrete measurements. Using spatially complex forested northern peatlands as an exemplar ecosystem, we explore the high resolution spatiotemporal thermal behaviour of this critical interface and its response to disturbances by using Fibre-Optic Distributed Temperature Sensing. Soil-surface thermal patterning was identified from 1.9 million temperature measurements under undisturbed, trees removed and vascular sub-canopy removed conditions. Removing layers of the structurally diverse vegetation canopy not only increased mean temperatures but it shifted the spatial and temporal distribution, range and longevity of thermal hotspots and hot-moments. We argue that linking hotspots and/or hot moments with spatially variable ecosystem processes and feedbacks is key for predicting ecosystem function and resilience.

2.2 INTRODUCTION

Soil-surface temperature acts as a "biocontroller" (Buchan, 2011) of terrestrial ecohydrological, biogeochemical (Jiménez *et al*., 2007) and micrometeorological (Johnson-Maynard *et al.,* 2001) processes, regulating carbon storage and release (Kirschbaum, 1995; Taggart *et al*., 2011), water use efficiency (Stout, 1992), metabolic processes (Dijkstra *et al*., 2011), and species competition (Brand, 1990). Temperatures at the pedosphere-atmosphere interface control ecosystem functioning, determining the rate and direction of energy and mass exchange with the atmosphere (e.g. Carbon and water fluxes), and act as the driving force of subsurface thermal dynamics (Kettridge *et al*., 2013; Wullschleger *et al*., 1991) and associated biogeochemical processes. Despite this, there remains a critical gap in our understanding of how thermally driven processes vary both spatially and temporally across complex, heterogeneous or self-organised landscapes. This constrains our ability to accurately characterize the system function, resilience and service provisions of complex ecosystems, and project their response to disturbance.

Accurate, spatially explicit characterisation of spatiotemporal thermal dynamics at the soil-atmosphere interface will likely yield important new process understanding (Hrachowitz *et al*., 2013; Krause *et al*., 2015). Moreover, it will also allow the determination of how a landscape disturbance, such as canopy removal, produces non-uniform amplification or dampening of local-scale thermal variability, and redistribution of thermal patterning in both space and time. The detection of thermal hot-spots and hot moments (i.e. Hotspots that do not fully persist though time) will provide insight into the location, frequency and duration of areas where shifts in ecohydrological, biogeochemical (Jiménez *et al*., 2007), and micrometeorological (Johnson-Maynard *et al*., 2001) processes occur. These hotspots/moments may not only stress a system, but

may result in tipping points in ecosystem processes. That is, moments when critical thresholds are reached or surpassed irregularly across spatially diverse thermal landscapes may influence ecosystem resilience to perturbations. Examples of such critical thresholds and nonlinearity are numerous, from crops, where yield declines for corn, soybeans, and cotton past a defined threshold are greater than the yield increase approaching that temperature (Schlenker and Roberts, 2009), to changes in biogeochemical cycles as a result of shifts in soil bacterial populations (Biederbeck and Campbell, 1973; Zogg *et al*., 1997) (for example, soil NO_3^--N concentration, gross mineralization, and nitrification rates rapidly increase when soil temperatures increase from 2, 5 or 10 °C to 15 °C (Cookson *et al*., 2002)).

Applying high spatiotemporal resolution soil-temperature surveys to understand the temperature complexities at the interface have been limited by technological constraints until recently. Soil-temperature measurements within vegetated ecosystems have been restricted to small sample numbers (Morecroft *et al*., 1998) as a result of cost and logistical constraints (Krause *et al*., 2011; Webb *et al*., 2008) such as data storage (Kang *et al*., 2000), power, and time limitations. However, technological advances in the form of Fibre-Optic Distributed Temperature Sensing (FO-DTS) now enables extensive, high frequency and resolution, thermal measurements at the decimetre scale (Tyler *et al*., 2009), allowing exploration of interface thermal processes within vegetated ecosystems at unprecedented spatiotemporal scales and resolutions. This offers the opportunity to advance our understanding of dynamic interface processes, that are vital for understanding how ecosystems function as a whole, and how those functions change in response to disturbance stresses (Krause *et al*., 2015; Scheffer *et al*., 2001).

This study pioneers the application of high-resolution FO-DTS monitoring for characterising thermal patterns at the pedosphere-atmosphere interface of one of the most important and complex ecosystem interface types: carbon-rich northern peatlands (Belyea and Clymo, 2001; Belyea and Baird, 2006). The high-resolution data acquisition that may be acquired by the FO-DTS allows identification of thermal hotspots and hot moments and, for the first time, allows assessment of their response to vegetation removal at an appropriate scale and resolution. Peatland soil-temperatures provide a strong control on the pedosphere-atmosphere interface and ecosystem functions, regulating the cycling of carbon (Dunfield *et al*., 1993) and hydrological fluxes (Blok *et al*., 2011; Kettridge and Waddington, 2014). These peatland systems have distinctively complex surfaces, characterised by a mosaic of hummock and hollow features (spatial scale of ~ 10^1–10^2 m^2 ; Belyea and Clymo, 2001). This visible structural heterogeneity reflects the spatial heterogeneity observed in surface processes. For example, methane fluxes, for which temperature is a key driver, are more variable across a few metres than between peatland systems or regions (Moore *et al*., 1998) and respiration may vary significantly between micro-sites (Juszczak *et al*., 2013). Despite being long-term carbon stores, holding 25% of the world's soil carbon (Turunen *et al*., 2002), peatland ecosystems are greatly affected by multiple disturbances (Harden *et al*., 2000), which likely exert a strong influence on surface temperature and associated processes. For example, tree-canopy removal for linear seismic lines (Timoney and Lee, 2001), for thinning, and from insect infestations (Raffa *et al*., 2008), will influence surface temperatures because forest canopies induce variability in the transmission of incoming solar radiation to the ground due to variations in structure, height and density across spatial scales (Hardy *et al*., 2004). The spatial patterns in thermal shielding by vegetation also interact with other controls on ground temperatures, such as

climate and small-scale distributions in geomorphological, hydrological, thermal and aerodynamic properties (Al-Kayssi, 2002; Folwell *et al*., 2015; Peters-Lidard *et al*., 1998).

By utilising FO-DTS technology to measure soil-surface temperatures at high spatiotemporal resolution in a highly patterned, forested peatland, we determine, (i) the spatiotemporal variability in peat-surface temperatures and the magnitude and persistence of associated thermal hot spots; and (ii) the thermal response to tree-canopy removal and lower vascular vegetation removal how such changes are spatially and temporally distributed; and whether the distribution, intensity and duration of thermal hotspots and hot-moments changes in response to disturbance.

2.3 MATERIALS AND METHODS

2.3.1 Study Site

The study was conducted in a poor fen peatland in central Alberta, Canada (55.8°N, 115.1°W). The site was last burned in ~1935 and has a tree cover of *black spruce (Picea mariana)* with a basal area of 11 m^2 ha^{-1} and mean height of 2.3 m (Kettridge *et al*., 2012), characteristic of boreal peatland ecosystems (Wieder *et al*., 2009). The site is characterised by a surface micro topography of *Sphagnum fuscum* hummocks and *S. Angustifolium* hollows. In addition, there are considerable areas, primarily under areas of dense black spruce tree cover, where the surface is composed of feather mosses (e.g. *Pleurozium schreberi*) and bare peat surfaces. Sub-canopy vascular vegetation consists of *Rhododendron groenlandicum*, *Rubus chamaemorus*, *Chamaedaphne calyculata, Maianthemum trifolia*, and *Vaccinium spp.*

2.3.1 FO-DTS Monitoring and field manipulations

Temperatures at the pedosphere-atmosphere interface were measured using a Silixa Ltd. XT Fibre-Optic Distributed Temperature Sensing (FO-DTS) system. FO-DTS determines the temperature along a fibre-optic cable by analysing the Raman backscatter (inelastic collisions, and the thermal excitation of electrons) of a laser pulse propagating through a glass fibre. Raman backscatter causes a shift in the return energy level below (Stokes band) or above (anti-Stokes band) the Rayleigh scatter band (the return of backscatter at the original laser pulse frequency). The resultant Stokes/anti-Stokes output ratio is used to determine temperature. For a detailed overview of the FO-DTS, measurement approach, its capabilities, limitations and methodological challenges, the reader is directed to a number of recent reviews including (Selker *et al*., 2006; Tyler *et al*., 2009; Krause *et al*., 2012; Krause and Blume, 2013).

A gel-coated fibre-optic (FO) cable was installed at 0.02 m depth below the surface at the study site in May 2015. This depth of 0.02 m allowed measurements of peat/moss temperature in close proximity of the peat surface whilst avoiding solar radiation directly heating the cable. The cable was installed carefully at a depth of 0.02 m by cutting the peat/moss with scissors and enabling the moss to expand back around the cable. Whilst the impact of this installation approach is considered minimal (see photos of cable installation in supporting information Figures SI2-4 to SI2-6), limited disturbance to the peat structure should be borne in mind. The maximum likely range in temperature as a result of variations in burial depth of ±0.015 m is predicted to be between ±3.2 and 5.9 °C (Table SI2-1). A full uncertainty analysis on the impact of a 0.015 m deviation in burial depth is presented in section SI2-1 of the supporting information (Kettridge and Baird, 2008, 2007).

The experimental setup comprised a sequence of eleven 10 m long rows spaced 1 m apart (Figure SI2-3). Two additional control rows were deployed to extend the measurement array 10 m to the north and 10 m to the west of the primary measurement plot. Due to the undulating surface (up to 0.41 m topographic variation), the actual cable length varied from the 10 m plan-view length, resulting in a total of 121 m of cable being buried in the main plot and 22.8 m in the control rows. FO-DTS surveys were conducted in alternate single-ended monitoring mode, with calibration carried out using temperature matching to thermally controlled water baths at both ends of the monitoring cable (Tyler *et al.*, 2009; Krause and Blume, 2013). Within these control baths, sections of FO cable (> 20 times the sampling interval) were maintained at a constant temperature throughout the experiment. FO-DTS temperatures were calibrated to thermistor measurements of the bath temperature to account for potential drift caused by differential loss along the cable length.

Measurements were obtained at a 0.25 m interval along the length of the FO cable, averaged over 1 minute intervals. Surveys were run for four days under pre-manipulation conditions on the 21st, 22nd, 24th and 26th May 2015. All trees in the plot and within a 10 m buffer around the plot were cut and removed on 27th May 2015 and FO-DTS monitoring was repeated on 30th May 2015 (felled: trees removed). Trees were not disturbed around the two extended sections of cable to the north and west, thus providing a reference (control) for temperatures measured within the primary plot. All remaining vascular vegetation was removed from the primary plot on 31st May 2015 and FO-DTS measurements of surface temperatures taken subsequently on 3rd June 2015 (cleared: tree and vascular vegetation removed). For all treatments, FO-DTS monitoring was carried out between 06:30 and 20:30 local standard time. Weather conditions during the experiment periods were characterised by hot, dry, largely cloud-free conditions, with maximum air temperatures ranging

from 25 to 28°c, (Table SI2-2). No rain fell during the experimental period, except on the 31st May and 1st of June, between the felled and cleared treatment periods, a small rain event of 13 mm was recorded. Rain-free periods and high surface temperatures subsequently resumed prior to the cleared temperature measurements.

Due to undulations in the peat surface and shallow tree roots, small sections of the buried FO cable became exposed by the end of the overall experiment period. Exposed sections were re-buried and temperature differences pre and post-burial used to assess the length of affected measurements beyond the physically exposed section. A mean affected cable length of 0.58 m (±0.22m standard deviation) either side of the exposure was established for exposures greater than 0.15m in length, (i.e. 1.16 m of buried cable was affected in addition to the physically exposed length). Exposures less than 0.15 m in length did not influence measured temperatures. Data from exposed sections and the 0.58 m either side were removed from every exposed section greater than 0.15 m during the post-processing. At a sampling interval of 0.25m, this resulted in 305 sampling points within the primary plot, 1,024,800 temperature measurements under pre-manipulation conditions and 256,200 temperature measurements under each of the felled and cleared treatments. Control rows with 79 sampling points produced a total of 66,360 temperature measurements over the whole measurement period.

2.3.2 Data Analysis

A Wilcoxon rank sum test (significance threshold of 0.05) was used to determine any significant differences in mean temperatures between the primary plot and control rows for each measurement day under each treatment (pre-manipulation, felled and cleared). Hotspots were identified by

subtracting the daily mean temperature of the control rows from the daily mean temperature at each spatial location within the plot (ΔT ºC).

Empirical Orthogonal Functions (EOFs) were used to decompose space-time patterns in the soil temperature data (i.e. a space-time principal component analysis). EOFs illustrate patterns in the space-time data that explain most of the observed variability, with each EOF representing a mode of variation. The approach has been successfully applied previously to decompose patterns of soil moisture (Perry and Niemann, 2007) and has been used in atmospheric science for many decades (Hannachi *et al*., 2007; Lorenz, 1956). The time series principal components (also called expansion coefficients) indicate the importance of a particular EOF in time.

Due to the time and effort required for FO-DTS cable installation, only one plot, and two 10 m control sections were instrumented with FO-DTS cable. We are aware of the pseudo-replication (Hurlbert, 1984) this causes. We therefore undertake extensive additional data analysis (included in the supporting information) and note that the results of significance tests agree with existing literature.

2.4 RESULTS

2.4.1 Effects of vascular vegetation removal on surface temperatures

Wilcoxon rank sum tests showed that vascular vegetation removal significantly increased mean temperatures. Pre-manipulation, temperatures did not differ significantly between the primary plot (n=305) and control rows (n=79: May 21st: p =0.61, 22$^{nd:}$ p =0.94, 24$^{th:}$ p =0.39, 26$^{th:}$ p =0.56) (Figure 2-1a). Significant differences were found between the primary plot and control rows once felled (p <0.001) and when cleared (p <0.001). Peat-surface temperatures show substantial

variability in both space and time (Figure 2-1b). Sixty-minute mean temperatures range from 0 to 25 ºC, with the temperature range across the 10 m x 10 m plot regularly exceeding 25 ºC during the day. See also supporting information (Section SI2-2, Figures SI2-9, SI2-10 and SI2-11 for spatially interpolated hourly mean data for each treatment and Movies SM2-1 to 3 for a movie of spatially interpolated 10 minute mean data).

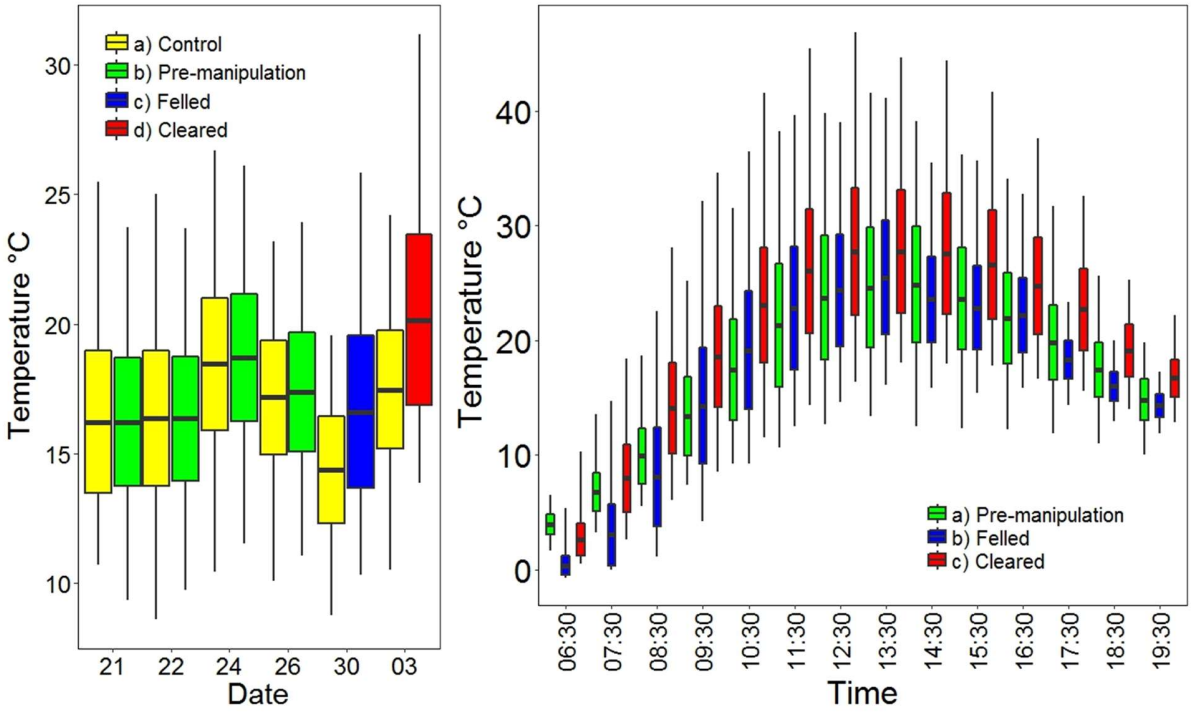

Figure 2-1, Boxplots representing the mean, ±SE and range of a) Daily mean plot temperature data presented for control (n = 79), pre-manipulation (n = 305), felled (trees removed; n = 305) and cleared (all vascular vegetation removed treatments; n = 305), b) Hourly mean plot temperature data presented for pre-manipulation, trees removed (felled) and all vascular vegetation removed (cleared) treatments (n=305)

2.4.2 Hot moments and hot spots in surface temperature patterns

Increases in mean temperatures with each successive treatment were not homogenous across the peat-surface in either space or time. The hotspot intensity (ΔT) increased from 6.7 ºC under pre-manipulation conditions to 11.4 ºC after felling and was more than double the pre-manipulation intensity when cleared, at 13.7 ºC (Figure 2-2).

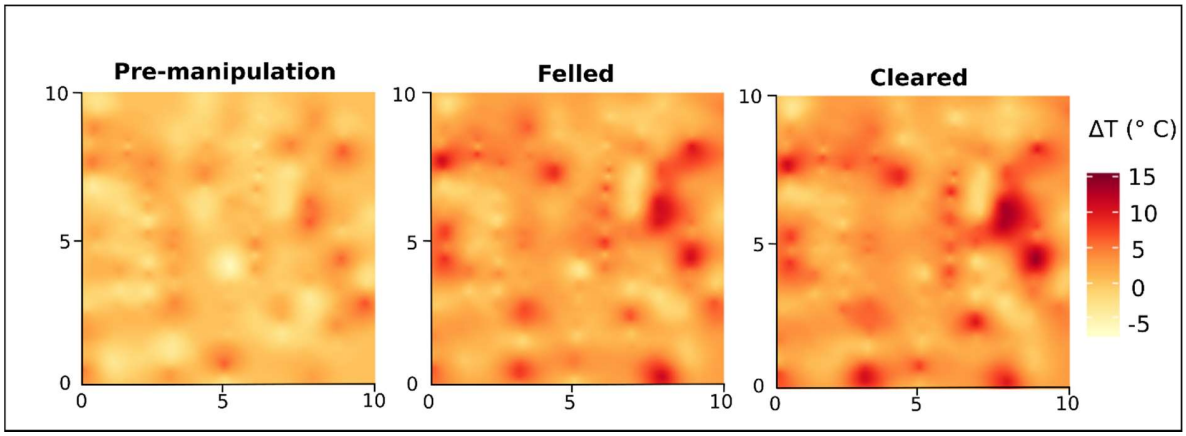

Figure 2-2, Mean daily hotspot intensity (ΔT ºC) under pre-manipulation, cleared and felled conditions. Hotspot intensity (ΔT ºC) was identified by subtracting the daily mean temperature of the control rows from the daily mean temperature at each spatial location within the plot.

The first three EOFs explain 57.7%, 21.1% and 9.1% of the variation observed under pre-manipulation conditions (Figure 2-3). Greater variance was explained by the first EOF after felling (80.1%) and clearing (77%) compared to pre-manipulation conditions (57.7%). EOFs 2 and 3 for felled (15.4 and 3.3% respectively) and cleared (18.1% and 3.2% respectively) explain less variance than their corresponding EOFs under pre-manipulation conditions.

There is very little change in EOF patterns among pre-manipulation days (Spearman's rank correlation coefficient; r = 0.95-0.97), but with felling and clearing, the spatial patterns change

substantially (r = 0.39-0.67 and r =0.38-0.59 respectively). The importance of the first three EOFs during the measurement period (PC's) also vary between pre- and post-manipulation conditions. Notably, principal component 1 and 2 of the first two EOFs are consistent between the felled and cleared conditions, but show the inverse pattern of principal component 1 and 2 under pre-manipulation conditions (Figure SI2-12). Further assessment of the heterogeneous nature of the shifts in spatial temporal temperature signatures are presented in Section SI2-2 (Vachaud *et al*., 1985).

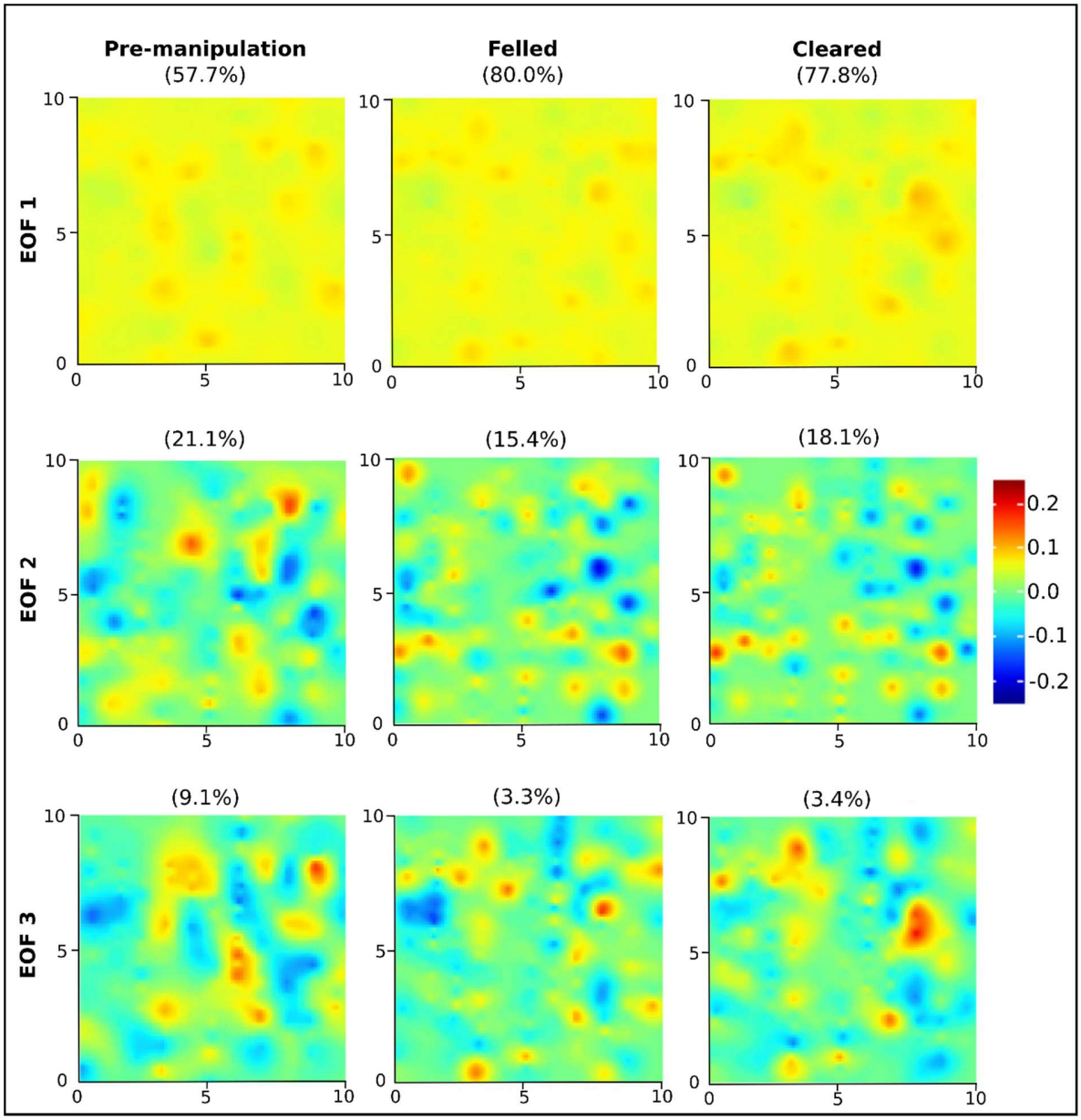

Figure 2-3, First three EOFs (dimensionless) for each treatment, derived from hourly mean temperature, with associated variance explained provided in parentheses.

2.5 DISCUSSION

2.5.1 Vegetation controls on spatial patterns and temporal dynamics of peatland surface temperatures

Significant surface temperature increases observed with both felling and clearing (also reported by Scull, (2007)) were not uniform across the peatland surface. Canopy disturbance induces shifts in the distribution, intensity (Figure 2-2, also supported by Section SI2-2: Figure SI2-7) and longevity (Figure 2-3, also supported by Section SI2-2: Figure SI2-8 to SI2-12) of high surface temperatures, with felling and clearing decreasing the spatial variability of incoming solar radiation in both space and time.

We consider that the intensity and longevity of such surface thermal hot spots is linked to peatland ecosystem heterogeneity; as shown in the conceptual model of Figure 2-4. Independent spatial patterns in surface processes, driven by high levels of peatland ecosystem heterogeneity, induce uniformity, because the summation of these processes induces short-lived-low intensity white noise (Figure 2-4, point a). Removing such layers and limiting the complexity of the pedosphere-atmosphere interface increases the potential for long lived positive effects to align, and to align for sustained periods. The most extreme spatial diversity thus results when the system is driven by a single process (Figure 2-4, point b). When the system is completely homogenous then inputs, such as solar radiation, are also spatially and temporally homogenous and hotspots and hot moments are not observed (Figure 2-4, point c). Within peatlands systems, ecological, hydrological and geomorphological heterogeneity drives variability in surface temperatures in addition to canopy complexity. These controls likely show strong co-dependence, maximising hotspot intensity in peat

surface temperatures. Canopy removal means such complexity is not further fragmented in space and time, and hotspot intensity is increased (Figure 2-4, moving the system from point d to e).

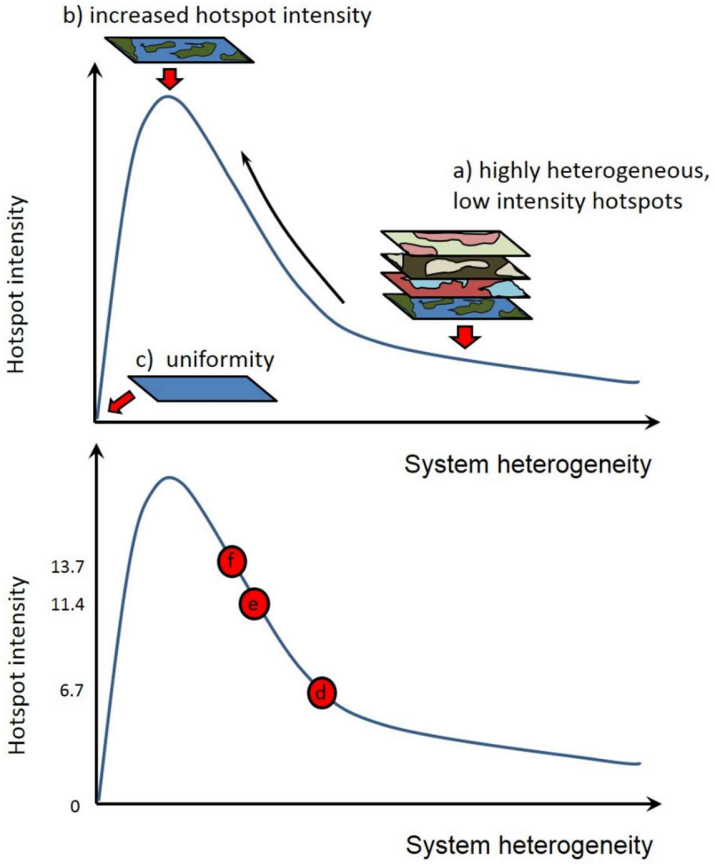

Figure 2-4, Conceptual dependence of peatland hotspot intensity on system heterogeneity. Above: A multi-layered heterogeneous peatland system (a) induce highly heterogeneous, low intensity outputs. Reducing peatland complexity to a single spatially disturbed parameter /processes (b) increases the intensity of associated hotspots. Uniformity with reduced system complexity is obtained only by limiting peatland heterogeneity to a minimum (c). *Below:* Points d, e and f represent positions of the observed peatland on the conceptual model under pre-manipulated, felled and cleared treatments, respectively. The y axis values on the lower panel represent the hotspot maxima observed (See Figure 2-2)

.

The removal of sub-canopy vascular vegetation had only a limited impact on the heterogeneity of surface temperatures in space and time (Figure 2-3, also supported by Section SI2-2 and Figures SI2-7e and SI2-7f, SI2-8, and SI2-12). This will be because (i) the vegetation is distributed comparatively uniformly in nature; (ii) it has limited impact on soil temperatures or, (iii) is strongly co-dependent with other drivers of system complexity function.

2.5.2 Implications for ecosystem functioning and resilience

Observed shifts in the location, longevity and intensity of thermal hotspots and hot moments after vegetation removal shows that the peatland system is now under discrete heterogeneous stress. Average transitions in system forcing in response to the disturbance resulted in part from intense concentrated changes within spatially isolated locations across the peatland. Spatial and temporal changes in process rates such as productivity, species competition, decomposition, and evapotranspiration will thus occur within a spatially irregular and locally extreme manner. The shift in hot spot locations also means such extremes do not map onto previous pre-disturbance hot spots in which the landscape has potential inherent resilience to mitigate the impact of such conditions. Heterogeneous stresses may therefore breach process thresholds and tipping points, and thus promote or dampen the strength of key system feedbacks (Waddington *et al*. 2015; Belyea, 2009; Rietkerk and Koopel, 2008).

The spatial dynamics and strengths of these competing feedbacks are integral to the spatial patterning and resilience of peatlands and wider ecosystems (Barbier *et al*., 2006; Guichard *et al*., 2003; Kéfi *et al*., 2007; Rietkerk *et al*., 2004). Intense, heterogeneous stresses may therefore change not only the ecosystem functioning but also, induce catastrophic shifts. For instance, the quick reduction in treed areas has been simulated in wind-disturbed forests associated with small

increases in gap fraction (Kizaki and Katori, 1999). Yet models used to predict changes to ecosystem functioning and resilience rarely consider the heterogeneous nature of applied stresses. Understanding the interconnected nature of feedbacks and heterogeneous stresses is an important consideration for assessing ecosystem dynamics, function and resilience (Schneider and Kéfi, 2016). Longer term studies that directly relate heterogeneous shifts in stresses to spatially and temporally varying system feedback mechanisms will advance our understanding of system responses to disturbances. Linking these poses a key research frontier for evaluating and predicting shifts in ecosystem function and assessing system resilience.

2.6 CONCLUSION

High spatiotemporal resolution surface-temperature data significantly improves our understanding of the complex thermal and radiative interactions at the peatland pedosphere-atmosphere interface and how these interactions change with vegetation removal. Vegetation removal increases mean temperatures as expected, but the high-resolution data and EOF analysis showed that the increase is not uniform in space or time across the peatland surface. The removal of these layers from the ecosystem decreases ecosystem complexity, but increases thermal diversity of the surface. The non-uniform response of thermal dynamics at the surface highlights the need to consider and link spatially explicit ecosystem functioning mechanisms (e.g. Soil-plant feedbacks) with the heterogeneous stresses placed on systems to fully assess their functioning and resilience.

2.7 REFERENCES

Al-Kayssi, A. W. (2002) Spatial variability of soil temperature under greenhouse conditions. *Renew. Energy* **27**(3), 453–462. doi:10.1016/S0960-1481(01)00132-X

Barbier, N., Couteron, P., Lejoly, J., Deblauwe, V. & Lejeune, O. (2006) Self-organized vegetation patterning as a fingerprint of climate and human impact on semi-arid ecosystems. *J. Ecol.* **94**(3), 537–547. doi:10.1111/j.1365-2745.2006.01126.x

Belyea, L R & Clymo, R. S. (2001) Feedback control of the rate of peat formation. *Proc. Biol. Sci.* **268**(1473), 1315–1321. doi:10.1098/rspb.2001.1665

Belyea, Lisa R. & Baird, A. J. (2006) Beyond 'the limits to peat bog growth': Cross-scale feedback in peatland development. *Ecol. Monogr.* **76**(3), 299–322. doi:10.1890/0012-9615(2006)076[0299:BTLTPB]2.0.CO;2

Belyea, Lisa R. (2009) Nonlinear Dynamics of Peatlands and Potential Feedbacks on the Climate System. In: *Carbon Cycling in Northern Peatlands* (A. J. Baird, L. R. Belyea & Co, eds.), Geophysica., 5–18. Washington, D.C.: American Geophysical Union.

Biederbeck, V. O. & Campbell, C. a. (1973) Soil Microbial Activity As Influenced By Temperature Trends and Fluctuations. *Can. J. Soil Sci.* **53**, 363–376. doi:10.4141/cjss73-053

Blok, D., Heijmans, M. M. P. D., Schaepman-Strub, G., Ruijven, J. van, Parmentier, F. J. W., Maximov, T. C. & Berendse, F. (2011) The Cooling Capacity of Mosses: Controls on Water and Energy Fluxes in a Siberian Tundra Site. *Ecosystems* **14**(7), 1055–1065. doi:10.1007/s10021-011-9463-5

Brand, D. G. (1990) Growth analysis of responses by planted white pine and white spruce to changes in soil temperature, fertility, and brush competition. *For. Ecol. Manage.* **30**(1–4), 125–138. doi:http://dx.doi.org/10.1016/0378-1127(90)90131-T

Buchan, G. D. (2011) *Encyclopedia of Agrophysics*. Springer. doi:10.1007/978-90-481-3585-1

Cookson, W. R., Cornforth, I. S. & Rowarth, J. S. (2002) Winter soil temperature (2 – 15 8 C) effects on nitrogen transformations in clover green manure amended or unamended soils ; a laboratory and field study. *Soil Biol. Biochem.* **34**, 1401–1415.

Dijkstra, P., Thomas, S. C., Heinrich, P. L., Koch, G. W., Schwartz, E. & Hungate, B. A. (2011) Effect of temperature on metabolic activity of intact microbial communities: Evidence for

altered metabolic pathway activity but not for increased maintenance respiration and reduced carbon use efficiency. *Soil Biol. Biochem.* **43**(10), 2023–2031. Elsevier Ltd. doi:10.1016/j.soilbio.2011.05.018

Dunfield, P., Knowles, R., Dumont, R. & Moore, T. R. (1993) Methane Production and Consumption in Temperate and Sub-Arctic Peat Soils - Response to Temperature and Ph. *Soil Biol. Biochem.* **25**(3), 321–326. doi:10.1016/0038-0717(93)90130-4

Folwell, S. S., Harris, P. P. & Taylor, C. M. (2015) Large-scale surface responses during European dry spells diagnosed from land surface temperature. *J. Hydrometeorol.* **17**, 975–993. doi:10.1175/JHM-D-15-0064.1

Génin, A., Majumder, S., Sankaran, S., Schneider, F. D., Danet, A., Berdugo, M., Guttal, V., *et al*. (2018) Spatially heterogeneous stressors can alter the performance of indicators of regime shifts. *Ecol. Indic.* (October). doi:10.1016/j.ecolind.2017.10.071

Guichard, F., Halpin, P. M., Allison, G. W., Lubchenco, J. & Menge, B. A. (2003) Mussel Disturbance Dynamics: Signatures of Oceanographic Forcing from Local Interactions. *Am. Nat.* **161**(6), 889–904. The University of Chicago Press. doi:10.1086/375300

Hannachi, A., Jolliffe, I. T. & Stephenson, D. B. (2007) Empirical orthogonal functions and related techniques in atmospheric science: A review. *Interntional J. Climatol.* **4**(December 2007), 1549-1555. doi:10.1002/joc

Harden, J. W., Trumbore, S. E., Stocks, B. J., Hirsch, A. & Gower, S. T. (2000) The role of fire in the boreal carbon budget. *Glob. Chang. Biol.* **6**, 174–184.

Hardy, J. P., Melloh, R., Koenig, G., Marks, D., Winstral, A., Pomeroy, J. W. & Link, T. (2004) Solar radiation transmission through conifer canopies. *Agric. For. Meteorol.* **126**(3–4), 257–270. doi:10.1016/j.agrformet.2004.06.012

Hrachowitz, M., Savenije, H. H. G., Blöschl, G., McDonnell, J. J., Sivapalan, M., Pomeroy, J. W., Arheimer, B., *et al*. (2013) A decade of Predictions in Ungauged Basins (PUB)—a review. *Hydrol. Sci. J.* **58**(6), 1198–1255. Taylor & Francis. doi:10.1080/02626667.2013.803183

Hurlbert, S. H. (1984) Pseudo replication and the design of ecological field experiments. *Ecol. Monogr.* **54**(2), 187–211.

Jiménez, C., Tejedor, M. & Rodríguez, M. (2007) Influence of land use changes on the soil temperature regime of Andosols on Tenerife, Canary Islands, Spain. *Eur. J. Soil Sci.* **58**(2), 445–449. doi:10.1111/j.1365-2389.2007.00897.x

Johnson-Maynard, J. L., Shouse, P., Graham, R., Castiglione, P. & Quideau, S. A. (2001) Microclimate and pedogenic implications in a 50-year-old chaparal and pine biosequence. *Soil Sci. Soc. Am. J.* **68**(3), 876–884.

Juszczak, R., Humphreys, E., Acosta, M., Michalak-Galczewska, M., Kayzer, D. & Olejnik, J. (2013) Ecosystem respiration in a heterogeneous temperate peatland and its sensitivity to peat temperature and water table depth. *Plant Soil* **366**(1–2), 505–520. doi:10.1007/s11104-012-1441-y

Kang, S., Kim, S., Oh, S. & Lee, D. (2000) Predicting spatial and temporal patterns of soil temperature based on topography, surface cover and air temperature. *For. Ecol. Manage.* **136**(1–3), 173–184. doi:10.1016/S0378-1127(99)00290-X

Kéfi, S., Rietkerk, M., Baalen, M. van & Loreau, M. (2007) Local facilitation, bistability and transitions in arid ecosystems. *Theor. Popul. Biol.* **71**(3), 367–379. doi:10.1016/j.tpb.2006.09.003

Kettridge, N. & Baird, A. (2008) Modelling soil temperatures in northern peatlands. *Eur. J. Soil Sci.* **59**(2), 327–338. doi:10.1111/j.1365-2389.2007.01000.x

Kettridge, N. & Baird, A. J. (2007) In situ measurements of the thermal properties of a northern peatland: Implications for peatland temperature models. *J. Geophys. Res. Earth Surf.* **112**(2), 1–12. doi:10.1029/2006JF000655

Kettridge, N., Thompson, D. K., Bombonato, L., Turetsky, M. R., Benscoter, B. W. & Waddington, J. M. (2013) The ecohydrology of forested peatlands: Simulating the effects of tree shading on moss evaporation and species composition. *J. Geophys. Res. Biogeosciences* **118**(2), 422–435. doi:10.1002/jgrg.20043

Kettridge, N., Thompson, D. K. & Waddington, J. M. (2012) Impact of wildfire on the thermal behavior of northern peatlands: Observations and model simulations. *J. Geophys. Res. Biogeosciences* **117**(G2), n/a-n/a. doi:10.1029/2011JG001910

Kettridge, Nicholas & Waddington, J. M. (2014) Towards quantifying the negative feedback regulation of peatland evaporation to drought. *Hydrol. Process.* **28**(11), 3728–3740. doi:10.1002/hyp.9898

Kirschbaum, M. U. F. (1995) The temperature dependence of soil organic matter decomposition, and the effect of global warming on soil organic C storage. *Soil Biol. Biochem.* **27**(6), 753–760. doi:10.1016/0038-0717(94)00242-S

Kizaki, S. & Katori, M. (1999) Analysis of Canopy-Gap Structures of Forests by Ising-Gibbs States - Equilibrium and Scaling Property of Real Forests -. *J. Phys. Soc. Japan* **68**(8), 2553–2560. The Physical Society of Japan. doi:10.1143/JPSJ.68.2553

Krause, S., Hannah, D. M., Fleckenstein, J. H., Heppell, C. M., Kaeser, D., Pickup, R., Pinay, G., *et al*. (2011) Inter-disciplinary perspectives on processes in the hyporheic zone. *Ecohydrology* **4**(4), 481–499. doi:10.1002/eco.176

Krause, S., Taylor, S. L., Weatherill, J., Haffenden, a., Levy, a., Cassidy, N. J. & Thomas, P. a. (2012) Fibre-optic distributed temperature sensing for characterizing the impacts of vegetation coverage on thermal patterns in woodlands. *Ecohydrology* **764**(August 2012), n/a-n/a. doi:10.1002/eco.1296

Krause, S & Blume, T. (2013) Impact of seasonal variability and monitoring mode on the adequacy of fiber-optic distributed temperature sensing at aquifer-river interfaces. *Water Resour. Res.* **49**, 2408–2423. doi:10.1002/wrcr.20232

Krause, S, Lewandowski, J., Dahm, C. N. & Tockner, K. (2015) Invited Commentary Frontiers in real-time ecohydrology – a paradigm shift in understanding complex environmental systems. *Ecohydrology* **537**, 529–537. doi:10.1002/eco.1646

Lorenz, E. N. (1956) Empirical Orthogonal Functions and Statistical Weather Prediction. *Tech. Rep. Stat. Forecast Proj. Rep. 1 Dep. Meteorol. MIT 49*.

Moore, T. R., Roulet, N. T. & Waddington, J. M. (1998) Uncertainty in predicting the effect of climatic change on the carbon cycling of Canadian peatlands. *Clim. Change*. doi:10.1023/A:1005408719297

Morecroft, M. D., Taylor, M. E. & Oliver, H. R. (1998) Air and soil microclimates of deciduous woodland compared to an open site. *Agric. For. Meteorol.* **90**(1–2), 141–156. doi:http://dx.doi.org/10.1016/S0168-1923(97)00070-1

Perry, M. A. & Niemann, J. D. (2007) Generation of soil moisture patterns at the catchment scale by EOF interpolation. *Hydrol. Earth Syst. Sci. Discuss.* **4**(5), 2837–2874. doi:10.5194/hessd-4-2837-2007

Peters-Lidard D., C., Blackburn, E., Liang, X., Wood F., E., Peters-Lidard, C. D., Blackburn, E., Liang, X., *et al*. (1998) The Effect of Soil Thermal Conductivity Parameterization on Surface Energy Fluxes and Temperatures. *J. Atmos. Sci.* **55**(7), 1209–1224. doi:10.1175/1520-0469(1998)055<1209:TEOSTC>2.0.CO;2

Raffa, K. F., Aukema, B. H., Bentz, B. J., Carroll, A. L. & Hicke, J. A. (2008) Cross-scale Drivers of Natural Disturbances Prone to Anthropogenic Amplification : The Dynamics of Bark Beetle Eruptions. *Bioscience* **58**(6), 501–517.

Rietkerk, M., Dekker, S. C., Ruiter, P. C. De & Koppel, J. van de. (2004) Self-Organized Patchiness and Catastrophic Shifts in Ecosystems. *Science (80-.).* **305**(5692), 1926–1929. doi:10.1126/science.1101867

Rietkerk, M. & Koppel, J. van de. (2008) Regular pattern formation in real ecosystems. *Trends Ecol. Evol.* **23**(3), 169–175. doi:10.1016/j.tree.2007.10.013

Scheffer, M., Carpenter, S., Foley, J. A., Folke, C. & Walker, B. (2001) Catastrophic shifts in ecosystems. *Nature* **413**(6856), 591–596.

Schlenker, W. & Roberts, M. J. (2009) Nonlinear temperature effects indicate severe damages to U.S. crop yields under climate change. *Proc. Natl. Acad. Sci.* **106**(37), 15594–15598. doi:10.1073/pnas.0906865106

Scull, P. (2007) Changes in Soil Temperature Associated with Reforestation in Central New York State. *Phys. Geogr.* **28**(4), 360–373. doi:10.2747/0272-3646.28.4.360

Selker, J. S., The, L., Huwald, H., Mallet, A., Luxemburg, W., Giesen, N. Van De, Stejskal, M., *et al*. (2006) Distributed fiber-optic temperature sensing for hydrologic systems. *Water Resour. Res.* **42**, 1–8. doi:10.1029/2006WR005326

Stout, W. L. (1992) Water-Use Efficiency of Grasses as Affected by Soil, Nitrogen, and Temperature. *Soil Sci. Soc. Am. J.* **56**. Madison, WI: Soil Science Society of America. doi:10.2136/sssaj1992.03615995005600030036x

Taggart, M. J., Heitman, J. L., Vepraskas, M. J. & Burchell, M. R. (2011) Surface shading effects on soil C loss in a temperate muck soil. *Geoderma* **163**(3–4), 238–246. Elsevier B.V. doi:10.1016/j.geoderma.2011.04.020

Timoney, K. & Lee, P. (2001) Environmental management in resource-rich Alberta, Canada: first world jurisdiction, Third World analogue? *J. Environ. Manage.* **63**(4), 387–405. doi:10.1006/jema.2001.0487

Turunen, J., Tomppo, E., Tolonen, K. & Reinikainen, A. (2002) Estimating carbon accumulation rates of undrained mires in Finland – application to boreal and subarctic regions. *The Holocene* **1**(2002), 69–80.

Tyler, S. W., Selker, J. S., Hausner, M. B., Hatch, C. E., Torgersen, T., Thodal, C. E. & Schladow, S. G. (2009) Environmental temperature sensing using Raman spectra DTS fiber-optic methods. *Water Resour. Res.* **45**(4), W00D23. doi:10.1029/2008WR007052

Vachaud, G., Passerat De Silans, A., Balabanis, P. & Vauclin, M. (1985) Temporal Stability of Spatially Measured Soil Water Probability Density Function1. *Soil Sci. Soc. Am. J.* **49**. Madison : Soil Science Society of America. doi:10.2136/sssaj1985.03615995004900040006x

Waddington, J. M., Morris, P. J., Kettridge, N., Granath, G., Thompson, D. & Moore, P. (2015) Hydrological feedbacks in northern peatlands. *Ecohydrology* (8), 113–127. doi:10.1002/eco.1493

Webb, B. W., Hannah, D. M., Moore, R. D., Brown, L. E. & Nobilis, F. (2008) Recent advances in stream and river temperature research. *Hydrol. Process.* **918**(February), 902–918. doi:10.1002/hyp

Wieder, R. K., Scott, K. D., Kamminga, K., Vile, M. a., Vitt, D. H., Bone, T., Xu, B., *et al*. (2009) Postfire carbon balance in boreal bogs of Alberta, Canada. *Glob. Chang. Biol.* **15**(1), 63–81. doi:10.1111/j.1365-2486.2008.01756.x

Wullschleger, S. D., Cahoon, J. E., Ferguson, J. a & Oosterhuis, D. M. (1991) SURFTEMP : Simulation of Soil Surface Temperature Using the Energy Balance Equation. *J. Agron. Educ.* **20**(1).

Zogg, G. P., Zak, D. R., Ringelberg, D. B., White, D. C., MacDonald, N. W. & Pregitzer, K. S. (1997) Compositional and Functional Shifts in Microbial Communities Due to Soil Warming. *Soil Sci. Soc. Am. J.* **61**, 475–481. Madison, WI: Soil Science Society of America. doi:10.2136/sssaj1997.03615995006100020015x

2.8 SUPPORTING INFORMATION FOR CHAPTER TWO

Supporting information is composed of two distinct sections: Section SI2-1 and Section SI2-2.

Section SI2-1 supports the methods section of the main article and provides:

- An evaluation of the impact of cable depth on measured peat surface temperatures and
- Digital photographs of the overall field site, cable installation and vegetation treatments.

Contents of this section;

- Text SI2-1
- Figures SI2-1 to SI2-6
- Table SI2-1 to SI2-2

Section SI2-2 supports the results section of the main article and provides additional data analysis and results supporting claims that spatial and temporal temperature signatures vary with treatment.

Contents of this section;

- Text SI2-2
- Figures SI2-7 to SI2-12
- Movie SI2-1 to SI2-3

2.8.1 Section SI2.1 Uncertainty analysis of cable burial depth and images of experimental set-up

This section supports the methods section of the chapter by providing an evaluation of the impact of cable depth on measured peat surface temperatures and illustrates the overall field site, cable installation and vegetation treatments using digital photographs.

Uncertainty analysis: Impact of cable depth on measured peat surface temperatures.

FO-DTS cable was installed at a depth of 0.02 m by carefully cutting the peat surface with scissors and inserting the FO cable with fingertips (See photos of installed cable in Figures SI2-4 to SI2-6 below). Whilst the installation depth was 0.02 m, the actual depth of installation may deviate slightly. For this reason, we explore a) the potential that cable depth provides a primary control on observed temperature patterns and b) the magnitude of the impact of expected errors in cable depth installation.

Method

i) Peatland temperature model

Peat/moss temperatures were simulated with a finite difference Fourier based peatland temperature model comparable to the HIP-Dlet model of *Kettridge and Baird (2008)*. The soil profile was discretised in to 120 nodes at 0.005 cm depth increments through the vertical profile, with simulations undertaken at a 60 second time interval. The heat flux between adjacent nodes, q (W m^{-2}), is calculated as:

$$q = -k \frac{dT}{dz} \qquad \text{(Equation SI 2-1)}$$

Where T is temperature (K), z is depth (m) and the proportionality constant k is the thermal conductivity (W m^{-1} K^{-1}). The volumetric heat capacity (C) and k are assumed spatially constant with depth through the soil profile, with a thermal diffusivity equivalent to a dry peatland soil profile (1.4 m^2 s^{-1} 10^{-7} (*Kettridge and Baird*, 2007)). The surface and basal boundary temperatures within the model temperature were defined from measured temperatures.

ii) Peat temperature measurements used to set the model boundary conditions

Simulations were conducted using temperature data from the measurement period when all vascular vegetation was removed. This minimizes the complexity of the surface boundary and thus allows a better assessment of the effect of cable depth. Soil temperatures were measured in a one dimension temperature string installed within a hollow microform within the study site, outside the FO-DTS plot. Temperatures were measured using copper-constant thermocouples at 20 minute intervals over the study period at a depth of 0.015 m, 0.07 m, 0.13 m, 0.22 m, 0.4 m and 0.6 m. Initial model temperatures were derived from these measured temperatures from the hollow and interpolated based on a polynomial best fit regression model. The lower model boundaries were set from observed peat temperatures at a depth of 0.6 m. The temperatures applied to the surface varied between different model scenarios:

Model scenarios were used to assess;

1) The Depth necessary to induce the observed temperature variations:

   To attempt to replicate observed temperatures, solely as a result of measurement depth, peat surface temperature must equal the maximum measured temperatures (subsequent cooler temperatures are as a result of depth). Therefore, the location within the study

plot with the highest maximum daily temperatures was applied as the surface temperature.

2) The impact of expected depth variations on observed temperatures.

We selected three locations, the maximum temperatures of which fell on the 25, 50 and 75th percentile of the 304 measurement locations, respectively.

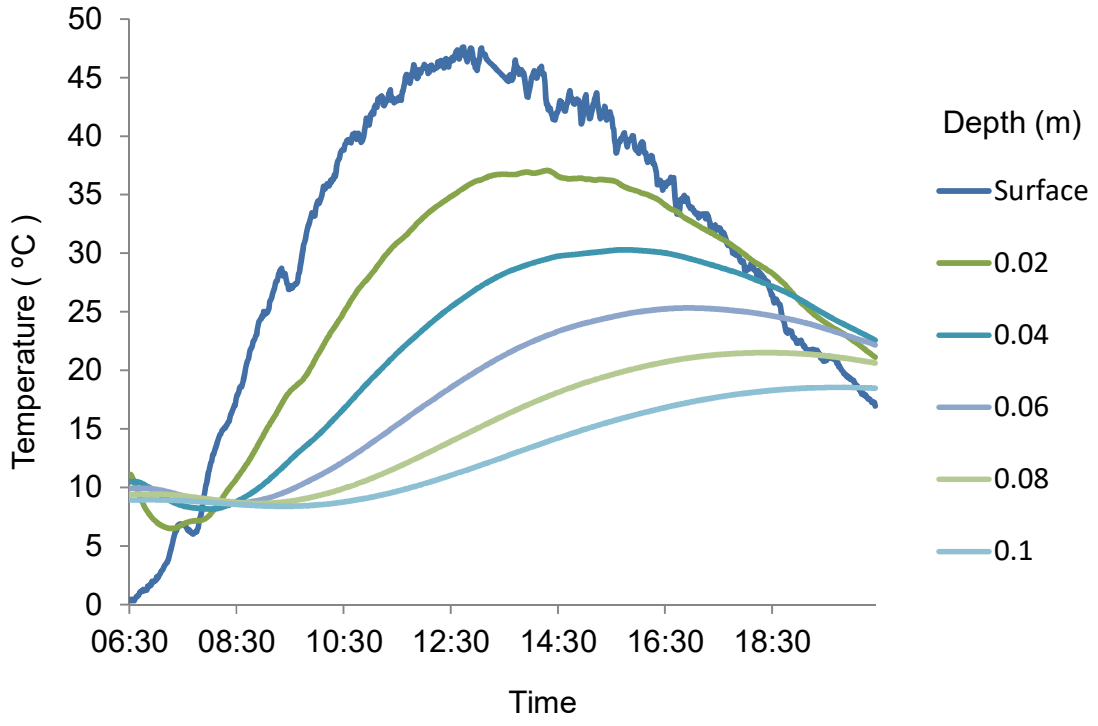

Figure SI 2-1, Peat temperatures at depths of 0 to 0.1m. Surface boundary temperatures are observed, peat temperatures at depth are modelled.

Results

Model scenario 1: The maximum observed temperature within the measurement plot under cleared conditions (the treatment showing highest temperatures) was 47.6 °C. During this same

measurement day, the coolest maximum temperature observed within the study site was 19.5 °C. The depth necessary to induce this temperature variation within the simulated peatland was between 0.09m and 0.1m (Figure SI2-1). Such an increase in depth also results in a lag in maximum temperatures of approx. 7 hours. A comparison of maximum measured peatland temperatures at a depth of 0.02m and the corresponding time of maximum temperature measurement is presented in Figure SI2-2. The data show a positive correlation, with maximum temperatures observed during the middle of the day, and minimum temperatures within the morning.

Model scenario 2: An increase in the average cable depth of 0.01m, over a 0.25 m segment, results in a predicted decrease in median temperature observed by the FO-DTS of 2.8 °C, (Table SI2-1). At locations of higher maximum temperature, the impact of altering the average cable depth increases slightly; a 0.01m increase in depth within a Q75 profile is predicted to equal 3.5 °C, whilst for a Q25 location it is equal to 2.2 °C, (Table SI2-1).

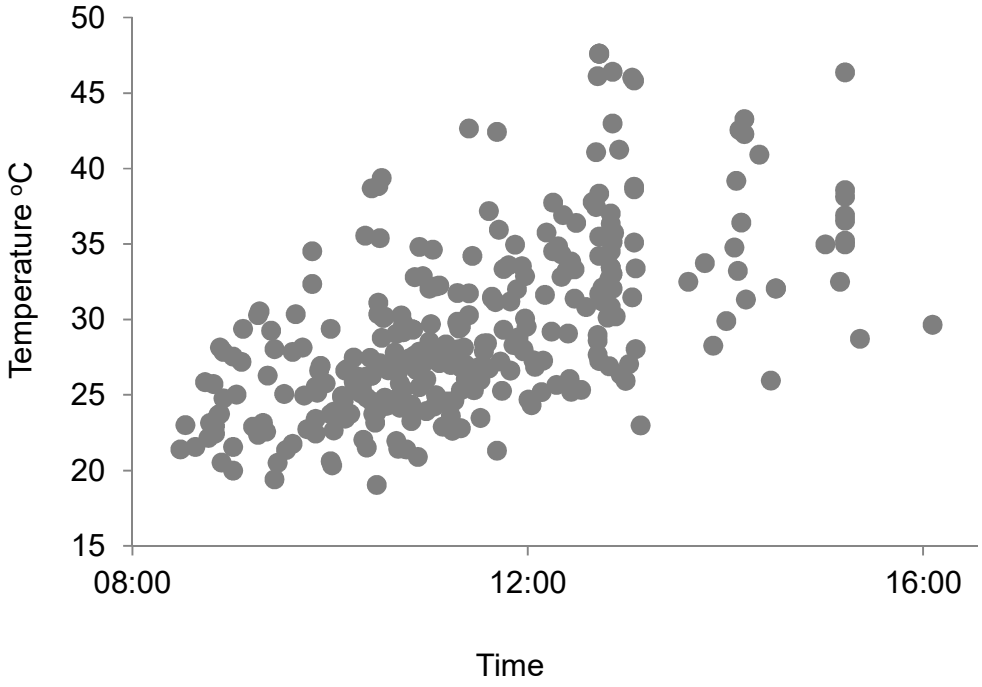

Figure SI 2-2, Maximum temperatures observed under cleared conditions against time of maximum temperature observation.

Table SI 2-1, Difference in simulated median temperature between a likely range of installation depths and the desired installation depth of 0.02m. The observed 1 minute interval data from locations whose maximum temperature were at the 25th, 50th and 75th percentile under cleared conditions was applied as the surface boundary condition. Zero values indicate no temperature change, resulting from temperatures differences calculated from the 0.02 m reference depth.

Installation depth (m)

	0.005	**0.01**	**0.015**	**0.02**	**0.025**	**0.03**	**0.035**
Q25	4.08	2.57	1.22	0	-1.11	-2.15	-3.12
Q50	5.47	3.42	1.61	0	-1.47	-2.81	-4.05
Q75	6.80	4.30	2.04	0	-1.85	-3.51	-5.02

Discussion

Variation in the cable depth cannot explain the temperature patterns observed within the study site. Firstly, an unrealistic range of average burial depths for 0.25 m sections of the FO cable (up to 10 cm below the peat surface; the range of depths required to produce the observed temperature range) would be required. Secondly, such variations in the average burial depth would induce substantial time lags between observed maximum temperatures (Figure SI2-1), with a strong negative correlation between maximum temperature and time to maximum temperature. However, a positive correlation is observed (Figure SI2-2).

Whilst cable depth cannot explain observed temperature patterns, variations in cable depth might influence observed temperatures. The actual burial depth is unlikely to vary more than ±1.5 cm because of the installation technique used. The cable was manually and carefully installed. Notably,

if the cable was installed any shallower than 0.005 m deep, the cable would have been exposed and the resulting data excluded from the analysis. Further, the cable is unlikely to be buried deeper than 0.03m as a small grove of 0.02m in depth was cut through the peat by hand with scissors into which the cable was placed by hand. The maximum likely range in temperature as a result of variations in burial depth of ±0.015 m is predicted to be between ±3.2 and 5.9 °C (Table SI2-1). This compares to the range in measured average temperatures under cleared conditions of 17 ºC, and the range in average hourly surface temperatures of 30 ºC.

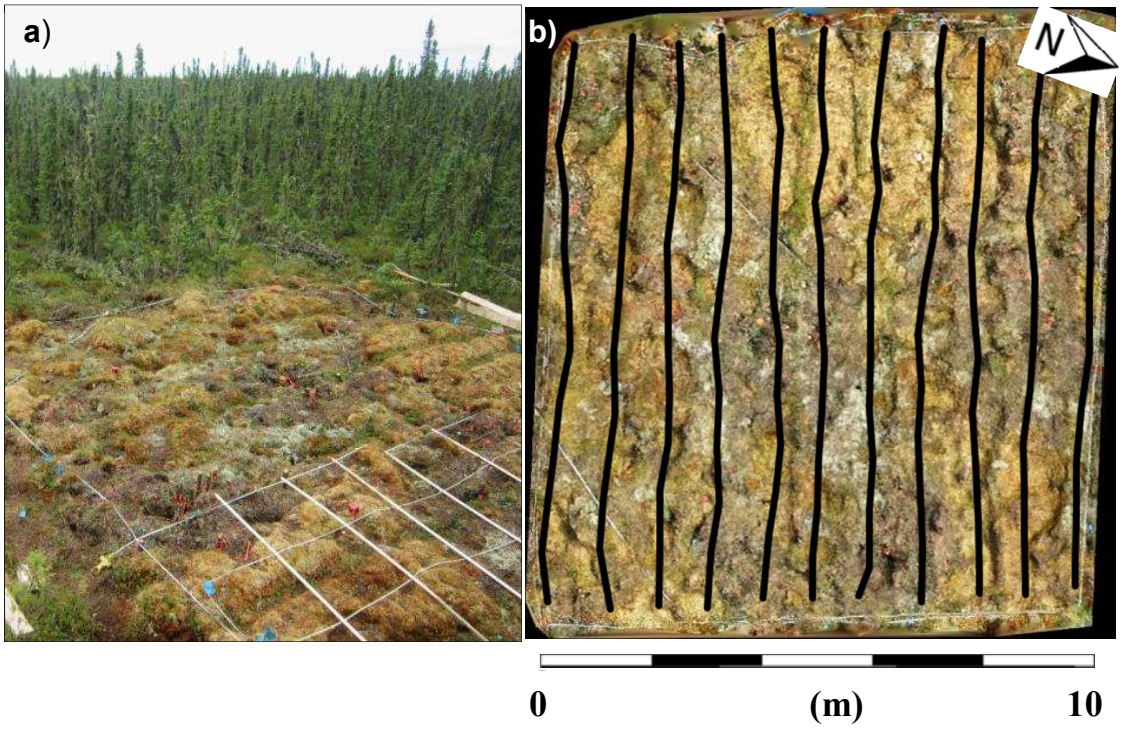

Figure SI 2-3, View of plot after clearing (removal of trees and all other vascular vegetation) looking south; white squares are 1 m2). B) Plan view of plot showing cable locations indicated by black lines.

Figure SI 2-4, Picture of field site with trees removed, before removing vascular vegetation.

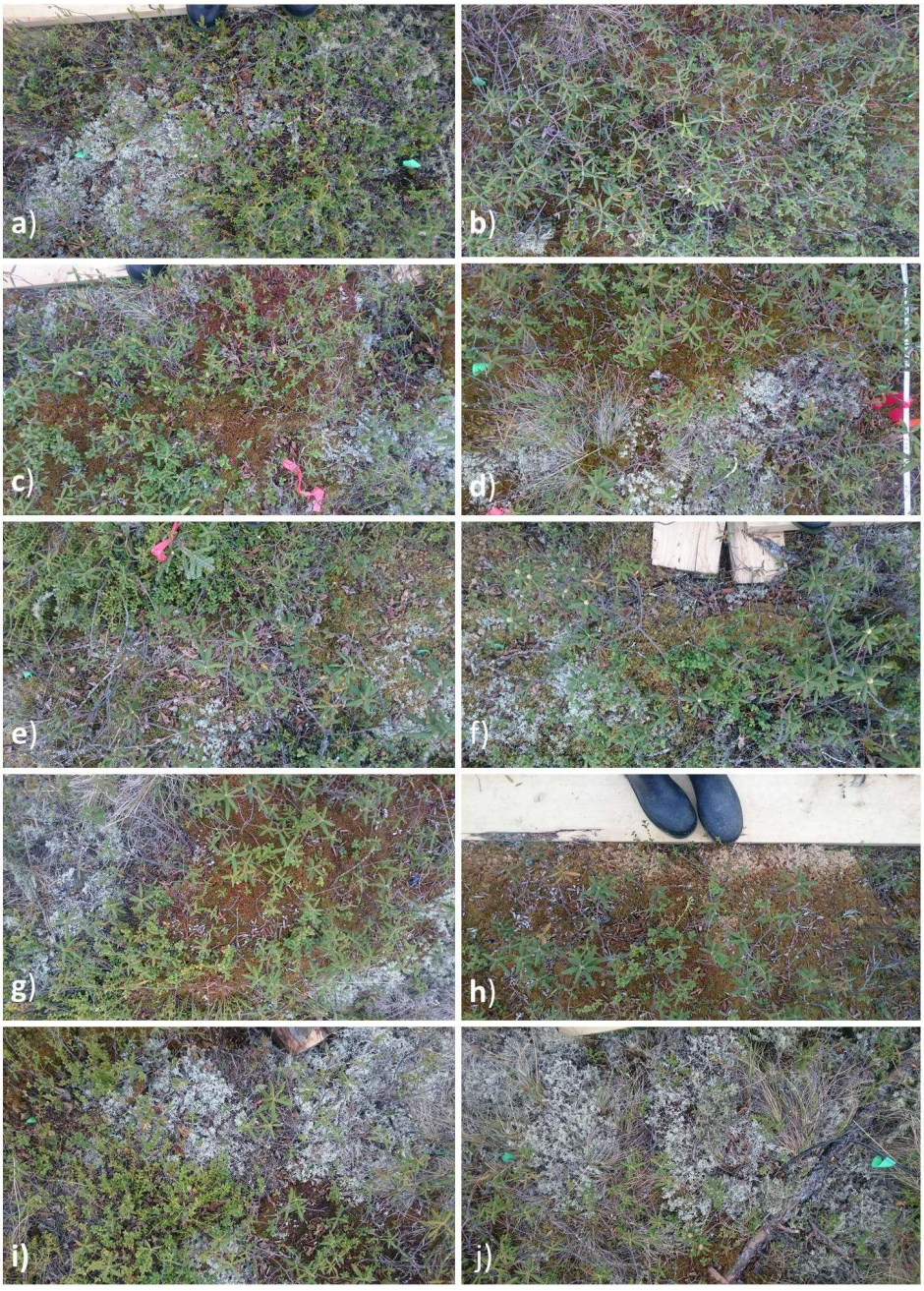

Figure SI 2-5, Photo of buried cable. Green tape marks 1 m intervals along cable length. Board walk used between the cable rows to avoid compaction. Photos of cable installed: a) in lichen/bare ground, b), c) and d) in *Sphagnum fuscum*, e) in *Pleurozium schreberi* and lichen f) *Pleurozium schreberi, Sphagnum fuscum* and lichen, g) *in Sphagnum fuscum* and lichen, h) in *Sphagnum fuscum*, i) in lichen, and j) in lichen with example exposed section of cable.

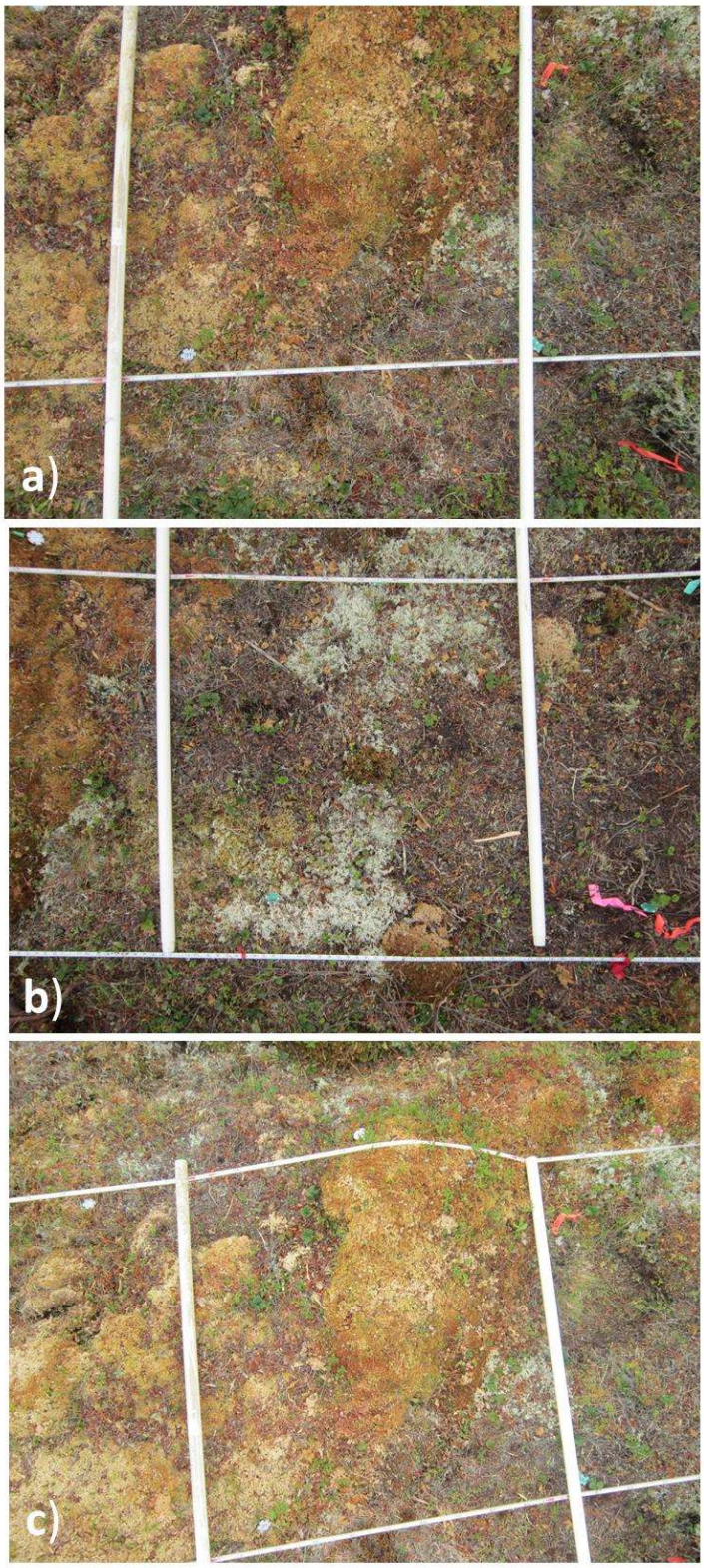

Figure SI 2-6, Photo of buried cable with all vascular vegetation removed. Poker chips mark 1 m intervals along cable length. White lines indicate approximately 1 m^2 sections of the plot. Images show cable buried in a*) Sphagnum fuscum* and bare ground, b) *Pleurozium schreberi,* bare ground, lichen and *Sphagnum fuscum* and c) *Sphagnum fuscum* and bare ground

Table SI 2-2, Air temperature and Relative humidity data for the experimental site, spanning the entire measurement period.

Date		Air Temperature (° C)	Relative Humidity (%)	Date		Air Temperature (° C)	Relative Humidity (%)
	Max	26.2	91.9		Max	15	92.2
21/05/2015	Min	-2.6	19.5	**28/05/2015**	Min	-2.4	30
	Mean	15.4	43		Mean	7.7	60.1
	Max	28.4	93.6		Max	19	93.5
22/05/2015	Min	-2.3	19.1	**29/05/2015**	Min	-4.8	30.3
	Mean	16	48		Mean	9.1	55
	Max	27.8	77.2		Max	21.5	93.6
23/05/2015	Min	6.4	22.6	**30/05/2015**	Min	-3.4	34.1
	Mean	19.2	41		Mean	12	57.2
	Max	28.2	92.3		Max	16.6	96.8
24/05/2015	Min	-0.3	21.3	**31/05/2015**	Min	8.4	59.2
	Mean	16.9	51		Mean	11.7	81.1
	Max	28.3	93.4		Max	13.9	95.3
25/05/2015	Min	1.9	25.8	**01/06/2015**	Min	-2.7	53.4
	Mean	16.9	57		Mean	8	79.3
	Max	23.7	95		Max	17.9	96.7
26/05/2015	Min	1.2	28.9	**02/06/2015**	Min	-4.5	46.9
	Mean	14.9	60.6		Mean	8.9	68.7
	Max	25.3	93.9		Max	25.1	96.4
27/05/2015	Min	-1.7	34.5	**03/06/2015**	Min	0.5	36.6
	Mean	11.1	70		Mean	15.9	61.8

2.8.2 Section SI2.2 Additional analyses and results

Here we describe additional data analysis and results to support claims that spatial and temporal temperature signatures vary with treatment.

Data analysis for additional results:

Treatment comparisons use temperature differences relative to the plot spatial mean, calculated as per *Vachaud et al.* (1985) and mapped in ArcMap (ESRI) by ordinary kriging. This allows a robust identification of the hot-spots and hot-moments that are a direct consequence of the felling and clearing and not the result of climate variability between measurement days or increases in mean temperatures. Relative (dimensionless) temperature deviation $\delta t(j)$ was calculated as:

$$\boldsymbol{\delta t(j) = \frac{Tt(j) - u[Tt(j)]}{u[Tt(j)]}} \qquad \text{(Equation SI 2-2)}$$

Where $Tt(j)$ Is the temperature (T) at a given time (t) for a horizontal spatial location (j) and $u[Tt(j)]$ is the mean soil temperature across the measurement space at the given time (t).

Stability in $\delta t(j)$ between treatments, and between hourly time steps within treatment days (e.g. Comparison of $\delta t(j)$ at 06:30 and 07:30) was determined by spearman rank correlations on sub-sampled data (to remove autocorrelation), conducted in R. A Spearman's rank correlation coefficient of one shows no change in spatial distribution, whereas a value of zero indicates maximum change in spatial distribution. Data used in spearman rank correlation analysis was conducted on subsampled (minimum distance of 1 m) data to ensure spatial independence.

Description of additional results

Daily mean temperatures exhibited more spatial homogeneity under pre-manipulation conditions than the felled and cleared treatment conditions (Figure SI2-7), with less pronounced anomalies in relative temperature difference ($\delta t(j)$). Maximum pre-manipulation $\delta t(j)$ was observed on 26th May, equal to 0.2 (Figure SI2-7 a). This is compared to a maximum of 0.4 under both felled and cleared conditions (compare Figure SI2-7 a, b and c). The spatial distribution in $\delta t(j)$ also varied in response to treatment (Figure SI2-7 a, b and c). The spatial distribution in $\delta t(j)$ correlates strongly between pre-manipulation days (r = 0.95-0.97), but correlation reduces substantially when trees are felled (r = 0.67-0.74) and when subsequent remaining vascular vegetation is removed (cleared) (r =0.59-0.65). The spatial distribution in $\delta t(j)$ for the felled treatment is not substantially modified by clearance of the remaining vascular vegetation cover (r = 0.93).

The spatial variation in $\delta t(j)$ is indicative of hot thermal moments. Under pre-manipulation conditions, for example at 10:00 and 14:00 (Figure SI2-7 d, g), local $\delta t(j)$ hotspots are more intense than the daily mean (Figure SI2-7 a), reaching 0.5. When felled and cleared, this intensity increases to 0.7 (Figure SI2-7 e, h, f, i).

In addition to the increased intensity and changes in daily ($\delta t(j)$), the position of high intensity zones shifts with time and treatment. Figures SI2-9, SI2-10 and SI2-11 and Movies SM2-1, SM2-2 and SM2-3, show that spatial patterning changes with time, within and between treatments with the greatest changes observed between pre-manipulation and felled conditions. These observed changes in spatial patterning through time are quantified by comparing the spatial stability in $\delta t(j)$ between neighbouring hourly time points (Spearman's rank correlation). The greatest variability between hourly $\delta t(j)$ is observed under pre-manipulation conditions; r broadly ranges between 0.7 and 0.9 (Figure SI2-8). Under treatment conditions, the spatial distribution in $\delta t(j)$ is more

consistent between hourly time-steps (Figure SI2-8), indicating greater stability in the spatial distribution of hourly $\delta t(j)$ through the measurement period. The principal component associated with each EOF further supports these results with the greatest differences in the principal components (PC's) observed when comparing pre-manipulation and felled conditions. Principal component 1 and 2 of the first two EOFs are consistent between felled and cleared conditions, but show the inverse pattern of PC 1 and 2 under pre-manipulation conditions (Figure SI2-12).

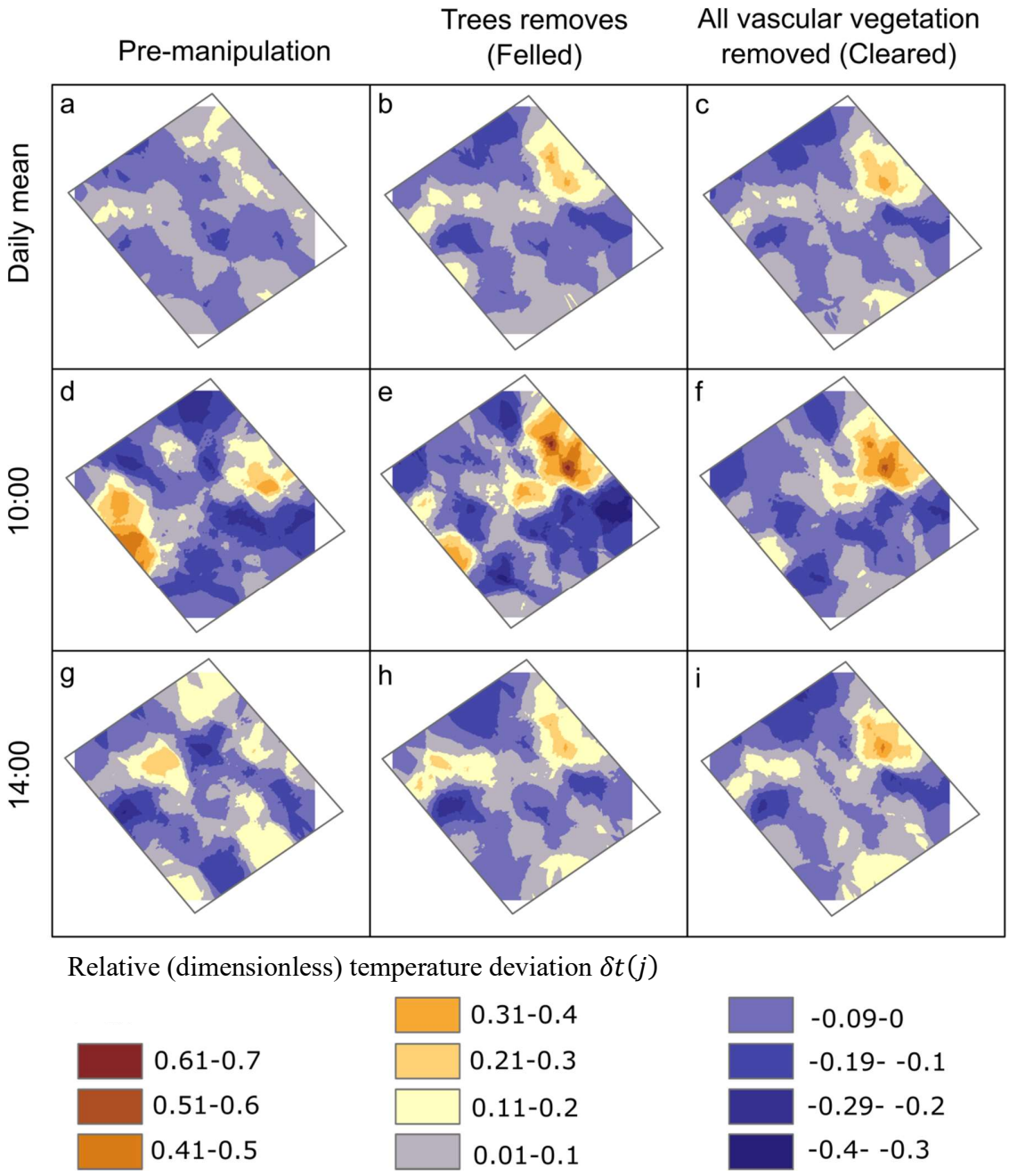

Figure SI 2-7, Maps of relative standard deviation for daily mean data (a,b,c), 10:00 time point (d,e,f) and 14:00 time point (g,h,i) for pre-manipulation (a,d,g), felled (b,e,h), and cleared treatments (c,f,i).

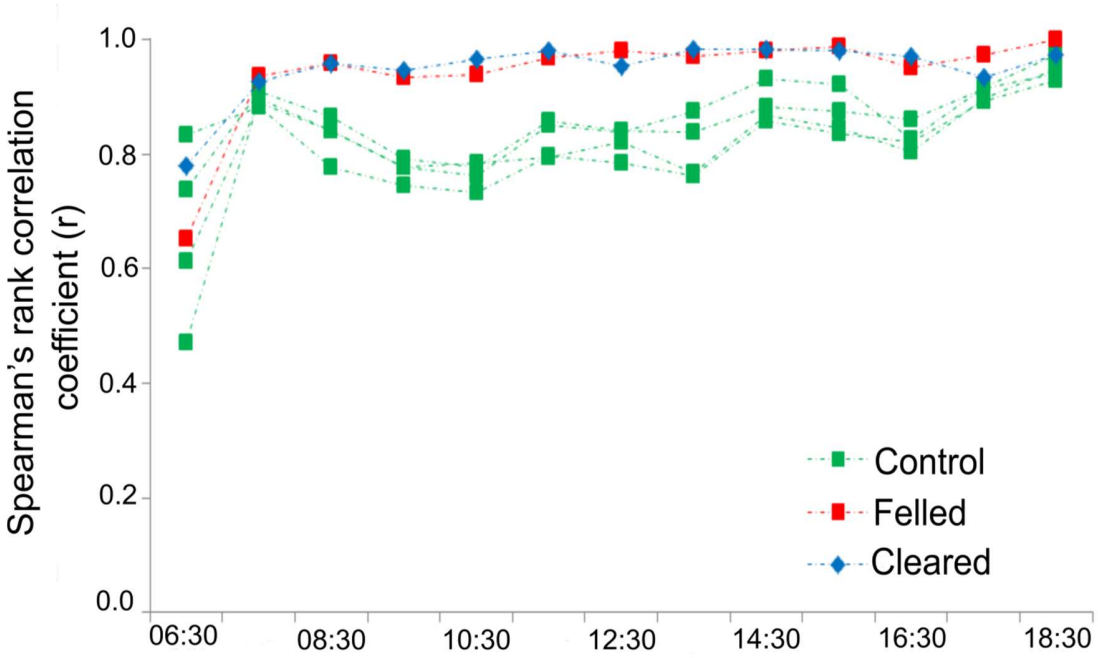

Figure SI 2-8, Spearman rank correlation data points illustrating change in spatial patterning in data between neighbouring hourly means (values of 1 indicate no changes in spatial patterning. Values of 0 indicate maximum change in spatial patterning.).

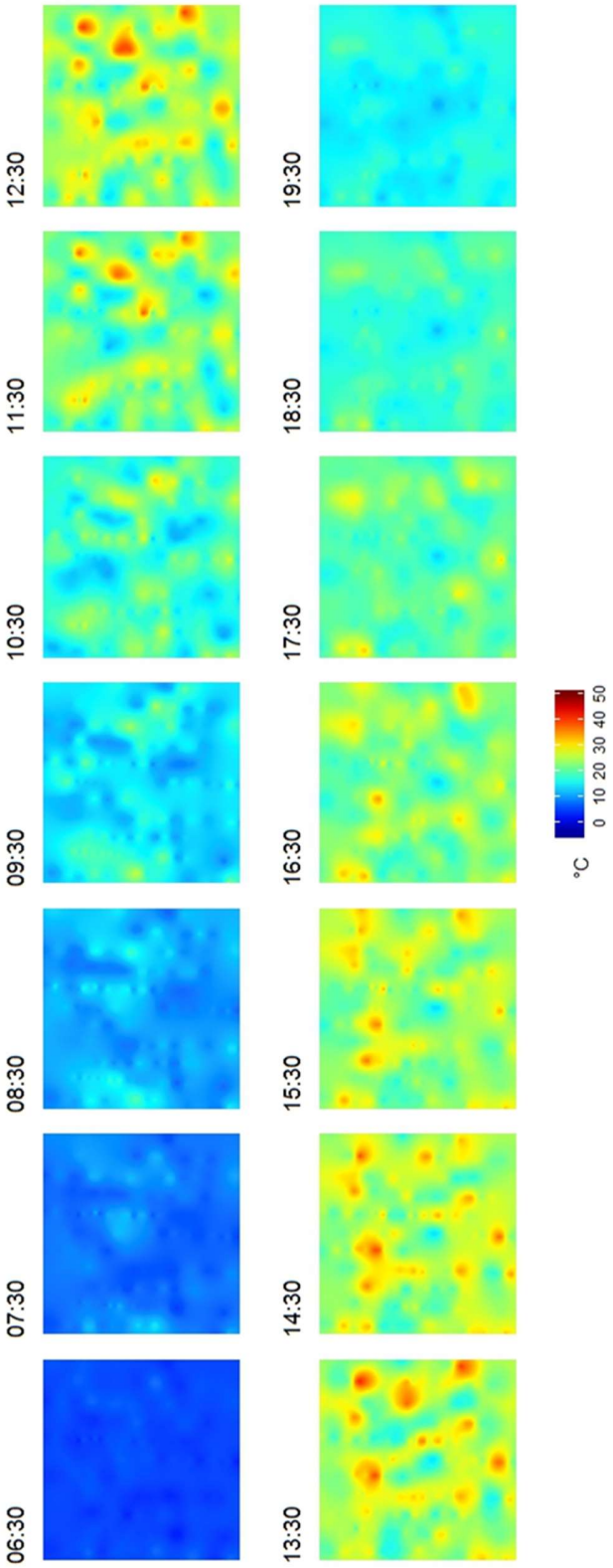

Figure SI 2-9, Mean hourly temperature data under pre-manipulation conditions for hourly time-steps.

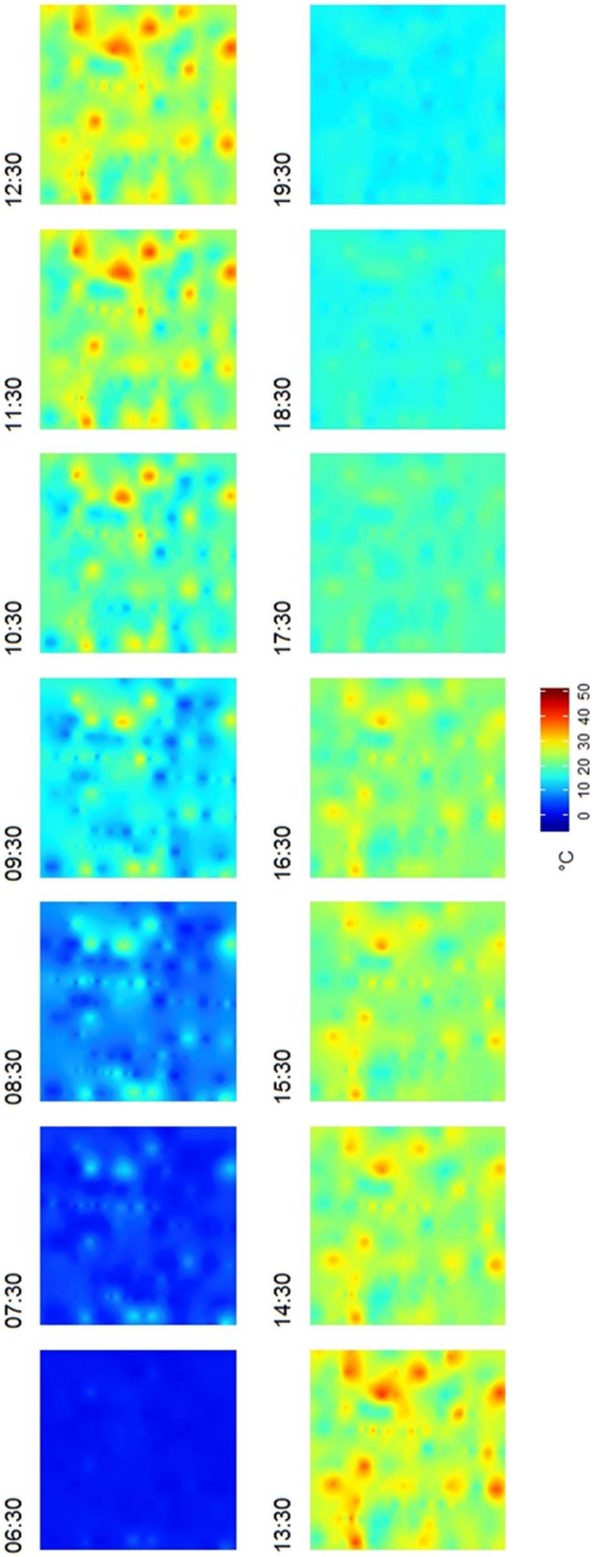

Figure SI 2-10, Mean hourly temperature data under felled conditions for hourly time-steps.

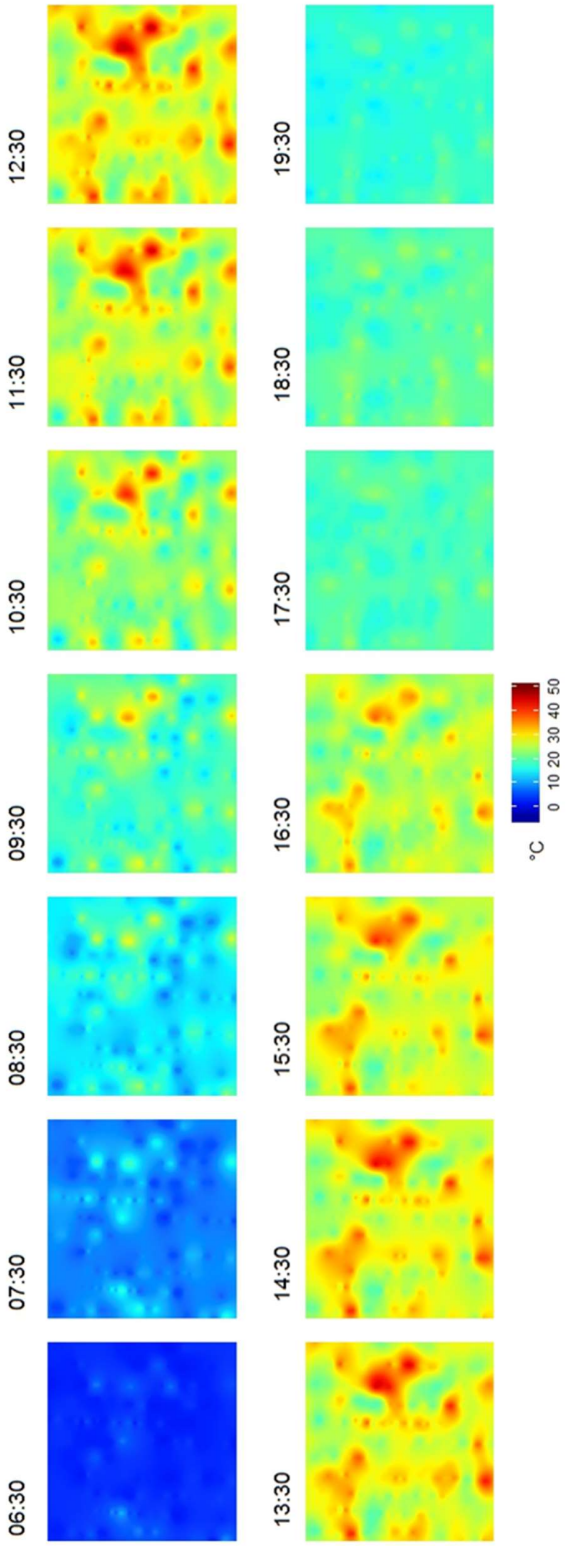

Figure SI 2-11, Mean hourly temperature data under cleared conditions for hourly time-steps.

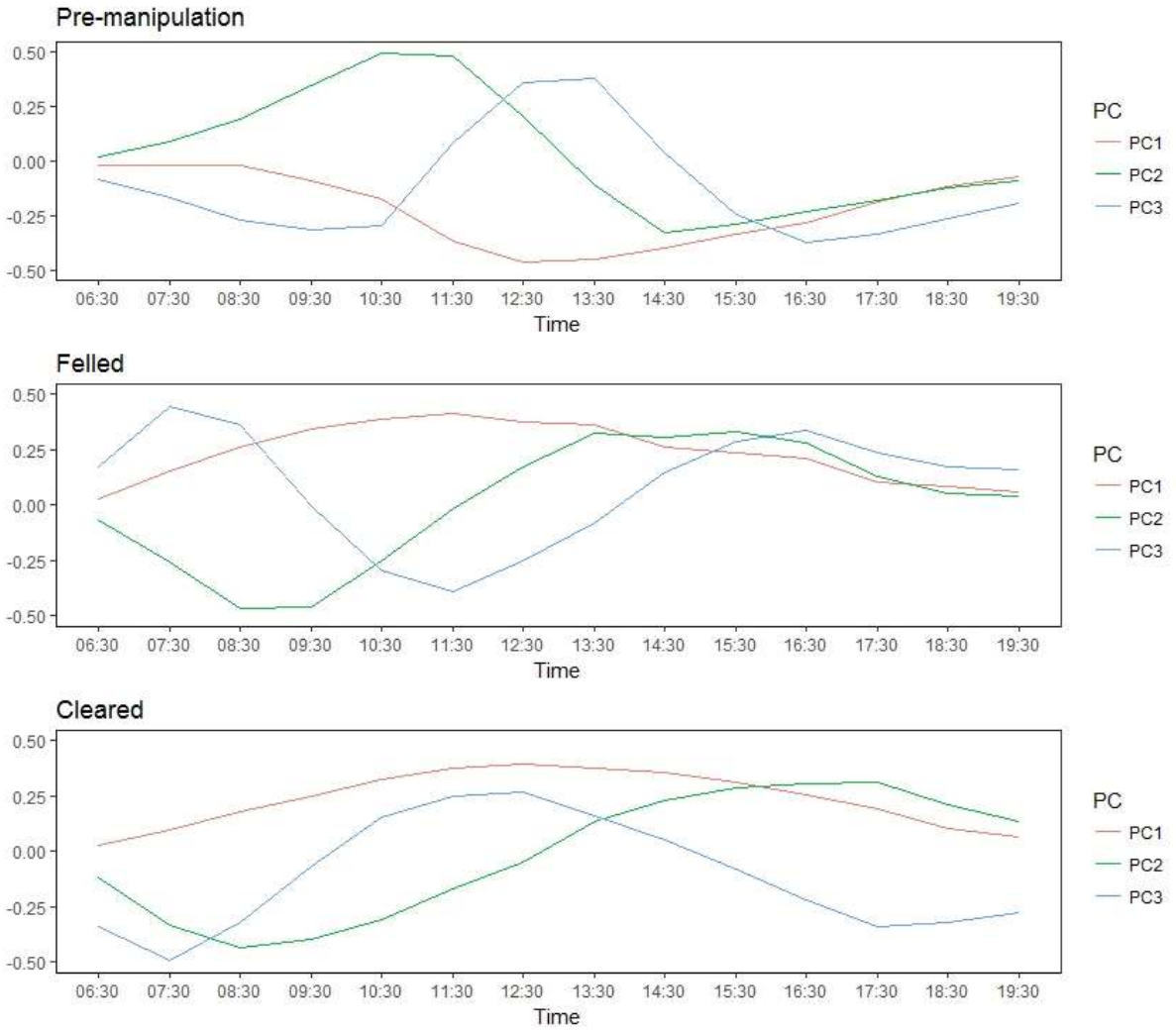

Figure SI 2-12, Principal components of the first three EOF's for each treatment.

Movie SI 2-1: Movie of peat surface temperatures at 10 minute intervals across the measurement plot under pre-manipulation conditions. (**grl56819-sup-0001-2017GL075974-ms01.avi**)

Movie SI 2-2. Movie of peat surface temperatures at 10 minute intervals across the measurement plot under felled conditions. (**grl56819-sup-0002-2017GL075974-ms02.avi**)

Movie SI 2-3. Movie of peat surface temperatures at 10 minute intervals across the measurement plot under cleared conditions (**grl56819-sup-0003-2017GL075974-ms03.avi**)

CHAPTER THREE : THE INFLUENCE OF SYSTEM HETEROGENEITY ON PEAT-SURFACE TEMPERATURE DYNAMICS

3.1 ABSTRACT

Temperatures at the soil-surface interface influence ecosystem functioning by driving non-linear terrestrial biogeochemical, ecohydrological, and micrometeorological processes. Understanding the dynamic and small-scale nature of key system processes such as these, is increasingly identified as a priority for peatland research. The ability to simulate not only mean peat-surface temperatures but the thermal complexity in space and time, will propel our ability to assess system functioning through advanced understanding of the spatial distribution, frequency, and duration of thermally driven processes. A recently produced surface temperature dataset of unprecedented spatio-temporal resolution (1.9 million temperature measurements over 100 m^2) was used, to critically and rigorously assess the spatio-temporal thermal regime simulated by the PHI-BETA-THETA model. This model simulates the peatland thermal behaviour in three dimensions, within the forested boreal peatland plot used to collect the empirical temperature measurements. We subsequently use the evaluated model to simulate not only the influence of individual ecosystem structural layers (tree canopy and sub-canopy, subsurface ice-layers, ground cover vegetation and microtopography) on surface temperature distributions but how different combinations of these heterogeneous layers influence peat-surface thermal regimes. The simulations of peat temperature using different combinations of heterogeneous layers allows us to determine how ecosystem layers may simplify or complicate surface thermal patterns and promote or dampen temperature extremes. Critically, the results show that changes in the spatio-temporal dynamics may occur without significant changes in median temperatures. This study provides important insight into spatial and temporal variability in temperature driven peatland processes and highlights key considerations for future research.

3.2 INTRODUCTION

The soil-surface is a critical interface, controlling mass and energy exchange between terrestrial ecosystems and the atmosphere. Dynamic, spatially complex soil-surface temperatures regulate the rates of such interface exchanges, governing processes such as carbon storage and release (Johnstone *et al.*, 2016; Juszczak *et al.*, 2013; Kirschbaum, 1995; Lafleur *et al.*, 2005; Taggart *et al.*, 2011), water fluxes (Delucia, 1986), species competition (Brand, 1990), metabolic (Dijkstra *et al.*, 2011) and biogeochemical cycling (Frei *et al.*, 2012). Surface temperatures also impact processes at depth by driving the thermal regime of the soil profile (Kettridge *et al.*, 2013; Wullschleger *et al.*, 1991). This control of system processes by surface temperature is of notable importance within peatland ecosystems where complex peat-surfaces act to regulate deeper stores of organic carbon (Belyea & Clymo, 2001; Belyea & Baird, 2006) that account for one-third of the global soil carbon pool (Turunen *et al.*, 2002).

Despite a past focus on point measurements (Kellner, 2001; Kellner & Halldin, 2002; Kettridge *et al.*, 2012; Kettridge & Baird, 2007; Lafleur *et al.*; 2005; Mckenzie *et al.*, 2007), peatland surface temperatures are rarely uniform. Peat-surface temperatures can vary by over 25 °C at the decimetre scale in undisturbed, forested conditions (Chapter 2, Leonard *et al*., 2018). This complex thermal signature emerges from interactions between meteorological regime, energy interception by vegetation (Hardy *et al*., 2004; Chapter 2, Leonard *et al*., 2018), and organisation of geomorphological, hydrological (Al-Kayssi, 2002; Folwell *et al.*, 2015), thermal (Peters-Lidard *et al.*, 1998) and aerodynamic (Green *et al.*, 1984) properties. Within temperate peatlands, the distinctive micro-topography of hummocks and hollows (Foster *et al.*, 1983; Sjörs, 1961) can induce surface temperature variations of up to 13°C between northern and southern slopes less than a meter apart, primarily as a result of sun angle and direct short-wave radiation input (Kettridge & Baird, 2010). But microtopography is also intrinsically

linked to water table depths and soil moisture which further modify peat temperatures (Kettridge & Baird, 2008). Peat groundcover also has a significant influence over peat-surface temperatures (Soudzilovskaia *et al.*, 2013), with 20 °C temperature variations observed between neighbouring patches of *Pleurozium schreberi* and *Sphagnum fuscum* (Stoy *et al*., 2012). Processes inducing such temperature differences between ground-cover types include, significant differences in evaporative cooling (Blok *et al.*, 2011; Brown *et al.*, 2010) and surface albedo (Stoy *et al*., 2012). Subsurface heterogeneity may also impact surface thermal regimes. When seasonally frozen, uneven ice thawing results in the presence of frozen peat and frost-free peat patches well into the growing season (Petrone *et al.*, 2008). With the spatial variations in peatland surface temperatures similar in magnitude to diurnal fluctuations (Chapter 2, Leonard *et al*., 2018), understanding the variation in the thermal response of peatlands to climatic shifts or more localised disturbance is likely as important as determining the average system behaviour. Whilst both the complex spatiotemporal distribution in peat surface temperatures and the processes that induce them have been highlighted, the magnitude of the impact of individual layers of heterogeneity and their interactions on system thermal complexity is unknown. The extent to which combinations of layers induce hotspots or hot moments of varying intensity and longevity, that may induce thermally complex ecosystems that can support biological and biogeochemical diversity or exceed localised tipping points, is not known. It is further unclear how heterogeneity develops from, or can be maximised within, homogeneous peatland landscapes, such within harvested peatlands. This chapter aims to determine the influence both of individual layers of heterogeneity (subsurface ice-layers, ground cover vegetation, microtopography, tree, and sub-canopy vascular cover) on surface temperature distributions, and how different combinations of these layers influence peat-surface temperature patterns. This chapter further tests the conceptual understanding posed by Leonard

et al., (2018, Chapter 2) that individual layers of system heterogeneity may, alone, create sustained heterogeneity in the peat thermal regime, producing sustained hotspots at the peat surface but when multiple layers of heterogeneity are stacked, heterogeneity in the thermal regime reduces because the combined effect of layers results in short-lived low intensity events i.e. less intense hotspots.

To achieve this goal we utilise high spatio-temporal peat temperature measurements (Leonard *et al*., 2018) to critically evaluate the spatio-temporal thermal regime simulated by PHI-BETA-THETA, a peatland thermal model (Kettridge *et al*., 2013). The ability to predict not only mean peat-surface temperatures but the thermal complexity in space and time, will propel our ability to assess system functioning through advanced understanding of the spatial distribution, frequency, and duration of thermally driven processes. The novel evaluation of simulated temperature distributions will identify model strengths and weaknesses, providing guidance and focus to future research and model development efforts. This model advancement is key in order to further our understanding and ability to predict the resilience of such heterogeneous and globally significant systems.

3.3 STUDY SITE

Empirical data was collected from a poor fen (peat-depth ≥ 3m) in central Alberta, Canada (55.81°N, 115.11°W). The site has a tree cover of *Picea mariana* with a basal area of 11 m^2 ha^{-1}, and an average height of 2.3 m (Kettridge *et al.*, 2012), which is characteristic of boreal peatlands (Wieder *et al.*, 2009). The vascular sub-canopy includes *Rhododendron groenlandicum, Rubus chamaemorus, Chamaedaphne calyculata, Maianthemum trifolia, Oxycoccus microcarpus, Vaccinium vitus-idea* and *Eriophorum spp.* Ground cover consists of a mosaic of *S. fuscum* (43%), *P. schreberi* (9%)*, Cladina sp., Cladonia sp.* (11%) and bare peat (see Figure SI3-1; 26%), the combination of which gives the peatland its characteristic,

patterned (Foster *et al.*, 1983; Sjörs, 1961), hummock-hollow features that vary in height by up to 0.41m within the measurement area, which is consistent with other accounts (Lewis & Dowding, 1926).

3.4 METHODS

3.4.1 High resolution spatio-temporal data

Soil-surface temperature data was collected using a Silixa Ltd. XT Fiber-Optic Distributed Temperature Sensing (FO-DTS) system. A fibre-optic cable was buried at 0.02m depth in the formation of 11 rows spaced 1m apart in a 10 x 10 m plot. Temperatures were measured at 0.25m spatial and 1-minute temporal intervals between 0630 and 2030 for each measurement day. Temperatures were recorded between the 21st of May and the 3rd of June 2015 and consist of 4 days of undisturbed conditions, 1 day of trees removed conditions (felled) and 1 day of all vascular vegetation removed (cleared) conditions. Two 10 m lengths of cable were buried outside the plot and remained undisturbed throughout the measurement period as a control. For additional information on the experimental set-up and data-collection methods the reader is directed to (Chapter 2, Leonard *et al*., 2018) and associated supplemental material.

3.4.2 PHI-BETA-THETA Model Summary

PHI-BETA-THETA is a finite difference Fourier based model that simulates the 1D thermal behaviour through numerous vertical peat profiles discretised at 0.01 m intervals. The thermal properties of each node are determined based on the peat bulk density and volumetric water content. Volumetric water contents are calculated from the van Genuchten equation, with pore water retention determined from the water table depth assuming hydrostatic equilibrium through the peat profile. The volumetric heat capacity is calculated by summing soil constituents multiplied by their respective heat capacities. The impact of ice melt is represented

by an increased volumetric heat capacity during periods of melt (*cf.* Mckenzie *et al*., 2007). The thermal conductivity is calculated according to Farouki (1986). Water table depth and soil temperature were measured by a pressure transducer throughout the simulation period and applied to set the water table position and the lower boundary temperature of the model. The water table depth varies amongst soil profiles (by up to 0.41 m) due to the surface micro topography of the simulation plot. Initial peat near-surface temperatures are defined from measured temperatures across the simulation areas at 0630 taken from the FO-DTS at a depth of 0.02m. Peat profile initial conditions were set using a cubic spline interpolation from measured soil temperatures at the beginning of the simulation period.

The surface boundary of PHI-BETA-THETA is driven by standard meteorological data used to calculate the net short and longwave radiation, sensible and latent heat fluxes. Short and long wave radiation are calculated using a spatially explicit 3D radiation model. Trees within the measurement plot were photographed, and their structures represented as collections of voxels (SI3-1). Trees are placed within the 3D landscape and the direct and diffuse shortwave radiation (through time) and sky view factor (constant) at the surface of each peat profile determined following an approach similar to that presented by Essery *et al*. (2008). The net longwave radiation is calculated in accordance with Stefan-Boltzmann law and Beer's law (Aber and Melillo, 1991) applying the predetermined sky view factor. Additionally, the model accounts for the influence of micro-topography by incorporating the effect of, measured variations in elevation, slope, aspect and shading of the peat surface on the short and long wave radiation balance (Kettridge and Baird, 2010). Ice depth measurements are used to inform the spatially varying depth of increased volumetric heat capacity during periods of melt. Latent heat is calculated according to the Penman-Monteith model and sensible heat is calculated according to Newton's law of cooling. PHI-BETA-THETA builds upon previous modelling efforts,

namely 1-D HIP (Kettridge and Baird, 2010), radiative transfer model (Essery *et al*., 2008) and BETA (Kettridge and Waddington, 2014). A full description of the model is available in the supporting information, Section SI3-1.

3.4.3 Description of simulations

Model performance was evaluated by numerically replicating the experimental setup of Leonard *et al*. (2018), with vegetation layers removed in the same sequence and at the same time (Trees removed (felled) then all other vascular vegetation removed (Cleared)). Subsequently, 80 scenarios were simulated, using meteorological data between 0630 and 2030 on the 24th of May (a predominantly cloud free day with air temperature ranging from 4.7 to 28.2 °C). Scenarios comprised all permutations of the following options: trees (On/Off), shrubs (On/Off), microtopography (On/Off), surface-cover (On/Off), ice cover (On/Off), initial surface temperature (On/Off). Surface-cover was simulated using either a median surface resistance value (Median r_s) or a surface resistance value selected from a log normal distribution (log-normal distribution r_s) of surface resistance values obtained for each groundcover type (SI3-1). When surface-cover was set to 'Off', uniform groundcover was simulated for each of the following conditions; *S. fuscum* (Median r_s), *S. fuscum* (log normal distribution r_s), *P. schreberi* (Median r_s), *P. schreberi* (log normal distribution r_s), bare ground (Median r_s), *b*are ground (log normal distribution r_s), *Cladina sp* (Median r_s), *Cladina sp* (log normal distribution r_s). When surface-cover was set to 'On', the groundcover is simulated with the species that were present in each location, a mosaic (of *S. fuscum* (43%), *P. schreberi* (9%), (*Cladina sp., Cladonia sp.* (11%) and bare peat (26%)) for a median and log-normal r_s. Ice cover was simulated as the average observed depth to ice (Off) and observed depth to ice at each measurement location (On). Initial surface temperatures were set by either observed surface temperatures (On) or average of the observed surface temperatures (Off). Data was simulated

for a depth of 0.02 m below the peat surface. The model outputs the temperature for each spatial location at 10-minute intervals.

3.4.4 Analysis

Due to the dynamic non-uniform nature of peat-surface temperatures, empirical orthogonal functions (EOFs) were used to provide a compact representation of the intricate and complex data (Rajic, 2002) by spatially representing the variance of a dataset. Each EOF represents a proportion of the dataset's variance with the first EOF representing the largest proportion of the total variance meaning that one or two EOFs will provide insight into most of the variability within a dataset (Dawson, 2016). Spearman rank correlation analysis (*rho*) was applied to compare spatial patterning of the EOFs. A single daily hotspot value (ΔT °C) was calculated for each scenario by subtracting the plot mean temperature (Figure SI3-3) from the greatest mean temperature value at a single location (Figure SI3-4).

3.5 RESULTS

3.5.1 Model performance

The change in spatial patterning of near surface temperatures between treatments shows very similar behaviour between measured and modelled temperatures (Figure 3-1 and Table 3-1). The greatest decrease in *rho* values (which indicates the greatest shift in spatial patterning) is observed in both modelled and measured data sets when undisturbed and felled conditions are compared (average decrease in *rho* value of 0.35 and 0.23 for measured and modelled respectively). A further, much smaller, decrease is observed in both modelled and measured temperatures when comparing felled and cleared scenarios (average decrease in *rho* values is 0.09 and 0.07 for measured and modelled respectively). The simulated EOF extremes are lower

than measured, which likely reflects the conservative extreme values simulated by the model compared to the measured data (Figure 3-1 and Figure SI3-2).

Model simulations regularly overestimate peat surface temperatures under all treatment conditions between the hours of 0630 and 0830 (Figure SI3-2). Under undisturbed conditions the model underestimates surface temperatures between 0930 and 1730. All model scenarios show best alignment with measured data between 1730 and 1930. Cleared conditions show better replication of the median and quartile data, although the first and fourth quartile data underestimate the observed range. High extreme temperatures are best replicated at the start and end of each measurement period but are conservative during daytime/peak median temperatures (Figure SI3-2) under felled and cleared conditions.

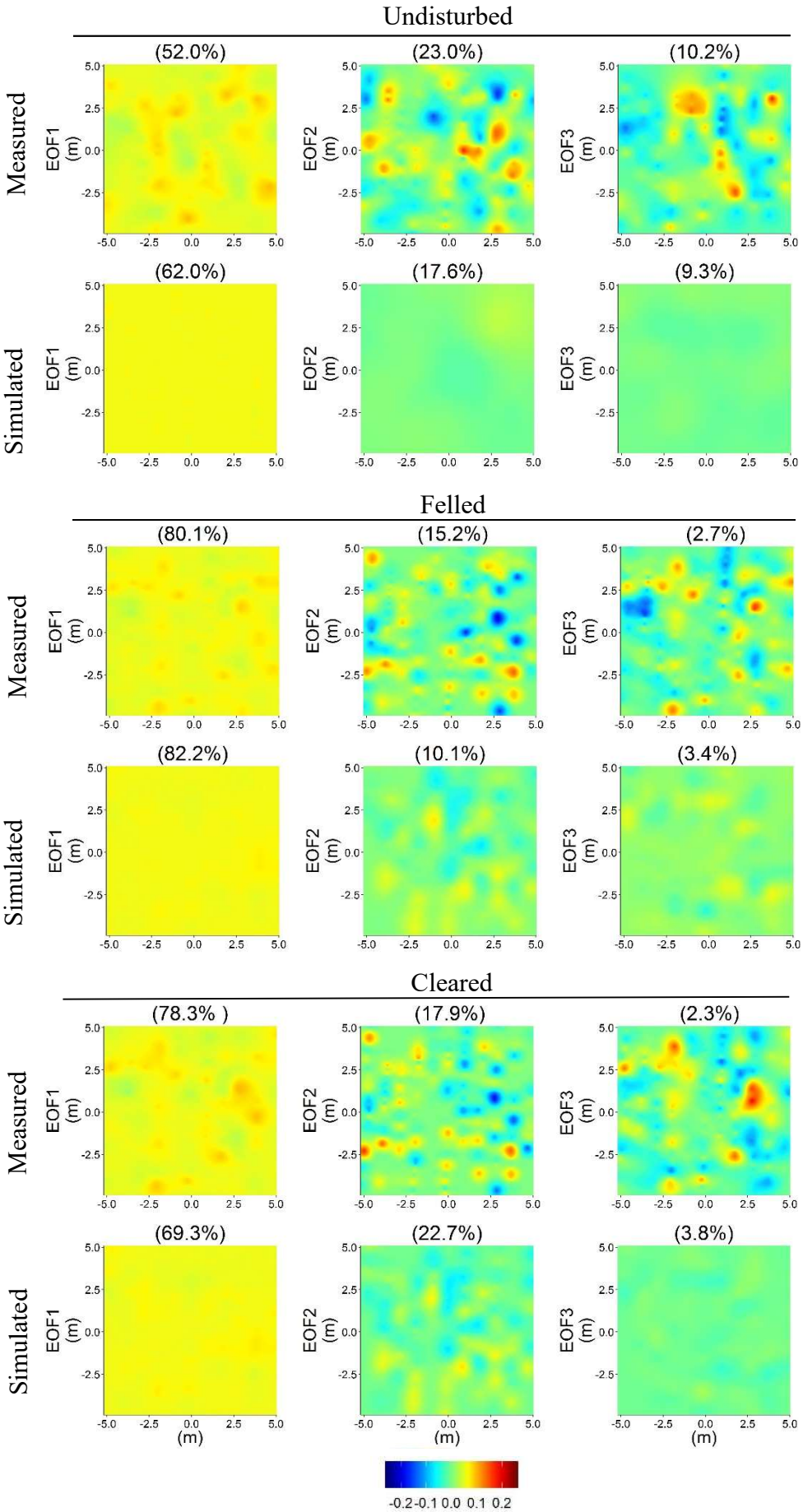

Figure 3-1, The first three EOFs (dimensionless) and associated variance explained for measured and simulated data, derived from hourly mean temperature.

Table 3-1, Spearman's rank correlation coefficient (r) comparing the spatial patterns of EOF1 between undisturbed and treatment conditions for measured data and simulated data.

		Undisturbed *21/05/2015*	Undisturbed *22/05/2015*	Undisturbed *24/05/2015*	Undisturbed *26/05/2015*
Measured Data	Undisturbed *21/05/2015*	1.00	0.96	0.96	0.97
	Undisturbed *22/05/2015*	0.96	1.00	0.96	0.94
	Undisturbed *24/05/2015*	0.96	0.96	1.00	0.96
	Undisturbed *26/05/2015*	0.97	0.94	0.96	1.00
	Felled *30/05/2015*	**0.58**	**0.60**	**0.67**	**0.63**
	Cleared *03/06/2015*	**0.49**	**0.49**	**0.60**	**0.56**
Simulated Data	Undisturbed *21/05/2015*	1.00	0.74	0.78	0.77
	Undisturbed *22/05/2015*	0.74	1.00	0.87	0.79
	Undisturbed *24/05/2015*	0.78	0.87	1.00	0.88
	Undisturbed *26/05/2015*	0.77	0.79	0.88	1.00
	Felled *30/05/2015*	**0.60**	**0.60**	**0.69**	**0.56**
	Cleared *03/06/2015*	**0.49**	**0.53**	**0.65**	**0.51**

3.5.2 Model Scenarios

Peat surface hotspots are zero when the system is homogeneous, i.e. simulations with no tree cover, no shrub cover, no microtopography, with no variation in surface cover species (single species cover), uniform depth to ice, uniform initial surface temperatures and fixed surface resistance values (Figure 3-2). Increasing the layers of heterogeneity increases the hotspot intensity up to 5 layers of system heterogeneity. The most extreme hotspot intensity is observed with shrubs, microtopography, *S. fuscum* only groundcover, spatially explicit ice depths and starting surface temperatures, and a log-normal distribution of resistance. On average, increasing the number of layers of heterogeneity above five reduces the hotspot intensity. The observed significant changes in hotspots may be due to either changes in the mean temperatures (Figure SI3-3), as a result of changes in shading and incidents of direct radiation reaching the

ground surface or changes in maximum temperatures (Figure SI3-4) as a result of variations in slope and aspect, and/or both.

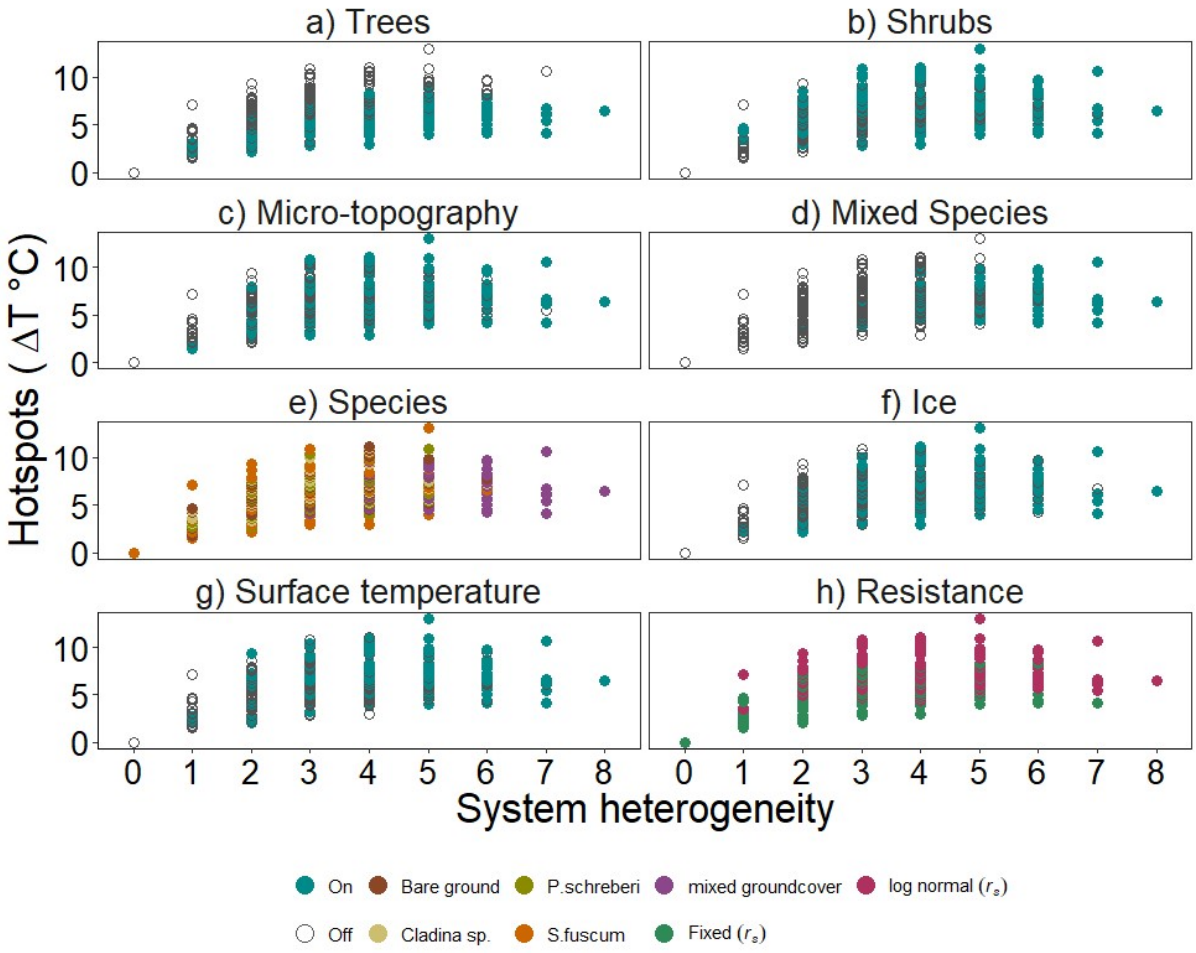

Figure 3-2, each tile shows hotspots values (ΔT °C) of all simulations (at depth 2cm), with the different colours representing each tested component of the system. a) Trees *(On vs Off),* b) Shrubs *(On vs Off),* c) Micro-topography *(On vs Off),* d) Mixed *(mixed species groundcover vs single species groundcover),* e) Species *(each groundcover type),* f) Ice *(On vs Off*), g) Initial surface temperature (observed surface temperatures *(On)* vs average of the observed surface temperatures *(Off))* and h) *Resistance (log-normal distribution vs fixed value surface resistance).*

Tree layer presence significantly decreases the simulated median temperatures and hotspot temperature. It also significantly alters the spatial patterning of surface temperatures (Figure 3-3. Table SI3-6). The presence of a shrub layer significantly decreases median simulated temperatures and significantly increases hotspot temperature but has no significant influence

on thermal patterning. Micro-topography significantly shifts spatial patterning and hotspot location but has no significant impact on median temperatures. The spatially varying ice layer has no significant effect on hotspots, median temperatures or the spatial thermal regime. Data where observed initial surface temperatures were used showed significantly greater hotspots compared to data where average initial surface temperatures were used. No significant differences were found in median temperatures or thermal patterning. The spatial patterning of surface temperatures significantly changes when uniform ground covers are compared to mixed groundcovers, but no significant changes are seen in hotspots or median temperatures. *S. fucum* and mixed groundcover scenarios showed significantly reduced median temperatures but no significant influence over hotspots. Only mixed groundcover scenarios showed significant increases in spatial patterning (Figure 3-3, Table SI3-7, SI3-6). All model scenarios where the ground cover layer surface resistance is drawn from a log-normal distribution shows no differences in median temperatures but shows significantly greater hotspots and significantly greater deviance in thermal patterning from undisturbed conditions (Figure 3-3).

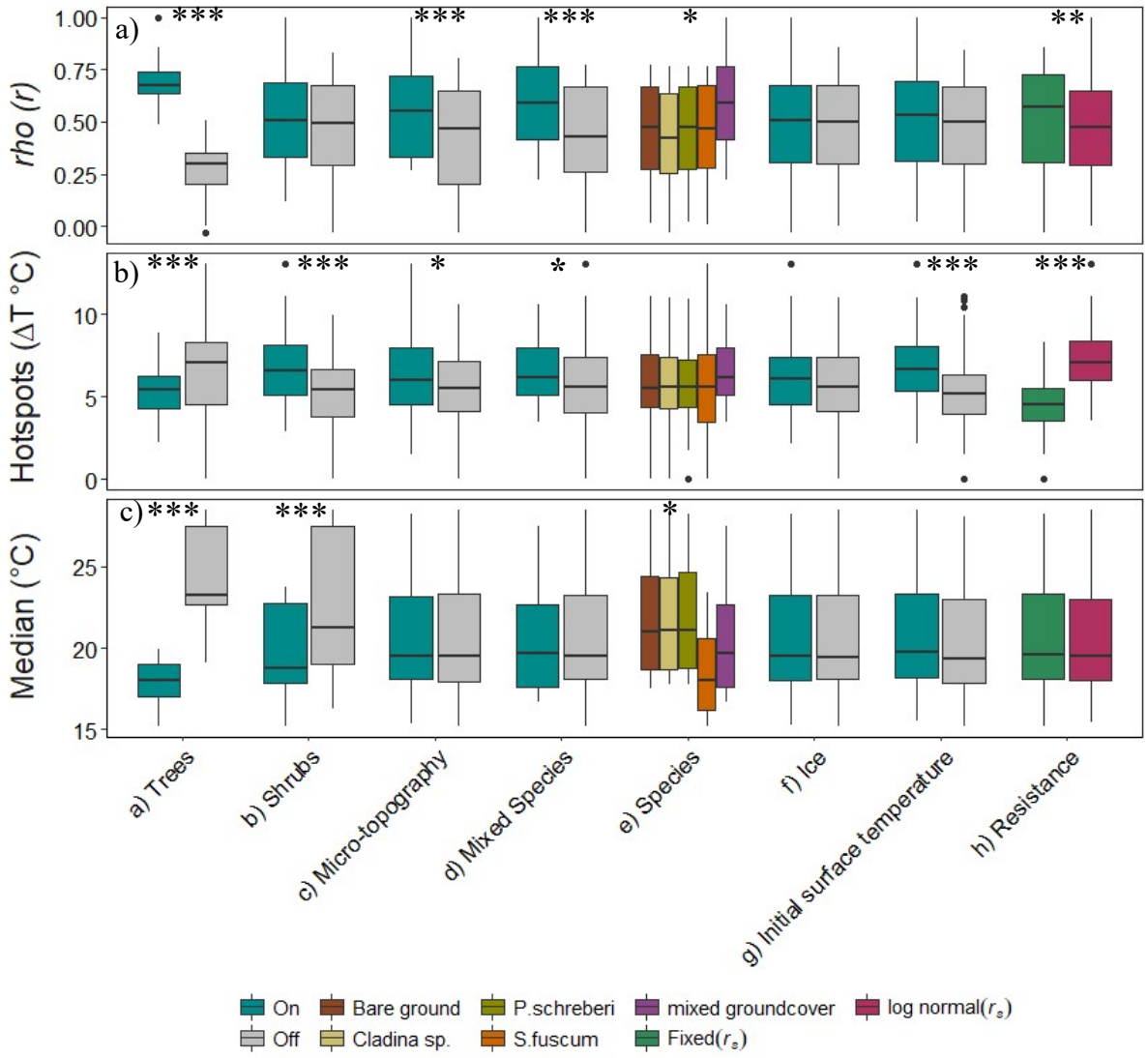

**Figure 3-3, Each of the three tiles contain data relating to the daily median temperature (°C), daily hotspots (Δ*T* °C) and changes in spatial distributions (rho (*r*) values closest to one show least change from the undisturbed system). Each component on the x-axis represents data from all scenarios, with the different colours representing the presence/absence/type of layer heterogeneity tested. i.e. a) Trees *(data from all scenarios with trees on vs data from all scenarios with trees off)*, b) Shrubs *(data from all scenarios with shrubs on vs data from all scenarios with shrubs off)*, c) Micro-topography *(data from all scenarios with micro-topography on vs data from all scenarios with microtopography off)*, d) Mixed Species *(data from all scenarios with mixed groundcover on vs data from all scenarios with single species groundcover)*, e) Species *(data from all scenarios comparing each groundcover type*), f) Ice Shrubs *(data from all scenarios with ice on vs data from all scenarios with ice off)* g) Initial surface temperature (*observed surface temperatures (On) vs average of the observed surface temperatures (Off)* and h) Resistance *(data from all scenarios with log-normal distribution of surface resistances (r_s) vs data from all scenarios with fixed value surface resistances (r_s)). Boxplots represent the median, 25th and 75th percentile (whiskers: smallest and largest observed value that's less than*

*or equal to the lower/upper hinge -/+ 1.5 * IQR). Asterisks denote significant differences between each layer option (Table SI3-6).*

3.6 DISCUSSION

3.6.1 Model evaluation

PHI-BETA-THETA represented the spatio-temporal peat-surface temperature dynamics well, replicating observed changes in spatial patterning of EOF1 between undisturbed, felled and cleared conditions (Figure 3-1, Table 3-1). Further, the average *rho* values decreased between undisturbed and felled and when cleared was also well replicated. However, greater variation in spatial patterning (*rho* (*r*)) of EOF1 was observed within simulated than observed undisturbed temperatures (range of 1 to 0.74 compared to 1 to 0.94; Table 3-1), which may be the result of variations in the cable burial depth (+/ 1.5 cm). Cable buried deeper will be consistently cooler and cable buried shallower consistently warmer during the simulated daytime growing season temperatures. Any such bias in the measured peat temperatures will impact the ranking of values in the spearman rank correlation analysis, providing stronger correlations between the patterns in EOF 1 derived from measured undisturbed data (Table 3-1).

Warmer simulated morning temperatures, compared to measured, are highly likely the result of over-night soil moisture recharge processes such as fog, dew deposition and distillation (Carleton & Dunham, 2003), and capillary rise (Admiral & Lafleur, 2007; Yazaki *et al.*, 2006) lowering the surface temperatures. Dew was also observed to freeze the peat surface to ~1 cm depth and remain frozen during the start of some measurement days. Recharge and surface freezing processes were not captured by the model and were the likely source of greater deviance between the measured and simulated temperatures early in the day (Figure SI3-2).

Lower day-time temperatures simulated by the model compared to measured temperatures may in part result from the model not adequately representing aerodynamic properties. Aerodynamic resistance is assumed to be constant for all treatment conditions (calculated according to Kettridge *et al*., (2013)). However, vegetation height influences soil temperatures (Green *et al.*, 1984; Kelliher *et al.*, 1993) through increasing aerodynamic resistance (Kettridge *et al*., 2013).

3.6.2 Influence of heterogeneity on surface thermal regime and system functioning

Simulations broadly support the hypothesis of Leonard *et al*., (2018) that peat surface hotspot intensity is linked to ecosystem heterogeneity (Figure 3-2). However, maximum hotspots were observed when five layers of heterogeneity are present (Figure 3-2) rather than one as previously hypothesised. The 9.1 °C range in hotspot temperature when five layers are present suggests that not all system layers of heterogeneity have an equal influence. The hypothesis that the maximum hotspots are observed only when one layer of heterogeneity is present (Leonard *et al*., 2018) is likely true if all layers have equal influence over the thermal regime and the heterogeneity of each layer was independent from the next. However, co-dependence in the observed system layers is likely (e.g. between trees and sub-canopy vascular species as they compete for resources such as light) resulting in layers of heterogeneity with varying influences over system hotspots. Ice depth variation and groundcover type are the only layers that do not significantly influence peat surface hotspots (Figure 3-3, Table SI3-6, Table SI3-7).

Critically, results show that changes in the spatio-temporal dynamics may occur, potentially inducing an overall shift in system functioning, without a significant change in median temperature (Figure 3-3, Table SI3-6, Table SI3-7). Peatland system functioning is a balance of spatially varying process feedbacks that include; hydrological processes, ecological succession and competition, productivity and decomposition (Waddington *et al.*, 2015) (which often produce distinctive peatland surface patterning ; Aber *et al*., 2002). Shifts in peat-surface

thermal patterning and dynamics will shift rates and locations of thermally driven processes such as productivity, species competition, decomposition, and evapotranspiration. As a result, the system is placed under a heterogeneous stress because hotspots have shifted locations and may have dis-proportionate effects on system process rates (Johnstone *et al.*, 2016). Locations where inherent resilience to increased peat surface temperatures had developed, e.g. microbial acclimation to elevated temperatures (Bradford *et al.*, 2008; Kaiser *et al.*, 2014), no longer align with the new peat-surface temperature signature. If spatial changes result in process rates that breech thresholds and tipping points, they could irreversibly shift the balance of key system feedbacks (Belyea, 2009, Rietkerk & van de Koppel, 2008, Waddington *et al.*, 2015) and cause significant shifts in system functioning (Génin *et al.*, 2018; Johnstone *et al.*, 2016; Schneider & Kefi, 2016).

Models used to predict changes to system functioning rarely consider the heterogeneous nature of disturbances on systems where significant changes in the average values of process drivers are observed, let alone heterogeneous shifts where no significant changes in average process drivers are observed. To fully understand system functioning and its response to disturbance, a more comprehensive understanding of spatio-temporal responses to heterogeneous stresses is recommended. Researchers should consider the spatio-temporally heterogeneous nature of any disturbance and the likely impact of this on the spatio-temporal dynamics of balanced system feedback mechanisms.

3.7 REFERENCES

Aber, J. S., Aaviksoo, K., Karofeld, E. & Aber, A. W. (2002) Patterns in Estonian bogs as depicted in color kite aerial photographs. *Suo* **53**(1), 1–15.

Admiral, S. W. & Lafleur, P. M. (2007) Partitioning of latent heat flux at a northern peatland.

Aquat. Bot. **86**(2), 107–116. doi:10.1016/j.aquabot.2006.09.006

Al-Kayssi, A. W. (2002) Spatial variability of soil temperature under greenhouse conditions. *Renew. Energy* **27**(3), 453–462. doi:10.1016/S0960-1481(01)00132-X

Belyea, L R & Clymo, R. S. (2001) Feedback control of the rate of peat formation. *Proc. Biol. Sci.* **268**(1473), 1315–1321. doi:10.1098/rspb.2001.1665

Belyea, Lisa R. & Baird, A. J. (2006) Beyond 'the limits to peat bog growth': Cross-scale feedback in peatland development. *Ecol. Monogr.* **76**(3), 299–322. doi:10.1890/0012-9615(2006)076[0299:BTLTPB]2.0.CO;2

Belyea, Lisa R. (2009) Nonlinear Dynamics of Peatlands and Potential Feedbacks on the Climate System. In: *Carbon Cycling in Northern Peatlands* (A. J. Baird, L. R. Belyea & Co, eds.), Geophysica., 5–18. Washington, D.C.: American Geophysical Union.

Blok, D., Heijmans, M. M. P. D., Schaepman-Strub, G., Ruijven, J. van, Parmentier, F. J. W., Maximov, T. C. & Berendse, F. (2011) The Cooling Capacity of Mosses: Controls on Water and Energy Fluxes in a Siberian Tundra Site. *Ecosystems* **14**(7), 1055–1065. doi:10.1007/s10021-011-9463-5

Bradford, M. A., Davies, C. A., Frey, S. D., Maddox, T. R., Melillo, J. M., Mohan, J. E., Reynolds, J. F., *et al.* (2008) Thermal adaptation of soil microbial respiration to elevated temperature. *Ecol. Lett.* **11**(12), 1316–1327. doi:10.1111/j.1461-0248.2008.01251.x

Brand, D. G. (1990) Growth analysis of responses by planted white pine and white spruce to changes in soil temperature, fertility, and brush competition. *For. Ecol. Manage.* **30**(1–4), 125–138. doi:http://dx.doi.org/10.1016/0378-1127(90)90131-T

Brown, M. & Lowe, D. G. (2005) Unsupervised 3D Object Recognition and Reconstruction in Unordered Datasets. *Fifth Int. Conf. 3-D Digit. Imaging Model.*, 56–63. doi:doi:10.1109/3DIM.2005.81, 2005.

Brown, S. M., Petrone, R. M., Mendoza, C. & Devito, K. J. (2010) Surface vegetation controls on evapotranspiration from a sub-humid Western Boreal Plain wetland. *Hydrol. Process.* **24**(8), 1072–1085. doi:10.1002/hyp.7569

Bubier, J. L., Rock, B. N. & Crill, P. M. (1997) Spectral reflectance measurements of boreal wetland and forest mosses. *J. Geophys. Res. Atmos.* **102**(D24), 29483–29494. doi:10.1029/97JD02316

Carleton, T. J. & Dunham, K. M. M. (2003) Distillation in a boreal mossy forest floor. *Can. J. For. Res.* **33**(4), 663–671. NRC Research Press. doi:10.1139/x02-197

Croft, P. J., Shulman, M. D. & Avissar, R. (1993) Cranberry stomatal conductivity. *HortScience* **28**(11), 1114–1116.

Dawson, A. (2016) eofs: A Library for EOF Analysis of Meteorological, Oceanographic, and Climate Data. *J. Open Res. Softw.* **4**, 4–7. doi:10.5334/jors.122

Delucia, E. H. (1986) Effect of low root temperature on net photosynthesis, stomatal conductance and carbohydrate concentration in Engelmann spruce (Picea engelmannii Parry ex Engelm.) seedlings. *Tree Physiol.* **2**(1_2_3), 143–154. Retrieved from http://www.ncbi.nlm.nih.gov/pubmed/14975849

Dijkstra, P., Thomas, S. C., Heinrich, P. L., Koch, G. W., Schwartz, E. & Hungate, B. A. (2011) Effect of temperature on metabolic activity of intact microbial communities: Evidence for altered metabolic pathway activity but not for increased maintenance respiration and reduced carbon use efficiency. *Soil Biol. Biochem.* **43**(10), 2023–2031. Elsevier Ltd. doi:10.1016/j.soilbio.2011.05.018

Essery, R., Bunting, P., Rowlands, A., Rutter, N., Hardy, J., Melloh, R., Link, T., *et al*. (2008) Radiative Transfer Modeling of a Coniferous Canopy Characterized by Airborne Remote Sensing. *J. Hydrometeorol.* **9**(2), 228–241. doi:10.1175/2007JHM870.1

Folwell, S. S., Harris, P. P. & Taylor, C. M. (2015) Large-scale surface responses during European dry spells diagnosed from land surface temperature. *J. Hydrometeorol.* **17**, 975–993. doi:10.1175/JHM-D-15-0064.1

Foster, D. R., King, G. A., Glaser, P. H. & Wright Jr, H. E. (1983) Origin of string patterns in boreal peatlands. *Nature* **306**, 256. Nature Publishing Group. Retrieved from http://dx.doi.org/10.1038/306256a0

Frei, S., Knorr, K. H., Peiffer, S. & Fleckenstein, J. H. (2012) Surface micro-topography causes

hot spots of biogeochemical activity in wetland systems: A virtual modeling experiment. *J. Geophys. Res. Biogeosciences* **117**(4), 1–18. doi:10.1029/2012JG002012

Génin, A., Majumder, S., Sankaran, S., Schneider, F. D., Danet, A., Berdugo, M., Guttal, V., *et al*. (2018) Spatially heterogeneous stressors can alter the performance of indicators of regime shifts. *Ecol. Indic.* (October). doi:10.1016/j.ecolind.2017.10.071

Genuchten, M. T. Van. (1980) A closed-form equation for predicting the hydraulic conductivity of unsaturated soils. *Soil Sci. Soc. Am. J.* **44**(5), 892–898. doi:10.2136/sssaj1980.03615995004400050002x

Green, F. H. W., Harding, R. J. & Oliver, H. R. (1984) The relationship of soil temperature to vegetation height. *J. Climatol.* **4**(3), 229–240. doi:10.1002/joc.3370040302

Hardy, J. P., Melloh, R., Koenig, G., Marks, D., Winstral, A., Pomeroy, J. W. & Link, T. (2004) Solar radiation transmission through conifer canopies. *Agric. For. Meteorol.* **126**(3–4), 257–270. doi:10.1016/j.agrformet.2004.06.012

Hopkinson, C., Chasmer, L. E., Sass, G., Creed, I. F., Sitar, M., Kalbfleisch, W. & Treitz, P. (2005) Vegetation class dependent errors in lidar ground elevation and canopy height estimates in a boreal wetland environment. *Can. J. Remote Sens.* **31**(2), 191–206. Taylor & Francis. doi:10.5589/m05-007

Idso, S. B., Jackson, R. D., Reginato, R. J., Kimball, B. A. & Nakayama, F. S. (1975) The Dependence of Bare Soil Albedo on Soil Water Content. *J. Appl. Meteorol.* doi:10.1175/1520-0450(1975)014<0109:TDOBSA>2.0.CO;2

Johnstone, J. F., Allen, C. D., Franklin, J. F., Frelich, L. E., Harvey, B. J., Higuera, P. E., Mack, M. C., *et al*. (2016) Changing disturbance regimes, ecological memory, and forest resilience. *Front. Ecol. Environ.* **14**(7), 369–378. doi:10.1002/fee.1311

Juszczak, R., Humphreys, E., Acosta, M., Michalak-Galczewska, M., Kayzer, D. & Olejnik, J. (2013) Ecosystem respiration in a heterogeneous temperate peatland and its sensitivity to peat temperature and water table depth. *Plant Soil* **366**(1–2), 505–520. doi:10.1007/s11104-012-1441-y

Kaiser, C., Franklin, O., Dieckmann, U. & Richter, A. (2014) Microbial community dynamics

alleviate stoichiometric constraints during litter decay. *Ecol. Lett.* **17**(6), 680–690. doi:10.1111/ele.12269

Kelliher, F. M., Leuning, R. & Schulze, E. D. (1993) Evaporation and canopy characteristics of coniferous forests and grasslands. *Oecologia* **95**(2), 153–163. doi:10.1007/BF00323485

Kellner, E. (2001) Surface energy fluxes and control of evapotranspiratoin from a Swedish Sphagnum mire. *Agric. For. Meteorol.* **110**(2), 101–123. doi:10.1016/S0168-1923(01)00283-0

Kellner, Erik & Halldin, S. (2002) Water budget surface-layer water storage in a Sphagnum bog in Central Sweden. *Hydrol. Process.* **16**(1), 87–103. doi:10.1002/hyp.286

Kettridge, N. & Baird, a. (2008) Modelling soil temperatures in northern peatlands. *Eur. J. Soil Sci.* **59**(2), 327–338. doi:10.1111/j.1365-2389.2007.01000.x

Kettridge, N. & Baird, a. J. (2007) In situ measurements of the thermal properties of a northern peatland: Implications for peatland temperature models. *J. Geophys. Res. Earth Surf.* **112**(2), 1–12. doi:10.1029/2006JF000655

Kettridge, N., Lukenbach, M. C., Hokanson, K. J., Hopkinson, C., Devito, K. J., Petrone, R. M., Mendoza, C. A., *et al*. (2017) Low Evapotranspiration Enhances the Resilience of Peatland Carbon Stocks to Fire. *Geophys. Res. Lett.* 9341–9349. doi:10.1002/2017GL074186

Kettridge, N., Thompson, D. K., Bombonato, L., Turetsky, M. R., Benscoter, B. W. & Waddington, J. M. (2013) The ecohydrology of forested peatlands: Simulating the effects of tree shading on moss evaporation and species composition. *J. Geophys. Res. Biogeosciences* **118**(2), 422–435. doi:10.1002/jgrg.20043

Kettridge, N., Thompson, D. K. & Waddington, J. M. (2012) Impact of wildfire on the thermal behavior of northern peatlands: Observations and model simulations. *J. Geophys. Res. Biogeosciences* **117**(G2), n/a-n/a. doi:10.1029/2011JG001910

Kettridge, Nicholas & Baird, A. J. (2010) Simulating the thermal behavior of northern peatlands with a 3-D microtopography. *J. Geophys. Res.* **115**(G3), G03009. doi:10.1029/2009JG001068

Kirschbaum, M. U. F. (1995) The temperature dependence of soil organic matter decomposition, and the effect of global warming on soil organic C storage. *Soil Biol. Biochem.* **27**(6), 753–760. doi:10.1016/0038-0717(94)00242-S

Lafleur, P. M., Moore, T. R., Roulet, N. T. & Frolking, S. (2005) Ecosystem respiration in a cool temperate bog depends on peat temperature but not water table. *Ecosystems* **8**(6), 619–629. doi:10.1007/s10021-003-0131-2

Leonard, R. M., Kettridge, N., Devito, K. J., Petrone, R. M., Mendoza, C. A., Waddington, J. M. & Krause, S. (2018) Disturbance Impacts on Thermal Hot Spots and Hot Moments at the Peatland-Atmosphere Interface. *Geophys. Res. Lett.* 1–9. doi:10.1002/2017GL075974

Lewis, F. J. & Dowding, E. S. (1926) The Vegetation and Retrogressive Changes of Peat Areas (" Muskegs ") in Central Alberta. *Br. Ecol. Soc.* **14**(2), 317–341.

Mckenzie, J. M., Siegel, D. I., Rosenberry, D. O., Glaser, P. H. & Voss, C. I. (2007) Heat transport in the Red Lake Bog , Glacial Lake Agassiz Peatlands **378**(December 2006), 369–378. doi:10.1002/hyp

McKenzie, J. M., Voss, C. I. & Siegel, D. I. (2007) Groundwater flow with energy transport and water–ice phase change: Numerical simulations, benchmarks, and application to freezing in peat bogs. *Adv. Water Resour.* **30**(4), 966–983. doi:http://dx.doi.org/10.1016/j.advwatres.2006.08.008

Moore, P. A., Lukenbach, M., Thompson, D. K., Kettridge, N., Granath, G. & Waddington, J. M. (2019) Assessing the peatland hummock-hollow classification framework using high-resolution elevation models: Implications for appropriate complexity ecosystem modelling. *Biogeosciences Discuss.* (in review). doi:https://doi.org/10.5194/bg-2019-20

Peters-Lidard D., C., Blackburn, E., Liang, X., Wood F., E., Peters-Lidard, C. D., Blackburn, E., Liang, X., *et al*. (1998) The Effect of Soil Thermal Conductivity Parameterization on Surface Energy Fluxes and Temperatures. *J. Atmos. Sci.* **55**(7), 1209–1224. doi:10.1175/1520-0469(1998)055<1209:TEOSTC>2.0.CO;2

Petrone, R. M., Devito, K. J., Silins, U., Mendoza, C., Brown, S. C., Kaufman, S. C. & Price, J. S. (2008) Transient peat properties in two pond-peatland complexes in the sub-humid

Western Boreal Plain , Canada. *Mires Peat* **3**, 1–13.

Rajic, N. (2002) Principal component thermography for flaw contrast enhancement and flaw depth characterisation in composite structures. *Compos. Struct.* **58**(4), 521–528. doi:10.1016/S0263-8223(02)00161-7

Redding, T. E. & Devito, K. J. (2006) Particle densities of wetland soils in northern Alberta, Canada. *Can. J. Soil Sci.* **86**(1), 57–60. NRC Research Press. doi:10.4141/S05-061

Rietkerk, M. & Koppel, J. van de. (2008) Regular pattern formation in real ecosystems. *Trends Ecol. Evol.* **23**(3), 169–175. doi:10.1016/j.tree.2007.10.013

Schneider, F. D. & Kefi, S. (2016) Spatially heterogeneous pressure raises risk of catastrophic shifts. *Theor. Ecol.* 207–217. doi:10.1007/s12080-015-0289-1

Sjörs, H. (1961) Surface patterns in boreal peatland. *Endeavour* **20**, 217-24.

Soudzilovskaia, N. A., Bodegom, P. M. van & Cornelissen, J. H. C. (2013) Dominant bryophyte control over high-latitude soil temperature fluctuations predicted by heat transfer traits, field moisture regime and laws of thermal insulation. *Funct. Ecol.* **27**(6), 1442–1454. doi:10.1111/1365-2435.12127

Stoy, P. C., Street, L. E., Johnson, A. V., Prieto-Blanco, A. & Ewing, S. A. (2012) Temperature, Heat Flux, and Reflectance of Common Subarctic Mosses and Lichens under Field Conditions: Might Changes to Community Composition Impact Climate-Relevant Surface Fluxes? *Arctic, Antarct. Alp. Res.* **44**(4), 500–508. doi:10.1657/1938-4246-44.4.500

Taggart, M. J., Heitman, J. L., Vepraskas, M. J. & Burchell, M. R. (2011) Surface shading effects on soil C loss in a temperate muck soil. *Geoderma* **163**(3–4), 238–246. Elsevier B.V. doi:10.1016/j.geoderma.2011.04.020

Thompson, D. K., Benscoter, B. W. & Waddington, J. M. (2014) Water balance of a burned and unburned forested boreal peatland. *Hydrol. Process.* **28**(24), 5954–5964. doi:10.1002/hyp.10074

Thompson, D. K. & Waddington, J. M. (2013) Wildfire effects on vadose zone hydrology in forested boreal peatland microforms. *J. Hydrol.* **486**, 48–56.

doi:10.1016/j.jhydrol.2013.01.014

Turunen, J., Tomppo, E., Tolonen, K. & Reinikainen, A. (2002) Estimating carbon accumulation rates of undrained mires in Finland – application to boreal and subarctic regions. *The Holocene* **1**(2002), 69–80.

Waddington, J. M., Morris, P. J., Kettridge, N., Granath, G., Thompson, D. K. D. & Moore, P. a. P. (2015) Hydrological feedbacks in northern peatlands. *Ecohydrology* (8), 113–127. doi:10.1002/eco.1493

Wieder, R. K., Scott, K. D., Kamminga, K., Vile, M. a., Vitt, D. H., Bone, T., Xu, B., *et al*. (2009) Postfire carbon balance in boreal bogs of Alberta, Canada. *Glob. Chang. Biol.* **15**(1), 63–81. doi:10.1111/j.1365-2486.2008.01756.x

Woods, K. D., Feiveson, A. H. & Botkin, D. B. (1991) Statistical error analysis for biomass density and leaf area index estimation. *Can. J. For. Res.* **21**(7), 974–989. NRC Research Press. doi:10.1139/x91-135

Wullschleger, S. D., Cahoon, J. E., Ferguson, J. a & Oosterhuis, D. M. (1991) SURFTEMP : Simulation of Soil Surface Temperature Using the Energy Balance Equation. *J. Agron. Educ.* **20**(1).

Yazaki, T., Urano, S. I. & Yabe, K. (2006) Water balance and water movement in unsaturated zones of Sphagnum hummocks in Fuhrengawa Mire, Hokkaido, Japan. *J. Hydrol.* **319**(1–4), 312–327. doi:10.1016/j.jhydrol.2005.06.037

3.8 SUPPORTING INFORMATION FOR CHAPTER THREE

Supporting information for Chapter three is composed of two distinct sections: Section SI3-1 and Section SI3-2.

Section SI3-1 supports the methods section of the main article and provides a detailed description of the numerical modelling components of PHI- BETA-THETA.

Contents of this section;

- Text S1
- Table SI3-1 to SI3-4
- Figure SI3-1

Section SI3-2 supports the results and discussion sections of Chapter 3

Contents of this section;

- Text S2
- Figure SI3-2 to SI3-5
- Table SI3-5 to SI3-8

3.8.1 Section SI3-1 Model description and information on model parameters

This section supports the methods section of the main article by providing a more detailed description of the numerical model used. In addition, more details of data collection methods, analysis and results are provided for site specific model parameters; Microtopography, Albedo, Surface and stomatal resistance, and other additional data for model parameterization.

PHI-BETA-THETA

The peatland hydrological impacts (PHI) model is a physio-empirical model developed to investigate the role of peatland ecosystem complexity through process interactions and feedbacks. Fluxes of energy and mass in the simulation domain are one-dimensional (1D), where surface energy balance is simulated using BETA (Kettridge *et al.*, 2013), and soil thermal dynamics using the PHI version of HIP-1D (Kettridge & Baird, 2008); THErmal Transfer Algorithm (THETA). THETA is simply a MATLAB encoded version of HIP-1D which integrates with other PHI components. Although mass and energy transfer through the soil-vegetation-atmosphere continuum is modelled in 1D, this chapter investigated the role of spatial heterogeneity of vegetation, surface cover, and microtopography.

Microtopography

A digital elevation model (DEM) of the simulation domain (the 10 x 10 m plot) was created from a 3D point cloud generated using a structure-from-motion approach (Brown & Lowe, 2005, Moore *et al.*, 2019). Ground control points, surveyed using a dGPS, were used to scale, level, and orient the point cloud. The DEM was produced on a 0.01 m × 0.01 m grid using the MATLAB function TriSctteredInterp (MATLAB R2017a, The Mathworks) and smoothed using a 3 × 3 mean filter window. Surface slope and aspect were calculated from a planar fit to

the eight-connected neighbours of a given point. Elevation at a given point was used to set the local water table depth.

THETA

THETA is a finite-difference Fourier-based heat transfer algorithm which simulates soil temperature using vertically discretized soil layers, where energy transfer is governed by conduction and vapour diffusion. The effect of freezing/thawing on temperature change is incorporated using an energy sink/source term (*cf.* McKenzie *et al.*, 2007), where ice affects soil thermal properties through a change in both heat capacity (C) and thermal conductivity (k). For soil temperature to cross the freezing point, the heat of fusion for water must first be satisfied. This heat transfer algorithm is implemented in THETA using conditional statements and simple book-keeping of latent heat storage of a given layer based on volumetric water content (θ). Volumetric water content was calculated based soil pore-water pressure (ψ) using the van Genuchten parameterization of soil water retention (Van Genuchten, 1980);

$$\boldsymbol{\theta(\psi) = \theta_r + \frac{\theta_s - \theta_r}{(1+|\alpha\psi|^n)^{1-1/n}}} \qquad \text{(Equation SI 3-1)}$$

where θ_s and θ_r are the saturated and residual water contents, respectively. The inverse of air-entry pressure (α), and pore size index (n) are fitted parameters. Herein, we set α and n based on empirical relations to bulk density (ρ_b) derived from Thompson & Waddington (2013). The θ_s is estimated from peat bulk density (ρ_b, Mg m^{-3}) according to Redding & Devito, (2006):

$$\boldsymbol{\theta_s = 1 - \frac{\rho_b}{1470}} \qquad \text{(Equation SI 3-2)}$$

Residual water contents (θ_r) was set to zero in the simulations, since this assumption was made in deriving α and n in Thompson & Waddington (2013). Pore-water pressure is prescribed in our simulations, where the magnitude of ψ is equal to the height above the water table for a given node. Initial boundary conditions were set by linearly interpolating measured peat

temperature with depth. The lower boundary condition was set using the temperature measured at depth from the water level recorder (0.8 m below a hollow). The solution for ground heat flux (see BETA below) is used as an upper boundary condition for THETA, and where THETA passes soil temperature and thermal properties of the first soil layer to BETA.

BETA

The Boreal Ecohydrology Tree Algorithm (BETA) is a 1D surface-vegetation-atmosphere transfer model which simulates the energy and radiation balance for a forested peatland (Kettridge *et al.*, 2013). Using the Penman-Monteith model, latent, sensible, and ground heat flux at the surface are calculated by iteratively solving for the surface temperature which closes the energy balance equation. Aerodynamic resistance is calculated according Kettridge *et al.*, (2013) and surface resistance is prescribed based on measured values. For each ground cover type (bare peat, *Sphagnum fuscum, Pleurozium schreberi*, and *Cladina sp.*), the measured distribution of surface resistance from chamber measurements (SI3-2) are used to run multiple iterations of the simulation, with surface resistance randomly chosen from the ground cover-dependent distribution. Sub-canopy latent heat flux is modelled using the same approach and is parameterized based on measured vegetation type, leaf area index, and average leaf-level resistance. The radiation balance is calculated based on how the size and spatial arrangement of trees affect radiation interception, and is modelled after Essery *et al.*, (2008).

Solar insolation

The effect of surface slope and aspect on solar insolation were calculated according to Kettridge & Baird, (2010), where terrain shading is not taken into account. Tree shading in BETA is modelled after Essery *et al.*, (2008) who present an analytical solution for calculating path lengths through the canopy based on sun-earth geometry and by representing canopy cross-

sectional area as an ellipse. Transmissivity of radiation through the canopy is based on Beer's law:

$$\boldsymbol{p_c = e^{-G(\theta)\sum \lambda l_t}} \qquad \text{(Equation SI 3-3)}$$

where p_c is the probability of light passing through the canopy, G is the foliage projection function (default parameterization is a random foliage distribution), θ is the solar elevation angle, and l_t is the ray path length. A volumetric representation of the tree canopy was implemented so that tree shape can be prescribed and foliage density can be made non-uniform/heterogeneous. Individual trees are represented by voxels of user-definable size (0.05 m × 0.05 m × 0.05 m herein) each with its own foliage area volume density (λ) ($m^2_{\text{foliage area}}$ m^{-3}_{volume}). Unlike analytical solutions to calculate path length through the canopy (e.g. Essery *et al.*, 2008), the voxel representation of the tree canopy requires projection of each voxel onto the simulated surface. Based on solar azimuth and elevation, the projected location on the surface is calculated using the centroid of each voxel in the tree canopy. The peatland surface is discretized as a raster with pixel of user-definable dimensions (0.01 m × 0.01 m herein) on which voxel centroids are projected. Based on voxel size and solar azimuth-elevation, the voxel 'shadow' is distributed about projected centroid location. Total incident radiation at the surface in a given pixel is the sum of the product of individual voxel path length and foliage density. For computational efficiency and to reduce memory requirements for large number of voxels, location data for both voxels and surface location are stored as integers, and p_c calculations done using single-precision numbers. The use of integers for the coordinate system allows the position of data within a 2- D (surface) or 3D array (tree voxels) to correspond with its physical location, allowing for rapid indexing.

Canopy structure from imagery

Canopy imagery (from the trees within the 10 x 10 m plot) was used to gather information on canopy light interception with height and radially from the tree trunk (*cf.* Kettridge *et al.*, 2013). Probability of light interception was evaluated based on voxel dimensions (i.e. 0.05 m × 0.05 m area). Because of the unknown horizontal path length through the tree along the axis of the camera view, the percentage of pixels classified as vegetation was used as a weighting function to assign foliage area volume in the canopy. Vegetation weights were averaged both radially and with height, then rotated about the central axis of the tree to produce a 3D representation of the tree canopy. Although direct estimates of foliage area volume were not possible, it was assumed that the average number of vegetation classified pixels per unit volume scaled with average foliage area volume. Tree volume was estimated from the projected area of trees derived from photos. Average (±std) foliage area volume for a given tree was assigned by scaling the distribution of average vegetation-classified pixel density to 3.87 ± 1.7 m^{-1}. The position of each tree within the plot was measured using a differential GPS to 2 cm accuracy.

Albedo

The albedo of *Cladina sp* was set to 0.22 (Stoy *et al.*, 2012), *Sphagnum* spp was set to 0.135 (Bubier *et al.*, 1997), *P. schreberi* was set to 0.19 (Bubier *et al.*, 1997), Bare ground albedo was set to 0.13 (Idso *et al.*, 1975).

Surface and stomatal resistance

Between June and August 2014 surface resistance to evapotranspiration was measured from areas with a 100% cover of; *S. fuscum* (n=32), *P. schreberi* (n=43), *Cladina sp* (n=21) and bare ground (n=33). A closed chamber setup was used to measure surface resistance, following the McLeod *et al.,* (2004) approach. A 12.6 L plexiglass chamber was lowered over the ground for

a time period of two minutes while the air inside was mixed by a small fan. Measurements of humidity were recorded every 1.6s using a PP systems EGM4 infra-red gas analyser. Soil surface temperatures were recorded from a depth of 0.02 m below the ground/bryophyte surface. The linear change in vapour density within the first 35 seconds allowed calculation of evapotranspiration rate (ET) (Stannard, 1988). All measurement dates and locations were randomly selected between May and August, provided there was no precipitation on the day of measurement.

The surface resistance to evaporation (r_s) is calculated as follows:

$$\boldsymbol{r_s} = \frac{\rho_{vs}^{*} - \rho_{va}}{ET} - \boldsymbol{r_a} \qquad \text{(Equation SI 3-4)}$$

where, ρ_{vs} is the saturation vapour density of the peat surface, ρ_{va} is the vapour density of the air within the chamber, r_a, the aerodynamic resistance within the chamber during a measurement, was calculated by placing the chamber over a water bath at room temperature (r_s = 0) and calculating evaporation accordingly using the same method and duration as the field measurements).

Stomatal resistance (s m^{-1}) was calculated from measurements of stomatal conductance (mm s^{-1}) taken by an AP4 Delta-T leaf Porometer. Measurements were taken between 9 am and 4 pm on dry days during the 2014 and 2015 growing seasons. Plants were randomly located and, where possible, 3 leaves of each plant were measured.

Mean leaf area was calculated from n = 67 leaves each of the following species; *Rhododendron groenlandicum, Rubus chamaemorus*, *Chamaedaphne calyculata, Maianthemum trifolia*, and *Vaccinium vitus-idea*. Leaves were carefully hand-picked from stems in the field,

photographed against a white background and later processed in Image J to obtain individual leaf area values (cm^2).

The surface resistance of the mosses and vascular species are calculated according to (Kettridge *et al.*, 2017). The stomatal resistance of the dominant species (*Vaccinium vitus-idea;* 252 s m^{-1}) was divided by the LAI of each plot to give a conservative estimate of $r_{vascular}$.

$$r_{total} = \frac{1}{\frac{1}{r_{ground\ surface}} + \frac{1}{r_{vascular}}} + r_{a\ chamber} \qquad \text{(Equation SI 3-5)}$$

Results: Stomatal resistance and Leaf Area

Table SI 3-1, Descriptive statistics of stomatal resistance (sm^{-1}) of vascular sub-canopy species found at the study site (BC35).

	Median	st dev	n	st error
Maianthemum trifolia	231.95	126.41	26	25.28
Rubus chamaemorus	607.97	303.15	218	20.58
Chamaedaphne calyculata	520.13	193.15	62	24.73
Rhododendron groenlandicum	551.49	286.79	213	19.70
Vaccinium vitus-idea	252.12	109.07	177	8.22

Our results are comparable to the range of stomatal resistances found in literature of 215 sm^{-1} (Kettridge *et al.*, 2017) to 546 sm^{-1} (Thompson *et al.*, 2014) for *Rhododendron groenlandicum* 395 +/- 196 sm^{-1} (Kettridge *et al*., 2017*)* for *Rubus chamaemorus,* and 500 to 125 sm^{-1} (Croft *et al.*, 1993) for *Vaccinium spp.*

Table SI 3-2, Statistics describing leaf area of vascular sub-canopy species found at the study site (BC35).

Species	Mean (cm^2)	Standard deviation	Standard error
Vaccinium vitus-idea	0.28	0.14	0.02
Rubus chamaemorus	11.61	7.64	0.94
Rhododendron groenlandicum	0.84	0.54	0.07
Maianthemum trifolia	3.63	1.76	0.22
Chamaedaphne calyculata	0.76	0.37	0.05

.

Results: Groundcover Surface and Sub-canopy vascular surface resistance

Relative humidity (%) and air temperature did not differ significantly between species plots (Kruskal-Wallis chi-squared = 1.74, df = 3, p-value = 0.63; Kruskal-Wallis chi-squared = 3.78, df = 3, p-value = 0.29). *P. schreberi, S. fuscum,* Bare ground and *Cladina sp* showed median r_{moss} of 791, 88, 456 and 778 sm^{-1} respectively. r_{moss} was significantly different between species (r_{moss} is significantly lower in *S. fucum* plots: Kruskal-Wallis chi-squared = 41.95, df = 3, p-value = <0.001). Median $r_{GroundSurface}$ for *S. fucum* are within the range reported in literature (Thompson *et al.,* 2014, 78-56 s m^{-1}; Kettridge *et al.,* 2017, 207-295 s m^{-1}).

Table SI 3-3, Comparing surface resistance of r_s, $r_{GroundSurface}$ and $r_{vascular}$ for each category of ground cover.

	r_s (s m^{-1})	standard deviation	$r_{GroundSurface}$ (s m^{-1})	standard deviation	$r_{vascular}$ (s m^{-1})	standard deviation	*n*
Cladina sp.	492.1	75363.1	778.3	23103.1	1716.5	11296.8	18
Bare ground	394.0	18924.5	455.8	1232.4	1361.4	4350.2	27
P.schreberi	499.7	270595.1	790.7	888.8	1044.1	1693.4	37
S. fuscum	83.2	19040.8	87.9	299.7	886.9	4350.2	31

Table SI 3-4, Dunn test results showing the differences in $r_{GroundSurface}$ between species are only significant for *S. fuscum*

comparison	Z	P.unadj	P.adj
Bare -P. schreberi	-0.93	0.35	0.53
Bare-S. fuscum	4.60	**<0.001**	**<0.001**
P. schreberi - S. fuscum	5.93	**<0.001**	**<0.001**
Bare-Cladina sp	-0.53	0.60	0.72
P. schreberi-Cladina sp	0.26	0.80	0.80
S. fuscum-Cladina sp	-4.63	**<0.001**	**<0.001**

Additional data for model parameterization

Standard meteorological data were collected from a 10m tower approx. 350m from the plot throughout the measurement period. At the start of the measurement period, Leaf Area Index (LAI) (measured using LICOR LAI 2000), ice depth (measured using a steel rod), soil moisture (measured using a ML3 Theta probe) and ground cover type (visual identification) at each measurement and simulation location (0.25 intervals along the length of the FO-DTS cable) were recorded.

Figure SI 3-1, Showing a typical bare peat patch from the study site (BC35).

3.8.2 Section SI3-2 Additional results.

This section supports the results and discussion of the main article.

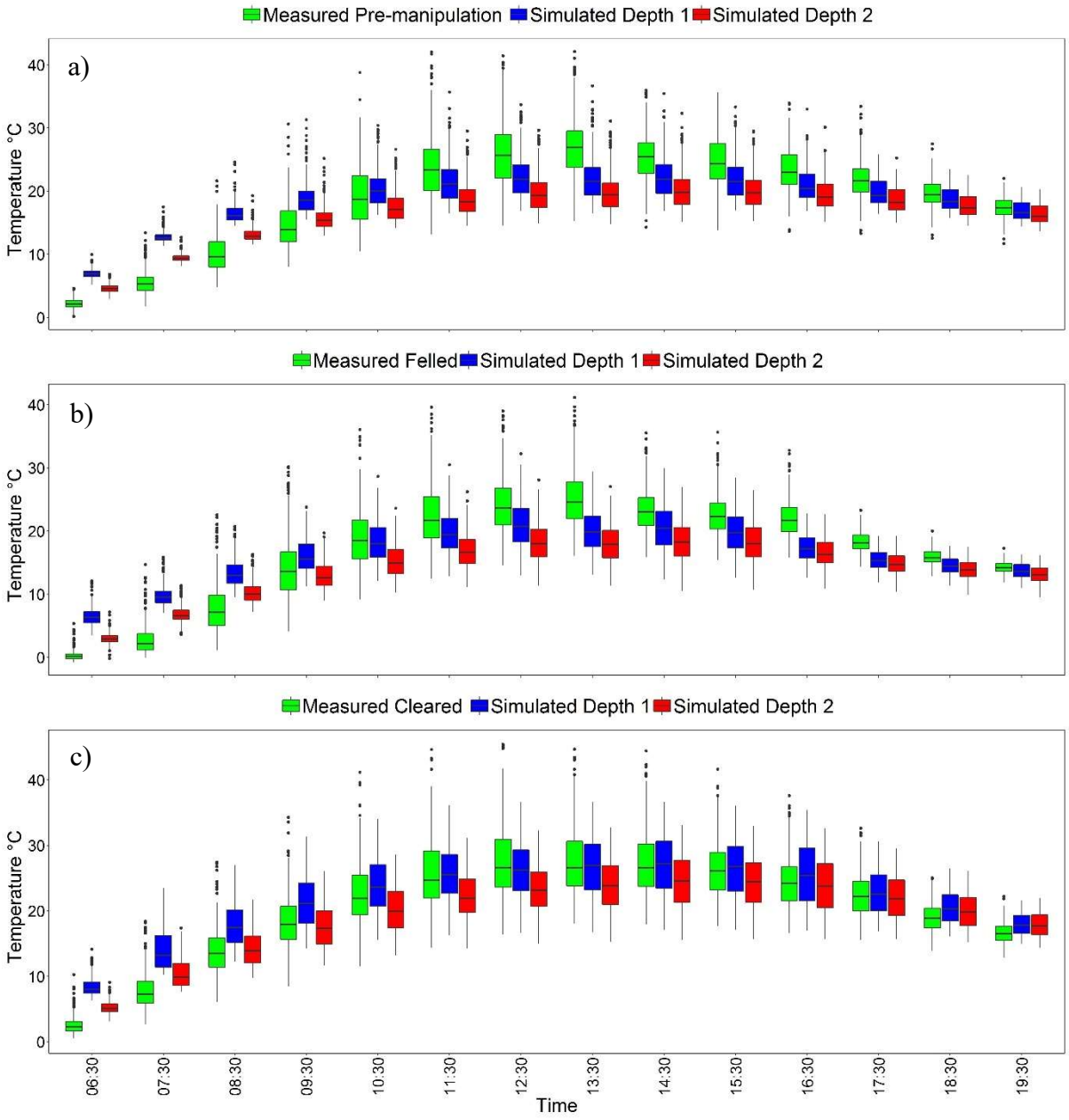

Figure SI 3-2, Box plots representing the median, 25th and 75th percentile (whiskers: smallest and largest observed value that's less than or equal to the lower/upper hinge -/+ 1.5 * IQR) derived from hourly mean measured and simulated data (depth 1cm and depth 2cm) under (a) Undisturbed conditions, (b) Felled conditions, and (c) Cleared conditions (n = 305)

Table SI 3-5, Showing % groundcover sampled from plot and % groundcover used for evaluation of model performance.

	% data points modelled locations for evaluation	% data points sampled from plot
S. fuscum	56	43
Bare ground	24	25
Cladina sp	13	11
P. schreberi	7	9
Cotton grass	0	4
missing data	0	4
other non-sphagnum species	0	3

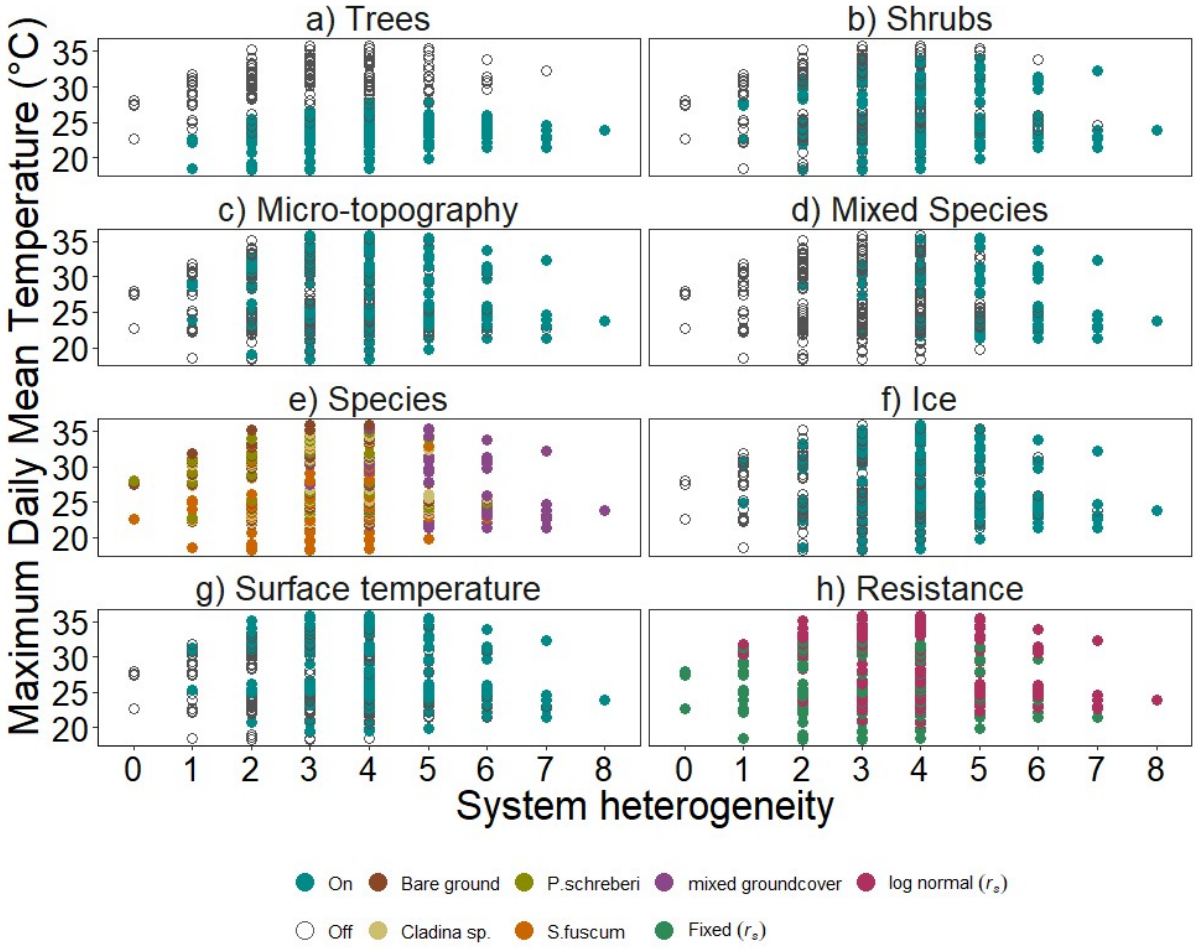

Figure SI 3-3, Each tile shows the maximum temperatures (°C) (i.e. maximum value of daily mean temperatures (°C) at each spatial location) of each simulation (at depth 2cm), with the different colours representing each tested component of the system. a) Trees *(On vs Off)*, b) Shrubs *(On vs Off)*, c) Micro-topography *(On vs Off)*, d) Mixed *(mixed species groundcover vs single species groundcover)*, e) Species *(each groundcover type)*, f) Ice *(On vs Off)*, g) Initial surface temperature (*observed surface temperatures (On) vs average of the observed surface temperatures (Off)* and h) Resistance *(log-normal distribution vs fixed value surface resistance).*

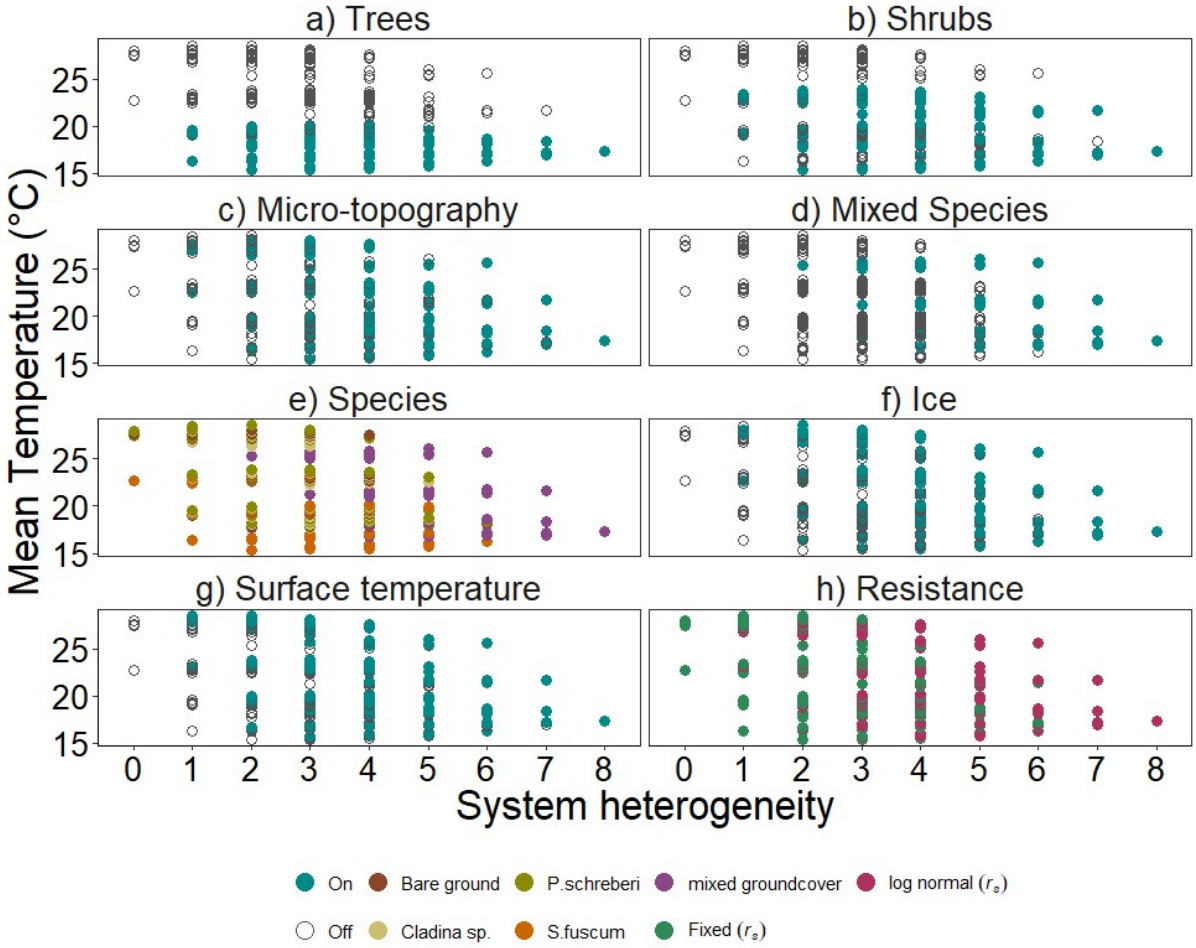

Figure SI 3-4, Each tile shows mean daily temperature values (°C) (i.e. mean value of daily mean temperatures (°C) at each spatial location) of each simulation (at depth 2cm), with the different colours representing each tested component of the system. a) Trees *(On vs Off)*, b) Shrubs *(On vs Off)*, c) Micro-topography *(On vs Off)*, d) Mixed *(mixed species groundcover vs single species groundcover)*, e) Species *(each groundcover type)*, f) Ice *(On vs Off)*, g) Initial surface temperature (*observed surface temperatures (On) vs average of the observed surface temperatures (Off)* and h) Resistance *(log-normal distribution vs fixed value surface resistance)*

Table SI 3-6, Wilcoxon rank sum test results to show which layers have a significant impact on Median temperatures, Hotspots and changes in spatial distributions of temperatures (*rho* values of each scenario compared to undisturbed conditions; EOF1).

	Spearman rank	**Median**	**Hotspots**
	p -value	p -value	p -value
Trees (With vs Without)	**<0.0001*** **	**<0.0001*** **	**<0.0001*** **
Shrubs (with Vs without)	0.09	**<0.0001*** **	**<0.0001*** **
Micro-topography (On Vs flat)	**<0.0001*** **	0.97	**0.042***
Surface cover (mixed vs single species)	**<0.0001*** **	0.82	**0.027***
Ice (with Vs without)	0.96	0.80	0.18
Initial surface temerature (average vs observed)	0.17	0.10	**<0.0001*** **
Resistance (Log normal distirbution of r_{moss} vs fixed value r_{moss}.	**0.001***	0.70	**<0.0001*** **

Table SI 3-7, Dunn test results to show which species are have significant differences of Median temperatures, Hotspots and changes in spatial distributions of temperatures (*rho* values of each scenario compared to undisturbed conditions; EOF1).

	Hotspots			*rho*			Median		
	Z-statistic	**unadjusted P- value**	**adjusted P- value**	**Z-statistic**	**unadjusted P- value**	**adjusted P- value**	**Z-statistic**	**unadjusted P- value**	**adjusted P- value**
Bare ground- *P.schreberi*	0.284	0.777	0.971	-0.049	0.961	0.961	-0.826	0.409	0.511
Bare ground - *Cladina ps.*	0.137	0.891	0.891	0.723	0.470	0.783	-0.287	0.774	0.774
P.schreberi* - *Cladina ps.	-0.147	0.883	0.981	0.772	0.440	0.880	0.540	0.589	0.655
Bare ground - Mixed	-1.464	0.143	0.358	**-3.741**	**0.000**	**0.001**	**2.335**	**0.020**	**0.028**
***P.schreberi* - Mixed**	-1.747	0.081	0.403	**-3.692**	**0.000**	**0.001**	**3.161**	**0.002**	**0.004**
***Cladina ps.* - Mixed**	-1.600	0.110	0.365	**-4.464**	**0.000**	**0.000**	**2.621**	**0.009**	**0.018**
Bare ground - *S. fuscum*	0.695	0.487	0.975	0.062	0.950	1.000	**4.945**	**0.000**	**0.000**
P.schreberi* - *S. fuscum	0.411	0.681	0.973	0.111	0.912	1.000	**5.771**	**0.000**	**0.000**
Cladina ps.* - *S. fuscum	0.558	0.577	0.961	-0.661	0.509	0.727	**5.231**	**0.000**	**0.000**
Mixed - *S. fuscum*	2.158	0.031	0.309	**3.803**	**0.000**	**0.001**	**2.610**	**0.009**	**0.015**

CHAPTER FOUR : FOREST STAND COMPLEXITY CONTROLS ECOSYSTEM-SCALE EVAPOTRANSPIRATION DYNAMICS: IMPLICATIONS FOR LANDSCAPE FLUX SIMULATIONS

4.1 ABSTRACT

Forest structure and organisation in open-canopy systems exhibit substantial controls on system process dynamics such as evapotranspiration (ET). The energy reaching sub-canopy forest layers is greater in open-canopy systems compared to closed canopy systems, inducing variability in the distribution of energy that drives ET as well as species composition and organisation. Open-canopy forested systems are found across a range of terrestrial biomes yet, the impact of their structural complexity and organisation on whole system ET dynamics is poorly understood. Using the PHI-BETA-THETA model and measured Eddy Covariance data from a boreal treed peatland, this chapter critically evaluate how stand compositional and organisational complexity influences ET dynamics. Model simulations iteratively increase complexity from a simple 'big-leaf' model, to a model representing spatial and temporal variability of all system layers. This chapter shows the effect of each complex system component on stand ET dynamics. Critically, we demonstrate that including spatio-temporal canopy and radiation variability increases ET model estimates by ~25.5 %, reduces unexplained variance by 8% and reduces hysteresis in model outputs. These results have clear implications for flux modelling of forest systems, demonstrating that substantial improvements to model simulations can be made by spatially and temporally defining the variability in incoming solar radiation.

4.2 INTRODUCTION

Globally, forests occupy ~30% of the land surface (Bonan, 2008) and exhibit strong controls over the hydrological cycle (Ellison *et al.*, 2017). Forest evapotranspiration (ET) is a globally important process responsible for re-distributing water both locally and globally (by re-charging atmospheric moisture) whilst, simultaneously, acting as an important water loss mechanism that controls the hydrological balance and system functioning of forests (Jackson *et al.*, 2001). Accurate quantification and prediction of forest ET and its components is crucial to improve understanding of hydrological, climatic, and ecosystem processes, benefiting water resource management (Brutsaert, 2010; McNaughton & Jarvis, 1983), hydrological modelling (Zhao *et al.*, 2013), weather forecasts, and forest vulnerability to fire (Boer *et al.*, 2016), especially under a changing climate (Brümmer *et al.*, 2012).

Vascular plants primarily control atmospheric exchange processes in dense, closed canopy systems (Black *et al.*, 1996; Ferretti *et al.*, 2003; Hossein *et al.*, 1994; Leuning *et al.*, 1994; Wallace *et al.*, 1993; Williams *et al.*, 2004; Wilson *et al.*, 2001). However, many forests are composed of sparsely distributed vascular vegetation, often due to limiting factors such as nutrient availability and hydrological status. As a result, a large proportion of energy reaches sub-canopy layers (Baldocchi *et al.*, 2000) and ET is dominated by energy exchange within the under-story (Allen, 1990; Baldocchi *et al.*, 2000; Villegas *et al.*, 2014; Villegas *et al.*, 2010; Vogel & Baldocchi, 1996; Yunusa *et al.*, 1997). Sparse canopies of this type thus have complicated ET dynamics. These complicated ET dynamics are impacted by the number of contributing vertical layers and their interaction as a result of stand structure and complexity (Villegas *et al.*, 2014; Villegas *et al.*, 2010). Plants act as roughness elements and influence airflow, turbulence regimes, mass and energy exchange through this subcanopy (Breshears *et al.*, 2009; Martens *et al.*, 2000). Canopy attributes such as height, extent of leaf coverage along

the stem, tree density, and leaf density and clumping also modify spatio-temporal patterns in drivers (Green *et al.* 1984; Villegas *et al*. 2010; Kettridge *et al.* 2013) and controllers of ET. Canopy individuals not only modify the environment directly beneath them but also the environment in adjacent areas. Notably, shading reduces energy inputs directly below the canopy as well as within canopy gaps (Villegas *et al.,* 2014). The spatial distribution of environmental conditions is not the only mechanism by which forest architecture influences ET. The physical effects of forest architecture also influence the species composition and organisation of lower layers through processes of competition, extinction and establishment. In fact, open-canopy systems show relatively high sub-canopy diversity because of the increased variability in environmental conditions found in the sub-canopy layers (Sagar *et al.*, 2008). This variability in sub-canopy species is an important influence on ET dynamics because different plant species (within and between functional groups) have variable albedo and show significant differences in their ability to conduct water to the atmosphere (Heijmans *et al.*, 2004; Lafleur, 1990; De Sena *et al.*, 2007). Evapotranspiration from the under-storey layers is therefore highly variable in space and time due to the complicated eco-hydrological system organisation. This highly variable nature of ET in open canopy systems illustrates that vertical and/or horizontal aggregation of complex non-linear systems to 'big-leaf' behaviours (common within empirical models; Shuttleworth, 2007) may be inappropriate for representing stand level ET dynamics (Friend, 2001; Villegas *et al.*, 2014; Villegas *et al.*, 2010).

Using a boreal peatland forest as an exemplar ecosystem, this chapter assesses how stand structure and compositional organisation influence ET. Characteristically open-canopy, treed peatlands occupy ~24% of the boreal forest region (Joosten & Clarke, 2002), which itself makes up ~33% of global forest cover (~10% of the earth's vegetated surface; McGuire *et al*., 1995). Boreal peatlands are one of the world's largest terrestrial carbon stores, accounting for a

conservative estimate of ~500 GtC (Bradshaw & Warkentin, 2015; Yu, 2012), which is ~60% of the global atmospheric carbon pool (~830 GtC) (Ciais *et al.*, 2013; Joos *et al.*, 2013; Prather *et al.*, 2012) and about equal to all of the carbon in living terrestrial vegetation (450 to 650 GtC; Prentice and Harrison 2009; Ciais *et al.* 2013). Boreal peatland forests further perform key hydrological functions at the landscape scale (Devito *et al.*, 2005; Holden, 2005), for example by acting as important landscape water sources through the sub-humid climate of the boreal plain (Devito *et al.*, 2017). Forested peatlands and their vital system service provisions are also subject to regular and increasing disturbances such as fire (Chapin *et al.*, 2000); with almost 1,500 km^2 affected annually, releasing 6,300 Gg C yr^{-1} in western Canada alone (Turetsky *et al*., 2002). Despite their hydrological and biogeochemical importance, and exposure to increasing disturbance, boreal forest regions remain under-represented in ET literature (Fatichi & Pappas, 2017; Watras, 2017; Zhang *et al.*, 2009), especially boreal wetlands (Chapin *et al.*, 2000). Advances have been made to incorporate increasing levels of heterogeneity within Boreal peatland ET modelling (Kettridge *et al.*, 2013; Sutherland *et al.*, 2014; Sutherland *et al.*, 2017), however, to my knowledge, assessment of how small-scale stand complexity, composition and layer inter-dependencies affect ET dynamics remains largely unknown and un-explored.

Using Boreal peat forests to assess how stand structure and related organisational complexity influence ET (informing understanding of open canopy forest ET more generally) has clear advantages over other such systems. Boreal forests have some of the simplest structural architecture of any forest biome (Landsberg & Gower, 1997), comprised of even-aged communities as a result of frequent stand-initiating disturbances such as wildfires, insect outbreaks, and felling (Kurz & Apps, 1993; McCarthy, 2001). This relatively simple structure, combined with their relatively low taxonomic diversity (Burton, 2013) means more

concentrated efforts can be applied to defining the species specific characteristics, responses and behaviours, thus providing advantages to modelling, computing capacity and confidence in interpretation. In addition, the distribution of heterogeneity is relatively even across a flat open landscape (Figure 4-1). This reduces the impact of potentially confounding factors that would add uncertainty, such as, high variability in within stand tree density/size and topographical influences. This reduction of potentially confounding factors will increase confidence in model outputs and interpretation that relate directly to stand complexity effects.

This chapter critically evaluates how stand compositional and organisational complexity influences ET dynamics by using PHI-BETA-THETA, comparing sub hourly ET simulations against Eddy Covariance (EC) flux tower measurements. Understanding how ET dynamics change by representing various system complexities within the modelling domain will provide advanced understanding of how ET is controlled by the system structure and facilitate more informed and targeted future research efforts in open-canopy forested systems.

4.3 STUDY SITE

Data was collected from a deep peat (≥ 3m), poor fen in central Alberta (55.81°N, 115.11°W), Figure 4-1. The surface is characterised by a ground cover mosaic, consisting of *S. fuscum* (43% cover), *P. schreberi* (9% cover), *Cladina. sp., Cladonia sp.* (11% cover) and bare peat (26% cover). The lower vascular layer comprises *Rhododendron groenlandicum*, *Rubus chamaemorus*, *Chamaedaphne calyculata, Maianthemum trifolia*, *Vaccinium oxycoccus*, *Vaccinium vitus-idea* and *Eriophorum sp.* The upper vascular layer comprises solely of *Picea mariana* with a stand density of 16 000 stems ha^{-1}, basal area and average height of 11 $m^2\ ha^{-1}$ and 2.3 m respectively (Kettridge *et al.*, 2012). Surface microtopography varies in height by up to 0.41m (Chapter 2).

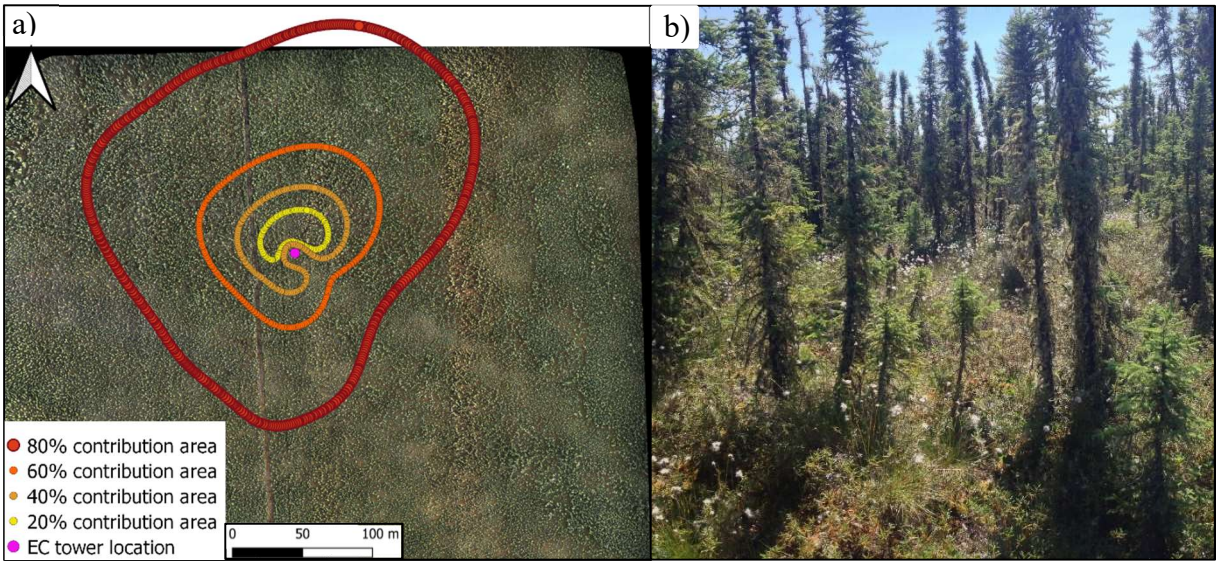

Figure 4-1, a) Aerial image of study site showing the location of the Eddy Covariance flux tower, and the areas contributing to 20%, 40%, 60% and 80% of the total flux measured between 24th of July to 13th of August 2014 and b) a photo of the vegetation structure

4.4 METHODS

4.4.1 PHI-BETA-THETA Model Summary

PHI-BETA-THETA simulates evapotranspiration from a treed boreal peatland. PHI-BETA-THETA uniquely accounts for small scale complexity when simulating the surface energy balance, ground-layer cover type and peat thermal behaviour and builds on previous modelling work, principally, PHI-BETA-THETA (Chapter 3), the Boreal Ecohydrology Tree Algorithm (BETA : Kettridge *et al.,* 2013), 3-D HIP (Kettridge and Baird, 2010) and the radiative transfer model (Essery *et al.,* 2008). Tree heights and locations are generated by a Canopy Height Model (CHM: See further description in SI4-1, supporting information) using Lidar data collected from the study site. The distribution of groundcover species (and their respective resistance and albedo values) is determined by Multivariate Adaptive Regression Splines (MARS) in accordance with (Elith & Leathwick, 2007) (See SI4-2). Sub-canopy vascular vegetation leaf area index (LAI) is randomly selected from a measured distribution (SI4-2).

Meteorological data from a 10 m high tower, (collecting net radiation, upwelling shortwave radiation, air temperature, relative humidity and wind speed data) drives the surface boundary of PHI-BETA-THETA within which net short and longwave radiation, latent heat and sensible heat fluxes were calculated. The separation of net radiation into its short and long wave components was determined using a spatially explicit 3D radiation model that depends on tree size/position and ground cover species distribution. Trees were represented within the simulated 3D landscape as crowns (SI4-1), following an approach similar to Essery *et al.,* (2008) and adapted by (Kettridge *et al*. 2013), which allows the determination of direct and diffuse shortwave radiation (through time) and sky view factor (constant) at the sub-canopy/ground surface. Net longwave radiation is calculated from Stefan-Boltzmann law, Beer's law (Aber and Melillo, 1991) and the above generated sky view factor. The model accounts for the influence of micro-topography on the short and long wave radiation by incorporating variations in elevation, slope, aspect and shading of the peat surface (surface topography of points randomly selected from measured distributions: see SI3-1, Chapter 3 supporting information) (Kettridge and Baird, 2010). Newton's law of cooling was used to calculate sensible heat flux. The Penman-Monteith model is used to calculate latent heat flux. ,

$$LE = \frac{s(T_s - T_a) + vdd_a}{r_a + r_s} \qquad \text{(Equation 4-1)}$$

Where s is the slope of the saturation vapour versus temperature curve (kg $m^{-3}K^{-1}$), T_s is surface temperature and T_a is air temperature (K), vdd_a is vapour density deficit of air (kg m^{-3}), r_a and r_s are aerodynamic and surface resistance (s m^{-1}), respectively Surface resistance (r_s) is derived from field measurements of both groundcover surface resistance ($r_{GroundSurface}$) and sub-canopy stomatal resistance ($r_{vascular}$) (See Chapter 3 supporting information for methods and results, SI3-1). Tree transpiration rates are derived from 15 instrumented trees at the study site (SI4-1).

The 1D thermal behaviour of isolated peat profiles are simulated by a finite difference Fourier based model, discretised at 0.01 m intervals. Bulk peat density and volumetric water content (VWC) are used to calculate the thermal properties at each node. The Van Genuchten equation is used to determine the VWC, with pore water retention determined from depth to water table with assumed hydrostatic equilibrium through the peat profile. The volumetric heat capacity of the soil profile is the sum of each soil constituent multiplied by their respective heat capacities. The latent heat of fusion is represented by increasing the volumetric heat capacity at 0^{o}C (*cf.* Mckenzie *et al.,* 2007). Peat thermal conductivity is calculated in accordance with Farouki (1986). Depth to water table and peat temperature were measured throughout the simulation period and used to define the water table position and the lower boundary temperature of the simulated peat profiles. When micro-topography is represented in a spatially explicit manner within PHI-BETA-THETA, the water level remains spatially uniform but the WTD varies spatially as a consequence of the defined distribution in surface elevation. When a surface micro-topography is excluded within the model, the water table depth (WTD) is uniform in space, with the peat surface elevation assumed equal to the mean surface elevation (Chapter 3, Leonard *et al.,* (2018)). Initial surface temperatures were assumed equal to air temperatures (simulations initiated at midnight). A polynomial was fitted to the surface (air) and measured peat sub surface temperatures within a single temperature string within the study site to define the initial subsurface temperatures. A detailed description of the model is available in SI3-1 (Chapter 3 supporting information).

4.4.2 Eddy Covariance

Eddy covariance data were collected from a10 m tower between 25th July and 14th August 2014 by an open path infrared gas analyser (IRGA LI7500) and sonic anemometer (CSAT 3D). Data was sampled at a rate of 20 Hz and averaged every 30 minutes (Brown *et al.,* 2010). Fluxes

were de-spiked and corrected for density effects (Leuning & Judd, 1996; Webb *et al.*, 1980), coordinate rotation corrections follow (Kaimal & Finningan, 1994; Tanner & Thurtell, 1969) and sensors were installed level and < 0.1m apart (verified by Blanford and Gay analysis; (Blanford & Gay, 1992)) to avoid the need to account for sensor separation. Friction velocity threshold of <0.15 m s^{-1} was applied (based on the friction velocity versus energy balance closure point of inflection). 60% of the data were dismissed through the QA/QC process. Measured latent and sensible heat accounted for an average of 89% of the available energy in filtered data (this is consistent with the mean of ~80 % found in EC literature :Wilson 2002). A final correction was applied to force closure of the energy balance by preserving the ratio of the turbulent fluxes, i.e. Bowen ratio, β (Barr *et al.*, 2006; Blanken *et al.*, 1997; Petrone *et al.*, 2001; Sutherland *et al.*, 2017; Twine *et al.*, 2000). Data were gap filled according to Petrone *et al.* (2007), applying the α value from the ratio of actual evapotranspiration (AET) and potential evapotranspiration (PET) to PET. Potential evapotranspiration was determined by the Priestley Taylor method. Where gap-filled data are included within figures, this is noted in figure captions.

4.4.3 Description of simulations

The modelling domain was parameterised with spatially explicit data from a 250 m radius of the EC tower (80% of the total flux is contributed from within 250 m of the measurement tower 90% of the time, Figure 4-1a). Within the 250 m radius ~12 thousand, $1m^2$, simulation locations were randomly defined. For each 30-minute time interval the 2D flux foot print was used to select and weight the contributions from the given simulations' points. 2D flux footprint contribution areas are calculated in accordance with Kljun *et al.* (2015), every 30 min. Simulations were run at 30-minute intervals for the time-period 24/07/2014 00:00 to 13/08/2014 23:30:00 MST. A total of ten scenarios were simulated (Table 3-1), each simulation

represents increasing levels of observed system complexity, to try and understand how this system complexity influences ET dynamics. The model was initially run as a simple 'big-leaf' with no representation of spatial variation within the vertical system layers and a single, uniform groundcover-type of either bare ground, *P. schreberi, S. fucsum,* or *Cladina sp.* These simulations are referred to as SGBL-BG, SGBLPS, SGBL-SF and SGBL-C. This simulation was then repeated but with the modelling parameters associated with groundcover type (surface resistance and albedo) weighted by the observed relative proportions of each groundcover type (WGBL). The next simulation in the series, WGBL- FFP, is the same as WGBL but the mean radiation and canopy openness data is the mean value for each footprint area per time interval, rather than the mean value for a 250m radius of the tower. WGSC is the same as the WBGL-FFP simulation but instead of having uniform radiation inputs, the canopy is defined, and the radiation inputs vary accordingly in space and time. The SGSC simulation then uses the spatially distributed canopy and incoming radiation parameters to predict the spatial distribution of each groundcover type using the MARS sub-model (SI4-1). The SGSCSM simulation further adds micro-topography influences, representing variability in slope and elevation (and WTD) by randomly drawing from a measured distribution. The model representing most complexity (SE) again builds on the previous simulation (SGSCSM) and adds spatial variability in the leaf area index (LAI) of dominant sub-canopy vascular species and surface resistance values (of both the simulated groundcover species and vascular plants) by randomly selecting values from measured distributions.

Table 4-1, Combinations of a uniform or spatially explicit parameterisation of forest layers for each simulated scenario.

		SGBL-PS ***(P.schreberi -big-leaf)***	**SGBL-SF** ***(S.fuscum big-leaf)***	**SGBL-C** ***(Cladonia sp. big-leaf)***	**SGBL-BP** ***(Bare Peat big-leaf)***	**WGBL** ***(Weighted groundcover big-leaf)***	**WGBL FFP** ***(Weighted groundcover & mean canopy of footprint area)***	**WGSC** ***(Weighted groundcover & Spatially explicit canopy)***	**SGSC** ***(Spatially distributed groundcover, & Spatially explicit canopy)***	**SGSCSM** ***(Spatially distributed groundcover, micro- topography & canopy)***	**SE** ***(Everything is spatially explicit)***
Radiation and canopy openness	Uniform (Mean value within 250m radius of the flux measurement tower)	✓	✓	✓	✓	✓					
	Mean value (within the footprint at each time interval)						✓				
	Spatially explicit							✓	✓	✓	✓
LAI of sub-canopy vascular	Uniform (Median value)	✓	✓	✓	✓	✓	✓	✓	✓	✓	
	Randomly assigned from measured distribution										✓
Ground cover sepcies	Uniform cover Bare peat				✓						
	Uniform cover *Cladonia. sp*			✓							
	Uniform cover *S.fuscum/*		✓								
	Uniform cover *P.schreberi*	✓									
	Weighted based on % cover					✓	✓	✓			
	Spatially explicit (Mars)								✓	✓	✓
Surface resistance (ground cover & sub-canopy vascular)	Uniform (Median value)	✓	✓	✓	✓	✓	✓	✓	✓	✓	
	Randomly assigned from measured distribution										✓

Micro-topography	Uniform (Median value)	✓	✓	✓	✓	✓	✓	✓	✓		
	Randomly assigned from measured distribution									✓	✓

4.5 RESULTS

4.5.1 Comparison of simulated and measured data.

All model scenarios, except WGBL (filtered), differ significantly from measured ET ($p<0.05$) (Table 4-2). Mean measured ET for filtered (F) and gap-filled (GF) was 6.27 mm d^{-1} (± 2.97 SD) and 2.43 mm d^{-1} (± 3.71 SD), respectively. The big leaf scenario with a uniform cover of *Cladina spp*. (SGBL-C) shows the lowest simulated ET, underestimating measured ET by 10.68% (46.8%; GF figure provided here and subsequently, in brackets). ET estimates are higher in SGBL-PS and SGBL-BP scenarios. A noticeable increase in mean ET is observed between SGBL-BP and SGBL-SF of 2.11 mm d^{-1} (1.02 mm d^{-1}). When the groundcover surface resistance (r_s) and albedo is weighted to account for species composition (WGBL) the mean simulated ET is 6.25 mm d^{-1} (3.15 mm d^{-1}). The simulated mean ET rises slightly by 0.79 mm d^{-1} (0.48 mm d^{-1}) when the mean radiation input for each time interval is used (WGBL-FFP) as opposed to the mean for the 250m radius (80% contribution area of entire simulation period).When spatially explicit canopy and radiation input is included (WGSC), mean simulated ET shows a large increase, rising by 2.17 mm d^{-1} (0.89 mm d^{-1}). A slight increase in mean simulated ET is observed when the MARS sub-model is added (predicting ground cover distribution, SGSC), increasing average ET by 0.31 mm d^{-1} (0.13 mm d^{-1}). Minimal increase (<0.1 mm d^{-1}) is observed in mean simulated ET when microtopography is included (SGSCSM). Mean simulated ET reduces by 1.55 mm d^{-1} (0.74 mm d^{-1}) in the most detailed simulation (SE), when LAI of sub-canopy vascular species and the surface resistance of both

groundcover and sub-canopy vascular layer are randomly drawn from measured distributions (Table 4-2, Figure 4-2).

Table 4-2, Descriptive statistics and Mann-Whitney U Test results comparing measured Eddy Covariance flux data and data from each simulation (data shown in Figure 4-2). Data are split into filtered and gap-filled/un-filtered data.

	Scenario	Mean (mm d^{-1})	±SD	*p*-value (<0.05)	% difference from measured	R^2	RMSE
Filtered data	SGBL-BP	4.98	2.29	<0.001	-25.85	0.55	51.68
	SGBL -C	4.27	1.93	<0.001	-46.80	0.52	53.23
	SGBL-PS	4.56	2.08	<0.001	-37.23	0.53	52.612
	SGBL -SF	7.08	3.29	<0.001	11.54	0.57	50.226
	WGBL	6.25	2.91	0.40	-0.22	0.57	50.16
	WGBL-FFP	7.04	3.32	<0.001	11.05	0.60	48.43
	WGSC	9.21	3.99	<0.001	31.93	0.69	42.62
	SGSC	9.52	4.15	<0.001	34.17	0.69	42.90
	SGSCSM	9.59	4.20	<0.001	34.65	0.69	43.10
	SE	8.04	3.62	<0.001	22.02	0.7	42.14
	EC ET	6.27	2.97	-	-	-	-
Un-filtered modelled data and gap-filled measured data	SGBL-BP	2.54	2.63	<0.001	4.39	0.75	47.93
	SGBL -C	2.20	2.25	<0.001	-10.68	0.74	49.23
	SGBL-PS	2.34	2.41	<0.001	-3.76	0.75	48.75
	SGBL -SF	3.56	3.78	<0.001	31.6	0.77	46.25
	WGBL	3.15	3.33	<0.001	22.82	0.77	46.41
	WGBL-FFP	3.47	3.76	<0.001	30.24	0.79	44.01
	WGSC	4.38	4.87	<0.001	44.45	0.87	35.18
	SGSC	4.51	5.05	<0.001	46.14	0.87	35.31
	SGSCSM	4.55	5.09	<0.001	46.52	0.87	35.47
	SE	3.81	4.32	<0.001	36.10	0.88	35.24
	EC ET	2.43	3.71	-	-	-	-

4.5.2 Impact of complexity on simulated ET dynamics.

Big-leaf (SGBL) models account for the smallest proportion of the variance observed in measured ET. Of these simulations SGBL-SF has the highest explained variance with an R^2 of 0.79 (0.57) (Table 4-2). The scenario where the groundcover was weighted to represent the relative contributions of each cover type (WGBL) has an R^2 of 0.57. Using mean radiation

inputs from the footprint area at each time interval (WGBL-FFP) only improves R^2 by 1%. A marked increase in explained variance (R^2 increases by 8% (9%)) and reduction in Root Mean Square Error (RMSE) are observed when canopy and radiation are included in a spatially explicit manner within the simulation (Table 4-2). The increase in explained variance corresponds with a reduction in hysteresis amplitude between measured and simulated ET (Figure 4-2, compare a) to f) with g) to j)). No substantial changes in explained variance are observed when micro-topography, spatially distributed groundcover species, LAI and variable surface resistances are included in model simulations (Table 4-2). Trees, sub-canopy vascular and groundcover relative contributions to ET vary among scenarios. Tree transpiration is consistently the lowest contributor, ranging from 0.22% to 1.36% of total ET. Groundcover contributions to ET dominate in all scenarios except SGBL-BP/C/PS (Table 4-3; Figure 4-2), where sub-canopy vascular contributions show highest contributions to ET. Figure 4-3 shows how the ratio of temperature to vapour pressure deficit changes throughout the day. Between the hours of 0900 and 1230, the ratio is ≥1, while between the hours of 1300 and 0830, the ratio is < 1.

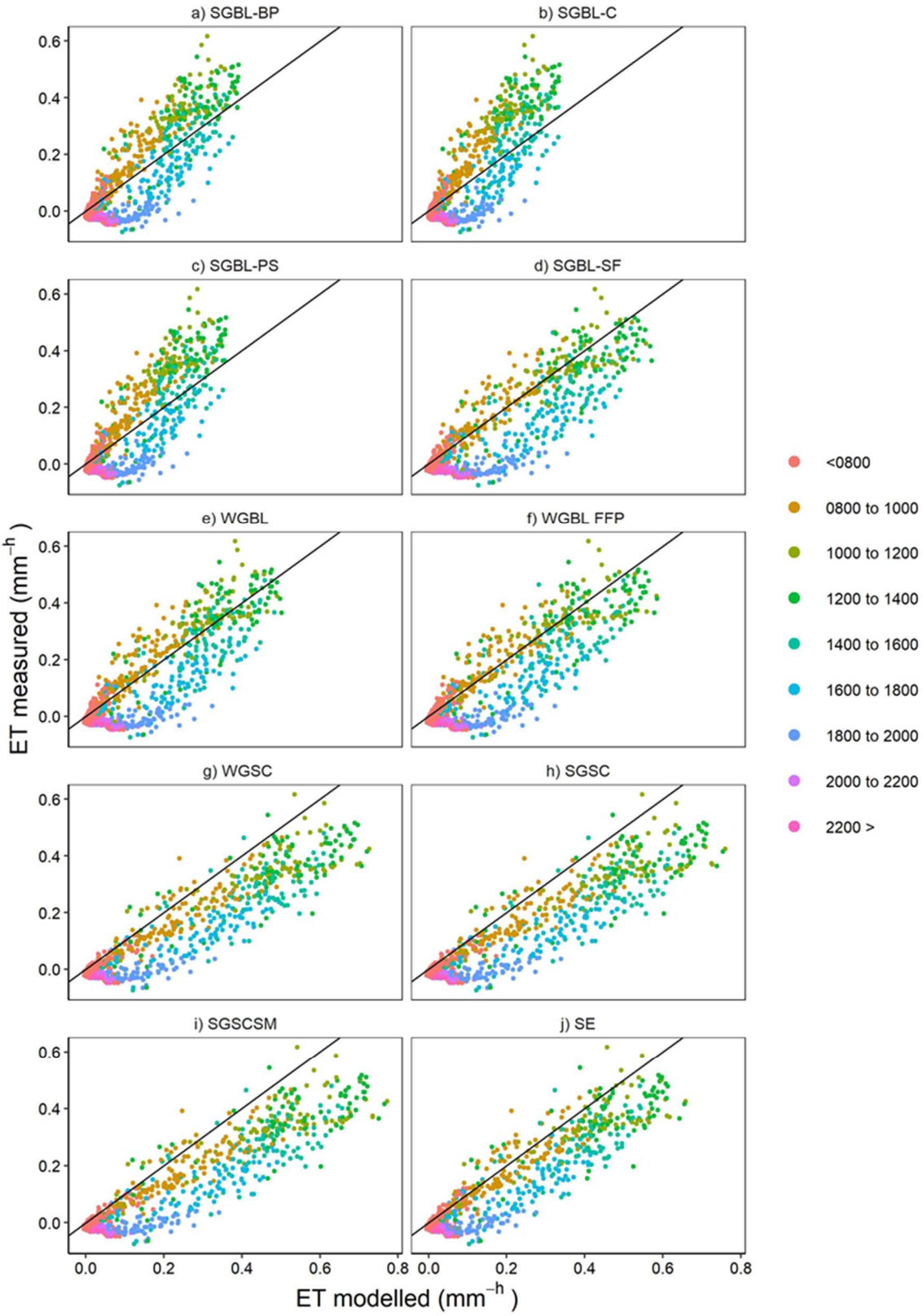

Figure 4-2, Correlation between 60-minute eddy covariance ET data and ET modelled from corresponding footprint area for each simulation.1:1 line shown on each tile (Gap-filled EC data included (60% gap-filled)). Colours show time of day.

Table 4-3, Relative contributions of each vertical system layer to ET (unfiltered modelled data), for each scenario.

	Ground cover ET (%)	**Tree ET** (%)	**Sub-canopy vascular ET** (%)	**Ground cover ET** (mm d^{-1})	**Tree ET** (mm d^{-1})	**Sub-canopy vascular** (mm d^{-1})	**Total Mean** (mm d^{-1})
SGBL-BP	44.49	1.18	54.33	1.13	0.03	1.38	2.54
SGBL -C	34.55	1.36	64.09	0.76	0.03	1.41	2.20
SGBL-PS	39.15	1.28	59.57	0.92	0.03	1.40	2.34
SGBL - SF	60.11	0.84	39.04	2.14	0.03	1.39	3.56
WGBL	59.37	0.95	39.68	1.87	0.03	1.25	3.15
WGBL-FFP	59.94	0.28	37.75	2.08	0.01	1.31	3.47
WGSC	54.69	0.23	45.08	2.39	0.01	1.97	4.38
SGSC	56.19	0.22	43.58	2.54	0.01	1.97	4.52
SGSCSM	56.48	0.22	43.30	2.57	0.01	1.97	4.55
SE	63.42	0.26	36.32	2.41	0.01	1.38	3.81

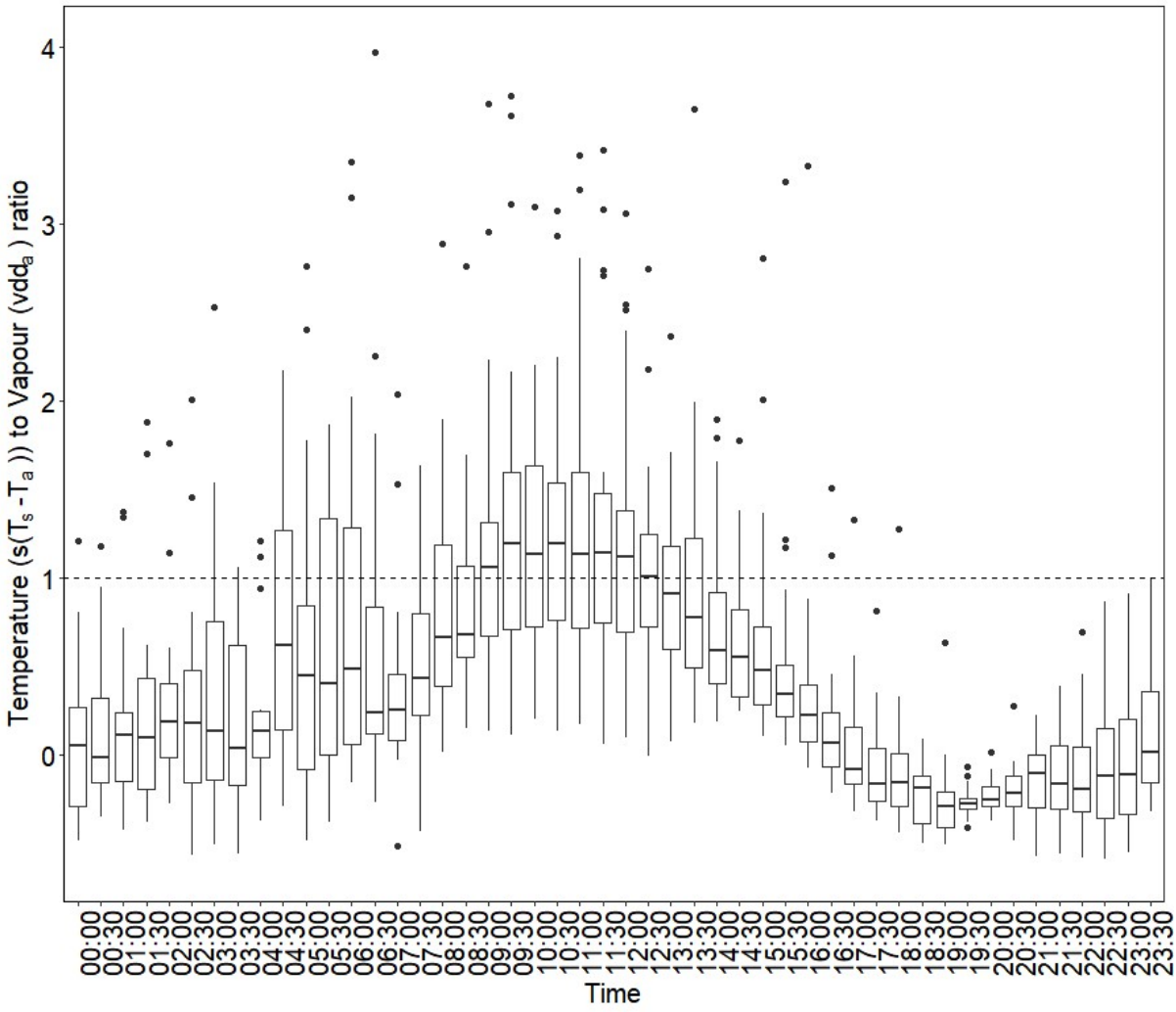

Figure 4-3, Boxplots of the ratio between the temperature (s (Ts-Ta)) and humidity (vdda) component of the Penman-Monteith equation. Data are taken from entire simulation period and plotted at 30-minute intervals between 0000 and 2330 from modelled data (SE). ***Boxplots represent the median, 25th and 75th percentile (whiskers: smallest and largest observed value that's less than or equal to the lower/upper hinge -/+ 1.5 * IQR)***

4.6 DISCUSSION

4.6.1 How do the model scenarios and measured data estimates compare?

All simulations, except SGBL-PS and SGBL-C, overestimate ET (Table 4-2). In all scenarios where *S. fuscum* (the dominant groundcover type in the measured system) is represented, ET

from the ground layer is the dominant ET contributor and supports wider research findings (Bisbee *et al.*, 2001; Bond-Lamberty *et al.*, 2011; Gabrielli, 2016; Heijmans *et al.*, 2004a). Where the relative proportions of groundcovers and their respective surface resistance and albedo properties are represented (WGBL and WGBL-FFP), where the low surface resistance S*phagnum* only represents 43% cover, ET estimates are lower than SGBL-SF but still higher than SGBL-C/BP/PS. Big-leaf model simulations with uniform groundcover of *Cladonia. sp*, *P. schreberi* and bare peat (SGBL – C/PS/BP) show lowest ET estimates and are considerably lower than a uniform cover of *S. fuscum* (SGBL-SF; Table 4-2). The large difference between mean ET estimates within the four SGBL scenarios is because *Sphagnum* surface resistance (r_s) is significantly lower than other groundcover types (Chapter 3, Chapter 5 : Heijmans *et al*. 2004), resulting in greater ground layer ET rates (Table 4-3). Increases in ET estimates when mean radiation and canopy openness from the flux footprint at each time interval is used, as opposed to the mean canopy and radiation inputs from 250m radius of the tower, is likely due to differences in radiation inputs between the mean radiation input for the 250m radius and the mean for each time interval (based on footprint area).

The higher ET rates in simulations incorporating a spatially explicit canopy (WGSE, SGSC, SGSCSM and SE) likely results from the non-linear response of groundcover ET to increased energy inputs. Spatial variability in canopy and associated radiation inputs induce highly variable surface temperatures (Chapter 2, (Leonard *et al.*, 2018) ; Chapter 3). High energy input, higher temperature surfaces with a given ground cover contribute dis-proportionately more to ET than low energy areas of the same ground cover types. This disproportional effect results from the non-linearity in the slope of the saturation humidity vs temperature curve (s) (Oke, 1987). Surfaces receiving mean energy inputs therefore evaporate less than surfaces receiving patches of higher and lower energy inputs. Tree transpiration was the lowest contributor to the

overall ET budget in all simulations (0.22 to 1.36%: Table 4-3), which is in agreement with literature estimates of 0.4% to 34% (Thompson *et al.*, 2014; Warren *et al.*, 2018) and findings from other open-canopy systems (Allen 1990; Vogel and Baldocchi 1996; Yunusa *et al*. 1997; Baldocchi *et al*. 2000; Villegas *et al*. 2010, 2014). The very low contribution of transpiration to ET is largely due to the low sapwood area (from short (2.3m average height) and sparse (11 m^2 ha^{-1}) black spruce canopy) in northern peatlands (Angstmann *et al.*, 2012; Mao *et al.*, 2017; Wieder *et al.*, 2009) in combination with waterlogged, nutrient-poor, cold conditions adversely affecting transpiration (Bovard *et al.*, 2005; Lieffers & Macdonald, 1989; Oren & Pataki, 2001; Simard *et al.*, 2007). There is a slight decrease in transpiration rates when the scenario accounts for footprint area. The likely cause of this difference is variability in sapwood density mean values derived from 250m radius area and the footprint area at each time interval.

The inclusion of spatially variable LAI and groundcover/sub-canopy surface resistance reduced ET overestimation. The log normal distribution in groundcover r_s creates areas of high surface resistance and low ground layer ET (Table 4-3). In addition, ET from the sub-canopy vascular layer in this simulation is reduced more substantially (Table 4-3). This is likely the combined effect of the log-normal distribution in sub-canopy LAI and stomatal resistance creating areas of low LAI and areas of high stomatal resistance that reduces the contribution of the vascular layer to system ET. Micro-topography and a distributed groundcover had relatively little impact on simulated ET (Figure 4-2, Table 4-2).

4.6.2 Why does including complexity induce changes in system dynamics?

Including spatially explicit parameterisation of the canopy and radiation inputs has a noticeable impact on simulated ET (Table 4-2, Figure 4-2). Incorporation of small-scale spatio-temporal variability in canopy and radiation inputs reduced the magnitude of hysteresis in simulated ET rates (Figure 4-2) because of the more detailed representation of the surface temperature

component of the Penman-Monteith equation (s$(T_s$-$T_a)$), Eq. 4-1. The reduction in the hysteresis loop results from increased simulated ET in the mornings (0800 to 13:00), with negligible shift in ET through the subsequent afternoons (Figure 4-2). During the morning, between ~08:00 and ~13:00, the simulated ET is driven both by the surface atmosphere temperature gradient and vapour density deficit of the air (vdd_a; Figure 4-3). After ~13:00, vdd_a is the dominant driver of simulated ET (Figure 4-3). Spatial variation in surface temperature therefore has a minimal impact on ET during this time (Figure 4-2).

A likely reason for this overestimation of ET in the afternoon and remaining hysteresis (Figure 4-2) is that the surface resistance values in the model do not change throughout the day (and are based on measurements between 10:00 and 16:00), whereas in the measured system, ET values are probably increasing substantially in the afternoons (~1600). Surface resistance is at around 100–300 sm^{-1} during the day, increasing towards the afternoon, and shows a strong increase from 1500 to 1800 of up to ~350% (Kellner, 2001). It is likely that evaporation demand exceeds supply in the afternoons. Different mosses/groundcover types have different capacities for meeting evaporative demand. *S. fuscum* can normally meet evaporative demands by wicking water up from depth using capillary rise (Hayward & Clymo, 1982; Mccarter & Price, 2014; Price *et al.*, 1997), however, other groundcover types, (including other *Sphagna*, (Mccarter & Price, 2014), feather mosses (Carleton & Dunham, 2003) and lichens) may dry out in afternoons due to their inability to access water from depth at a rate that meets evaporative demands. Overnight recharge processes that include fog, dew, distillation and capillary rise (Admiral & Lafleur, 2007; Carleton & Dunham, 2003; Yazaki *et al.*, 2006) then function to reduce surface resistances at the start of the following day. The inclusion of diurnal trends in surface resistance values would likely improve ET simulations and reduce the observed hysteresis even further by reducing afternoon ET. Simulations that incorporate microtopography and the MARS sub-

model predicting groundcover species distributions show relatively little changes in either mean ET, data variability (Figure 4-2, Table 4-2) or how the different layers contribute to overall ET (Table 4-3).

4.6.3 Implications and further considerations for flux modelling

Results demonstrate that in open canopy systems, spatial variability of the energy inputs are important consideration for ET. Including spatio-temporal canopy and radiation variability in the model increases ET estimates by ~25.5% (gap filled data, 30.8 % filtered data) and reduces unexplained variance by 8%. (when comparing big leaf simulation with weighted groundcover (WGBL-FFP) to spatially explicit canopy with weighted groundcover (WGSC)). Additionally, the inclusion of spatio-temporal canopy and radiation variability reduces hysteresis in model outputs. Without this investigation into how complexity impacts ET and the data presented here, the observed hysteresis in big-leaf modelling results may have been explained solely as unaccounted for controls on ET, such as temporally dependent vegetation controls on surface resistance that vary diurnally, and in response to water availability (Betts *et al.*, 2004; Kellner, 2001). The results here however, suggest a substantial proportion of model variance may be explained by the spatio-temporal variability in energy inputs at the evaporating surface. This substantial decrease in unexplained variance is an important finding that quantifies the value added to predicting ET dynamics by incorporating the spatial variability of energy inputs. These results point out that even though the big-leaf model showed good estimations of ET, it is not representing some important mechanisms controlling and driving ET, and in order to capture sub-daily ET dynamics a spatially explicit model would be advantageous. The importance of this finding is highlighted further by the fact that the simulated system has a relatively uniform distribution of heterogeneity, i.e. the tree canopy is variable in space, but the distribution of the trees is relatively even (Figure 4-1). The observed effects of including a spatially explicit

canopy and radiation representation would likely be stronger in a more heterogeneous system with even greater variability in energy inputs reaching the under-story (Kettridge *et al.*, 2013). Accurate parameterisation of system structural layers that influence the spatio-temporal distribution of energy reaching lower layers will provide more accurate morning ET predictions, especially for open canopy systems such as boreal forested peatlands.

4.7 REFERENCES

Admiral, S. W. & Lafleur, P. M. (2007) Partitioning of latent heat flux at a northern peatland. *Aquat. Bot.* **86**(2), 107–116. doi:10.1016/j.aquabot.2006.09.006

Allen, S. J. (1990) Measurement and estimation of evaporation from soil under sparse barley crops in northern Syria. *Agric. For. Meteorol.* **49**(4), 291–309. doi:https://doi.org/10.1016/0168-1923(90)90003-O

Angstmann, J. L., Ewers, B. E. & Kwon, H. (2012) Size-mediated tree transpiration along soil drainage gradients in a boreal black spruce forest wildfire chronosequence. *Tree Physiol.* **32**(5), 599–611. doi:10.1093/treephys/tps021

Baldocchi, D., Kelliher, F. M., Black, T. A. & Jarvis, P. (2000) Climate and vegetation controls on boreal zone energy exchange. *Glob. Chang. Biol.* **6**(S1), 69–83. John Wiley & Sons, Ltd (10.1111). doi:10.1046/j.1365-2486.2000.06014.x

Barr, A. G., Morgenstern, K., Black, T. A., McCaughey, J. H. & Nesic, Z. (2006) Surface energy balance closure by the eddy-covariance method above three boreal forest stands and implications for the measurement of the CO2 flux. *Agric. For. Meteorol.* **140**(1–4), 322–337. doi:10.1016/j.agrformet.2006.08.007

Betts, A. K., Goulden, M. L. & Wofsy, S. C. (2004) Controls on evaporation in a black spruce forest. *J. Clim.* **12**, 1601–1618. doi:10.1029/2003GB002128

Bisbee, K., Gower, S., Norman, J. & Nordheim, E. (2001) Environmental controls on ground cover species composition and productivity in a boreal black spruce forest. *Oecologia* **129**(2), 261–270. doi:10.1007/s004420100719

Black, T. A., Hartog, G. Den, Neumann, H. H., Blanken, P. D., Yang, P. C., Russell, C., Nesic, Z., *et al*. (1996) Annual cycles of water vapour and carbon dioxide fluxes in and above a boreal aspen forest. *Glob. Chang. Biol.* **2**(3), 219–229. doi:10.1111/j.1365-2486.1996.tb00074.x

Blanken, P. D., Black, T. A., Yang, P. C., Neumann, H. H., Nesic, Z., Staebler, R., Hartog, G. den, *et al*. (1997) Energy balance and canopy conductance of a boreal aspen forest: Partitioning overstory and understory components. *J. Geophys. Res. Atmos.* **102**(D24), 28915–28927. doi:10.1029/97jd00193

Boer, M. M., Bowman, D. M. J. S., Murphy, B. P., Cary, G. J., Cochrane, M. A., Fensham, R. J., Krawchuk, M. A., *et al*. (2016) Future changes in climatic water balance determine potential for transformational shifts in Australian fire regimes. *Environ. Res. Lett.* **11**(6), 65002. {IOP} Publishing. doi:10.1088/1748-9326/11/6/065002

Bonan, G. B. (2008) Forests and Climate Change : Climate Benefits of Forests (June).

Bond-Lamberty, B., Gower, S. T., Amiro, B. & Ewers, B. E. (2011) Measurement and modelling of bryophyte evaporation in a boreal forest chronosequence. *Ecohydrology* **4**, 26–35. doi:10.1002/eco.118

Bovard, B. D., Curtis, P. S., Vogel, C. S., Su, H. B. & Schmid, H. P. (2005) Environmental controls on sap flow in a northern hardwood forest. *Tree Physiol.* **25**(1), 31–38. doi:10.1093/treephys/25.1.31

Bradshaw, C. J. A. & Warkentin, I. G. (2015) Global estimates of boreal forest carbon stocks and flux. *Glob. Planet. Change* **128**, 24–30. Elsevier B.V. doi:10.1016/j.gloplacha.2015.02.004

Breshears, D. D., Whicker, J. J., Zou, C. B., Field, J. P. & Allen, C. D. (2009) A conceptual framework for dryland aeolian sediment transport along the grassland-forest continuum: Effects of woody plant canopy cover and disturbance. *Geomorphology* **105**(1–2), 28–38. Elsevier B.V. doi:10.1016/j.geomorph.2007.12.018

Brümmer, C., Black, T. A., Jassal, R. S., Grant, N. J., Spittlehouse, D. L., Chen, B., Nesic, Z., *et al*. (2012) How climate and vegetation type influence evapotranspiration and water use efficiency in Canadian forest, peatland and grassland ecosystems. *Agric. For. Meteorol.*

doi:10.1016/j.agrformet.2011.04.008

Brutsaert, W. (2010) *Evaporation Into the Atmosphere: Theory, History, and Applications*. doi:10.1007/978-94-017-1497-6_1

Burgess, S. S. O., Adams, M. A., Turner, N. C., Beverly, C. R., Ong, C. K., Khan, A. A. H. & Bleby, T. I. M. M. (2001) An improved heat pulse method to measure low and reverse rates of sap flow in woody plants † **21**(1998), 589–598.

Burton, P. J. (2013) Exploring complexity in boreal forests. In: *Managing Forests as Complex Adaptive Systems: Building Resilience to the Challenge of Global Change* (M. Christian, K. J. Puettmann & D. Coates, eds.), 79–110. New York: Routledge. doi:10.4324/9780203122808

Carleton, T. J. & Dunham, K. M. M. (2003) Distillation in a boreal mossy forest floor. *Can. J. For. Res.* **33**(4), 663–671. NRC Research Press. doi:10.1139/x02-197

Chapin, F. S., Mcguire, A. D., Randerson, J., Pielke, R., Baldocchi, D., Hobbie, S. E., Roulet, N., *et al*. (2000) Arctic and boreal ecosystems of western North America as components of the climate system. *Glob. Chang. Biol.* **6**, 211–223. doi:10.1046/j.1365-2486.2000.06022.x

Ciais, P., Sabine, C., Bala, G., Bopp, L., Brovkin, V., Canadell, J., Chhabra, A., *et al*. (2013) Carbon and other Biogeochemical cycles. In: *Climate Change 2013: The Physical Science Basis. Working Group I Contribution to the 5th Assessment of the Intergovernmental Panel on Climate Change* (V. B. and P. M. M. Stocker, T.F., D. Qin, G.-K. Plattner, M. Tignor, S.K. Allen, J. Boschung, A. Nauels, Y. Xia, ed.), 1535. Cambridge and New York: Cambridge University Press.

Davis, T. W., Kuo, C.-M., Liang, X. & Yu, P.-S. (2012) Sap Flow Sensors: Construction, Quality Control and Comparison. *Sensors* **12**(12), 954–971. doi:10.3390/s120100954

Devito, K., Creed, I., Gan, T., Mendoza, C., Petrone, R., Silins, U. & Smerdon, B. (2005) A framework for broad-scale classification of hydrologic response units on the Boreal Plain: Is topography the last thing to consider? *Hydrol. Process.* **19**(8), 1705–1714. doi:10.1002/hyp.5881

Devito, K. J., Hokanson, K. J., Moore, P. A., Kettridge, N., Anderson, A. E., Chasmer, L.,

Hopkinson, C., *et al*. (2017) Landscape controls on long-term runoff in subhumid heterogeneous Boreal Plains catchments. *Hydrol. Process.* **31**(15), 2737–2751. doi:10.1002/hyp.11213

Elith, J. & Leathwick, J. (2007) Predicting species distributions from museum and herbarium records using multiresponse models fitted with multivariate adaptive regression splines. *Divers. Distrib.* **13**(3), 265–275. doi:10.1111/j.1472-4642.2007.00340.x

Ellison, D., Morris, C. E., Locatelli, B., Sheil, D., Cohen, J., Murdiyarso, D., Gutierrez, V., *et al*. (2017) Trees , forests and water : Cool insights for a hot world. *Glob. Environ. Chang.* **43**, 51–61. Elsevier Ltd. doi:10.1016/j.gloenvcha.2017.01.002

Essery, R., Bunting, P., Rowlands, A., Rutter, N., Hardy, J., Melloh, R., Link, T., *et al*. (2008) Radiative Transfer Modeling of a Coniferous Canopy Characterized by Airborne Remote Sensing. *J. Hydrometeorol.* **9**(2), 228–241. doi:10.1175/2007JHM870.1

Fatichi, S. & Pappas, C. (2017) Constrained variability of modeled T:ET ratio across biomes. *Geophys. Res. Lett.* **44**(13), 6795–6803. doi:10.1002/2017GL074041

Ferretti, D. F., Pendall, E., Morgan, J. A., Nelson, J. A., LeCain, D. & Mosier, A. R. (2003) Partitioning evapotranspiration fluxes from a Colorado grassland using stable isotopes: Seasonal variations and ecosystem implications of elevated atmospheric CO2. *Plant Soil* **254**(2), 291–303. doi:10.1023/A:1025511618571

Friend, A. D. (2001) Modelling canopy CO2 fluxes: are 'big-leaf' simplifications justified? *Glob. Ecol. Biogeogr.* **10**(6), 603–619. doi:10.1046/j.1466-822x.2001.00268.x

Gabrielli, E. C. (2016) Partitioning Evapotranspiration in Forested Peatlands within the Western Boreal Plain , Fort.

Green, F. H. W., Harding, R. J. & Oliver, H. R. (1984) The relationship of soil temperature to vegetation height. *J. Climatol.* **4**(3), 229–240. doi:10.1002/joc.3370040302

H. Blanford, J. & W. Gay, L. (1992) *Test of a robust eddy correlation system for sensible heat flux*. *Theor. Appl. Climatol.*, Vol. 46. doi:10.1007/BF00866448

Hayward, P. M. & Clymo, R. S. (1982) *Profiles of Water Content and Pore Size in Sphagnum and Peat, and their Relation to Peat Bog Ecology*. *Proc. R. Soc. London. Ser. B, Biol. Sci.*,

Vol. 215. doi:10.1098/rspb.1982.0044

Heijmans, M. M. P. D., Arp, W. J. & Chapin, F. S. (2004) Carbon dioxide and water vapour exchange from understory species in boreal forest. *Agric. For. Meteorol.* **123**, 135–147. doi:10.1016/j.agrformet.2003.12.006

Heijmans, M. M. P. D., Arp, W. J. & Chapin, F. S. (2004) Controls on moss evaporation in a boreal black spruce forest. *Global Biogeochem. Cycles* **18**(2), n/a-n/a. doi:10.1029/2003GB002128

Holden, J. (2005) Peatland hydrology and carbon release: why small-scale process matters. *Philos. Trans. R. Soc. A Math. Phys. Eng. Sci.* **363**(1837), 2891–913. doi:10.1098/rsta.2005.1671

Hossein, A., O., P. W. & T., P. U. K. (1994) Partitioning of Evapotranspiration Using Lysimeter and Micro-Bowen-Ratio System. *J. Irrig. Drain. Eng.* **120**(2), 450–464. American Society of Civil Engineers. doi:10.1061/(ASCE)0733-9437(1994)120:2(450)

Jackson, R. B., Carpenter, S. R., Dahm, C. N., McKnight, D. M., Naiman, R. J., Postel, S. L. & Running, S. W. (2001) Water in a changing world. *Ecol. Appl.* **11**(4), 1027–1045. John Wiley & Sons, Ltd. doi:10.1890/1051-0761(2001)011[1027:WIACW]2.0.CO;2

Joos, F., Roth, R., Fuglestvedt, J. S., Peters, G. P., Enting, I. G., Bloh, W. Von, Brovkin, V., *et al*. (2013) Carbon dioxide and climate impulse response functions for the computation of greenhouse gas metrics: A multi-model analysis. *Atmos. Chem. Phys.* **13**(5), 2793–2825. doi:10.5194/acp-13-2793-2013

Joosten, Hans; Clarke, D. (2002) *Wise Use of Mires and Peatlands - and Including Framework for Decision - Making. Transformation*.

Kaimal, J. C. & Finningan, J. . (1994) *Atmospheric Bournary Layer Flows: Their Structure and Measurement*. New York: Oxford University Press.

Kellner, E. (2001) Surface energy fluxes and control of evapotranspiratoin from a Swedish Sphagnum mire. *Agric. For. Meteorol.* **110**(2), 101–123. doi:10.1016/S0168-1923(01)00283-0

Kettridge, N., Thompson, D. K., Bombonato, L., Turetsky, M. R., Benscoter, B. W. &

Waddington, J. M. (2013) The ecohydrology of forested peatlands: Simulating the effects of tree shading on moss evaporation and species composition. *J. Geophys. Res. Biogeosciences* **118**(2), 422–435. doi:10.1002/jgrg.20043

Kettridge, N., Thompson, D. K. & Waddington, J. M. (2012) Impact of wildfire on the thermal behavior of northern peatlands: Observations and model simulations. *J. Geophys. Res. Biogeosciences* **117**(G2), n/a-n/a. doi:10.1029/2011JG001910

Kljun, N., Calanca, P., Rotach, M. W. & Schmid, H. P. (2015) A simple two-dimensional parameterisation for Flux Footprint Prediction (FFP). *Geosci. Model Dev.* **8**(11), 3695–3713. doi:10.5194/gmd-8-3695-2015

Kurz, W. A. & Apps, M. J. (1993) Contribution of Northern Forests to the Global C Cycle: Canada as a Case Study BT - Terrestrial Biospheric Carbon Fluxes Quantification of Sinks and Sources of CO2. (J. Wisniewski & R. N. Sampson, eds.), 163–176. Dordrecht: Springer Netherlands. doi:10.1007/978-94-011-1982-5_10

Lafleur, P. (1990) Evaporation From Wetlands. *Can. Geogr. / Le Géographe Can.* **34**(1), 79–82. doi:10.1111/j.1541-0064.1990.tb01072.x

Landsberg, J. J. & Gower, S. T. (1997) *Applications of physiological ecology to forest management*. San Diego : Academic Press. Retrieved from http://lib.ugent.be/catalog/rug01:000478902

Leonard, R. M., Kettridge, N., Devito, K. J., Petrone, R. M., Mendoza, C. A., Waddington, J. M. & Krause, S. (2018) Disturbance Impacts on Thermal Hot Spots and Hot Moments at the Peatland-Atmosphere Interface. *Geophys. Res. Lett.* 1–9. doi:10.1002/2017GL075974

Leuning, R., Condon, A. G., Dunin, F. X., Zegelin, S. & Denmead, O. T. (1994) Rainfall interception and evaporation from soil below a wheat canopy. *Agric. For. Meteorol.* **67**(3–4), 221–238. doi:10.1016/0168-1923(94)90004-3

Leuning, Ray & Judd, M. J. (1996) The relative merits of open- And closed-path analysers for measurement of eddy fluxes. *Glob. Chang. Biol.* **2**(3), 241–253. doi:10.1111/j.1365-2486.1996.tb00076.x

Lieffers, V. J. & Macdonald, S. E. (1989) Growth and foliar nutrient status of black spruce and tamarack in relation to depth of water table in some Alberta peatlands. *Can. J. For. Res.*

20(6), 805–809. doi:10.1139/x90-106

Mao, L., Bater, C. W., Stadt, J. J., White, B., Tompalski, P., Coops, N. C. & Nielsen, S. E. (2017) Environmental landscape determinants of maximum forest canopy height of boreal forests. *J. Plant Ecol.* **12**(1), 96–102. doi:10.1093/jpe/rtx071

Martens, S. N., Breshears, D. D. & Meyer, C. W. (2000) Spatial distributions of understory light along the grassland/forest continuum: Effects of cover, height, and spatial pattern of tree canopies. *Ecol. Modell.* **126**(1), 79–93. doi:10.1016/S0304-3800(99)00188-X

Mccarter, C. P. R. & Price, J. S. (2014) Ecohydrology of Sphagnum moss hummocks: Mechanisms of capitula water supply and simulated effects of evaporation. *Ecohydrology* **7**(1), 33–44. doi:10.1002/eco.1313

McCarthy, J. (2001) Gap dynamics of forest trees: A review with particular attention to boreal forests. *Environ. Rev.* **9**(2), 129. doi:10.1139/er-9-2-129

McGuire, D. A., Melillo, J. M., Kicklighter, D. W. & Joyce, L. A. (1995) Equilibrium Responses of Soil Carbon to Climate Change: Empirical and Process-Based Estimates. *J. Biogeogr.* **22**(4/5), 785–796. Wiley. Retrieved from http://www.jstor.org/stable/2845980

McNaughton, K. G. & Jarvis, P. G. (1983) Predicting effects of vegetation changes on transpiration and evaporation. In: *Water Deficits and Plant Growth* (T. . Kozlowski, ed.), 1–47. New York: Acadmic Press.

Nungesser, M. K. (2003) Modelling microtopography in boreal peatlands: hummocks and hollows. *Ecol. Modell.* **165**(2–3), 175–207. doi:10.1016/S0304-3800(03)00067-X

Oke, T. R. (1987) *Boundary layer climates*, 2nd ed. New York: Routledge.

Oren, R. & Pataki, D. E. (2001) Transpiration in response to variation in microclimate and soil moisture in southeastern deciduous forests. *Oecologia* **127**(4), 549–559. doi:10.1007/s004420000622

Oren, R., Zimmermann, R. & Terbough, J. (1996) Transpiration in Upper Amazonia Floodplain and Upland Forests in Response to Drought- Breaking Rains. *Ecology* **77**(3), 968–973. Retrieved from https://www.jstor.org/stable/2265517

Petrone, R. M., Waddington, J. M. & Price, J. S. (2001) Ecosystem scale evapotranspiration

and net CO2 exchange from a restored peatland. *Hydrol. Process.* **15**(14), 2839–2845. doi:10.1002/hyp.475

Petrone, R., Silins, U. & Devito, K. (2007) Dynamics of evapotranspiration from a riparian pond complex in the Western Boreal Forest, Alberta, Canada. *Hydrol. Process.* **21**, 1391–1401.

Prather, M. J., Holmes, C. D. & Hsu, J. (2012) Reactive greenhouse gas scenarios: Systematic exploration of uncertainties and the role of atmospheric chemistry. *Geophys. Res. Lett.* **39**(9). doi:10.1029/2012GL051440

Prentice, I. C. & Harrison, S. P. (2009) Ecosystem effects of CO2 concentration: Evidence from past climates. *Clim. Past* **5**(3), 297–307. doi:10.5194/cp-5-297-2009

Price, A. ., Dunham, K., Carleton, T. & Band, L. (1997) Variability of water fluxes through the black spruce (Picea mariana) canopy and feather moss (*Pleurozium schreberi*) carpet in the boreal forest of Northern Manitoba. *J. Hydrol.* **196**(1–4), 310–323. doi:10.1016/S0022-1694(96)03233-7

Sagar, R., Singh, A. & Singh, J. S. (2008) Differential effect of woody plant canopies on species composition and diversity of ground vegetation: A case study. *Trop. Ecol.* **49**(2), 189–197.

Sena, J. O. A. De, Zaidan, H. A. & Camargo e Castro, P. R. De. (2007) Transpiration and stomatal resistance variations of perennial tropical crops under soil water availability conditions and water deficit. *Brazilian Arch. Biol. Technol.* **50**(2), 225–230.

Shuttleworth, W. J. (2007) Putting the 'vap' into evaporation. *Hydrol. Earth Syst. Sci.* **11**(1), 210–244. doi:10.5194/hess-11-210-2007

Simard, M., Lecomte, N., Bergeron, Y., Bernier, P. Y. & Paré, D. (2007) Forest productivity decline caused by successional paludification of boreal soils. *Ecol. Appl.* **17**(6), 1619–1637. John Wiley & Sons, Ltd. doi:10.1890/06-1795.1

Sutherland, G., Chasmer, L. E., Petrone, R. M., Kljun, N. & Devito, K. J. (2014) Evaluating the use of spatially varying versus bulk average 3D vegetation structural inputs to modelled evapotranspiration within heterogeneous land cover types. *Ecohydrology* **7**(6), 1545–1559. doi:10.1002/eco.1477

Sutherland, George, Chasmer, L. E., Kljun, N., Devito, K. J. & Petrone, R. M. (2017) Using High Resolution LiDAR Data and a Flux Footprint Parameterization to Scale Evapotranspiration Estimates to Lower Pixel Resolutions. *Can. J. Remote Sens.* **43**(2), 215–229. doi:10.1080/07038992.2017.1291338

Tanner, B. C. & Thurtell, G. W. (1969) Anemoclinometer measurements of Reynolds stress and heat transport in the atmospheric surface layer.

Thompson, D. K., Benscoter, B. W. & Waddington, J. M. (2014) Water balance of a burned and unburned forested boreal peatland. *Hydrol. Process.* **28**(24), 5954–5964. doi:10.1002/hyp.10074

Turetsky, M., Wieder, K., Halsey, L. & Vitt, D. (2002) Current disturbance and the diminishing peatland carbon sink. *Geophys. Res. Lett.* **29**(11), 7–10. doi:10.1029/2001GL014000

Twine, T. E., Kustas, W. P., Norman, J. M., Cook, D. R., Houser, P. R., Meyers, T. P., Prueger, J. H., *et al*. (2000) Correcting eddy-covariance flux underestimates over a grassland. *Agric. For. Meteorol.* **103**(3), 279–300. doi:10.1016/S0168-1923(00)00123-4

Villegas, J. C., Espeleta, J. E., Morrison, C. T., Breshears, D. D. & Huxman, T. E. (2014) Factoring in canopy cover heterogeneity on evapotranspiration partitioning: Beyond big-leaf surface homogeneity assumptions. *J. Soil Water Conserv.* **69**(3), 78A-83A. doi:10.2489/jswc.69.3.78a

Villegas, Juan Camilo, Breshears, D. D., Zou, C. B. & Law, D. J. (2010) Ecohydrological controls of soil evaporation in deciduous drylands: How the hierarchical effects of litter, patch and vegetation mosaic cover interact with phenology and season. *J. Arid Environ.* **74**(5), 595–602. Elsevier Ltd. doi:10.1016/j.jaridenv.2009.09.028

Vogel, C. A. & Baldocchi, D. D. (1996) Energy and CO2 flux densities above and below a temperate broad-leaved forest and a boreal pine forest. *Tree Physiol.* **16**, 5–16.

Wallace, J. S., Lloyd, C. R. & Sivakumar, M. V. K. (1993) Measurements of soil, plant and total evaporation from millet in Niger. *Agric. For. Meteorol.* **63**(3–4), 149–169. doi:10.1016/0168-1923(93)90058-P

Warren, R. K., Pappas, C., Helbig, M., Chasmer, L. E., Berg, A. A., Baltzer, J. L., Quinton, W. L., *et al*. (2018) Minor contribution of overstorey transpiration to landscape

evapotranspiration in boreal permafrost peatlands. *Ecohydrology* **11**(5), 1–10. doi:10.1002/eco.1975

Watras, C. J. (2017) Estimates of evapotranspiration from contrasting Wisconsin peatlands based on diel water table oscillations (August 2016). doi:10.1002/eco.1834

Webb, E. K., Pearman, G. I. & Leuning, R. (1980) Correction of Flux Measurements for Density Effects. *Q. J. R. Meteorol. Soc.* **106**, 85–100.

Wieder, R. K., Scott, K. D., Kamminga, K., Vile, M. a., Vitt, D. H., Bone, T., Xu, B., *et al*. (2009) Postfire carbon balance in boreal bogs of Alberta, Canada. *Glob. Chang. Biol.* **15**(1), 63–81. doi:10.1111/j.1365-2486.2008.01756.x

Williams, D. G., Cable, W., Hultine, K., Hoedjes, J. C. B., Yepez, E. A., Simonneaux, V., Er-Raki, S., *et al*. (2004) Evapotranspiration components determined by stable isotope, sap flow and eddy covariance techniques. *Agric. For. Meteorol.* **125**(3–4), 241–258. doi:10.1016/j.agrformet.2004.04.008

Wilson, K. (2002) Energy balance closure at FLUXNET sites. *Agric. For. Meteorol.* **113**(1–4), 223–243. doi:10.1016/S0168-1923(02)00109-0

Wilson, K. B., Hanson, P. J., Mulholland, P. J., Baldocchi, D. D. & Wullschleger, S. D. (2001) A comparison of methods for determining forest evapotranspiration and its components: Sap-flow, soil water budget, eddy covariance and catchment water balance. *Agric. For. Meteorol.* **106**(2), 153–168. doi:10.1016/S0168-1923(00)00199-4

Yazaki, T., Urano, S. I. & Yabe, K. (2006) Water balance and water movement in unsaturated zones of Sphagnum hummocks in Fuhrengawa Mire, Hokkaido, Japan. *J. Hydrol.* **319**(1–4), 312–327. doi:10.1016/j.jhydrol.2005.06.037

Yu, Z. C. (2012) Northern peatland carbon stocks and dynamics: A review. *Biogeosciences* **9**(10), 4071–4085. doi:10.5194/bg-9-4071-2012

Yunusa, I. A. M., Walker, R. R. & Guy, J. R. (1997) Partitioning of seasonal evapotranspiration from a commercial furrow-irrigated Sultana vineyard. *Irrig. Sci.* **18**(1), 45–54. doi:10.1007/s002710050043

Zhang, K., Kimball, J. S., Mu, Q., Jones, L. A., Goetz, S. J. & Running, S. W. (2009) Satellite

based analysis of northern ET trends and associated changes in the regional water balance from 1983 to 2005. *J. Hydrol.* **379**(1–2), 92–110. Elsevier B.V. doi:10.1016/j.jhydrol.2009.09.047

Zhao, L., Xia, J., Xu, C. yu, Wang, Z., Sobkowiak, L. & Long, C. (2013) Evapotranspiration estimation methods in hydrological models. *J. Geogr. Sci.* **23**(2), 359–369. doi:10.1007/s11442-013-1015-9

4.8 SUPPORTING INFORMATION FOR CHAPTER FOUR

Supporting information for chapter four is composed of two distinct sections: Section SI4-1 and

Section SI4-2

Section SI4-1 supports the methods section of the main article with additional information on the numerical modelling components of PHI- BETA-THETA. To avoid repetition, information presented in this section is in addition to the detailed description provided in Chapter three supplementary information (SI3-1)

Contents of this section;

- Text SI4-1
- Table SI4-1

Section SI4-2 provides additional results that support findings in the main article.

Contents of this section;

- Figure SI4-1 and SI4-2

4.8.1 Section SI4-1 Additional modelling description.

This section supports the methods section of the main article with additional information on the numerical modelling components of PHI- BETA-THETA. To avoid repetition, details of methods here are of modelling components / parameters that differ from those described in Chapter 3 supporting information (SI3-1), which provides a full model description.

Tree height and Location (Canopy Height Model, CHM) and structure

Lidar data were acquired August 2008. Once accessed, laser pulse returns were classified into ground and non-ground within TerraScan (Terrasolid Inc., Finland). A digital elevation model (DEM) was created from ground-classified returns for the ground surface at 1 m resolution using a triangular irregular network (TIN) model, while a digital surface model (DSM) was created for all non-ground returns using an inverse distance weighted algorithm (1 m pixel resolution), representing the vegetated canopy (Golden Software Surfer, Inc.). A canopy height model (CHM) was developed by subtracting the DEM from the DSM. Tree density was determined by assuming that vegetation exceeding a height of 1.5 m within the CHM represents a tree. A 1.5 m threshold was used to determine location of tree stems and crowns at that height, such that all trees within the CHM that were less than 1.5 m were excluded. The maximum (99th percentile) of the canopy height within the CHM was used to determine a) the existence of a tree and b) tree height.

Idealized shapes are used to represent the tree canopy. Due to the relatively low tree density at the study site, we represent black spruce trees as cones. Allometric relations are used to relate tree height to tree crown length (Woods *et al*., 1991) and crown base radius (Kettridge *et al*., 2013). Tree location and height were derived from Lidar data of the study area using a canopy

height model (Hopkins *et al*., 2006). To minimize misclassification of trees, a height threshold of 1.5 m was used relative to ground-return heights. Foliage area volume density was randomly assigned to each tree voxel based on the measured distribution of λ for black spruce (Kettridge *et al*., 2013).

Tree transpiration

Transpiration was measured every 20 minutes, from n =30 black spruce trees between the 6th July and 29th August 2014. Heat ratio method (HRM) sapflow sensors were constructed according to *Davis et al.,* [2012] and connected to CR10 X campbell dataloggers. However, due to the small diameter of the trees, we used 10-mm length sensors, covered with aluminium casing, and installed at ground level. Volumetric sap flow was calculated as described in detail by (Burgess *et al.*, 2001), accounting for both correction of wounding and probe misalignment. Due to gaps in the transpiration data and to extend the data set, multiple linear regression models were run in R, relating transpiration to using relative humidity, air temperature and total radiation averaged over the same time interval of 20 minutes. Only datasets showing R^2 of ≥ 0.6 were selected, resulting in n=15 with an R^2 range of 0.60 to 0.91 (Table SI4-1). Transpiration rates ranged from 0.07 to 0.49 mm d^{-1} ha^{-1} (n=15), which is greater than those observed in a similar environment (<0.000001 and 0.000003 mm d^{-1} ha^{-1} : Warren *et al.,* 2018) but lower than those observed previously at the same site (0.2 to 1.2 mm d^{-1} ha^{-1} (n=*3*) :Thompson *et al.,* 2014). Average transpiration efficiency (Oren *et al.*, 1996) was 234 mm d^{-1} kPa^{-1}. Tree transpiration is modelled empirically based on measured vapour pressure deficit (cf. Thompson *et al*., 2014) using a transpiration efficiency derived from the 15 replicate sap-flow sensors.

$$T = A_{tb} E_{st} VPD \qquad \text{(Equation S4-1)}$$

Where, (T is Tree transpiration (mm d^{-1}) A_{tb} is the tree basal area per m^2 (-), VPD is the average daytime vapour pressure deficit (kPa) (Oren *et al.,* 1996) and E_{st} is the sapwood transpiration efficiency (mm d^{-1} kPa^{-1}).

Table SI 4-1, Diameter at stem base of each sap-flow measurement tree and corresponding R^2 value for data modelled using relative humidity, air temperature and total radiation averaged over the same time interval.

Diameter at base (cm)	R^2	Diameter at base (cm)	R^2	Diameter at base (cm)	R^2
6.1	0.2	4.3	**0.88***	6.8	0.46
11.4	0.36	6.90	**0.80***	7.50	0.34
2.2	N/A	2.40	**0.86***	3.80	**0.62***
4.7	0.51	3.10	0.04	3.80	0.19
9.2	**0.88***	1.60	**0.84***	2.60	0.50
6.7	**0.87***	5.20	0.43	8.40	**0.71***
4.3	**0.91***	1.70	**0.60***	5.20	0.41
2.6	**0.74***	7.20	**0.89***	3.20	N/A
4.9	**0.62***	7.50	**0.79***	5.10	N/A
4.0	0.12	4.30	**0.83***	2.80	0.05

*** - data used in PHI-BETA-THETA**
N/A - bad data.

Predicting ground layer and sub-canopy vegetation presence/absence.

Multivariate Adaptive Regression with Spline (MARS) model was fitted to environmental variable data relating to each groundcover type (bare peat, *P. schreberi, S. fuscum* and *Cladonia sp..)* as described in Elith & Leathwick (2007). Environmental variable data was obtained from two transects of 80m and 100m at the study site in 2014. The following measurements were taken from 0.04 m^2 plots every 1m along each transect: estimated % of each ground-cover species (following the Domin scale), leaf counts for each sub-canopy vascular species, leaf area

of representative sample of each sub-canopy vascular species (multiplied by leaf counts for each species to give LAI), % litter, ice depth, moisture of upper 6 cm and 3 cm, distance to the nearest tree, diameter of the nearest tree, slope, aspect, gradient, water table depth, electrical conductivity and water temperature. From fish eye hemispherical photographs and the subsequent processing of images in Gap Light Analyser software, the following was derived: % Canopy Openness (the percentage of open sky seen from beneath a forest canopy), Transmitted Direct (the amount of direct solar radiation transmitted by the canopy), Transmitted Diffuse (the amount of diffuse solar radiation transmitted by the canopy), Transmitted Total (the sum of Transmitted Direct and Transmitted Diffuse), % Transmitted Direct (the ratio of Transmitted Direct to Above Direct Mask multiplied by 100%), % Transmitted Diffuse (the ratio of Transmitted Diffuse to Above Diffuse Mask multiplied by 100%) , % Transmitted Total (the ratio of Transmitted Total to Above Total Mask multiplied by 100%). Due to missing data from 23 plots, $n = 157$. Water table depth and moisture data was excluded from analysis because it strongly correlated with *S. fuscum* due to its ability to grow tall, creating a surface that is further from the water table (Nungesser, 2003) but still maintain access to water at depth through capillary rise (Mccarter & Price, 2014).

Included in the final model are variables that can be used to predict the distribution of groundcover species; Distance to nearest tree, diameter of nearest tree, Aspect, Ice depth, % Canopy Openness (the percentage of open sky seen from beneath a forest canopy), Transmitted Direct (the amount of direct solar radiation transmitted by the canopy), Transmitted Diffuse (the amount of diffuse solar radiation transmitted by the canopy), Transmitted Total (the sum of Transmitted Direct and Transmitted Diffuse), % Transmitted Direct (the ratio of Transmitted Direct to Above Direct Mask multiplied by 100%), % Transmitted Diffuse (the ratio of Transmitted Diffuse to Above Diffuse Mask multiplied by 100%) , % Transmitted Total (the

ratio of Transmitted Total to Above Total Mask multiplied by 100%), electrical conductivity, total leaf area of shrubs.

MARS analysis relating vascular species presence/absence data to environmental variables showed no significant relationships that allowed prediction of abundance distributions of vascular sub-canopy species. The presence of each dominant sub-canopy vascular species is therefore randomly assigned, based on the likelihood of its occurrence in the transect: (*Rhododendron groenlandicum* (0.92), *Rubus chamaemorus,* (0.61) *and Vaccinium vitus-idea* (0.98). Their LAI values are randomly drawn from a log-normal distribution of values found for each species in the transect measurements.

4.8.2 Section SI4-2 Additional results

This section includes additional results that support findings in the main article.

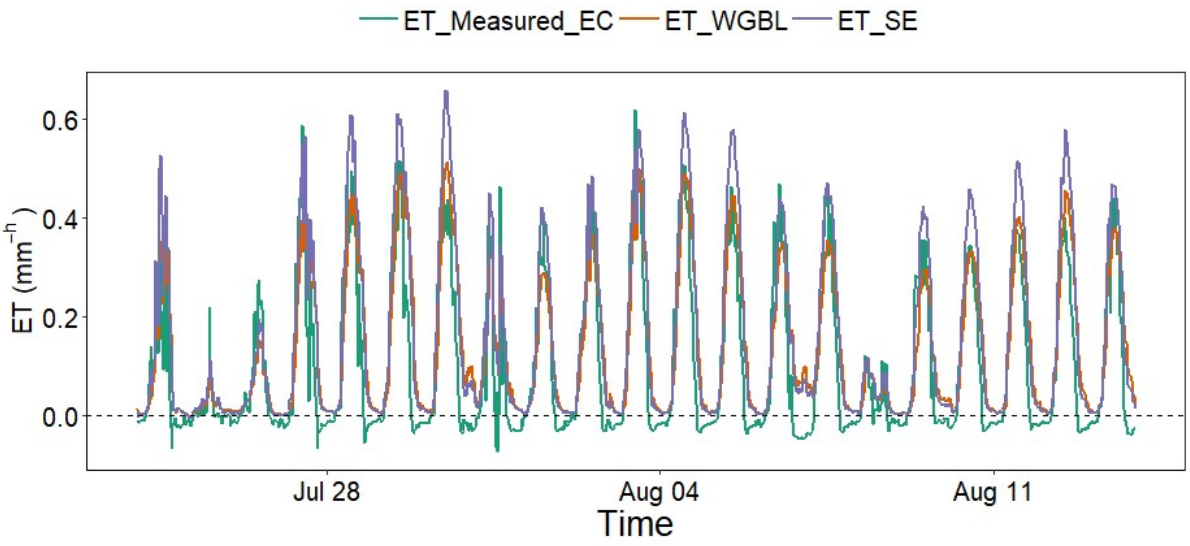

Figure SI 4-1, Time series of measured ET (gap-filled) from the EC tower, modelled ET from the detailed simulation (SE) and ET modelled from simulation with 'big-leaf' canopy parameterization and weighted groundcover (WGBL).

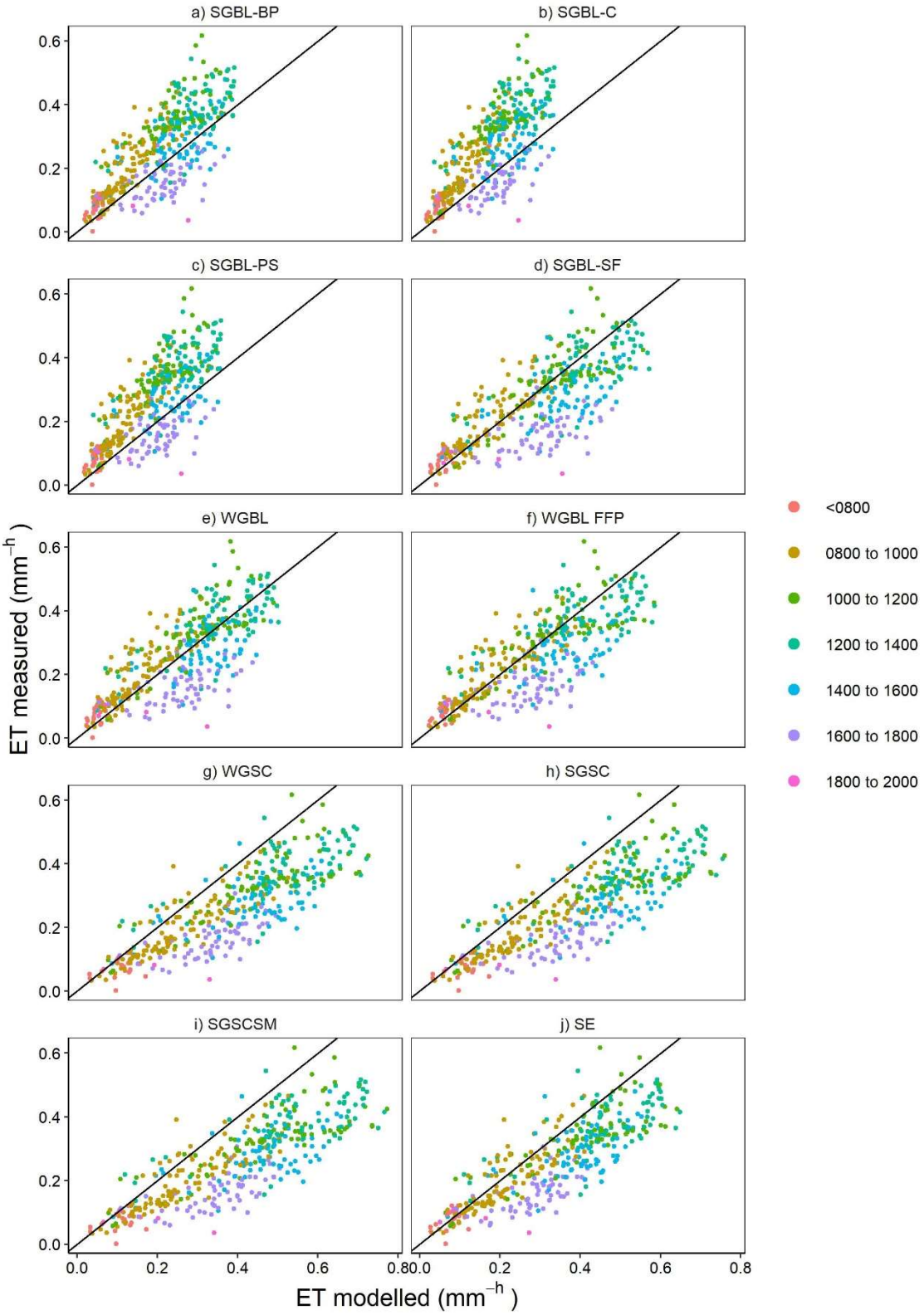

Figure SI 4-2, Correlation between 60-minute eddy covariance ET data and ET modelled from corresponding footprint area for each simulation.1:1 line shown on each tile (Filtered data only; 40% of data). Colours show time of day.

CHAPTER FIVE : PEATLAND BRYOPHYTE RESPONSES TO INCREASED LIGHT FROM BLACK SPRUCE REMOVAL

5.1 ABSTRACT

The ecohydrological impact of tree-canopy removal on moss and peat, which provide a principal carbon store, is just starting to be understood. Different mosses have contrasting contributions to carbon and water fluxes (e.g. *Sphagnum fuscum, Pleurozium schreberi*) and are strongly influenced by tree-canopy cover. Changes in tree-canopy cover may therefore lead to long-term shifts in species composition and associated ecohydrological function. However, the medium-term response to such disturbance, the associated lag in this transition to a new ecohydrological and biogeochemical regime, is not understood in detail. We investigate this medium-term (4 year) ecohydrological, biogeochemical and species compositional response to tree-canopy removal using a randomised plot design within a northern peatland. This is the only study to test for the influence of increased light alone. We demonstrate that changes in treatment plots four years after tree-canopy removal were not significant. Notably, *P. schreberi* and *S. fuscum* remained within their respective plots post treatment and there was no significant difference in plot resistance to evapotranspiration or carbon exchange. Results show that tree-canopy removal alone has little impact on bryophyte ecohydrology in the short/medium-term. This resistance to disturbance contrasts strongly with short-term changes observed within mineral soils, suggesting that concurrent shifts in the large-scale hydrology induced within such disturbances are necessary to cause rapid ecohydrological transitions. Understanding this lagged response is critical to determine the strength of medium to long-term negative ecohydrological feedbacks within peatlands in addition to carbon and water fluxes on a decadal timescale in response to disturbance.

5.2 INTRODUCTION

Boreal forests occupy approximately 10% of the earth's vegetated surface (McGuire *et al.,* 1995), of which, peatlands are a dominant feature. These northern peatlands are estimated to be one of the world's largest carbon stores (Yu, 2012). Despite this, northern forested peatlands are subject to widespread tree-canopy disturbances. Linear tree clearance from seismic lines exceeds 1.5 M km in Alberta, Canada alone (Timoney and Lee, 2001). This equates to a 19 M ha disturbance assuming a 60 m edge effect. Thinning of spruce stands is used as a fire control method. In addition, insect infestations have the potential to act as a significant future disturbance with increases in the frequency and severity of fire and drought projected to reduce tree-canopy resistance to insects and disease (Raffa *et al.,* 2008). Such disturbances not only remove the tree-canopy, but impact the ecohydrological function of the moss and peat (Kettridge *et al.,* 2013) which provide the principal carbon store within these carbon rich ecosystems.

Mosses play an integral role in ecosystem functioning with their ability to equal or exceed tree-canopy productivity within northern forested peatlands (Bisbee *et al.,* 2001) and contribute up to 69% of total ecosystem evapotranspiration (Bond-Lamberty *et al.,* 2011). Typically, feather mosses (e.g. *Pleurozium schreberi*) are associated with a high black spruce stand density and *Sphagnum* carpets are more typical of open tree-canopy peatlands. A combination of these floor cover types exist on peatlands with low stand density. Since tree cover controls the moss layer environment (e.g. Temperature and radiation), its loss or thinning results in different ground layer species compositions as a result of competition and extinction-colonization dynamics. Feather moss groundcover percentage is negatively related to tree-canopy transmittance of photosynthetically active radiation (PAR), when *Sphagnum* is present while percentage ground cover of *Sphagnum* is positively related to tree-canopy PAR transmittance (Bisbee *et al.,* 2001).

This suggests that thinning of tree canopies will increase *Sphagnum* cover. Carbon and water fluxes would alter as a result since *S. fuscum* is three times more productive than *P. schreberi* (Bisbee *et al.,* 2001) and evaporates much more due to its enhanced water transport abilities (Mccarter and Price, 2014).

Short-term studies within mineral soils suggest that *S. fuscum* cover increases in the first years after tree-canopy removal (Fenton and Bergeron, 2007) and *P. schreberi* shows complete absence after one year (Shields *et al.,* 2007) or significant decreases in cover after four years (Fenton *et al.,* 2003). Despite the extent of tree-canopy disturbance within carbon rich forested peatlands, and their strong control over water and carbon fluxes, the medium-term response of moss species composition that characterises the transitional periods of lagged responses and their associated carbon and water fluxes, remain largely unstudied. It may be argued that transitional phases dominate peatland composition and function, particularly in boreal Alberta. The cycling of disturbances such as fire, thinning, clear cutting, and seismic line creation etc. is continuous in this region, resulting in a patchwork of continually responding ecosystems, yet work at the response/transitional phase (medium-term) timescale is rarely considered. Findings of short-term studies may change in the medium-term because the disturbance/treatment response processes may take longer than their study period. For example, a decline in *S. fuscum* two years after tree-canopy removal is suggested to have been a result of physiological shock due to exposure to new conditions (Fenton and Bergeron, 2007) and is likely to recover (Clymo and Duckett, 1986). In addition to lack of medium-term studies, we are not aware of any that report or demonstrate minimal changes in water-table depth and/or the impact of machinery. These are common confounding factors in large-scale timber clearances where most tree-canopy removal studies have taken place.

We target these key knowledge gaps by investigating the ecohydrological, biogeochemical and compositional response of two key northern bryophytes to tree-canopy removal. The experiment is uniquely conducted with before and after treatment (tree-canopy removal) plots in a black spruce peatland, with no additional factors (e.g. disturbance related changes in water levels and surface micro-topography) allowing unequivocal evaluation of medium-term moss response to changes in light conditions alone. The isolation of light as a process that likely induces changes to the influential moss layer will allow more robust and flexible modelling and predictions of peatland ecohydrological functioning to various disturbances including, tree removal, insect infestations and any other light increasing disturbances.

5.3 STUDY SITE

Experiments were conducted on a poor fen in central Alberta, Canada (55.81°N, 115.11°W). The depth of peat is ≥ 3m and the hydrological regime is such that it is part of a larger flow-through system within the landscape resulting in a stable water table. Total annual precipitation for (the study period) 2010, 2011, 2012, 2013, 2014, 2015 was 282 mm, 489 mm, 497 mm, 523 mm, 376 mm and 387 mm respectively. The study site is characterised by a tree cover of *Picea mariana* with a basal area and average height of 11 m^2 ha^{-1} and 2.3 m respectively. Tree basal areas for northern Albertan peatlands range from 0.3 to 47.3 m^2 ha^{-1} for peatlands that are 21 to 100 years since fire, respectively (Wieder *et al.,* 2009). Ground layer vegetation is composed of *Sphagnum fuscum, Sphagnum angustifolium*, *and Pleurozium schreberi* with vascular species that include *Rhododendron groenlandicum, Rubus chamaemorus*, *Chamaedaphne calyculata, Maianthemum trifolia, Vaccinium oxycoccus* and *Vaccinium vitus-idea.*

5.4 METHODS

In May, 2010, 20 polyvinyl chloride collars (inside diameter of 0.17 m, length 0.10 m) were installed in the ground based on the species present (10 x *S. fuscum* and 10 x *P. schreberi,* each

with 100% cover). No significant differences in sky view factor between the proposed control (0.60 ± 0.08) and treatment (0.65 ± 0.09) plots ($p > 0.05$, t = –1.58) or between the *S. fuscum* (0.60 ± 0.06) and *P. schreberi* (0.64 ± 0.11) plots ($p > 0.05$, t = –1.16) were found. On the 17th of June 2010, trees around five randomly selected *S. fuscum* collars and five randomly selected *P. schreberi* collars were cut by hand to increase sky view factor at the collar. Trees within a 5 m radius that influence the available light at the plot were removed, which significantly increased the sky view factor in the treatment plots (0.85 ± 0.03) relative to the control plots (0.60 ± 0.08) ($p < 0.001$, t = 9.7). Relative humidity (%) did not differ significantly between treatment and control plots ($p = 0.91$, t = -0.11) or between species ($p = 0.22$, t = 1.3). Air temperature did not differ significantly between treatment and control plots (W = 42, $p = 0.58$) or between species (W = 62, $p = 0.39$) either. Between June and August 2010, soil moisture and surface resistance to evapotranspiration was measured fifteen times within each collar. Between July and August, 2014, measurements of species composition, and five repeat measurements of surface resistance (r_s), CO_2 exchange (net primary productivity, respiration, net ecosystem exchange) and soil moisture were undertaken within each collar. Moss stress (chlorophyll fluorescence) was measured in all plots at intervals between 0700 and 1800 in 2015. All measurement dates were randomly selected between May and August of each respective year, provided there was no precipitation on the day of measurement.

Bryophyte species cover was estimated as a percentage for each collar. Moisture measurements were taken at 0.06 m depth (repeats of n=5 were taken during 2010 and 2014). Resistance to evapotranspiration and CO_2 exchange were measured using a closed chamber system in accordance with McLeod *et al.,* (2004). A cylindrical clear plexiglass chamber (volume of 12.6 L) was placed over the collar for two minutes and the air inside mixed continuously using a small fan. Changes in the humidity and CO_2 concentration within the chamber were measured

every 1.6 seconds using a PP systems EGM4 infra-red gas analyser. A dark (opaque) chamber with the same dimensions was used to measure respiration (respiration assumed equal to dark chamber CO_2 flux) by the same method as described for resistance to evapotranspiration. Light chamber measurements were immediately followed by dark chamber measurements between 0900 and 1700. Temperature measurements were taken at 0.02 m below the bryophyte surface. Evapotranspiration rate (ET) was calculated from the slope of the linear change in vapour density (Stannard, 1988) during the first 35 seconds of measurement since changes in vapour density reduce significantly after the first minute (also reported by Kettridge *et al.,* (2013)). The surface resistance to evaporation (r_s) is equal to:

$$\boldsymbol{r_s} = \frac{\rho^*_{vs} - \rho_{va}}{ET} - \boldsymbol{r_a} \qquad \text{(Equation 5-1)}$$

Where, ρ_{vs} and ρ_{va} are the saturation vapour density of the peat surface and the vapour density of the air within the chamber respectively, and r_a is the aerodynamic resistance within the chamber during a measurement (calculated by placing the chamber over a water bath at room temperature ($r_s = 0$) and calculating evaporation accordingly using the same setup and duration as the field method).

5.4.1 CO_2 flux

Net ecosystem exchange (NEE) was calculated from (Shaver *et al.,* 2007),

$$\boldsymbol{NEE} = \frac{\boldsymbol{\rho V}}{\boldsymbol{A}} \frac{\boldsymbol{dC}}{\boldsymbol{dt}} \qquad \text{(Equation 5-2)}$$

Where ρ is air density (mol m^{-3}), V is the volume of the chamber plus base (m^3), A is the projected horizontal surface area of the chamber (m^2) and dC/dt is the rate of change in CO_2 concentration within the plexiglass chamber (μmol mol^{-1} s^{-1}). Ecosystem respiration (RE; μmol m^{-2} s^{-1}) was calculated in accordance with equation 5-2, but with dC/dt determined within a

dark (opaque) chamber. Gross ecosystem photosynthesis (GEP) is equal to NEE-RE, where a negative value indicates carbon uptake, and a positive value indicates carbon release.

5.4.2 Chlorophyll fluorescence measurements

Maximum quantum yield of photosystem II (F_v/F_m) was used to assess plant stress in response to tree-canopy removal due to its sensitivity as an indicator of plant photosynthetic performance (Maxwell and Johnson, 2000). An OS30p hand held chlorophyll fluorometer was used to measure F_v/F_m after 20 minutes of dark adaptation *(*Maxwell and Johnson, 2000) of mosses in each treatment. The theoretical maximum of F_v/F_m is between 0.78 and 0.89 (Adams and Demmig-Adams, 2004). Individual species will have different optimal values when un-stressed. Lower than optimal values indicate a lowered photosynthetic capacity (or stress); normally, this is water stress for bryophytes (Maxwell and Johnson, 2000). Chlorophyll fluorescence measurements were taken from all plots at regular intervals between 0600 and 1800 on the 17th July, 2015 to compare between control and treatment diurnal patterns.

All statistical analyses were conducted in R. A Wilcoxon rank-sum test was used to determine differences between % cover of bryophyte abundance between control and treatment plots (2014), daily average F_v/F_m treatment and control plots of each species (2015). Repeat measures of moisture, GEP and r_s from each collar were averaged. An ANOVA comparing species, year (where appropriate: moisture and r_s) and treatment was undertaken.

5.5 RESULTS

5.5.1 Species cover

Plots in 2010 were selected to include 100% cover of the respective species. *Sphagnum fuscum* and *P. schreberi* were still present in the relevant treatment and control plots in 2014. No significant difference was observed in either species abundance as a result of treatment. All *S.*

fuscum plots contained 100% *S. fuscum* cover in treatment and control plots. Although *P. schreberi* showed a decline (mean of percentage cover in control = 99% (SE ± 0.89, median = 100, range = 95 to 100), mean of percentage cover in treatment = 60% (SE ± 17.1, median =75, range = 2 to 100), this was not significant (p = 0.06, n = 5). *Pleurozium schreberi* remained present in all ten collars in 2014.

5.5.2 Surface resistance, gross ecosystem photosynthesis and moisture.

In 2014, Gross Ecosystem Productivity, did not differ significantly between treatment types but did show significant differences with species (Table 5-2: Figure 5-1) with *S. fucsum* (mean: -6, ±0.6 SE) more productive than *P. schreberi* (mean: -12, ±0.9 SE). Surface resistance was significantly different between species (i.e. R_s greater in *P. schreberi* plots: Figure 5-2) but did not show a treatment effect (Table 5-2). Moisture in the top 0.06 m also did not differ significantly with treatment but did show a significant species and year effect (Table 5-2: Figure 5-3).

Table 5-1, Species cover percentages for all plots (5 of each species) in 2010 and 2014

			Control 2010	Open 2010	Control 2014	Open 2014
P. schreberi plots	*Pleurozium schreberi*	Mean	100.0	100.0	99.0	60.4
		SE±	0.0	0.0	2.0	17.1
		Median	100.0	100.0	100.0	75.0
		Range	0.0	0.0	5.0	98.0
	Bare ground	Mean	-	-	0.0	21.4
		SE±	-	-	0.0	16.5
		Median	-	-	0.0	2.0
		Range	-	-	0.0	95.0
	Aulacomnium palustre	Mean	-	-	0.0	4.6
		SE±	-	-	0.0	3.5
		Median	-	-	0.0	0.0
		Range	-	-	0.0	20.0
	Polytrichum strictum	Mean	-	-	0.6	1.0
		SE±	-	-	0.5	0.9
		Median	-	-	0.0	0.0
		Range	-	-	3.0	5.0
S. fuscum plots	*Sphagnum fuscum*	Mean	100.0	100.0	100.0	100.0
		SE±	0.0	0.0	0.0	0.0
		Median	100.0	100.0	100.0	100.0
		Range	0.0	0.0	0.0	0.0

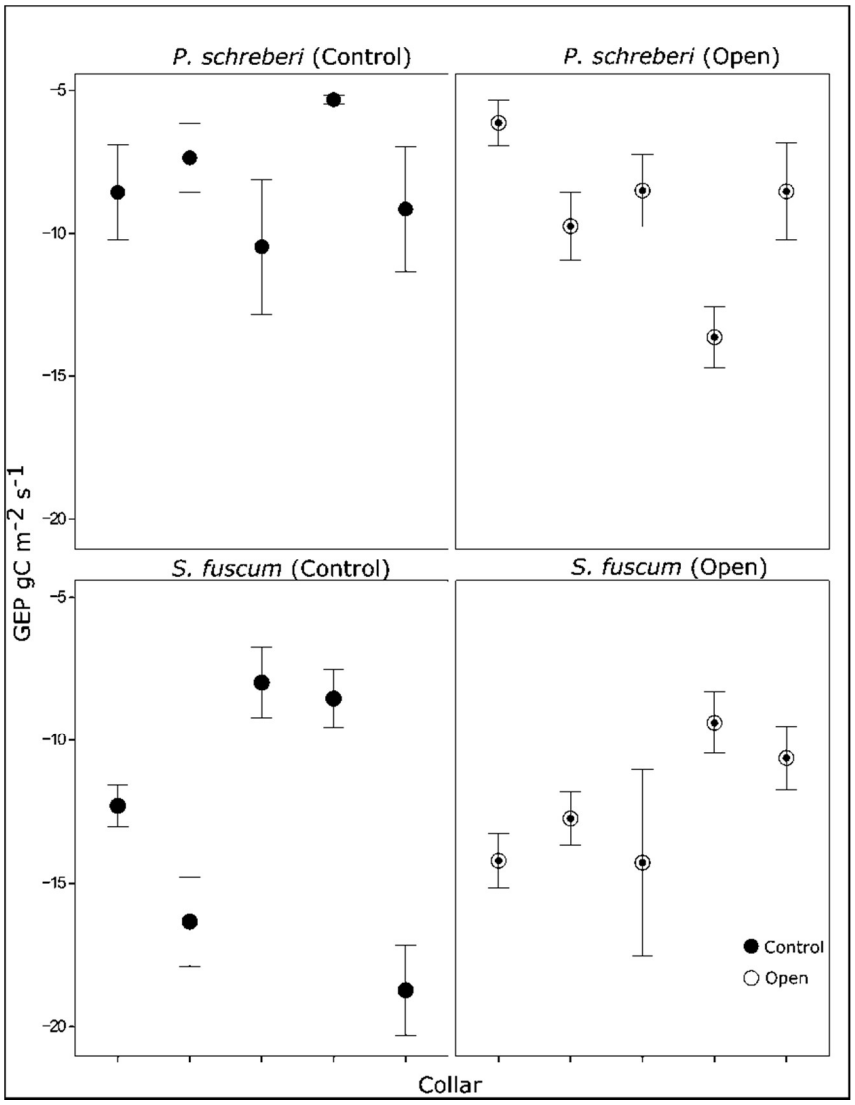

Figure 5-1, Mean (± SE) gross ecosystem productivity for each collar (n=5) with five repeat measurements, 2014.

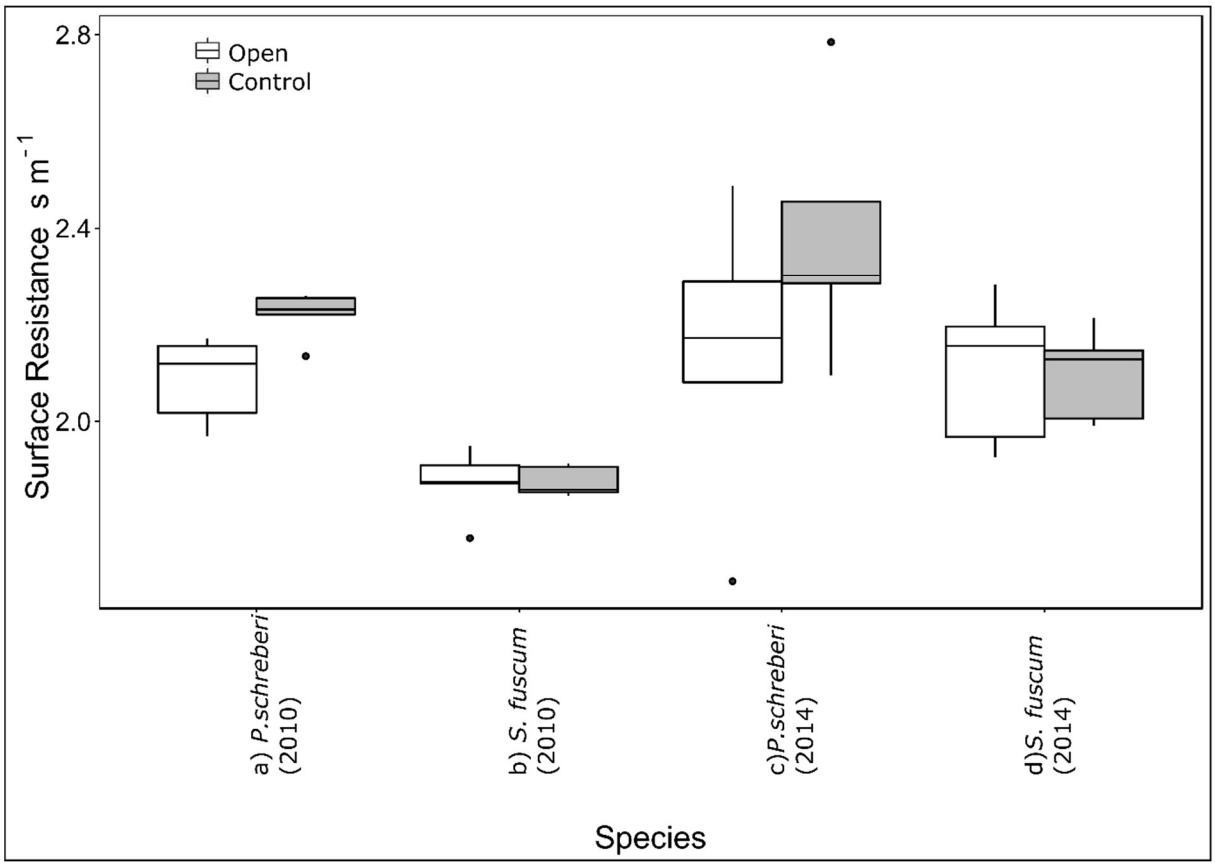

Figure 5-2, Mean (± SE) surface resistance of *Pleurozium schreberi* and *Sphagnum fuscum* in open and control plots, 2010 and, 2014 (n =5).

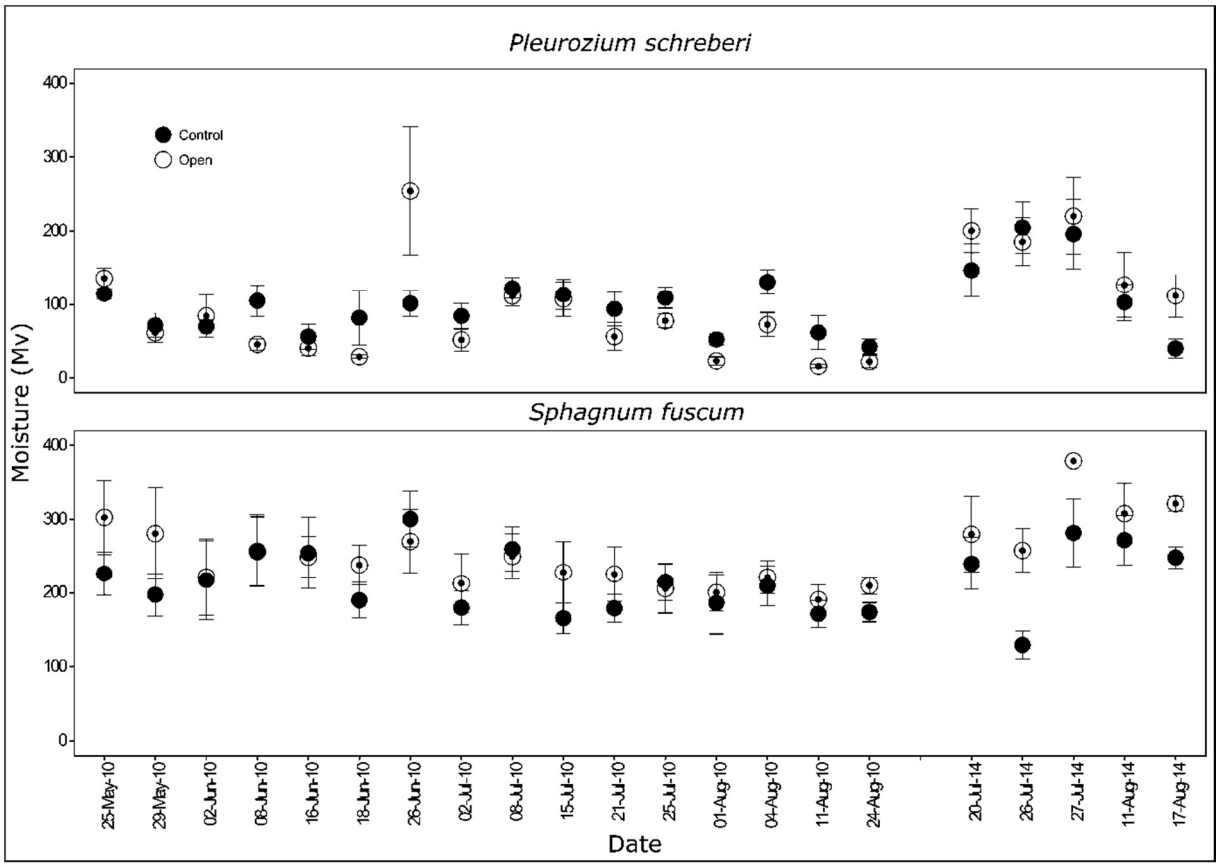

Figure 5-3, Mean (± SE) moisture data (n=5) for treatment and control plots of *Pleurozium schreberi* and *Sphagnum fuscum* before and after treatment.

5.5.3 Chlorophyll fluorescence

In 2015 both mean *P. schreberi* and *S. fuscum* F_v/F_m in the control collars remained near optimal throughout the day, only reaching a low of 0.66 for *S. fuscum* (Figure 5-4). The *Sphagnum fuscum* treatment fell as low as 0.63. The *P. schreberi* treatment plots on the other hand showed a drop in mean F_v/F_m later in the day to 0.46 at 1600. Differences between treatment and control *S. fuscum* F_v/F_m were not significant (p = 0.69, n = 5). However, the treatment did cause significant reductions in *P. schreberi* F_v/F_m values (p = 0.0079, n = 5).

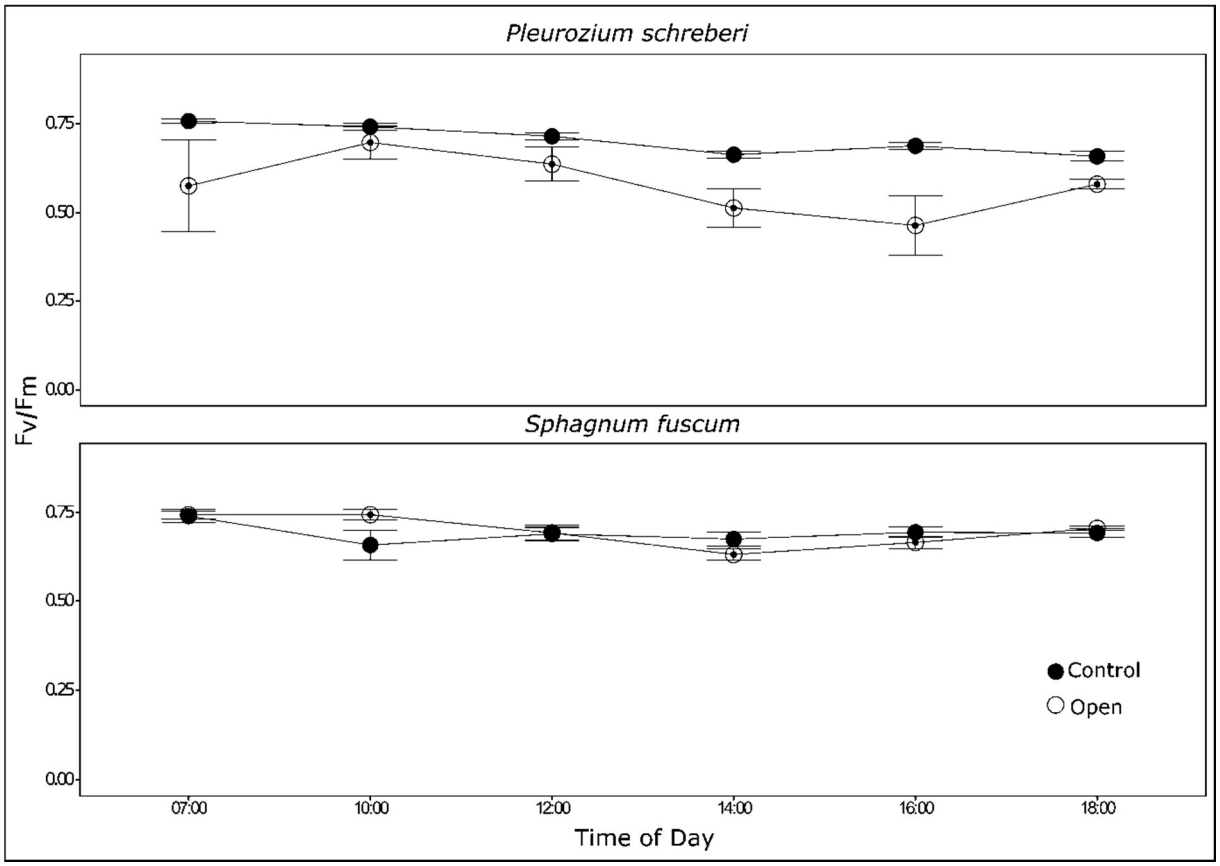

Figure 5-4, Mean (± SE) Fv/Fm values for control and treatment *Pleurozium schreberi* (2015), and control and treatment *Sphagnum fuscum* (2015), n =5.

Table 5-2, ANOVA results of comparisons between species, treatment and year for Moisture, Surface resistance and Gross Ecosystem Productivity (* = significant).

	Moisture (Mv)		Gross Ecosystem Productivity (gc m^{-2} s^{-1})		Surface resistance (s m^{-1})	
	F-value (1/16)	P-value	F-value (1/16)	P-value	F-value (1/16)	P-value
(Intercept)	201.70	<.0001	207.73	<.0001	90.57	<.0001
Species	22.52	0.0002*	22.85	0.0002*	21.21	0.0003*
Treatment	0.16	0.7	0.13	0.72	0.03	0.87
Year	21.77	0.0003*			0.40	0.53
Species:Treatment	0.58	0.46	0.62	0.44	0.07	0.79
Species:Year	1.05	0.32			0.33	0.58
Treatment:Year	0.16	0.7			3.54	0.08
Species:Treatment:Year	0.02	0.89			1.72	0.21

5.6 DISCUSSION

5.6.1 Species response to disturbance

Pleurozium schreberi is negatively correlated to the tree-canopy PAR transmittance when *Sphagnum* is present, and is typically found under dense tree covers (Bisbee *et al.,* 2001). *Sphagnum* is positively correlated with tree-canopy PAR transmittance and associated with open tree-canopy areas (Bisbee *et al.,* 2001). It is therefore likely that long-term shifts toward a *S. fuscum* dominated system will occur in response to tree-canopy removal. Despite this, tree-canopy removal alone did not cause any significant changes in species compositions in the medium-term. *Pleurozium schreberi* was present in all treatment collars four years after tree-canopy removal and showed no significant decrease in cover. We suggest here that the tree-canopy PAR transmittance, substrate type, depth and its associated hydrology not only control the species distribution (Bisbee *et al.,* 2001) but also modify the rate of this transition in response to tree-canopy removal.

Decline in *P. schreberi* has been attributed to increased evaporation stress. If tree-canopy cover is not adequate to prevent evaporation stress, feather mosses dry out and die because they are nearly independent of the substrates' water supply (Johnson, 1981). Thus evaporative stress will provide the likely driver for the expected long-term transition from *P. schreberi* to *S. fuscum* after tree-canopy removal. *Pleurozium schreberi* treatment plots exhibit less optimal F_v/F_m, values compared to control plots, resulting in reduced carbon accumulation which slowly reduces their competitive strength and groundcover. Further work is required to determine how the duration and intensity in *P. schreberi* stress varies on a diurnal cycle, its association with tree-canopy removal, its link with evaporative demand and near-surface moisture/tension. However, this evaporative stress is the probable cause of the observed decline of *P. schreberi* abundance and long-term shift to a *Sphagnum* dominated system. We observed that if increased evaporative stress associated with increased solar radiation is acting alone, the resulting shift in species occurs much slower, with no significant changes found within four years, suggesting the response is lagged. This lagged response left sub-canopy species outside of their niche environment, in this experiment, for a period of greater than four years.

Despite the slower response observed in this study, Shields *et al.,* (2007) and Fenton *et al.,* (2003) observed a complete loss of *P. schreberi* within mineral soils one year after tree-canopy removal, and a significant decrease after four years, respectively. This significant and rapid decrease/absence of *P. schreberi* in response to tree-canopy removal in short-term, mineral soil studies may be a result of changes in near-surface moisture saturation levels. A change in the moisture regime as a side effect of tree-canopy removal may be due to a change in any combination of the following: substrate depth, substrate storage, transpiration rates (lack of, after disturbance), disturbance size and compaction. If the balance between the water storage available and reduction in evapotranspiration through tree removal results in a water table rise

to a level unfavourable for *P. schreberi*, changes in species compositions may occur at a faster rate. Tree removal can result in a water table rise (due to lack of transpiration; Pothier *et al.,* 2003), which causes negative effects in feather moss (Busby *et al.,* 1978) in as little as 4 months (Birse, 2016). However, near-surface moisture conditions did not change significantly within our study. It is also unlikely that water levels changed significantly, due to the small scale of the disturbance (and low pre-disturbance transpiration rate) and the fact that the system has groundwater through flow. This ground water through flow limits large water level fluctuation that would adversely affect the studied mosses. The small scale nature of the experiment on a large groundwater fed fen, facilitates the minimisation of water level changes as a confounding effect (which is supported by soil moisture results; Figure 5-4). Further, such a rapid transition may be exacerbated by the tree clearance method employed. For instance, machinery used for harvesting can cause variable changes in forest floor depth by substrate compaction (Mariani *et al.,* 2006). Trees were cut by hand in this study, therefore, eliminating the influence of such disturbance. The lack of observed ecohydrological changes may have also been due to low pre-disturbance tree densities, resulting in a less extreme increase in light than in comparative studies (Shields *et al.,* 2007; Fenton *et al.*, 2003). However, the sky view factor was significantly reduced in the treatment plots. At a sky view factor of 0.85, both species could maintain their presence and ecohydrological functioning. Further work is required to assess whether the pre-disturbance tree density/sky view factor has an impact on species presence and ecohydrological function. However, given the high sky view factor values for treatment plots, this study highlights that light alone is not enough to rapidly change species composition.

Sphagnum fuscum percentage cover did not change between control and treatment collars. This was expected since *S. fuscum* usually grows in areas with a less dense tree cover (Bisbee *et al.,* 2001). *Sphagnum fuscum* decline in literature has been attributed to a physiological shock in

response to increased light levels (Fenton and Bergeron, 2007). This may have occurred in the short-term after which the *S. fuscum* subsequently recovered (Clymo and Duckett, 1986). For example, Locky and Bayley (2007) found a decline in *Sphagnum* cover 1 to 4 years after tree-canopy removal but a subsequent increase after 9 to12 years.

5.6.2 Hydrological and biogeochemical response

Differences in *P. schreberi* GEP and r_s between treatment and control collars were not significant in this study (Figures 5-1 and 5-3). The lack of connectivity with a water supply means that *P. schreberi* can only evaporate until the water available (from precipitation (Busby *et al.,* 1978), dew and distillation (Carleton and Dunham, 2003)) runs out and then it becomes stressed. Surface resistance is a measure of resistance to evaporation from the peat surface: low surface resistance allows high evaporation rates and vice versa. Surface resistance varies with precipitation and is therefore highly variable within a sub-humid climate. This is supported by highly variable r_s, GEP and F_v/F_m measurements for control plots. Evaporative stress is likely happening for a greater proportion of the day and is likely the cause of the long-term decline in *P. schreberi* abundance. There was also no significant change observed in *S. fuscum* r_s and GEP. *Sphagnum fuscum* can access water at depth, allowing it to meet most increases in evaporative demand (e.g. increased energy at the surface) and maintain consistent r_s and GEP rates. This is supported by F_v/F_m values that were consistently near the optimum range in both treatment and control plots (Figure 5-2). Although no significant changes in r_s and GEP were observed between treatments, significant differences were found between species for GEP and r_s, supporting suggestions that species compositions have the dominant control over C and water fluxes (Heijmans *et al.,* 2004). In the short/medium-term, moss layer hydrology and biogeochemistry have not changed, suggesting that these peatlands show some degree of resistance to disturbances. The lack of changes in surface resistance and GEP coupled with a

decrease in transpiration from the tree-canopy suggest that less water is lost from the ecosystem through evapotranspiration, which facilitates the maintenance of the peatlands' existing, globally important, carbon stock. In the longer term, a shift towards a *S. fuscum* dominated moss layer is suggested by the F_v/F_m data, moss physiology and because feather mosses are characteristic of areas with low light levels (Bisbee *et al.,* 2001). Such a shift in species composition will significantly change the moss layer hydrology and biogeochemistry of moss layers by increasing evapotranspiration and carbon accumulation.

Bryophyte species act as a first order control on the small scale atmospheric carbon and water fluxes from peatlands. Ecohydrological feedback models that assume moss layer species change in equilibrium with tree-canopy PAR (BETA model; Kettridge *et al.,* 2013) may provide a poor estimation of water fluxes during any transition period. Although PAR is a distinguishing feature between *P. schreberi* and *S. fuscum* dominated peatlands, the species compositional response to increased PAR is not immediate. This delayed response, compared to immediate responses of the same species within other studies (Shields *et al.,* 2007) highlight that different environmental factors, have varying controls over species competitive strengths and response rates to disturbances. As such, including appropriate disturbance response rates in ecohydrological models could dramatically improve their carbon and water balance prediction capabilities. For example, in this study we predict a shift towards a *S. fuscum* dominated system and increased carbon accumulation and evaporation from the moss layer, provided trees do not re-establish quickly. However, if the rate at which trees re-establish is faster than the rate at which *P. schreberi* cover significantly declines, the system could revert back to the status quo without significant changes to biogeochemistry and hydrology. Understanding species response rates provides better insight into ecosystem resistance to disturbance, ecohydrological feedback

mechanisms and quantification of carbon and water fluxes within globally important peatland systems.

5.7 CONCLUSION

Within the studied peatland, no significant changes in species composition, surface resistance or carbon fluxes from the bryophyte layer were observed as a result of tree-canopy removal. This study was uniquely conducted in a peatland system where confounding changes associated with tree-canopy clearance (e.g. significant water table changes and machinery influences) were avoided, allowing confident interpretation of results that were a direct effect of tree-canopy removal. These results showed slower changes (40% decrease in *P. schreberi* after 4 years) than those observed in short-term studies undertaken within mineral soils which suggests water table variations and/or harvest method may modify the responses of species to tree-canopy removal. Long-term changes are likely to result in a shift towards a *S. fuscum* dominated system as a result of evaporative stress causing weakened competitive strength of *P. schreberi* and eventual mortality. Because species have a dominant control over carbon and water fluxes from the system after tree-canopy removal we argue that further process based understanding of moss species compositional change over medium to long-term is essential for more accurate estimations of carbon and water fluxes in these globally important ecosystems.

5.8 REFERENCES

Adams, W. & Demmig-Adams, B. (2004) Chlorophyll Fluorescence as a Tool to Monitor Plant Response to the Environment. In: *Chlorophyll a Fluorescence—a signature of photosynthesis*, Papageorgi., 583–604. Springer.

Birse, E. M. (2016) Ecological Studies on Growth-Form in Bryophytes : III . The Relationship Between the Growth-Form of Mosses and Ground-Water Supply. *J. Ecol.* **46**(1), 9–27.

Bisbee, K., Gower, S., Norman, J. & Nordheim, E. (2001) Environmental controls on ground cover species composition and productivity in a boreal black spruce forest. *Oecologia* **129**(2), 261–270. doi:10.1007/s004420100719

Bond-Lamberty, B., Gower, S. T., Amiro, B. & Ewers, B. E. (2011) Measurement and modelling of bryophyte evaporation in a boreal forest chronosequence. *Ecohydrology* **4**, 26–35. doi:10.1002/eco.118

Busby, J. R., Bliss, L. C. & Hamilton, C. D. (1978) Microclimate control of growth rates and habitat of boreal forest mosses, Thompentypnum nitens and Hylocomium splendens. *Ecol. Monogr.* **48**, 95–110.

Carleton, T. J. & Dunham, K. M. M. (2003) Distillation in a boreal mossy forest floor. *Can. J. For. Res.* **33**(4), 663–671. NRC Research Press. doi:10.1139/x02-197

Clymo, R. S. & Duckett, G. (1986) Regeneration of Sphagnum. *New Phytol.* **102**, 589–614.

Fenton, N. J. & Bergeron, Y. (2007) Sphagnum community change after partial harvest in black spruce boreal forests. *For. Ecol. Manage.* **242**, 24–33. doi:10.1016/j.foreco.2007.01.028

Heijmans, M. M. P. D., Arp, W. J. & Chapin, F. S. (2004) Carbon dioxide and water vapour exchange from understory species in boreal forest. *Agric. For. Meteorol.* **123**, 135–147. doi:10.1016/j.agrformet.2003.12.006

Johnson, E. A. (1981) Vegetation organization and dynamics of lichen woodland communities in the Northwest Territories, Canada. *Ecology* **62**(1), 200–215. doi:10.2307/1936682

Kettridge, N., Thompson, D. K., Bombonato, L., Turetsky, M. R., Benscoter, B. W. & Waddington, J. M. (2013) The ecohydrology of forested peatlands: Simulating the effects of tree shading on moss evaporation and species composition. *J. Geophys. Res. Biogeosciences* **118**(2), 422–435. doi:10.1002/jgrg.20043

Locky, D. A. & Bayley, S. E. (2007) Effects of logging in the southern boreal peatlands of Manitoba, Canada. *Can. J. For. Res.* **37**, 649–661. doi:10.1139/X06-249

Mariani, L., Chang, S. X. & Kabzems, R. (2006) Effects of tree harvesting, forest floor removal, and compaction on soil microbial biomass, microbial respiration, and N availability in a boreal aspen forest in British Columbia. *Soil Biol. Biochem.* **38**(7), 1734–1744.

doi:10.1016/j.soilbio.2005.11.029

Maxwell, K. & Johnson, G. N. (2000) Chlorophyll fluorescence — a practical guide **51**(345), 659–668.

Mccarter, C. P. R. & Price, J. S. (2014) Ecohydrology of Sphagnum moss hummocks: Mechanisms of capitula water supply and simulated effects of evaporation. *Ecohydrology* **7**(1), 33–44. doi:10.1002/eco.1313

McGuire, D. A., Melillo, J. M., Kicklighter, D. W. & Joyce, L. A. (1995) Equilibrium Responses of Soil Carbon to Climate Change: Empirical and Process-Based Estimates. *J. Biogeogr.* **22**(4/5), 785–796. Wiley.

McLeod, M. K., Daniel, H., Faulkner, R. & Murison, R. (2004) Evaluation of an enclosed portable chamber to measure crop and pasture actual evapotranspiration at small scale. *Agric. Water Manag.* **67**(1), 15–34. doi:10.1016/j.agwat.2003.12.006

Pothier, D., Prévost, M. & Auger, I. (2003) Using the shelterwood method to mitigate water table rise after forest harvesting. *For. Ecol. Manage.* **179**, 573–583. doi:10.1016/S0378-1127(02)00530-3

Raffa, K. F., Aukema, B. H., Bentz, B. J., Carroll, A. L. & Hicke, J. A. (2008) Cross-scale Drivers of Natural Disturbances Prone to Anthropogenic Amplification : The Dynamics of Bark Beetle Eruptions. *Bioscience* **58**(6), 501–517.

Shaver, G. R., Street, L. E., Rastetter, E. B., Wijk, M. T. Van & Williams, M. (2007) Functional convergence in regulation of net CO 2 flux in heterogeneous tundra landscapes in Alaska and Sweden. *J. Ecol.* **95**(4), 802–817. doi:10.1111/j.1365-2745.2007.01259.x

Shields, J. M., Webster, C. R. & Glime, J. M. (2007) Bryophyte community response to silvicultural opening size in a managed northern hardwood forest. *For. Ecol. Manage.* **252**(1–3), 222–229. doi:10.1016/j.foreco.2007.06.048

Stannard, D. I. (1988) Use of a Hemispherical Chamber for Measurement of Evapotranspiration,. Denver.

Timoney, K. & Lee, P. (2001) Environmental management in resource-rich Alberta, Canada: first world jurisdiction, Third World analogue? *J. Environ. Manage.* **63**(4), 387–405.

doi:10.1006/jema.2001.0487

Wieder, R. K., Scott, K. D., Kamminga, K., Vile, M. a., Vitt, D. H., Bone, T., Xu, B., Benscoter, B W., Bhatti, J.S. (2009) Postfire carbon balance in boreal bogs of Alberta, Canada. *Glob. Chang. Biol.* **15**(1), 63–81. doi:10.1111/j.1365-2486.2008.01756.x

Yu, Z. C. (2012) Northern peatland carbon stocks and dynamics: A review. *Biogeosciences* **9**(10), 4071–4085. doi:10.5194/bg-9-4071-2012

CHAPTER SIX : KEY RESEARCH FINDINGS, SYNTHESIS AND FUTURE DIRECTIONS

6.1 INTRODUCTION

The research presented here was motivated by the need to understand how forest structure and organisation influences the dynamic system functioning of globally significant forested peatlands. The aim of this research was, '*to determine how complexity and organisation in forest structure, controls peatland ecohydrological system processes and the associated impact of structural disturbance on these system dynamics'.* This research focussed on addressing four main research gaps. Chapter 2 illustrated the spatiotemporal variability in peat-surface temperatures and the magnitude and persistence of associated thermal hot spots. Chapter 2 also determined the response of the thermal regime to tree-canopy and lower vascular vegetation removal, and assessed whether or not the distribution, intensity and duration of thermal hotspots and hot-moments changes in response to the canopy disturbance. Chapter 3 assessed the influence of both individual layers of system heterogeneity (subsurface ice-layers, ground cover vegetation, microtopography, tree, and sub-canopy vascular cover) on surface temperature distributions, and how different combinations of these layers influence peat-surface temperature patterns. Chapter 4 investigated how stand structure and related organisational complexity (ground cover vegetation, microtopography, tree, and sub-canopy vascular cover) influences ET rates, and discusses the implications for flux modelling. Chapter 5 determined the eco-hydrological, biogeochemical and compositional response of two key northern bryophytes to tree-canopy removal. In this chapter (Chapter 6), the key research findings are discussed and synthesized, and an outlook for further research is provided. This research has direct implications for numerical representations of system processes, associated functioning and response to disturbances.

6.2 KEY RESEARCH FINDINGS

The research presented here is novel and unique in: (1) using new technology to characterise the complicated peat-surface thermal dynamics of an intact and disturbed system at an unprecedented spatio-temporal resolution (1.9 million temperature measurements over 10 m^2), (2) utilising this detailed surface temperature dataset to critically and rigorously assess the simulated spatio-temporal thermal regime (using the PHI-BETA-THETA model) and assess how different layers of forest complexity impact the surface thermal regime, (3) presenting the first evaluation of how forest structural complexity impacts peatland ET, providing important considerations for forest flux modelling efforts and (4) presenting the first medium-term assessment of the ecohydrological, biogeochemical, and compositional response of two key northern bryophytes to increased light from canopy removal. The main research findings are as follows:

1. Surface temperatures vary significantly in space and time in undisturbed systems. Removing canopy layers shifts the spatial and temporal distribution, range, and longevity of thermal hot spots and hot moments in addition to increasing mean temperatures. This finding has important implications for a range of temperature driven processes. Taking hot spots and/or hot moments into consideration when investigating spatially variable ecosystem processes and feedbacks may be key for advancing our capacity to predict ecosystem function and resilience. (Chapter 2).
2. Investigations using the PHI-BETA-THETA model show that different layers of ecosystem structure and complexity have varying controls on surface temperatures, i.e. not all system vertical layers have an equal influence over peat surface temperatures. A particularly notable finding is that changes in the spatio-temporal thermal dynamics of peat surfaces may occur, without a significant change in average temperatures. This

finding has implications for research addressing system functioning, resilience and disturbance responses, because important temperature driven processes may have shifted location, intensity, and duration without a detected change in overall mean (Chapter 3).

3. Incorporating spatial complexity in the canopy layer and radiation has a significant impact on simulated ET, increasing estimates by up to 25.5% and reducing unexplained variance in simulated data. This research uniquely highlights that the inclusion of spatially explicit canopy and radiation inputs can substantially reduce unexplained variability and hysteresis in ET model outputs (Chapter 4).
4. In strong contrast with similar studies on mineral soil, tree canopy removal from the peatland did not significantly affect bryophyte ecohydrology in the short or medium-term. Models simulating eco-hydrological feedbacks to disturbance should carefully consider any transition periods of disturbance responses (Chapter 5).

6.3 SYNTHESIS

6.3.1 Small-scale variability of forested peatlands

Due to the visually striking patterning of peatland surfaces (Aber *et al*. 2002), it has long been acknowledged that small scale spatio-temporal variability is likely important for fully understanding peatland system processes and functioning (Holden 2005; Kettridge and Baird 2010; Frei *et al*. 2012; Aleina *et al*. 2015; Premke *et al*. 2016; Griffiths *et al*. 2017), but availability of resources to accurately capture this variability has been a limiting factor in fully quantifying and assessing the importance of spatially and temporally varying small-scale processes. New data presented in this thesis demonstrates the significant variability at the small-scale in peatland-atmosphere interface processes. Significant thermal variability is observed at unprecedented spatio-temporal resolution within an open canopy forested peatland system;

where spatial variability is similar in magnitude to the diurnal variation (Chapter 2 & 3). Such variability is consistent with findings in process specific areas of peatland research e.g. pore-water biogeochemistry (Ulanowski and Branfireun 2013), methane fluxes (Moore *et al*. 1998; Girkin *et al*. 2019), respiration (Juszczak *et al*. 2013). The highly variable surface thermal dynamics has important implications for efforts to quantify and numerically represent, temperature driven mass flux and energy balance processes in space and time (e.g. respiration, productivity and ET ; Chapter 4) and hence, overall ecosystem functioning. Such improved understanding of the controls of system complexity on key processes will lead not only to better simulations of system fluxes (Chapter 4) but more informed cost/benefit analyses for deciding what scale of complexity should be included in empirical measurement and numerical modelling efforts.

6.3.2 Small-scale variability and understanding system resilience

Understanding the small-scale spatio-temporal variability of peatland surfaces is not only important for quantifying and understanding the dynamics of observed systems but is also important for assessing system resilience in response to disturbances (Limpens *et al.,* 2008). Peatland systems are regulated by a balanced myriad of stable, multi-scale, multi-direction eco-hydrological feedbacks at the peatland-atmosphere interface (Belyea and Baird, 2006; Eppinga *et al,.* 2008, 2009; Belyea, 2009; Waddington *et al,.* 2015). This balance of feedbacks regulates self-organisation of peatland surface structure and functioning (Rietkerk and van de Koppel, 2008), which can persist for up to 5,000 years (Moore, 1977). However, peatlands may also exhibit rapid transitions or 'catastrophic shifts' where systems can change abruptly to an alternate stable state, with a different surface structure (Belyea and Malmer, 2004) and associated functioning (Eppinga *et al.* 2009; Loisel and Yu, 2013), the cause of which are not fully understood.

Disturbance to the peatland-atmosphere interface structure impacts the small-scale functioning of processes (Chapter 2, 3 & 4) and feedbacks (Chapter 5) that balance a peatland's stable state. Disturbance to system structural layers have a spatially and temporally variable effect on system processes at the small-scale (Chapter 2, 3, 4 & 5), even when no significant changes are observed in the mean behaviour (Chapter 3 & 4). Such new heterogeneous regimes (irrespective of mean behaviour), may dis-proportionately affect the system functioning through non-linear shifts in system processes or the breeching of process tipping points. Such shifts may disrupt the balance of system feedbacks and potentially cause catastrophic shifts to an alternate stable state (Rietkerk and van de Koppel, 2008; Belyea, 2009; Waddington *et al*., 2015). The exact mechanisms controlling such catastrophic shifts are not fully understood and predicting rapid threshold responses remains a significant challenge. Understanding system functioning and disturbance responses at the scale of within system variability, as detailed in this thesis however, is likely an important step in understanding system resilience and response to pressing climatic and anthropogenic disturbances within the boreal biome.

6.3.3 Summary

The novel and detailed scale of the research presented in this thesis highlights the strong impact forest structure has on the small-scale dynamics of mass and energy exchanges between globally important ecosystems (that harbour vast reserves of Carbon) and the atmosphere. The research contributes not only to illustrate the scale and magnitude of system variability of both intact and disturbed systems but to inform how better estimates of energy balance, mass fluxes and resilience may be achieved.

6.4 FUTURE RESEARCH

The ecohydrological responses of northern peatlands to disturbance are of key importance to climate change predictions and regional water management. Work in this thesis identifies the

impact of considering the small-scale complexity of ET and considers the associated impacts on carbon fluxes and resilience predictions. Here I indicate key suggestions for future efforts in assessing peatland response to disturbance.

- Research linking the spatially and temporally variable peatland feedback mechanisms to the small-scale and non-linear responses to disturbances will likely yield crucial mechanistic understanding of peatland responses to disturbance and allow better prediction of any associated larger scale threshold responses.
- Eco-hydrological system functioning and resilience are controlled by feedbacks operating at and across a range of scales (Eppinga *et al*. 2009). However, peatland research has not yet identified all system regulating and disturbance response feedbacks (Page and Baird 2016), for example, the delayed bryophyte response to canopy removal is identified for the first time in Chapter 5 of this thesis. Detailed small-scale functional understanding, embedded in cross-scale research, may provide enhanced conceptualisations of (cross-scale) system feedbacks and may also support more confident predictions of any tipping-points / catastrophic shifts. Increases in available technologies to facilitate high-resolution direct measurement, such as used in this thesis (FO-DTS), along-side increasingly available and advancing remote sensing technology, are likely to propel the capacity of peatland and boreal researchers to better represent and simulate such small-scale system processes within peatland scale and potentially landscape scale studies.

6.5 FINAL REMARKS

This thesis provides new process understanding of how forest architecture impacts the eco-hydrological functioning of boreal peatlands. The research provides first-hand, original evidence of the small-scale variability of important system regulating processes and their non-

linear responses to disturbances. This evidence of small-scale spatio-temporal variability and non-linearity provides key challenges and opportunities to future functioning and resilience research.

6.6 REFERENCES

Aber, J. S., Aaviksoo, K., Karofeld, E. & Aber, A. W. (2002) Patterns in Estonian bogs as depicted in color kite aerial photographs. *Suo* **53**(1), 1–15.

Aleina, F. C., Runkle, B. R. K., Kleinen, T., Kutzbach, L., Schneider, J. & Brovkin, V. (2015) Modeling micro-topographic controls on boreal peatland hydrology and methane fluxes. *Biogeosciences* **12**(19), 5689–5704. doi:10.5194/bg-12-5689-2015

Belyea, L. R. (2009) Nonlinear Dynamics of Peatlands and Potential Feedbacks on the Climate System. In: *Carbon Cycling in Northern Peatlands* (A. J. Baird, L. R. Belyea & Co, eds.), Geophysica., 5–18. Washington, D.C.: American Geophysical Union.

Belyea, L. R. & Baird, A. J. (2006) Beyond 'the limits to peat bog growth': Cross-scale feedback in peatland development. *Ecol. Monogr.* **76**(3), 299–322. doi:10.1890/0012-9615(2006)076[0299:BTLTPB]2.0.CO;2

Belyea, L. R. & Malmer, N. (2004) Carbon sequestration in peatland: patterns and mechanisms of response to climate change. *Glob. Chang. Biol.* **10**(7), 1043–1052. John Wiley & Sons, Ltd (10.1111). doi:10.1111/j.1529-8817.2003.00783.x

Eppinga, M. B., Rietkerk, M., Borren, W., Lapshina, E. D., Bleuten, W. & Wassen, M. J. (2008) Regular Surface Patterning of Peatlands : Confronting Theory with Field Data 520–536. doi:10.1007/s10021-008-9138-z

Eppinga, M. B., Rietkerk, M., Wassen, M. J. & Ruiter, P. C. De. (2009) Linking habitat modification to catastrophic shifts and vegetation patterns in bogs. *Plant Ecol.* **200**(1), 53–68. doi:10.1007/s11258-007-9309-6

Frei, S., Knorr, K. H., Peiffer, S. & Fleckenstein, J. H. (2012) Surface micro-topography causes hot spots of biogeochemical activity in wetland systems: A virtual modeling experiment. *J. Geophys. Res. Biogeosciences* **117**(4), 1–18. doi:10.1029/2012JG002012

Girkin, N. T., Vane, C. H., Cooper, H. V., Moss-Hayes, V., Craigon, J., Turner, B. L., Ostle, N., *et al*. (2019) Spatial variability of organic matter properties determines methane fluxes in a tropical forested peatland. *Biogeochemistry* **142**(2), 231–245. doi:10.1007/s10533-018-0531-1

Griffiths, N. A., Hanson, P. J., Ricciuto, D. M., Iversen, C. M., Jensen, A. M., Malhotra, A., McFarlane, K. J., Norby, R J., Sargsyan, K, Sebestyen, S. D., Shi, X, Walker, A. P., Ward, E. J., Warren, J. M., Weston, David J.*et al*. (2017) Temporal and Spatial Variation in Peatland Carbon Cycling and Implications for Interpreting Responses of an Ecosystem-Scale Warming Experiment. *Soil Sci. Soc. Am. J.* **0**(0), 0. doi:10.2136/sssaj2016.12.0422

Holden, J. (2005) Peatland hydrology and carbon release: why small-scale process matters. *Philos. Trans. R. Soc. A Math. Phys. Eng. Sci.* **363**(1837), 2891–913. doi:10.1098/rsta.2005.1671

Juszczak, R., Humphreys, E., Acosta, M., Michalak-Galczewska, M., Kayzer, D. & Olejnik, J. (2013) Ecosystem respiration in a heterogeneous temperate peatland and its sensitivity to peat temperature and water table depth. *Plant Soil* **366**(1–2), 505–520. doi:10.1007/s11104-012-1441-y

Kettridge, N. & Baird, A. J. (2010) Simulating the thermal behavior of northern peatlands with a 3-D microtopography. *J. Geophys. Res.* **115**(G3), G03009. doi:10.1029/2009JG001068

Limpens, J., Berendse, F., Blodau, C., Canadell, J. G., Freeman, C., Holden, J., Roulet, N., Rydin, H., Schaepman-Strub, G. (2008) Peatlands and the carbon cycle: From local processes to global implications - A synthesis. *Biogeosciences* **5**(5), 1475–1491. doi:10.5194/bg-5-1475-2008

Loisel, J. & Yu, Z. (2013) Recent acceleration of carbon accumulation in a boreal peatland, south central Alaska. *J. Geophys. Res. Biogeosciences* **118**(1), 41–53. doi:10.1029/2012JG001978

Moore, P. D. (1977) Stratigraphy and Pollen Analysis of Claish Moss, North-West Scotland: Significance for the Origin of Surface-Pools and Forest History. *J. Ecol.* **65**(2), 375–397. [Wiley, British Ecological Society]. doi:10.2307/2259489

Moore, T. R., Roulet, N. T. & Waddington, J. M. (1998) Uncertainty in predicting the effect of climatic change on the carbon cycling of Canadian peatlands. *Clim. Change*. doi:10.1023/A:1005408719297

Page, S. E. & Baird, A. J. (2016) Peatlands and Global Change: Response and Resilience. *Ssrn*. doi:10.1146/annurev-environ-110615-085520

Premke, K., Attermeyer, K., Augustin, J., Cabezas, A., Casper, P., Deumlich, D., Gelbrecht, J., Gerke, H.H., Gessler, A., Grossart, H-P., Hilt, S., Hupfer, M., Kalettka, T., Kayler, Z., Lischeid, G., Sommer, M., Zak, D., (2016) The importance of landscape diversity for carbon fluxes at the landscape level: small-scale heterogeneity matters. *Wiley Interdiscip. Rev. Water* **3**(4), 601–617. doi:10.1002/wat2.1147

Rietkerk, M. & Koppel, J.V.D. (2008) Regular pattern formation in real ecosystems. *Trends Ecol. Evol.* **23**(3), 169–175. doi:10.1016/j.tree.2007.10.013

Ulanowski, T. A. & Branfireun, B. A. (2013) Small-scale variability in peatland pore-water biogeochemistry, Hudson Bay Lowland, Canada. *Sci. Total Environ.* **454**–**455**, 211–218. doi:10.1016/j.scitotenv.2013.02.087

Waddington, J. M., Morris, P. J., Kettridge, N., Granath, G., Thompson, D. & Moore, P. (2015) Hydrological feedbacks in northern peatlands. *Ecohydrology* (8), 113–127. doi:10.1002/eco.1493

APPENDIX : PEER-REVIEWED ARTICLES ACCEPTED FOR PUBLICATION

AGU PUBLICATIONS

Geophysical Research Letters

RESEARCH LETTER
10.1002/2017GL075974

Key Points:
- Temporal shifts in environmental stressors cause spatially explicit system feedbacks that define ecosystem resilience to change
- Layers of peatland ecosystem complexity reduce thermal hot spot intensity
- Novel application of Fiber-Optic Distributed Temperature Sensing gives soil-surface temperatures at unprecedented spatiotemporal resolution

Supporting Information:
- Supporting Information S1
- Movie S1
- Movie S2
- Movie S3

Correspondence to:
R. M. Leonard,
rml343@bham.ac.uk

Citation:
Leonard, R. M., Kettridge, N., Devito, K. J., Petrone, R. M., Mendoza, C. A., Waddington, J. M., & Krause, S. (2018). Disturbance impacts on thermal hot spots and hot moments at the peatland-atmosphere interface. *Geophysical Research Letters*, *45*, 185–193. https://doi.org/10.1002/2017GL075974

Received 12 OCT 2017
Accepted 19 DEC 2017
Accepted article online 27 DEC 2017
Published online 13 JAN 2018

Disturbance Impacts on Thermal Hot Spots and Hot Moments at the Peatland-Atmosphere Interface

R. M. Leonard[1], N. Kettridge[1], K. J. Devito[2], R. M. Petrone[3], C. A. Mendoza[4], J. M. Waddington[5], and S. Krause[1]

[1]School of Geography, Earth and Environmental Sciences, University of Birmingham, Birmingham, UK, [2]Department of Biological Sciences, University of Alberta, Edmonton, Alberta, Canada, [3]Department of Geography and Environmental Management, University of Waterloo, Waterloo, Ontario, Canada, [4]Department of Earth and Atmospheric Science, University of Alberta, Edmonton, Alberta, Canada, [5]School of Geography and Earth Sciences, McMaster University, Hamilton, Ontario, Canada

Abstract Soil-surface temperature acts as a master variable driving nonlinear terrestrial ecohydrological, biogeochemical, and micrometeorological processes, inducing short-lived or spatially isolated extremes across heterogeneous landscape surfaces. However, subcanopy soil-surface temperatures have been, to date, characterized through isolated, spatially discrete measurements. Using spatially complex forested northern peatlands as an exemplar ecosystem, we explore the high-resolution spatiotemporal thermal behavior of this critical interface and its response to disturbances by using Fiber-Optic Distributed Temperature Sensing. Soil-surface thermal patterning was identified from 1.9 million temperature measurements under *undisturbed, trees removed* and *vascular subcanopy removed* conditions. Removing layers of the structurally diverse vegetation canopy not only increased mean temperatures but it shifted the spatial and temporal distribution, range, and longevity of thermal hot spots and hot moments. We argue that linking hot spots and/or hot moments with spatially variable ecosystem processes and feedbacks is key for predicting ecosystem function and resilience.

Plain Language Summary Peatlands cover 3% of the Earth's surface but hold more carbon than the world's forests. Surface temperatures are a key control over many important peatland processes such as carbon storage and release. While peatland function and their response to disturbances has traditionally been examined as uniform, spatially isolated systems, peatland processes occur in a spatially complex and interconnected manner. New technology enables us to explore these fine-scale behaviors, examining near-surface temperatures spatially across a peatland. Temperatures were measured high spatial and temporal resolution in an undisturbed ecosystem, and subsequently repeated after the trees canopy was removed, and after the shrubs and grasses were cut and removed. We effectively removed layers of the ecosystem, reducing the complexity of the system. Results showed that average temperatures increased with removal of vegetation layers as expected. However, importantly, this temperature increase was uneven across the peatland surface and did not reflect predisturbance temperature patterns. We relate this system response to ecosystem layers and system complexity. As more layers are removed (e.g., shrub layer, and tree layer), the intensity of thermal hot spots increases. This has important implications for understanding ecosystem resilience and for predicting carbon storage ability of soils.

1. Introduction

Soil-surface temperature acts as a "biocontroller" (Buchan, 2011) of terrestrial ecohydrological, biogeochemical (Jiménez et al., 2007) and micrometeorological (Johnson-Maynard et al., 2001) processes, regulating carbon storage and release (Kirschbaum, 1995; Taggart et al., 2011), water use efficiency (Stout, 1992), metabolic processes (Dijkstra et al., 2011), and species competition (Brand, 1990). Temperatures at the pedosphere-atmosphere interface control ecosystem functioning, determining the rate and direction of energy and mass exchange with the atmosphere (e.g., carbon and water fluxes), and act as the driving force of subsurface thermal dynamics (Kettridge et al., 2013; Wullschleger et al., 1991) and associated biogeochemical processes. Despite this, there remains a critical gap in our understanding of how thermally driven processes vary both spatially and temporally across complex, heterogeneous or self-organized landscapes. This constrains our ability to accurately characterize the system function, resilience, and service provisions of complex ecosystems and project their response to disturbance.

Accurate, spatially explicit characterization of spatiotemporal thermal dynamics at the soil-atmosphere interface will likely yield important new process understanding (Hrachowitz et al., 2013; Krause et al., 2015). Moreover, it will also allow the determination of how a landscape disturbance, such as canopy removal, produces nonuniform amplification or dampening of local-scale thermal variability, and redistribution of thermal patterning in both space and time. The detection of thermal hot spots and hot moments (i.e., hot spots that do not fully persist though time) will provide insight into the location, frequency, and duration of areas where shifts in ecohydrological, biogeochemical (Jiménez et al., 2007), and micrometeorological (Johnson-Maynard et al., 2001) processes occur. These hot spots/hot moments may not only stress a system but may result in tipping points in ecosystem processes. That is, moments when critical thresholds are reached or surpassed irregularly across spatially diverse thermal landscapes may influence ecosystem resilience to perturbations. Examples of such critical thresholds and nonlinearity are numerous, from crops, where yield declines for corn, soybeans, and cotton past a defined threshold are greater than the yield increase approaching that temperature (Schlenker & Roberts, 2009), to changes in biogeochemical cycles as a result of shifts in soil bacterial populations (Biederbeck & Campbell, 1973; Zogg et al., 1997) (e.g., soil NO_3^--N concentration, gross mineralization, and nitrification rates rapidly increase when soil temperatures increase from 2, 5 or 10°C to 15°C (Cookson et al., 2002)).

Applying high spatiotemporal resolution soil-temperature surveys to understand the temperature complexities at the interface have been limited by technological constraints until recently. Soil-temperature measurements within vegetated ecosystems have been restricted to small sample numbers (Morecroft et al., 1998) as a result of cost and logistical constraints (Krause et al., 2011; Webb et al., 2008) such as data storage (Kang et al., 2000), power, and time limitations. However, technological advances in the form of Fiber-Optic Distributed Temperature Sensing (FO-DTS) now enables extensive, high frequency and resolution, thermal measurements at the decimeter scale (Tyler et al., 2009), allowing exploration of interface thermal processes within vegetated ecosystems at unprecedented spatiotemporal scales and resolutions. This offers the opportunity to advance our understanding of dynamic interface processes that are vital for understanding how ecosystems function as a whole, and how those functions change in response to disturbance stresses (Krause et al., 2015; Scheffer et al., 2001).

This study pioneers the application of high-resolution FO-DTS monitoring for characterizing thermal patterns at the pedosphere-atmosphere interface of one of the most important and complex ecosystem interface types: carbon-rich northern peatlands (Belyea & Baird, 2006; Belyea & Clymo, 2001). The high-resolution data acquisition that may be acquired by the FO-DTS allows identification of thermal hot spots and hot moments and, for the first time, allows assessment of their response to vegetation removal at an appropriate scale and resolution. Peatland soil temperatures provide a strong control on the pedosphere-atmosphere interface and ecosystem functions, regulating the cycling of carbon (Dunfield et al., 1993) and hydrological fluxes (Blok et al., 2011; Kettridge & Waddington, 2014). These peatland systems have distinctively complex surfaces, characterized by a mosaic of hummock and hollow features (spatial scale of ~ 10^1–10^2 m^2; Belyea & Clymo, 2001). This visible structural heterogeneity reflects the spatial heterogeneity observed in surface processes. For example, methane fluxes, for which temperature is a key driver, are more variable across a few meters than between peatland systems or regions (Moore et al., 1998) and respiration may vary significantly between microsites (Juszczak et al., 2013). Despite being long-term carbon stores, holding 25% of the world's soil carbon (Turunen et al., 2002), peatland ecosystems are greatly affected by multiple disturbances (Harden et al., 2000), which likely exert a strong influence on surface temperature and associated processes. For example, tree-canopy removal for linear seismic lines (Timoney & Lee, 2001), for thinning, and from insect infestations (Aukema et al., 2008), will influence surface temperatures because forest canopies induce variability in the transmission of incoming solar radiation to the ground due to variations in structure, height, and density across spatial scales (Hardy et al., 2004). The spatial patterns in thermal shielding by vegetation also interact with other controls on ground temperatures, such as climate and small-scale distributions in geomorphological, hydrological, thermal and aerodynamic properties (Al-Kayssi, 2002; Folwell et al., 2015; Peters-Lidard et al., 1998).

By utilizing FO-DTS technology to measure soil-surface temperatures at high spatiotemporal resolution in a highly patterned, forested peatland, we determine (i) the spatiotemporal variability in peat-surface temperatures and the magnitude and persistence of associated thermal hot spots and (ii) the thermal response to

tree-canopy removal and lower vascular vegetation removal how such changes are spatially and temporally distributed and whether the distribution, intensity, and duration of thermal hot spots and hot moments changes in response to disturbance.

2. Materials and Methods

2.1. Study Site

The study was conducted in a poor fen peatland in central Alberta, Canada (55.8°N, 115.1°W). The site was last burned in ~1935 and has a tree cover of black spruce (*Picea mariana*) with a basal area of 11 m^2 ha^{-1} and mean height of 2.3 m (Kettridge et al., 2012), characteristic of boreal peatland ecosystems (Wieder et al., 2009). The site is characterized by a surface microtopography of *Sphagnum fuscum* hummocks and *S. angustifolium* hollows. In addition, there are considerable areas, primarily under areas of dense black spruce tree cover, where the surface is composed of feather mosses (e.g., *Pleurozium schreberi*) and bare peat surfaces. Subcanopy vascular vegetation consists of *Rhododendron groenlandicum*, *Rubus chamaemorus*, *Chamaedaphne calyculata, Maianthemum trifolia*, and *Vaccinium* spp.

2.2. FO-DTS Monitoring and Field Manipulations

Temperatures at the pedosphere-atmosphere interface were measured using a Silixa Ltd. XT Fiber-Optic Distributed Temperature Sensing (FO-DTS) system. FO-DTS determines the temperature along a fiber-optic cable by analyzing the Raman backscatter (inelastic collisions, and the thermal excitation of electrons) of a laser pulse propagating through a glass fiber. Raman backscatter causes a shift in the return energy level below (Stokes band) or above (anti-Stokes band) the Rayleigh scatter band (the return of backscatter at the original laser pulse frequency). The resultant Stokes/anti-Stokes output ratio is used to determine temperature. For a detailed overview of the FO-DTS, measurement approach, its capabilities, limitations, and methodological challenges, the reader is directed to a number of recent reviews including Krause et al. (2012), Krause and Blume (2013), Selker et al. (2006), and Tyler et al. (2009).

A gel-coated fiber-optic (FO) cable was installed at 0.02 m depth below the surface at the study site in May 2015. This depth of 0.02 m allowed measurements of peat/moss temperature in close proximity of the peat surface whilst avoiding solar radiation directly heating of the cable. The cable was installed carefully at a depth of 0.02 m by cutting the peat/moss with scissors and enabling the moss to expand back around the cable. While the impact of this installation approach is considered minimal (see photos of cable installation in supporting information Figures S4–S6), limited disturbance to the peat structure should be borne in mind. The maximum likely range in temperature as a result of variations in burial depth of ±0.015 m is predicted to be between ±3.2 and 5.9°C (Table S1). A full uncertainty analysis on the impact of a 0.015 m deviation in burial depth is presented in section S1 in the supporting information (Kettridge & Baird, 2007, 2008).

The experimental setup comprised a sequence of eleven 10 m long rows spaced 1 m apart (Figure S3). Two additional control rows were deployed to extend the measurement array 10 m to the north and 10 m to the west of the primary measurement plot. Due to the undulating surface (up to 0.41 m topographic variation), the actual cable length varied from the 10 m plan view length, resulting in a total of 121 m of cable being buried in the main plot and 22.8 m in the control rows. FO-DTS surveys were conducted in alternate single-ended monitoring mode, with calibration carried out using temperature matching to thermally controlled water baths at both ends of the monitoring cable (Krause & Blume, 2013; Tyler et al., 2009). Within these control baths, sections of FO cable ($>$ 20 times the sampling interval) were maintained at a constant temperature throughout the experiment. FO-DTS temperatures were calibrated to thermistor measurements of the bath temperature to account for potential drift caused by differential loss along the cable length.

Measurements were obtained at a 0.25 m interval along the length of the FO cable, averaged over 1 min intervals. Surveys were run for 4 days under premanipulation conditions on 21, 22, 24, and 26 May 2015. All trees in the plot and within a 10 m buffer around the plot were cut and removed on 27 May 2015, and FO-DTS monitoring was repeated on 30 May 2015 (felled: trees removed). Trees were not disturbed around the two extended sections of cable to the north and west, thus providing a reference (control) for temperatures measured within the primary plot. All remaining vascular vegetation was removed from the primary plot on 31 May 2015 and FO-DTS measurements of surface temperatures taken subsequently on 3 June 2015 (cleared: tree and vascular vegetation removed). For all treatments, FO-DTS monitoring was carried

out between 06:30 and 20:30 local standard time. Weather conditions during the experiment periods were characterized by hot, dry, largely cloud-free conditions, with maximum air temperatures ranging from 25 to 28°C (Table S1). No rain fell during the experimental period, except on 31 May and 1 June, between the felled and cleared treatment periods, a small rain event of 13 mm was recorded. Rain-free periods and high surface temperatures subsequently resumed prior to the cleared temperature measurements.

Due to undulations in the peat surface and shallow tree roots, small sections of the buried FO cable became exposed by the end of the overall experiment period. Exposed sections were reburied and temperature differences preburial and postburial used to assess the length of affected measurements beyond the physically exposed section. A mean affected cable length of 0.58 m (±0.22 m standard deviation) either side of the exposure was established for exposures greater than 0.15 m in length, (i.e., 1.16 m of buried cable was affected in addition to the physically exposed length). Exposures less than 0.15 m in length did not influence measured temperatures. Data from exposed sections and the 0.58 m either side were removed from every exposed section greater than 0.15 m during the postprocessing. At a sampling interval of 0.25 m, this resulted in 305 sampling points within the primary plot, 1,024,800 temperature measurements under premanipulation conditions and 256,200 temperature measurements under each of the felled and cleared treatments. Control rows with 79 sampling points produced a total of 66,360 temperature measurements over the whole measurement period.

2.3. Data Analysis

A Wilcoxon rank sum test (significance threshold of 0.05) was used to determine any significant differences in mean temperatures between the primary plot and control rows for each measurement day under each treatment (premanipulation, felled, and cleared). Hot spots were identified by subtracting the daily mean temperature of the control rows from the daily mean temperature at each spatial location within the plot (ΔT °C).

Empirical orthogonal functions (EOFs) were used to decompose space-time patterns in the soil temperature data (i.e., a space-time principal component analysis). EOFs illustrate patterns in the space-time data that explain most of the observed variability, with each EOF representing a mode of variation. The approach has been successfully applied previously to decompose patterns of soil moisture (Perry & Niemann, 2007) and has been used in atmospheric science for many decades (Hannachi et al., 2007; Lorenz, 1956). The time series principal components (also called expansion coefficients) indicate the importance of a particular EOF in time.

Due to the time and effort required for FO-DTS cable installation, only one plot and two 10 m control sections were instrumented with FO-DTS cable. We are aware of the pseudoreplication (Hurlbert, 1984) this causes. We therefore undertake extensive additional data analysis (included in the supporting information) and note that the results of significance tests agree with existing literature.

3. Results

3.1. Effects of Vascular Vegetation Removal on Surface Temperatures

Wilcoxon rank sum tests showed that vascular vegetation removal significantly increased mean temperatures. Premanipulation, temperatures did not differ significantly between the primary plot (n = 305) and control rows (n = 79: 21 May: p = 0.61, 22 May: p = 0.94, 24 May: p = 0.39, 26 May: p = 0.56) (Figure 1a). Significant differences were found between the primary plot and control rows once felled ($p < 0.001$) and when cleared ($p < 0.001$). Peat-surface temperatures show substantial variability in both space and time (Figure 1b). Sixty minute mean temperatures range from 0 to 25°C, with the temperature range across the 10 m × 10 m plot regularly exceeding 25°C during the day. See also supporting information (section S2, Figures S9–S11 for spatially interpolated hourly mean data for each treatment, and Movies S1–S3 for a movie of spatially interpolated 10 min mean data).

3.2. Hot Moments and Hot Spots in Surface Temperature Patterns

Increases in mean temperatures with each successive treatment were not homogenous across the peat surface in either space or time. The hot spot intensity (ΔT) increased from 6.7°C under premanipulation conditions to 11.4°C after felling and was more than double the premanipulation intensity when cleared, at 13.7°C.

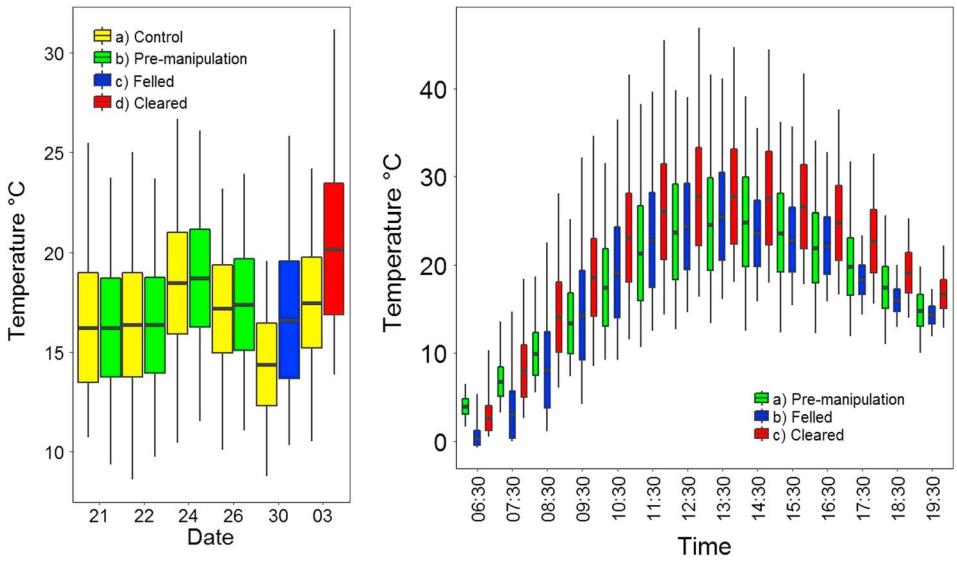

Figure 1. Box plots representing the mean, ±SE, and range of (a) daily mean plot temperature data presented for control (n = 79), premanipulation (n = 305), felled (trees removed; n = 305), and cleared (all vascular vegetation removed treatments; n = 305) and (b) hourly mean plot temperature data presented for premanipulation, trees removed (felled), and all vascular vegetation removed (cleared) treatments (n = 305).

The first three EOFs explain 57.7%, 21.1% and 9.1% of the variation observed under premanipulation conditions (Figure 3). Greater variance was explained by the first EOF after felling (80.1%) and clearing (77%) compared to premanipulation conditions (57.7%). EOFs 2 and 3 for felled (15.4 and 3.3% respectively) and cleared (18.1% and 3.2%, respectively) explain less variance than their corresponding EOFs under premanipulation conditions.

There is very little change in EOF patterns among premanipulation days (Spearman's rank correlation coefficient; r = 0.95–0.97), but with felling and clearing, the spatial patterns change substantially (r = 0.39–0.67 and r = 0.38–0.59, respectively). The importance of the first three EOFs during the measurement period (PC's) also vary between premanipulation and postmanipulation conditions. Notably, principal components 1 and 2 of the first two EOFs are consistent between the felled and cleared conditions but show the inverse pattern of principal component 1 and 2 under premanipulation conditions (Figure S12). Further assessment of the heterogeneous nature of the shifts in spatial temporal temperature signatures is presented in section S2 (Vachaud et al., 1985).

4. Discussion

4.1. Vegetation Controls on Spatial Patterns and Temporal Dynamics of Peatland Surface Temperatures

Significant surface temperature increases observed with both felling and clearing (also reported by Scull, 2007) were not uniform across the peatland surface. Canopy disturbance induces shifts in the distribution, intensity (Figure 2, also supported by section S2 and Figure S7), and longevity (Figure 3, also supported by section S2 and Figures S8–S12) of high surface temperatures, with felling and clearing decreasing the spatial variability of incoming solar radiation in both space and time.

We consider that the intensity and longevity of such surface thermal hot spots is linked to peatland ecosystem heterogeneity, as shown in the conceptual model of Figure 4. Independent spatial patterns in surface processes, driven by high levels of peatland ecosystem heterogeneity, induce uniformity, because the summation of these processes induces short-lived low-intensity white noise (Figure 4, point a). Removing such layers and limiting the complexity of the pedosphere-atmosphere interface increases the potential for long-lived positive effects to align, and to align for sustained periods. The most extreme spatial diversity thus results when the system is driven by a single process (Figure 4, point b). When the system is completely homogenous then inputs, such as solar radiation, are also spatially and temporally homogenous and hot

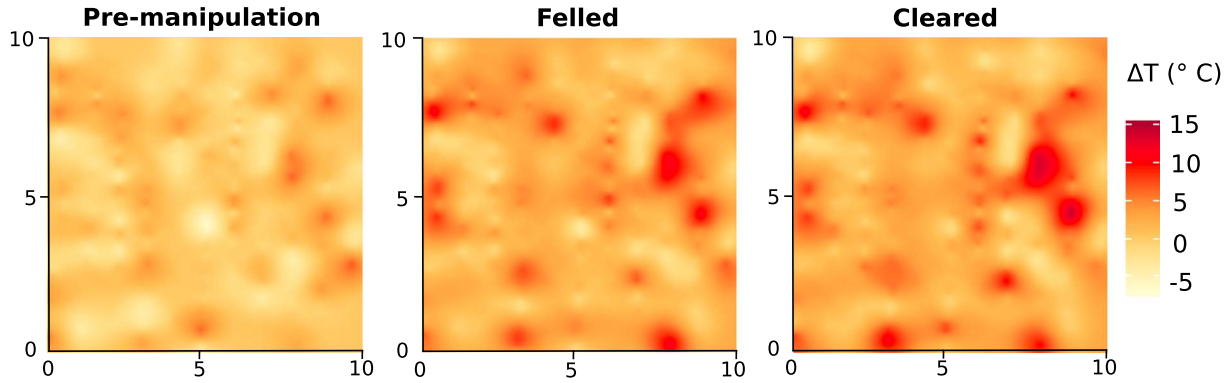

Figure 2. Mean daily hotspot intensity (ΔT °C) under premanipulation, cleared, and felled conditions. Hot spot intensity (ΔT °C) was identified by subtracting the daily mean temperature of the control rows from the daily mean temperature at each spatial location within the plot.

spots and hot moments are not observed (Figure 4, point c). Within peatlands systems, ecological, hydrological, and geomorphological heterogeneity drives variability in surface temperatures in addition to canopy complexity. These controls likely show strong codependence, maximizing hot spot intensity in peat surface temperatures. Canopy removal means such complexity is not further fragmented in space and time, and hot spot intensity is increased (Figure 4, moving the system from point d to e).

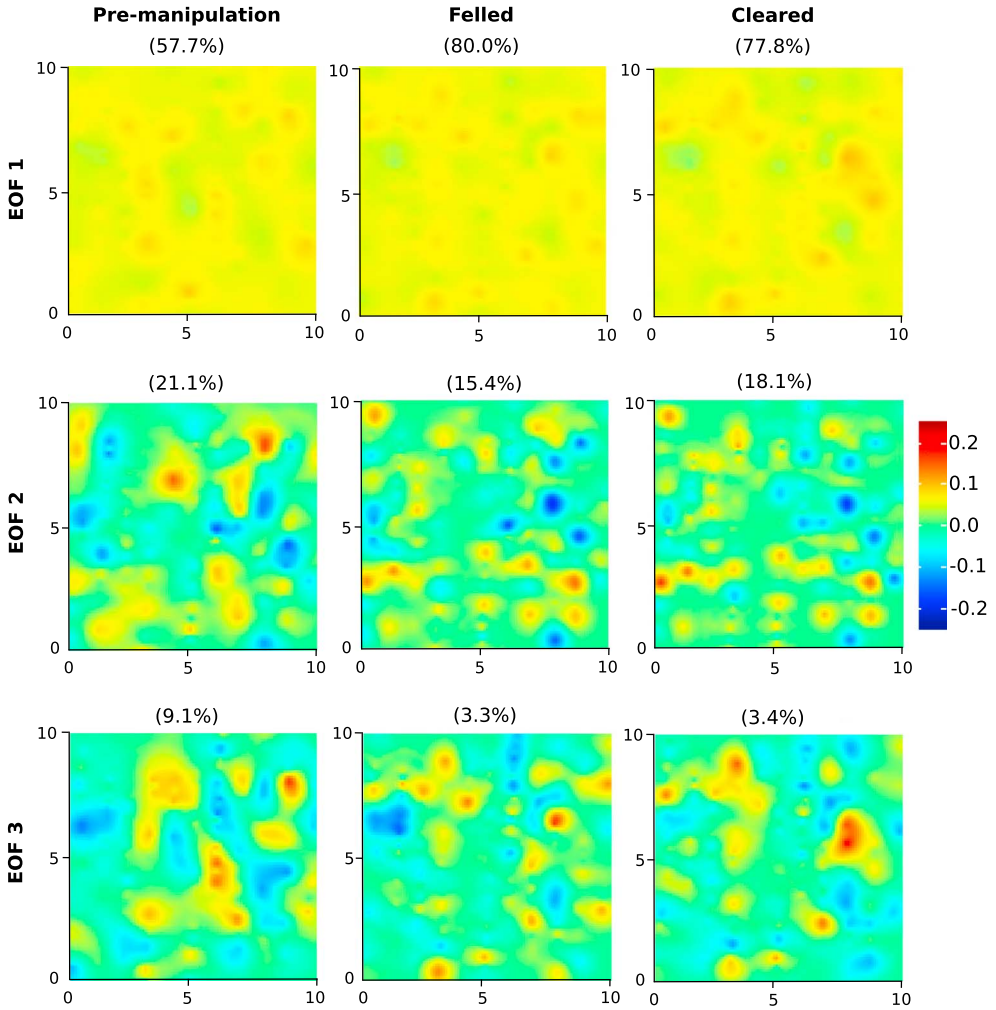

Figure 3. First three EOFs (dimensionless) for each treatment, derived from hourly mean temperature, with associated variance explained provided in parentheses.

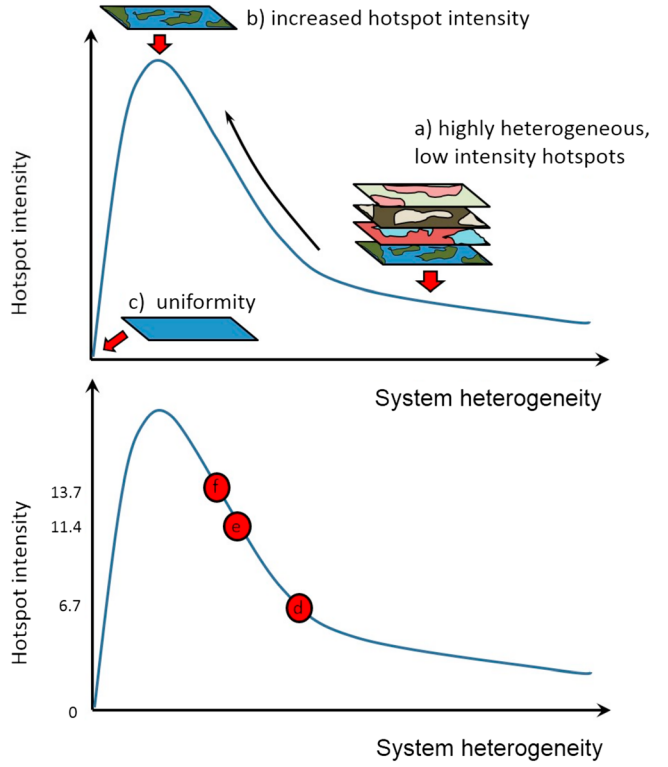

Figure 4. Conceptual dependence of peatland hotspot intensity on system heterogeneity. (top) A multilayered heterogeneous peatland system (point a) induces highly heterogeneous, low-intensity outputs. Reducing peatland complexity to a single spatially disturbed parameter/processes (point b) increases the intensity of associated hot spots. Uniformity with reduced system complexity is obtained only by limiting peatland heterogeneity to a minimum (point c). (bottom) Points d–f represent positions of the observed peatland on the conceptual model under premanipulated, felled, and cleared treatments, respectively. The *y* axis values on the lower panel represent the hot spot maxima observed (see Figure 2).

The removal of subcanopy vascular vegetation had only a limited impact on the heterogeneity of surface temperatures in space and time (Figure 3, also supported by section S2 and Figures S7e and S7f, S8, and S12). This will be because (i) the vegetation is distributed comparatively uniformly in nature; (ii) it has limited impact on soil temperatures or (iii) is strongly codependent with other drivers of system complexity function.

4.2. Implications for Ecosystem Functioning and Resilience

Observed shifts in the location, longevity, and intensity of thermal hot spots and hot moments after vegetation removal shows that the peatland system is now under discrete heterogeneous stress. Average transitions in system forcing in response to the disturbance resulted in part from intense concentrated changes within spatially isolated locations across the peatland. Spatial and temporal changes in process rates such as productivity, species competition, decomposition, and evapotranspiration will thus occur within a spatially irregular and locally extreme manner. The shift in hot spot locations also means such extremes do not map onto previous predisturbance hot spots in which the landscape has potential inherent resilience to mitigate the impact of such conditions. Heterogeneous stresses may therefore breach process thresholds and tipping points and thus promote or dampen the strength of key system feedbacks (Waddington et al., 2015; Belyea, 2009; Rietkerk & van de Koppel, 2008).

The spatial dynamics and strengths of these competing feedbacks are integral to the spatial patterning and resilience of peatlands and wider ecosystems (Barbier et al., 2006; Guichard et al., 2003; Kéfi et al., 2007; Rietkerk et al., 2004). Intense, heterogeneous stresses may therefore change not only the ecosystem functioning but also induce catastrophic shifts. For instance, the quick reduction in treed areas has been simulated in wind-disturbed forests associated with small increases in gap fraction (Kizaki & Katori, 1999). Yet models used to predict changes to ecosystem functioning and resilience rarely consider the heterogeneous nature of applied stresses. Understanding the interconnected nature of feedbacks and heterogeneous stresses is an important consideration for assessing ecosystem dynamics, function, and resilience (Schneider & Kéfi, 2016). Longer-term studies that directly relate heterogeneous shifts in stresses to spatially and temporally varying system feedback mechanisms will advance our understanding of system responses to disturbances. Linking these poses a key research frontier for evaluating and predicting shifts in ecosystem function and assessing system resilience.

5. Conclusion

High spatiotemporal resolution surface temperature data significantly improves our understanding of the complex thermal and radiative interactions at the peatland pedosphere-atmosphere interface and how these interactions change with vegetation removal. Vegetation removal increases mean temperatures as expected, but the high-resolution data and EOF analysis showed that the increase is not uniform in space or time across the peatland surface. The removal of these layers from the ecosystem decreases ecosystem complexity but increases thermal diversity of the surface. The nonuniform response of thermal dynamics at the surface highlights the need to consider and link spatially explicit ecosystem functioning mechanisms (e.g., soil-plant feedbacks) with the heterogeneous stresses placed on systems to fully assess their functioning and resilience.

Acknowledgments
We would like to thank and acknowledge Kristyn Housman and Rebekah Ingram for their support in the field when conducting this investigation. The data used are listed in the references, tables, and supporting information. Financial support was provided by Syncrude Canada Ltd. and Canadian Natural Resources Ltd. (SCL4600100599 to K. J. D., R. M. P., C. A. M., N. K., and J. M. W.) and Natural Sciences and Engineering Research Council (NSERC-CRD CRDPJ477235-14 to K. J. D., R. M. P., C. A. M., and J. M. W.) and the Natural Environment Research Council [NE/L501712/1]. We would also like to thank and acknowledge the suggestions made by M. Bayani Cardenas (Editor) and two anonymous reviewers on earlier versions of the manuscript.

References

Al-Kayssi, A. W. (2002). Spatial variability of soil temperature under greenhouse conditions. *Renewable Energy*, *27*(3), 453–462. https://doi.org/10.1016/S0960-1481(01)00132-X

Barbier, N., Couteron, P., Lejoly, J., Deblauwe, V., & Lejeune, O. (2006). Self-organized vegetation patterning as a fingerprint of climate and human impact on semi-arid ecosystems. *Journal of Ecology*, *94*(3), 537–547. https://doi.org/10.1111/j.1365-2745.2006.01126.x

Belyea, L. R. (2009). Nonlinear dynamics of peatlands and potential feedbacks on the climate system. In A. J. Baird, L. R. Belyea, & Co (Eds.), *Carbon cycling in northern peatlands*, *Geophysica* (pp. 5–18). Washington, DC: American Geophysical Union.

Belyea, L. R., & Baird, A. J. (2006). Beyond "the limits to peat bog growth": Cross-scale feedback in peatland development. *Ecological Monographs*, *76*(3), 299–322. https://doi.org/10.1890/0012-9615(2006)076%5B0299:BTLTPB%5D2.0.CO;2

Belyea, L. R., & Clymo, R. S. (2001). Feedback control of the rate of peat formation. *Proceedings Biological Sciences/The Royal Society*, *268*(1473), 1315–1321. https://doi.org/10.1098/rspb.2001.1665

Biederbeck, V. O., & Campbell, C. a. (1973). Soil microbial activity as influenced by temperature trends and fluctuations. *Canadian Journal of Soil Science*, *53*(4), 363–376. https://doi.org/10.4141/cjss73-053

Blok, D., Heijmans, M. M. P. D., Schaepman-Strub, G., van Ruijven, J., Parmentier, F. J. W., Maximov, T. C., & Berendse, F. (2011). The cooling capacity of mosses: Controls on water and energy fluxes in a Siberian tundra site. *Ecosystems*, *14*(7), 1055–1065. https://doi.org/10.1007/s10021-011-9463-5

Brand, D. G. (1990). Growth analysis of responses by planted white pine and white spruce to changes in soil temperature, fertility, and brush competition. *Forest Ecology and Management*, *30*(1-4), 125–138. https://doi.org/10.1016/0378-1127(90)90131-T

Buchan, G. D. (2011). Temperature Effects in Soil. In J. Gliński, J. Horabik, & J. Lipiec (Eds.), *Encyclopedia of Agrophysics, Encyclopedia of Earth Sciences Series*. Dordrecht, Netherlands: Springer.

Cookson, W. R., Cornforth, I. S., & Rowarth, J. S. (2002). Winter soil temperature (2–15 8°C) effects on nitrogen transformations in clover green manure amended or unamended soils: A laboratory and field study. *Soil Biology & Biochemistry*, *34*(10), 1401–1415. https://doi.org/10.1016/S0038-0717(02)00083-4

Dijkstra, P., Thomas, S. C., Heinrich, P. L., Koch, G. W., Schwartz, E., & Hungate, B. A. (2011). Effect of temperature on metabolic activity of intact microbial communities: Evidence for altered metabolic pathway activity but not for increased maintenance respiration and reduced carbon use efficiency. *Soil Biology and Biochemistry*, *43*(10), 2023–2031. https://doi.org/10.1016/j.soilbio.2011.05.018

Dunfield, P., Knowles, R., Dumont, R., & Moore, T. R. (1993). Methane production and consumption in temperate and sub-Arctic peat soils—Response to temperature and Ph. *Soil Biology & Biochemistry*, *25*(3), 321–326. https://doi.org/10.1016/0038-0717(93)90130-4

Folwell, S. S., Harris, P. P., & Taylor, C. M. (2015). Large-scale surface responses during European dry spells diagnosed from land surface temperature. *Journal of Hydrometeorology*, *17*(3), 975–993. https://doi.org/10.1175/JHM-D-15-0064.1

Guichard, F., Halpin, P. M., Allison, G. W., Lubchenco, J., & Menge, B. A. (2003). Mussel disturbance dynamics: Signatures of oceanographic forcing from local interactions. *The American Naturalist*, *161*(6), 889–904. https://doi.org/10.1086/375300

Hannachi, A., Jolliffe, I. T., & Stephenson, D. B. (2007). Empirical orthogonal functions and related techniques in atmospheric science: A review. *Interntional Journal of Climatology*, *4*(December 2007), 1549–1555. https://doi.org/10.1002/joc

Harden, J. W., Trumbore, S. E., Stocks, B. J., Hirsch, A., & Gower, S. T. (2000). The role of fire in the boreal carbon budget. *Global Change Biology*, *6*(S1), 174–184. https://doi.org/10.1046/j.1365-2486.2000.06019.x

Hardy, J. P., Melloh, R., Koenig, G., Marks, D., Winstral, A., Pomeroy, J. W., & Link, T. (2004). Solar radiation transmission through conifer canopies. *Agricultural and Forest Meteorology*, *126*(3-4), 257–270. https://doi.org/10.1016/j.agrformet.2004.06.012

Hrachowitz, M., Savenije, H. H. G., Blöschl, G., McDonnell, J. J., Sivapalan, M., Pomeroy, J. W., … Cudennec, C. (2013). A decade of Predictions in Ungauged Basins (PUB)—A review. *Hydrological Sciences Journal*, *58*(6), 1198–1255. https://doi.org/10.1080/02626667.2013.803183

Hurlbert, S. H. (1984). Psedo replication and the design of eclogical field experiments. *Ecological Monographs*, *54*(2), 187–211. https://doi.org/10.2307/1942661

Jiménez, C., Tejedor, M., & Rodríguez, M. (2007). Influence of land use changes on the soil temperature regime of Andosols on Tenerife, Canary Islands, Spain. *European Journal of Soil Science*, *58*(2), 445–449. https://doi.org/10.1111/j.1365-2389.2007.00897.x

Johnson-Maynard, J. L., Shouse, P., Graham, R., Castiglione, P., & Quideau, S. A. (2001). Microclimate and pedogenic implications in a 50-year-old chaparal and pine biosequence. *Soil Science Society of America Journal*, *68*(3), 876–884.

Juszczak, R., Humphreys, E., Acosta, M., Michalak-Galczewska, M., Kayzer, D., & Olejnik, J. (2013). Ecosystem respiration in a heterogeneous temperate peatland and its sensitivity to peat temperature and water table depth. *Plant and Soil*, *366*(1-2), 505–520. https://doi.org/10.1007/s11104-012-1441-y

Kang, S., Kim, S., Oh, S., & Lee, D. (2000). Predicting spatial and temporal patterns of soil temperature based on topography, surface cover and air temperature. *Forest Ecology and Management*, *136*(1-3), 173–184. https://doi.org/10.1016/S0378-1127(99)00290-X

Kéfi, S., Rietkerk, M., van Baalen, M., & Loreau, M. (2007). Local facilitation, bistability and transitions in arid ecosystems. *Theoretical Population Biology*, *71*(3), 367–379. https://doi.org/10.1016/j.tpb.2006.09.003

Kettridge, N., & Baird, A. (2008). Modelling soil temperatures in northern peatlands. *European Journal of Soil Science*, *59*(2), 327–338. https://doi.org/10.1111/j.1365-2389.2007.01000.x

Kettridge, N., & Baird, A. J. (2007). In situ measurements of the thermal properties of a northern peatland: Implications for peatland temperature models. *Journal of Geophysical Research*, *112*, F02019. https://doi.org/10.1029/2006JF000655

Kettridge, N., Thompson, D. K., Bombonato, L., Turetsky, M. R., Benscoter, B. W., & Waddington, J. M. (2013). The ecohydrology of forested peatlands: Simulating the effects of tree shading on moss evaporation and species composition. *Journal of Geophysical Research: Biogeosciences*, *118*, 422–435. https://doi.org/10.1002/jgrg.20043

Kettridge, N., Thompson, D. K., & Waddington, J. M. (2012). Impact of wildfire on the thermal behavior of northern peatlands: Observations and model simulations. *Journal of Geophysical Research*, *117*, G02014. https://doi.org/10.1029/2011JG001910

Kettridge, N., & Waddington, J. M. (2014). Towards quantifying the negative feedback regulation of peatland evaporation to drought. *Hydrological Processes*, *28*(11), 3728–3740. https://doi.org/10.1002/hyp.9898

Kirschbaum, M. U. F. (1995). The temperature dependence of soil organic matter decomposition, and the effect of global warming on soil organic C storage. *Soil Biology and Biochemistry*, *27*(6), 753–760. https://doi.org/10.1016/0038-0717(94)00242-S

Kizaki, S., & Katori, M. (1999). Analysis of canopy-gap structures of forests by Ising-Gibbs states—Equilibrium and scaling property of real forests. *Journal of the Physical Society of Japan*, *68*(8), 2553–2560. https://doi.org/10.1143/JPSJ.68.2553

Krause, S., & Blume, T. (2013). Impact of seasonal variability and monitoring mode on the adequacy of fiber-optic distributed temperature sensing at aquifer-river interfaces. *Water Resources Research*, *49*, 2408–2423. https://doi.org/10.1002/wrcr.20232

Krause, S., Hannah, D. M., Fleckenstein, J. H., Heppell, C. M., Kaeser, D., Pickup, R., … Wood, P. J. (2011). Inter-disciplinary perspectives on processes in the hyporheic zone. *Ecohydrology*, *4*(4), 481–499. https://doi.org/10.1002/eco.176

Krause, S., Lewandowski, J., Dahm, C. N., & Tockner, K. (2015). Invited commentary frontiers in real-time ecohydrology—A paradigm shift in understanding complex environmental systems. *Ecohydrology*, *8*(4), 529–537. https://doi.org/10.1002/eco.1646

Krause, S., Taylor, S. L., Weatherill, J., Haffenden, A., Levy, A., Cassidy, N. J., & Thomas, P. A. (2012). Fibre-optic distributed temperature sensing for characterizing the impacts of vegetation coverage on thermal patterns in woodlands. *Ecohydrology*, *764*. https://doi.org/10.1002/eco.1296

Lorenz, E. N. (1956). Empirical orthogonal functions and statistical weather prediction. Technical Report Statistical Forecast Project Report 1 Department of Meteorology MIT 49.
Moore, T. R., Roulet, N. T., & Waddington, J. M. (1998). Uncertainty in predicting the effect of climatic change on the carbon cycling of Canadian peatlands. *Climatic Change*, *40*(2), 229–245. https://doi.org/10.1023/A:1005408719297
Morecroft, M. D., Taylor, M. E., & Oliver, H. R. (1998). Air and soil microclimates of deciduous woodland compared to an open site. *Agricultural and Forest Meteorology*, *90*(1-2), 141–156. https://doi.org/10.1016/S0168-1923(97)00070-1
Perry, M. a., & Niemann, J. D. (2007). Generation of soil moisture patterns at the catchment scale by EOF interpolation. *Hydrology and Earth System Sciences Discussions*, *4*(5), 2837–2874. https://doi.org/10.5194/hessd-4-2837-2007
Peters-Lidard, D. C., Blackburn, E., Liang, X., Wood, F. E., Peters-Lidard, C. D., Blackburn, E., … Wood, E. F. (1998). The effect of soil thermal conductivity parameterization on surface energy fluxes and temperatures. *Journal of the Atmospheric Sciences*, *55*(7), 1209–1224. https://doi.org/10.1175/1520-0469(1998)055%3C1209:TEOSTC%3E2.0.CO;2
Raffa, K. F., Aukema, B. H., Bentz, B. J., Carroll, A. L., & Hicke, J. A. (2008). Cross-scale drivers of natural disturbances prone to anthropogenic amplification: The dynamics of bark beetle eruptions. *Bioscience*, *58*(6), 501–517. https://doi.org/10.1641/B580607
Rietkerk, M., Dekker, S. C., de Ruiter, P. C., & van de Koppel, J. (2004). Self-organized patchiness and catastrophic shifts in ecosystems. *Science*, *305*(5692), 1926–1929.
Rietkerk, M., & van de Koppel, J. (2008). Regular pattern formation in real ecosystems. *Trends in Ecology & Evolution*, *23*(3), 169–175. https://doi.org/10.1016/j.tree.2007.10.013
Scheffer, M., Carpenter, S., Foley, J. A., Folke, C., & Walker, B. (2001). Catastrophic shifts in ecosystems. *Nature*, *413*(6856), 591–596. https://doi.org/10.1038/35098000
Schlenker, W., & Roberts, M. J. (2009). Nonlinear temperature effects indicate severe damages to U.S. crop yields under climate change. *Proceedings of the National Academy of Sciences of the United States of America*, *106*(37), 15,594–15,598. https://doi.org/10.1073/pnas.0906865106
Schneider, F. D., & Kéfi, S. (2016). Spatially heterogeneous pressure raises risk of catastrophic shifts. *Theoretical Ecology*, *9*(2), 207–217. https://doi.org/10.1007/s12080-015-0289-1
Scull, P. (2007). Changes in soil temperature associated with reforestation in Central New York State. *Physical Geography*, *28*(4), 360–373. https://doi.org/10.2747/0272-3646.28.4.360
Selker, J. S., The, L., Huwald, H., Mallet, A., Luxemburg, W., Van De Giesen, N., … Parlange, M. B. (2006). Distributed fiber-optic temperature sensing for hydrologic systems. *Water Resources Research*, *42*, W12202. https://doi.org/10.1029/2006WR005326
Stout, W. L. (1992). Water-use efficiency of grasses as affected by soil, nitrogen, and temperature. *Soil Science Society of America Journal*, *56*. https://doi.org/10.2136/sssaj1992.03615995005600030036x
Taggart, M. J., Heitman, J. L., Vepraskas, M. J., & Burchell, M. R. (2011). Surface shading effects on soil C loss in a temperate muck soil. *Geoderma*, *163*(3-4), 238–246. https://doi.org/10.1016/j.geoderma.2011.04.020
Timoney, K., & Lee, P. (2001). Environmental management in resource-rich Alberta, Canada: First world jurisdiction, third world analogue? *Journal of Environmental Management*, *63*(4), 387–405. https://doi.org/10.1006/jema.2001.0487
Turunen, J., Tomppo, E., Tolonen, K., & Reinikainen, A. (2002). Estimating carbon accumulation rates of undrained mires in Finland—Application to boreal and subarctic regions. *The Holocene*, *1*(2002), 69–80.
Tyler, S. W., Selker, J. S., Hausner, M. B., Hatch, C. E., Torgersen, T., Thodal, C. E., & Schladow, S. G. (2009). Environmental temperature sensing using Raman spectra DTS fiber-optic methods. *Water Resources Research*, *45*, W00D23. https://doi.org/10.1029/2008WR007052
Vachaud, G., Passerat De Silans, A., Balabanis, P., & Vauclin, M. (1985). Temporal stability of spatially measured soil water probability density function1. *Soil Science Society of America Journal*, *49*. https://doi.org/10.2136/sssaj1985.03615995004900040006x
Waddington, J., Morris, P., Kettridge, N., Granath, G., Thompson, D., & Moore, P. (2015). Hydrological feedbacks in northern peatlands. *Ecohydrology*, *8*(1), 113–127. https://doi.org/10.1002/eco.1493
Webb, B. W., Hannah, D. M., Moore, R. D., Brown, L. E., & Nobilis, F. (2008). Recent advances in stream and river temperature research. *Hydrological Processes*, *918*, 902–918. https://doi.org/10.1002/hyp
Wieder, R. K., Scott, K. D., Kamminga, K., Vile, M. a., Vitt, D. H., Bone, T., … Bhatti, J. S. (2009). Postfire carbon balance in boreal bogs of Alberta, Canada. *Global Change Biology*, *15*(1), 63–81. https://doi.org/10.1111/j.1365-2486.2008.01756.x
Wullschleger, S. D., Cahoon, J. E., Ferguson, J. A., & Oosterhuis, D. M. (1991). SURFTEMP: Simulation of soil surface temperature using the energy balance equation. *Journal of Agronomic Education*, *20*(1).
Zogg, G. P., Zak, D. R., Ringelberg, D. B., White, D. C., MacDonald, N. W., & Pregitzer, K. S. (1997). Compositional and functional shifts in microbial communities due to soil warming. *Soil Science Society of America Journal*, *61*, 475–481. https://doi.org/10.2136/sssaj1997.03615995006100020015x

Received: 3 August 2016 | Revised: 30 October 2016 | Accepted: 30 October 2016

DOI 10.1002/eco.1804

WILEY

ECO LETTER

Peatland bryophyte responses to increased light from black spruce removal

R. Leonard[1] | N. Kettridge[1] | S. Krause[1] | K.J. Devito[2] | G. Granath[3] | R. Petrone[4] | C. Mendoza[5] | J.M. Waddington[6]

[1] School of Geography, Earth and Environmental Sciences, University of Birmingham, Edgbaston, Birmingham B15 2TT, UK

[2] Department of Biological Sciences, University of Alberta, Edmonton T6G 2E9AB, Canada

[3] Department of Ecology, Swedish University of Agricultural Sciences, Box 704475007 Uppsala, Sweden

[4] Department of Geography and Environmental Management, University of Waterloo, Waterloo, ON N2L 3G1, Canada

[5] Department of Earth and Atmospheric Science, University of Alberta, Edmonton, AB T6G 2E3, Canada

[6] School of Geography and Earth Sciencesz, McMaster University, Hamilton, ON L8S 4K1, Canada

Correspondence
Rhoswen Leonard, School of Geography, Earth and Environmental Sciences, University of Birmingham, Edgbaston, Birmingham, B15 2TT, UK.
Email: rml343@bham.ac.uk

Funding information
Natural Sciences and Engineering Research Council, Grant/Award Number: CRDPJ477235-14

Abstract

The ecohydrological impact of tree-canopy removal on moss and peat, which provide a principal carbon store, is just starting to be understood. Different mosses have contrasting contributions to carbon and water fluxes (e.g., *Sphagnum fuscum*, *Pleurozium schreberi*) and are strongly influenced by tree-canopy cover. Changes in tree-canopy cover may therefore lead to long-term shifts in species composition and associated ecohydrological function. However, the medium-term response to such disturbance, the associated lag in this transition to a new ecohydrological and biogeochemical regime, is not understood in detail. We investigate this medium-term (4 years) ecohydrological, biogeochemical, and species compositional response to tree-canopy removal using a randomized plot design within a northern peatland. This is the only study to test for the influence of increased light alone. We demonstrate that changes in treatment plots 4 years after tree-canopy removal were not significant. Notably, *P. schreberi* and *S. fuscum* remained within their respective plots post treatment, and there was no significant difference in plot resistance to evapotranspiration or carbon exchange. Results show that tree-canopy removal alone has little impact on bryophyte ecohydrology in the short or medium-term. This resistance to disturbance contrasts strongly with short-term changes observed within mineral soils, suggesting that concurrent shifts in the large scale hydrology induced within such disturbances are necessary to cause rapid ecohydrological transitions. Understanding this lagged response is critical to determine the strength of medium to long-term negative ecohydrological feedbacks within peatlands in addition to carbon and water fluxes on a decadal timescale in response to disturbance.

KEYWORDS

boreal, feathermoss, peat, Sphagnum, tree-canopy disturbance

1 | INTRODUCTION

Boreal forests occupy approximately 10% of the earth's vegetated surface (McGuire, Melillo, Kicklighter, & Joyce, 1995), of which, peatlands are a dominant feature. These northern peatlands are estimated to be one of the world's largest carbon stores (Yu, 2012). Despite this, northern forested peatlands are subject to widespread tree-canopy disturbances. Linear tree clearance from seismic lines exceeds 1.5 Mkm in Alberta, Canada, alone (Timoney & Lee, 2001). This equates to a 19-Mha disturbance assuming a 60-m edge effect. Thinning of spruce stands is used as a fire control method. In addition, insect infestations have the potential to act as a significant future disturbance with increases in the frequency and severity of fire and drought projected to reduce tree-canopy resistance to insects and disease (Raffa et al., 2008). Such disturbances not only remove the tree-canopy but also impact the ecohydrological function of the moss and peat (Kettridge et al., 2013), which provide the principal carbon store within these carbon rich ecosystems.

Mosses play an integral role in ecosystem functioning with their ability to equal or exceed tree-canopy productivity within northern

forested peatlands (Bisbee, Gower, Norman, & Nordheim, 2001) and contribute up to 69% of total ecosystem evapotranspiration (Bond-Lamberty, Gower, Amiro, & Ewers, 2011). Typically, feather mosses (e.g., *Pleurozium schreberi*) are associated with a high black spruce stand density and *Sphagnum* carpets are more typical of open tree-canopy peatlands. A combination of these floor cover types exist on peatlands with low stand density. Since tree cover controls the moss layer environment (e.g., temperature and radiation), its loss or thinning results in different ground layer species compositions as a result of competition and extinction-colonization dynamics. Feather moss groundcover percentage is negatively related to tree-canopy transmittance of photosynthetically active radiation (PAR), when *Sphagnum* is present while percentage ground cover of *Sphagnum* is positively related to tree-canopy PAR transmittance (Bisbee et al., 2001). This suggests that thinning of tree canopies will increase *Sphagnum* cover. Carbon and water fluxes would alter as a result because *Sphagnum fuscum* is three times more productive than *P. schreberi* (Bisbee et al., 2001) and evaporates much more due to its enhanced water transport abilities (McCarter & Price, 2014).

Short-term studies within mineral soils suggest that *S. fuscum* cover increases in the first years after tree-canopy removal (Fenton & Bergeron, 2007) and *P. schreberi* shows complete absence after 1 year (Shields, Webster, & Glime, 2007) or significant decreases in cover after 4 years (Fenton, Frego, & Sims, 2003). Despite the extent of tree-canopy disturbance within carbon rich forested peatlands, and their strong control over water and carbon fluxes, the medium-term response of moss species composition that characterizes the transitional periods of lagged responses and their associated carbon and water fluxes, remains largely unstudied. It may be argued that transitional phases dominate peatland composition and function, particularly in boreal Alberta. The cycling of disturbances such as fire, thinning, clear cutting, and seismic line creation is continuous in this region, resulting in a patchwork of continually responding ecosystems, yet work at the response/transitional phase (medium-term) timescale is rarely considered. Findings of short-term studies may change in the medium-term because the disturbance/treatment response processes may take longer than their study period. For example, a decline in *S. fuscum* 2 years after tree-canopy removal is suggested to have been a result of physiological shock due to exposure to new conditions (Fenton & Bergeron, 2007) and is likely to recover (Clymo & Duckett, 1986). In addition to lack of medium-term studies, we are not aware of any that report or demonstrate minimal changes in water-table depth and/or the impact of machinery. These are common confounding factors in large-scale timber clearances where most tree-canopy removal studies have taken place.

We target these key knowledge gaps by investigating the ecohydrological, biogeochemical, and compositional response of two key northern bryophytes to tree-canopy removal. The experiment is uniquely conducted with before and after treatment (tree-canopy removal) plots in a black spruce peatland, with no additional factors (e.g., disturbance related changes in water levels and surface micro topography), allowing unequivocal evaluation of medium-term moss response to changes in light conditions alone. The isolation of light as a process that likely induces changes to the influential moss layer will allow more robust and flexible modeling and predictions of peatland ecohydrological functioning to various disturbances including, tree removal, insect infestations, and any other light increasing disturbances.

2 | STUDY SITE

Experiments were conducted on a poor fen in central Alberta, Canada (55.81°N, 115.11°W). The depth of peat is ≥3 m and the hydrological regime is such that it is part of a larger flow-through system within the landscape, resulting in a stable water table. Total annual precipitation for (for the study period) 2010, 2011, 2012, 2013, 2014, 2015 was 282, 489, 497, 523, 376 and 387 mm, respectively. The study site is characterized by a tree cover of *Picea mariana* with a basal area and average height of 11 m^2 ha^{-1} and 2.3 m respectively. Tree basal areas for northern Albertan peatlands range from 0.3 to 47.3 m^2 ha^{-1} for peatlands that are 21 to 100 years since fire, respectively (Wieder et al., 2009). Ground layer vegetation is composed of *S. fuscum*, *Sphagnum angustifolium*, and *P. schreberi* with vascular species that include *Rhododendron groenlandicum*, *Rubus chamaemorus*, *Chamaedaphne calyculata*, *Maianthemum trifolia*, *Vaccinium oxycoccus*, and *Vaccinium vitus-idea*.

3 | METHODS

In May, 2010, 20 polyvinyl chloride collars (inside diameter of 0.17 m, length 0.10 m) were installed in the ground based on the species present (10 × *S. fuscum* and 10 × *P. schreberi*, each with 100% cover). No significant differences in sky view factor between the proposed control (0.60 ± 0.08) and treatment (0.65 ± 0.09) plots ($p > 0.05$, $t = -1.58$) or between the *S. fuscum* (0.60 ± 0.06) and *P. schreberi* (0.64 ± 0.11) plots ($p > 0.05$, $t = -1.16$) were found. On June 17, 2010, trees around five randomly selected *S. fuscum* collars and five randomly selected *P. schreberi* collars were cut by hand to increase sky view factor at the collar. Trees within a 5 m radius that influence the available light at the plot were removed, which significantly increased the sky view factor in the treatment plots (0.85 ± 0.03) relative to the control plots (0.60 ± 0.08) ($p < 0.001$, $t = 9.7$). Relative humidity (%) did not differ significantly between treatment and control plots ($p = 0.91$, $t = -0.11$) or between species ($p = 0.22$, $t = 1.3$). Air temperature did not differ significantly between treatment and control plots ($W = 42$, $p = 0.58$) or between species ($W = 62$, $p = 0.39$) either. Between June and August 2010, soil moisture and surface resistance to evapotranspiration were measured 15 times within each collar. Between July and August, 2014, measurements of species composition, and five repeat measurements of surface resistance (r_s), CO_2 exchange (net primary productivity, respiration, net ecosystem exchange), and soil moisture were undertaken within each collar. Moss stress (chlorophyll fluorescence) was measured in all plots at intervals between 7 a.m. and 6 p.m. in 2015. All measurement dates were randomly selected between May and August of each respective year, provided that there was no precipitation on the day of measurement.

Bryophyte species cover was estimated as a percentage for each collar. Moisture measurements were taken at 0.06 m depth (repeats of $n = 5$ were taken during 2010 and 2014). Resistance to evapotranspiration and CO_2 exchange were measured using a closed chamber system in accordance with McLeod, Daniel, Faulkner, and Murison

(2004). A cylindrical clear plexiglass chamber (volume of 12.6 L) was placed over the collar for 2 min and the air inside mixed continuously using a small fan. Changes in the humidity and CO_2 concentration within the chamber were measured every 1.6 s using a PP systems EGM4 infra-red gas analyser. A dark (opaque) chamber with the same dimensions was used to measure respiration (respiration assumed equal to dark chamber CO_2 flux) by the same method as described for resistance to evapotranspiration. Light chamber measurements were immediately followed by dark chamber measurements between 9 a.m. and 5 p.m. Temperature measurements were taken at 0.02 m below the bryophyte surface. Evapotranspiration rate (ET) was calculated from the slope of the linear change in vapor density (Stannard, 1988) during the first 35 s of measurement because changes in vapor density reduce significantly after the first minute (also reported by Kettridge et al. (2013)). The surface resistance to evaporation (r_s) is equal to

$$r_s = \frac{\rho^*_{vs} - \rho_{va}}{ET} - r_a, \quad (1)$$

where ρ_{vs} and ρ_{va} are the saturation vapor density of the peat surface and the vapor density of the air within the chamber, respectively and r_a is the aerodynamic resistance within the chamber during a measurement (calculated by placing the chamber over a water bath at room temperature (r_s = 0) and calculating evaporation accordingly using the same setup and duration as the field method).

3.1 | CO_2 flux

Net ecosystem exchange (NEE) was calculated from (Shaver, Street, Rastetter, Van Wijk, & Williams, 2007),

$$NEE = \frac{\rho V}{A}\frac{dC}{dt}, \quad (2)$$

where ρ is air density (mol/m^3), V is the volume of the chamber plus base (m^3), A is the projected horizontal surface area of the chamber (m^2), and dC/dt is the rate of change in CO_2 concentration within the plexiglass chamber (μmol mol^{-1} s^{-1}). Ecosystem respiration (RE; μmol m^{-2} s^{-1}) was calculated in accordance with Equation 2 but with dC/dt determined within a dark (opaque) chamber. Gross ecosystem productivity (GEP) is equal to NEE-RE, where a negative value indicates carbon uptake and a positive value indicates carbon release.

3.2 | Chlorophyll fluorescence measurements

Maximum quantum yield of photosystem II (F_v/F_m) was used to assess plant stress in response to tree-canopy removal due to its sensitivity as an indicator of plant photosynthetic performance (Maxwell & Johnson, 2000). An OS30p handheld chlorophyll fluorometer was used to measure F_v/F_m after 20 min of dark adaptation (Maxwell & Johnson, 2000) of mosses in each treatment. The theoretical maximum of F_v/F_m is between 0.78 and 0.89 (Adams & Demmig-Adams, 2004). Individual species will have different optimal values when un-stressed. Lower than optimal values indicate a lowered photosynthetic capacity (or stress); normally, this is water stress for bryophytes (Maxwell & Johnson, 2000). Chlorophyll fluorescence measurements were taken from all plots at regular intervals between 6 a.m. and 6 p.m. on July 17, 2015 to compare between control and treatment diurnal patterns.

All statistical analyses were conducted in R. A Wilcoxon rank-sum test was used to determine differences between percentage cover of bryophyte abundance between control and treatment plots (2014), daily average F_v/F_m treatment, and control plots of each species (2015). Repeat measures of moisture, GEP, and r_s from each collar were averaged. An ANOVA comparing species, year (where appropriate: moisture and r_s) and treatment were undertaken.

4 | RESULTS

4.1 | Species cover

Plots in 2010 were selected to include 100% cover of the respective species. *S. fuscum* and *P. schreberi* were still present in the relevant treatment and control plots in 2014 (Table 1). No significant difference was observed in either species abundance as a result of treatment. All *S. fuscum* plots contained 100% *S. fuscum* cover in treatment and

TABLE 1 Species cover percentages for all plots (5 of each species) in 2010 and 2014

			Control 2010	Open 2010	Control 2014	Open 2014
Pleurozium schreberi plots	*P. schreberi*	Mean	100.0	100.0	99.0	60.4
		SE ±	0.0	0.0	2.0	17.1
		median	100.0	100.0	100.0	75.0
		range	0.0	0.0	5.0	98.0
	Bare ground	Mean	—	—	0.0	21.4
		SE±	—	—	0.0	16.5
		median	—	—	0.0	2.0
		range	—	—	0.0	95.0
	Aulacomnium palustre	Mean	—	—	0.0	4.6
		SE±	—	—	0.0	3.5
		median	—	—	0.0	0.0
		range	—	—	0.0	20.0
	Polytrichum strictum	Mean	—	—	0.6	1.0
		SE±	—	—	0.5	0.9
		median	—	—	0.0	0.0
		range	—	—	3.0	5.0
Sphagnum fuscum plots	*S. fuscum*	Mean	100.0	100.0	100.0	100.0
		SE±	0.0	0.0	0.0	0.0
		median	100.0	100.0	100.0	100.0
		range	0.0	0.0	0.0	0.0

control plots. Although *P. schreberi* showed a decline (mean of percentage cover in control =99% (*SE* ± 0.89, median = 100, range = 95 to 100), mean of percentage cover in treatment =60% (*SE* ± 17.1, median = 75, range = 2 to 100), this was not significant (p = 0.06, n = 5). *P. schreberi* remained present in all 10 collars in 2014.

4.2 | Gross ecosystem productivity, surface resistance and moisture

In 2014, gross ecosystem productivity did not differ significantly between treatment types but did show significant differences with species (Table 2 and Figure 1) with *S. fucsum* (mean: −6, ±0.6 *SE*) more productive than *P. schreberi* (mean: −12, ±0.9 *SE*). Surface resistance was significantly different between species (i.e., r_s greater in *P. schreberi* plots: Figure 2) but did not show a treatment effect (Table 2). Moisture in the top 0.06 m also did not differ significantly with treatment but did show a significant species and year effect (Table 2 & Figure 3).

4.3 | Chlorophyll fluorescence

In 2015, both mean *P. schreberi* and *S. fuscum* F_v/F_m in the control collars remained near optimal throughout the day, only reaching a low of 0.66 for *S. fuscum*. The *S. fuscum* treatment fell as low as 0.63. The *P. schreberi* treatment plots on the other hand showed a drop in mean F_v/F_m later in the day to 0.46 at 4 p.m (Figure 4). Differences between treatment and control *S. fuscum* F_v/F_m were not significant (p = 0.69, n = 5). However, the treatment did cause significant reductions in *P. schreberi* F_v/F_m values (p = .0079, n = 5).

5 | DISCUSSION

5.1 | Species response to disturbance

Pleurozium schreberi is negatively correlated to the tree-canopy PAR transmittance when *Sphagnum* is present and is typically found under dense tree covers (Bisbee et al., 2001). *Sphagnum* is positively correlated with tree-canopy PAR transmittance and associated with open tree-canopy areas (Bisbee et al., 2001). It is therefore likely that long-term shifts toward an *S. fuscum* dominated system will occur in response to tree-canopy removal. Despite this, tree-canopy removal alone did not cause any significant changes in species compositions in the medium-term. *P. schreberi* was present in all treatment collars 4 years after tree-canopy removal and showed no significant decrease in cover. We suggest here that the tree-canopy PAR transmittance, substrate type, depth, and its associated hydrology not only control the species distribution (Bisbee et al., 2001) but also modify the rate of this transition in response to tree-canopy removal.

Decline in *P. schreberi* has been attributed to increased evaporation stress. If tree-canopy cover is not adequate to prevent evaporation stress, feather mosses dry out and die because they are nearly independent of the substrates' water supply (Johnson, 1981). Thus, evaporative stress will provide the likely driver for the expected long-term transition from *P. schreberi* to *S. fuscum* after tree-canopy removal. *P. schreberi* treatment plots exhibit less optimal F_v/F_m, values compared to control plots, resulting in reduced carbon accumulation which slowly reduces their competitive strength and groundcover. Further work is required to determine how the duration and intensity in *P. schreberi* stress varies on a diurnal cycle, its association with tree-canopy removal, its link with evaporative demand and near-surface moisture/tension. However, this evaporative stress is the probable cause of the observed decline of *P. schreberi* abundance and long-term shift to a *Sphagnum* dominated system. We observed that if increased evaporative stress associated with increased solar radiation is acting alone, the resulting shift in species occurs much slower, with no significant changes found within 4 years, suggesting the response is lagged. This lagged response left subcanopy species outside of their niche environment, for a period of greater than 4 years.

Despite the slower response observed in this study, Shields et al. (2007) and Fenton et al. (2003) observed a complete loss of *P. schreberi* within mineral soils 1 year after tree-canopy removal and a significant decrease after 4 years, respectively. This significant and rapid decrease/absence of *P. schreberi* in response to tree-canopy removal in short-term, mineral soil studies may be a result of changes in near-surface moisture saturation levels. A change in the moisture regime as a side effect of tree-canopy removal may be due to a change in any combination of the following: substrate depth, substrate storage, transpiration rates (lack of, after disturbance), disturbance size, and compaction. If the balance between the water storage available and reduction in evapotranspiration through tree removal results in a water table rise to a level unfavourable for *P. schreberi*, changes in species compositions may occur at a faster rate. Tree removal can result in a

TABLE 2 ANOVA results of comparisons between species, treatment and year for moisture, surface resistance and gross ecosystem productivity

	Moisture (Mv)		Gross ecosystem productivity (gC m^{-2} s^{-1})		Surface resistance (s/m)	
	F value (1/16)	*p* value	*F* value (1/16)	*p* value	*F* value (1/16)	*p* value
(Intercept)	201.70	<.0001	207.73	<.0001	90.57	<.0001
Species	22.52	.0002*	22.85	.0002*	21.21	.0003*
Treatment	0.16	.7	0.13	.72	0.03	.87
Year	21.77	.0003*			0.40	.53
Species:Treatment	0.58	.46	0.62	.44	0.07	.79
Species:Year	1.05	.32			0.33	.58
Treatment:Year	0.16	.7			3.54	.08
Species:Treatment:Year	0.02	.89			1.72	.21

Note. Asterisk (*) = significant.

water table rise (due to lack of transpiration; Pothier, Prévost, & Auger, 2003), which causes negative effects in feather moss (Busby, Bliss, & Hamilton, 1978) in as little as 4 months (Birse, 2016). However, near-surface moisture conditions did not change significantly within our study. It is also unlikely that water levels changed significantly, due to the small scale of the disturbance (and low predisturbance transpiration rate) and the fact that the system has groundwater through flow. This ground water through flow limits large water level fluctuation that would adversely affect the studied mosses. The small scale nature of the experiment on a large groundwater fed fen facilitates the minimization of water level changes as a confounding effect (which is supported by soil moisture results; Figure 3). Further, such a rapid transition may be exacerbated by the tree clearance method employed. For instance, machinery used for harvesting can cause variable changes in forest floor depth by substrate compaction (Mariani, Chang, & Kabzems, 2006). Trees were cut by hand in this study, therefore, eliminating the influence of such disturbance. The lack of observed ecohydrological changes may have also been due to low predisturbance tree densities, resulting in a less extreme increase in light than in comparative studies (Shields et al., 2007; Fenton et al., 2003). However, the sky view factor was significantly reduced in the treatment plots. At a sky view factor of 0.85, both species could maintain their presence and ecohydrological functioning. Further work is required to assess whether the predisturbance tree density or sky view factor has an impact on species presence and ecohydrological function. However, given the high sky view factor values for treatment plots, this study highlights that light alone is not enough to rapidly change species composition.

Sphagnum fuscum percentage cover did not change between control and treatment collars. This was expected because *S. fuscum* usually grows in areas with a less dense tree cover (Bisbee et al., 2001). *S. fuscum* decline in literature has been attributed to a physiological shock in response to increased light levels (Fenton & Bergeron, 2007). This may have occurred in the short-term after which the *S. fuscum* subsequently recovered (Clymo & Duckett, 1986). For example, Locky and Bayley (2007) found a decline in *Sphagnum* cover 1 to 4 years after tree-canopy removal but a subsequent increase after 9 to 12 years.

5.2 | Hydrological and biogeochemical response

Differences in *P. schreberi* GEP and r_s between treatment and control collars were not significant in this study (Figures 1 and 2). The lack of connectivity with a water supply means that *P. schreberi* can only evaporate until the water available (from precipitation (Busby et al., 1978), dew and distillation (Carleton & Dunham, 2003)) runs out and then it

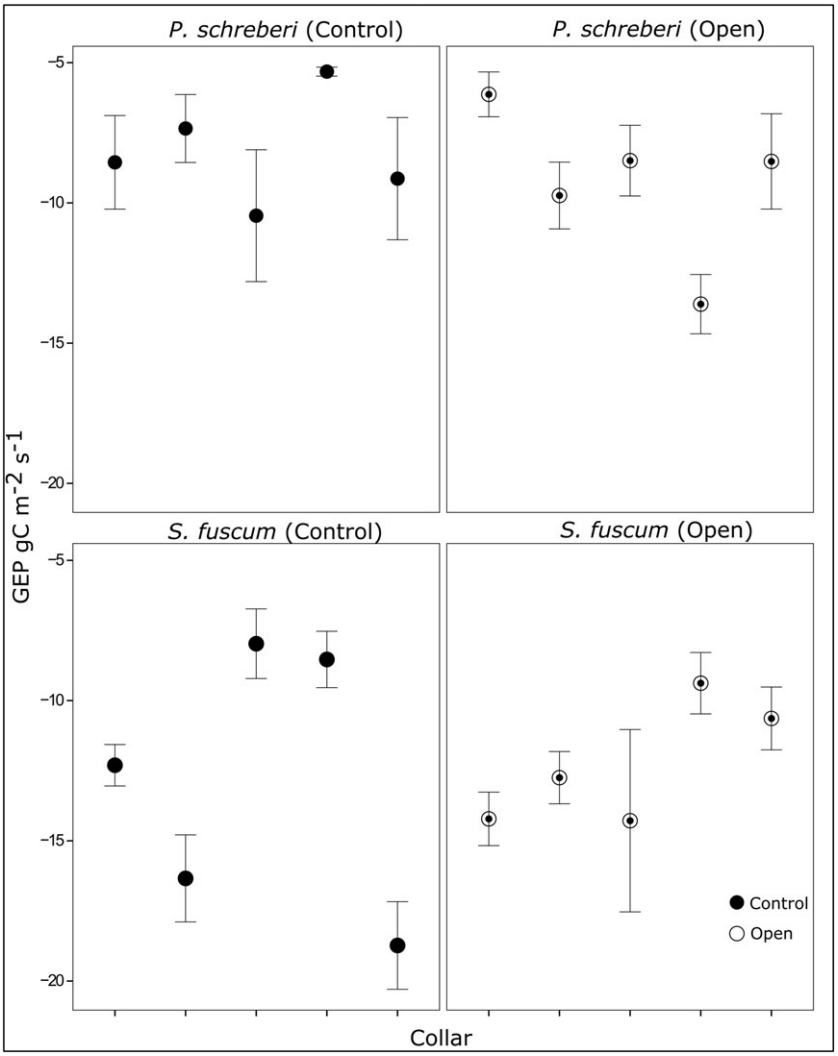

FIGURE 1 Mean (± *SE*) gross ecosystem productivity for each collar (n = 5) with five repeat measurements, 2014

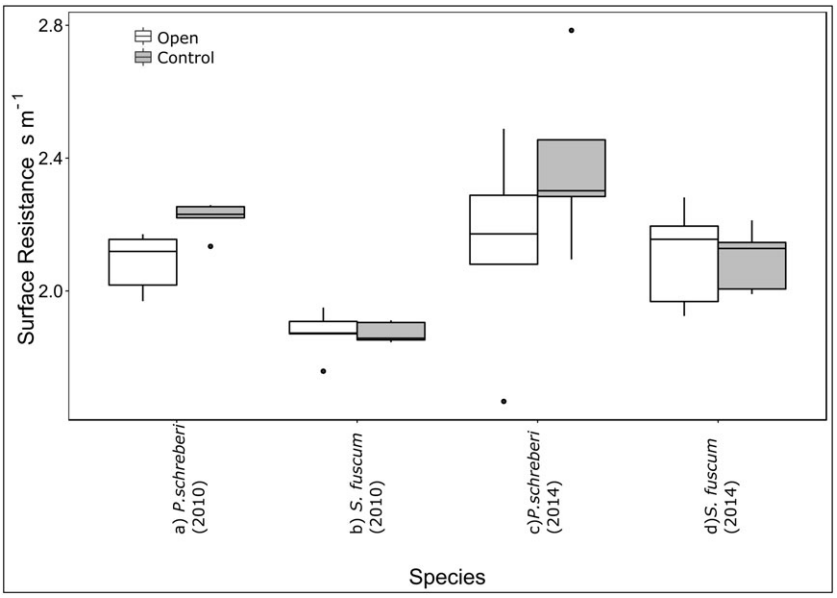

FIGURE 2 Mean (± *SE*) surface resistance of *Pleurozium schreberi* and *Sphagnum fuscum* in open and control plots, 2010 and, 2014 (*n* = 5)

becomes stressed. Surface resistance is a measure of resistance to evaporation from the peat surface: low surface resistance allows high evaporation rates and vice versa. Surface resistance varies with precipitation and is therefore highly variable within a subhumid climate. This is supported by highly variable r_s, GEP, and F_v/F_m measurements for control plots. Evaporative stress is likely happening for a greater proportion of the day and is likely the cause of the long-term decline in *P. schreberi* abundance. There was also no significant change observed in *S. fuscum* r_s and GEP. *S. fuscum* can access water at depth, allowing it to meet most increases in evaporative demand (e.g., increased energy at the surface) and maintain consistent r_s and GEP rates. This is supported by F_v/F_m values that were consistently near the optimum range in both treatment and control plots (Figure 4). Although no significant changes in r_s and GEP were observed between treatments, significant differences were found between species for GEP and r_s, supporting suggestions that species compositions have the dominant control over C and water fluxes (Heijmans, Arp, & Chapin, 2004). In the short/medium-term, moss layer hydrology and biogeochemistry have not

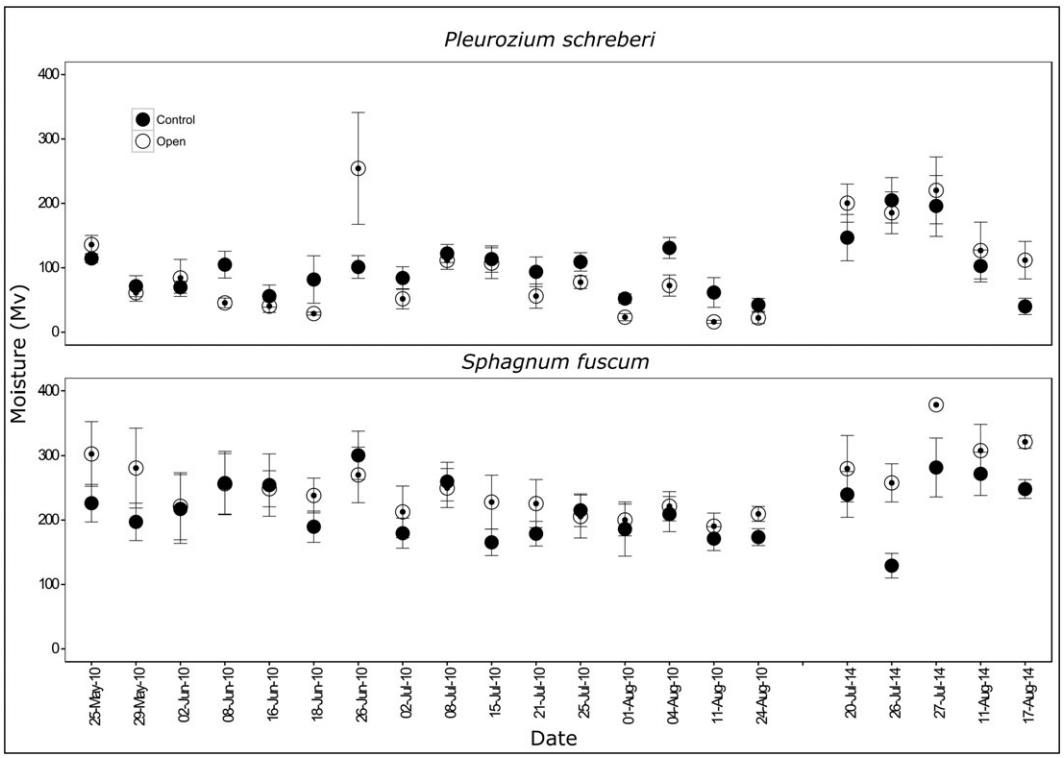

FIGURE 3 Mean (± *SE*) moisture data (*n* = 5) for treatment and control plots of *Pleurozium schreberi* and *Sphagnum fuscum* before and after treatment. (Black spruce canopy was removed on the 17th of June 2010)

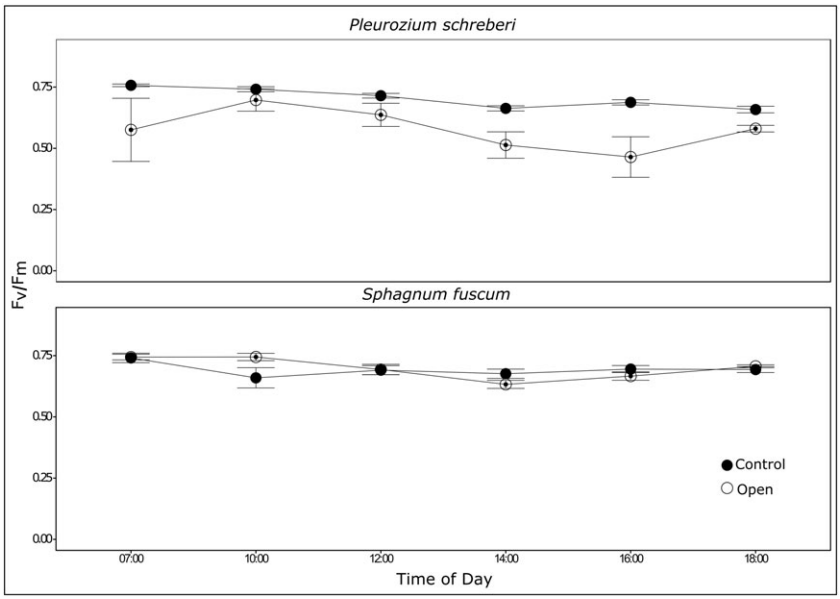

FIGURE 4 Mean (± *SE*) F_v/F_m values for control and treatment *Pleurozium schreberi* (2015),and control and treatment *Sphagnum fuscum* (2015), $n = 5$

changed, suggesting that these peatlands show some degree of resistance to disturbances. The lack of changes in surface resistance and GEP coupled with a decrease in transpiration from the tree-canopy suggests that less water is lost from the ecosystem through evapotranspiration, which facilitates the maintenance of the peatlands' existing, globally important, carbon stock. In the longer term, a shift toward an *S. fuscum* dominated moss layer is suggested by the F_v/F_m data, moss physiology and because feather mosses are characteristic of areas with low light levels (Bisbee et al., 2001). Such a shift in species composition will significantly change the moss layer hydrology and biogeochemistry of moss layers by increasing evapotranspiration and carbon accumulation.

Bryophyte species act a first order control on the small scale atmospheric carbon and water fluxes from peatlands. Ecohydrological feedback models that assume moss layer species change in equilibrium with tree-canopy PAR (BETA model; Kettridge et al., 2013) may provide a poor estimation of water fluxes during any transition period. Although PAR is a distinguishing feature between *P. schreberi* and *S. fuscum* dominated peatlands, the species compositional response to increased PAR is not immediate. This delayed response, compared to immediate responses of the same species within other studies (Shields et al., 2007) highlight that different environmental factors, has varying controls over species competitive strengths and response rates to disturbances. As such, including appropriate disturbance response rates in ecohydrological models could dramatically improve their carbon and water balance prediction capabilities. For example, in this study, we predict a shift toward an *S. fuscum* dominated system and increased carbon accumulation and evaporation from the moss layer, provided trees do not reestablish quickly. However, if the rate at which trees reestablish is faster than the rate at which *P. schreberi* cover significantly declines, the system could revert back to the status quo without significant changes to biogeochemistry and hydrology. Understanding species response rates provides better insight into ecosystem resistance to disturbance, ecohydrological feedback mechanisms, and quantification of carbon and water fluxes within globally important peatland systems.

6 | CONCLUSION

Within the studied peatland, no significant changes in species composition, surface resistance, or carbon fluxes from the bryophyte layer were observed as a result of tree-canopy removal. This study was uniquely conducted in a peatland system where confounding changes associated with tree-canopy clearance (e.g., significant water table changes and machinery influences) were avoided, allowing confident interpretation of results that were a direct effect of tree-canopy removal. These results showed slower changes (40% decrease in *P. schreberi* after 4 years) than those observed in short-term studies undertaken within mineral soils, which suggest that water table variations and/or harvest method may modify the responses of species to tree-canopy removal. Long-term changes are likely to result in a shift toward an *S. fuscum* dominated system as a result of evaporative stress causing weakened competitive strength of *P. schreberi* and eventual mortality. Because species have a dominant control over carbon and water fluxes from the system after tree-canopy removal, we argue that further process-based understanding of moss species compositional change over medium to long-term is essential for more accurate estimations of carbon and water fluxes in these globally important ecosystems.

ACKNOWLEDGMENTS

We would like to acknowledge and thank Laura Bombonato, Dan Thompson, and Steve Baisley for field support and initial set-up of this investigation. Financial support was provided by a Natural Environment Research Council studentship funding, Syncrude Canada Ltd and Canadian Natural Resources Ltd (SCL4600100599 to K. J. D., R. M. P, C. A. M., N. K., and J. M. W.) and Natural Sciences and Engineering Research Council (NSERC-CRD CRDPJ477235-14 to K. J. D., R. M. P., C. A. M., and J. M. W.).

REFERENCES

Adams, W. W., & Demmig-Adams, B. (2004). Chlorophyll fluorescence as a tool to monitor plant response to the environment. In G. C.

Papageorgiou, & Govindjee (Eds.), *Chlorophyll a fluorescence—A signature of photosynthesis*. 583–604. Netherlands: Springer.

Birse, E. M. (2016). Ecological studies on growth-form in bryophytes : III. The relationship between the growth-form of mosses and groundwater supply. *Journal of Ecology*, *46*(1), 9–27. doi:10.2307/2256900

Bisbee, K., Gower, S. T., Norman, J. M., & Nordheim, E. V. (2001). Environmental controls on ground cover species composition and productivity in a boreal black spruce forest. *Oecologia*, *129*(2), 261–270. doi:10.1007/s004420100719

Bond-Lamberty, B., Gower, S. T., Amiro, B., & Ewers, B. E. (2011). Measurement and modelling of bryophyte evaporation in a boreal forest chronosequence. *Ecohydrology*, *4*(1), 26–35. doi:10.1002/eco.118

Busby, J. R., Bliss, L. C., & Hamilton, C. D. (1978). Microclimate control of growth rates and habitats of the boreal forest mosses, *Tomenthypnum nitens* and *Hylocomium splendens*. *Ecological Monographs*, *48*(2), 95–110. doi:10.2307/2937294

Carleton, T. J., & Dunham, K. M. M. (2003). Distillation in a boreal mossy forest floor. *Canadian Journal of Forest Research*, *33*(4), 663–671. doi:10.1139/x02-197. Retrieved from http://dx.doi.org/10.1139/x02-197

Clymo, R. S., & Duckett, G. (1986). Regeneration of Sphagnum. *New Phytologist*, *102*, 589–614. doi:10.1111/j.1469-8137.1986.tb00834.x

Fenton, N. J., Frego, K. A., & Sims, M. R. (2003). Changes in forest floor bryophyte (moss and liverwort) communities 4 years after forest harvest. *Canadian Journal of Botany*, *81*(7), 714–731. doi:10.1139/b03-063

Fenton, N. J., & Bergeron, Y. (2007). Sphagnum community change after partial harvest in black spruce boreal forests. *Forest Ecology and Management*, *242*(1), 24–33. doi:10.1016/j.foreco.2007.01.028

Heijmans, M. M. P. D., Arp, W. J., & Chapin, F. S. (2004). Carbon dioxide and water vapour exchange from understory species in boreal forest. *Agricultural and Forest Meteorology*, *123*(3–4), 135–147. doi:10.1016/j.agrformet.2003.12.006

Johnson, E. A. (1981). Vegetation organization and dynamics of lichen woodland communities in the Northwest Territories Canada. *Ecology*, *62*(1), 200–215. doi:10.2307/1936682

Kettridge, N., Thompson, D. K., Bombonato, L., Turetsky, M. R., Benscoter, B. W., & Waddington, J. M. (2013). The ecohydrology of forested peatlands: Simulating the effects of tree shading on moss evaporation and species composition. *Journal of Geophysical Research: Biogeosciences*, *118*(2), 422–435. doi:10.1002/jgrg.20043

Locky, D. A., & Bayley, S. E. (2007). Effects of logging in the southern boreal peatlands of Manitoba Canada. *Canadian Journal of Forest Research*, *37*(3), 649–661. doi:10.1139/X06-249

Mariani, L., Chang, S. X., & Kabzems, R. (2006). Effects of tree harvesting forest floor removal and compaction on soil microbial biomass microbial respiration and N availability in a boreal aspen forest in British Columbia. *Soil Biology and Biochemistry*, *38*(7), 1734–1744. doi:10.1016/j.soilbio.2005.11.029

Maxwell, K., & Johnson, G. N. (2000). Chlorophyll fluorescence—a practical guide. *Journal of Experimental Botany*, *51*(345), 659–668. doi:10.1093/jexbot/51.345.659

McCarter, C. P. R., & Price, J. S. (2014). Ecohydrology of Sphagnum moss hummocks: Mechanisms of capitula water supply and simulated effects of evaporation. *Ecohydrology*, *7*(1), 33–44. doi:10.1002/eco.1313

McGuire, D. A., Melillo, J. M., Kicklighter, D. W., & Joyce, L. A. (1995). equilibrium responses of soil carbon to climate change: Empirical and process-based estimates. *Journal of Biogeography*, *22*(4/5), 785–796.

McLeod, M. K., Daniel, H., Faulkner, R., & Murison, R. (2004). Evaluation of an enclosed portable chamber to measure crop and pasture actual evapotranspiration at small scale. *Agricultural Water Management*, *67*(1), 15–34. doi:10.1016/j.agwat.2003.12.006

Pothier, D., Prévost, M., & Auger, I. (2003). Using the shelterwood method to mitigate water table rise after forest harvesting. *Forest Ecology and Management*, *179*(1–3), 573–583. doi:10.1016/S0378-1127(02)00530-3

Raffa, K. F., Aukema, B. H., Bentz, B. J., Carroll, A. L., Hicke, J. A., Turner, M. G., & Romme, W. H. (2008). Cross-scale drivers of natural disturbances prone to anthropogenic amplification: The dynamics of bark beetle eruptions. *BioScience*, *58*(6), 501–517. doi:10.1641/b580607

Shaver, G. R., Street, L. E., Rastetter, E. B., Van Wijk, M. T., & Williams, M. (2007). Functional convergence in regulation of net CO_2 flux in heterogeneous tundra landscapes in Alaska and Sweden. *Journal of Ecology*, *95*(4), 802–817. doi:10.1111/j.1365-2745.2007.01259.x

Shields, J. M., Webster, C. R., & Glime, J. M. (2007). Bryophyte community response to silvicultural opening size in a managed northern hardwood forest. *Forest Ecology and Management*, *252*(1–3), 222–229. doi:10.1016/j.foreco.2007.06.048

Stannard, D. I. (1988). Use of a hemispherical chamber for measurement of evapotranspiration. In *Open-File Report* (pp. 88–452). Denver, CO: United State Geological Survey.

Timoney, K., & Lee, P. (2001). Environmental management in resource-rich Alberta Canada: first world jurisdiction Third World analogue? *Journal of Environmental Management*, *63*(4), 387–405. doi:10.1006/jema.2001.0487

Wieder, R. K., Scott, K. D., Kamminga, K., Vile, M. A., Vitt, D. H., Bone, T., … Bhatti, J. S. (2009). Postfire carbon balance in boreal bogs of Alberta, Canada. *Global Change Biology*, *15*, 63–81. doi:10.1111/j.1365-2486.2008.01756.x

Yu, Z. C. (2012). Northern peatland carbon stocks and dynamics: A review. *Biogeosciences*, *9*(10), 4071–4085.

How to cite this article: Leonard, R., Kettridge, N., Krause, S., Devito, KJ., Granath, G., Petrone, R., Mendoza, C., Waddington, JM. Peatland bryophyte responses to increased light from black spruce removal. *Ecohydrol*. 2017;10:e1804. doi:10.1002/eco.1804.